THE AMERICAN PHYSICAL SOCIETY

[redacted]

OFFICERS OF THE SOCIETY

[redacted]

THE PHYSICAL REVIEW

[redacted]

[redacted]

Second Series *March, 1928* *Vol. 31, No. 3*

THE

PHYSICAL REVIEW

THE SPARK SPECTRUM OF SILVER (Ag II)

By A. G. Shenstone

Abstract

The spark spectrum of silver can be based on a set of terms as follows: ^3D, ^1D from the structure $4d^95s$; $^{3\&1}P$, D', F from $4d^95p$; ^3D, ^1D from $4d^96s$; $^{3\&1}S$, P', D, F', G from $4d^95d$. The theoretically lowest term $^1S_0$ ($4d^{10}$) has not been found, but an estimate of its position is given. There is evidence also for the structure $4d^94f$. All terms have intervals very different from the Landé values. The g-values also are evidently very irregular.

The separate limits calculated from the ^3D, ^1D series of two members show the same apparent divergence from theory as in Cu II, Ni I, Pd I. The intervals in the set $4d^95d$ also indicate divergence from theory. The calculated *ionization potential* is 17.1 volts from $5s^3D_3$.

MANY investigators have measured the spark spectrum of silver, the most recent being J. Frings.[1] It has been found in the present investigation, however, that the measures made by Exner and Haschek in 1911,[2] corrected, of course, to the international scale, give the most consistent results. Their measures have, therefore, been adopted down to λ2246. Beyond that point, it has been necessary to make new measurements using the copper standards previously given by the author.[3] Mr. C. W. Gartlein of Cornell University has kindly sent the author the measurements he has made of the stronger lines of the short wave-length region. They differ by about 0.8 wave numbers from the author's determinations, and it is not possible to determine which is the more accurate.

The identification of the lines as due to the first spark spectrum was made by photographing the spectrum of the arc as well as the spark and by photographing the spectrum of a spark sharply focussed on the spectrograph slit. (Hilger E. 1.) The Ag II lines may be divided into two classes, sharp and diffuse. As is usual in spectra of this type, it is found that the sharp lines are due entirely to transitions to the low levels, while the diffuse lines are always transitions to the middle set of terms. In addition to the lines which can be attributed to Ag II, numerous strong sharp lines occur in the spark but not in the arc. They are, undoubtedly, due to higher spark spectra. They are particularly numerous and strong in the region below

[1] J. Frings. Zeits. Wiss. Photog. **15**, p. 165 (1915).
[2] Kayser, "Handbuch der Spectroscopie. Vol. 7."
[3] A. G. Shenstone, Phys. Rev. **29**, p. 380 (1927).

λ2250 and can easily be differentiated from the Ag II lines by their polar character in the spark.

The present analysis is really an extension of that made by C. S. Beals.[4] Of his terms, only *A* and *M* have proved to be unreal, the remaining terms forming the main portion of the low ^3D, ^1D and their combining terms.

The Term Table (Table I) contains the terms identified, measured from the lowest term ($5s^3D_3$) as zero point. It will be seen from the table that they form the usual sets expected on the Hund theory, namely: (1) a low

TABLE I

Terms, intervals and limits in Ag II.

Designation Beals	Sh.	Term	Structure
B	$5s^3D_3$	0.0	$4d^95s$
C	$5s^3D_2$	1577.1	
	$5s^3D_1$	4574.8	
D	$5s^1D_2$	6881.3	
L	$5p^3P_2$	41008.3	
N	$5p^3F_3$	43003.2	
O	$5p^3P_1$	44457.0	
	$5p^3F_4$	44501.3	
	$5p^3D_2'$	46032.4	
	$5p^3P_0$	46972.1	$4d^95p$
P	$5p^3D_3'$	47292.4	
	$5p^3F_2$	47719.8	
Q	$5p^1F_3$	49966.4	
R	$5p^1P_1$	50727.1	
	$5p^3D_1'$	51166.6	
S	$5p^1D_2'$	51719.5	
	$6s^3D_3$	81362.7	
	$6s^3D_2$	81740.2	$4d^96s$
	$6s^3D_1$	85955.5	
	$6s^1D_2$	86233.9	
	$5d^3S_1$	86405.0	
	$5d^3G_5$	87496.6	
	$5d^3G_4$	87509.2	
	$5d^3P_2'$	87596.3	
	$5d^3P_1'$	87599.8	
	$5d^3D_3$	88041.1	
	$5d^3F_3'$	88320.6	
	$5d^3D_2$	88353.1	
	$5d^1S_0$	88356.9?	$4d^95d$
	$5d^3F_4'$	88437.9	
	$5d^1P_1'$	91592.1	
	$5d^3G_3$	92082.4	
	$5d^3D_1$	92336.6	
	$5d^1G_4$	92346.6	
	$5d^1D_2$	92620.0	
	$5d^3F_2'$	92985.0	
	$5d^1F_3'$	93027.9	
	$5d^3P_0'$	93904.5 ?	

Intervals (Higher *J*'s at left)		
$5s^3D$	1577.1	2997.7
$5p^3P$	3448.7	2515.1
$5p^3D'$	−1260.0	5134.2
$5p^3F$	−1498.0	4716.6
$6s^3D$	377.5	4215.3
$5d^3P'$	3.5	6304.7?
$5d^3D$	312.0	3983.5
$5d^3F'$	−117.3	4664.4
$5d^3G$	12.6	4573.2

Limits calculated from $5sD$ and $6sD$.

$^3D_3$ 138,000 = $^2D_3$ (Ag III)
$^3D_2$ 137,957
$^3D_1$ 142,595 = $^2D_2$ (Ag III)
$^1D_2$ 142,161

Ionization Potential
$^3D_3 \rightarrow {}^2D_3 = 17.1$ volts

$^3D^1D$ from the structure $4d^95s$; (2) an intermediate set $^{3,1}P$, D', F from $4d^95p$; (3) a high $^3D^1D$ from $4d^96s$; and (4) a high set $^{3,1}S$, P', D, F', G from $4d^95d$. The terms have been identified from intensities only, it being evident from Beals's measures of the unresolved Zeeman patterns that the *g*-values

[4] C. S. Beals, Phil. Mag. **2**, p. 770 (1926).

are mainly irregular. The terms are inverted with the exceptions that $5p^3F_4$, $5p^3D_3'$ and $5d^3F_4'$ are re-inverted. This re-inversion of the level of the middle set of highest j is the customary experience but the other two are unusual.

The term-nomenclature is designed, after the suggestion of Sommerfeld, to indicate the essentials of the atomic structure to which the term is due. This is possible in the present case since only one electron changes its quantum conditions during the process of emission of the spectrum. The term-prefixes, therefore, give the total quantum number of that electron and its azimuthal quantum number in the usual form of a letter (s, p, d etc.)

The intensities of the multiplets $4d^95p \rightarrow 4d^95s$ and $4d^96s \rightarrow 4d^95p$ are given in Table II and are in excellent agreement with theory. The intensities used are the author's visual estimates of the photographic intensities.

TABLE II

Intensities in multiplets in Ag II.

	$d^9p \rightarrow d^9s$				$d^9,s \rightarrow d^9p$.			
	$5s^3D$	$5s^3D_2$	$5s^3D_1$	$5s^1D_2$	$6s^3D_1$	$6s^3D_2$	$6s^3D_1$	$6s^1D_2$
$5p^3P_2$	100R	30	15	30	25u	—	—	—
$5p^3P_1$		80R	60	60		20u	2u	5u
$5p^3P_0$			70				8u	
$5p^3D'_3$	80R	50		80	30u	20u		5u
$5p^3D'_2$	10	75R	75	5	1u	30u	8u	1u
$5p^3D_1'$		15	60	1		1u	20u	—
$5p^3F_4$	100R				40u			
$5p^3F_3$	70R	90R		75	15u	35u		1u
$5p^3F_2$	—	45	70R	80	—	15u	15u	8u
$5p^1P_1$		15	10	75		3u	1u	20u
$5p^1D_2'$	8	20	40	60	1u	—	5u	20u
$5p^1F_3$	20	40		80R	1u	—		35u

The terms due to the structure d^9d combine with the d^9p terms to give very little except the diagonals of multiplets; but these are sufficient to fix the terms with considerable certainty. The term $5d^3G_5$ of course makes only one combination but that line is the strongest diffuse line in a wide region of the spectrum. The term $5d^3P_0'$ is doubtful because the three combinations from which it is calculated are all sharp instead of diffuse lines. The term $4d^1S_0$ is probably practically coincident with $5d^3D_2$, which makes an unexpectedly strong combination with $5p^1P_1$. In fact, this line has been observed as double by Frings and possibly the second member is $5p^1P_1 - 5d^1S_0$. $5d^1S_0$ has been calculated on that assumption.

The terms which might be expected but which have not been identified are the theoretically lowest term $^1S_0$ from the structure $5d^{10}$ and the pentad from $4d^94f$. The visible portion of the spectrum contains a considerable number of weak spark lines interspersed with a few strong ones, and the pentad referred to may produce these lines in combination with $4d^95d$. Some attempt as been made to find such terms but with insufficient success to warrant publication at present.

The position of $^1S_0(d^{10})$ may be very roughly estimated from analogy with Cu I and Cu II. The position of $^1S_0$ in Cu II was calculated from series in Cu I as being about 22,200 wave-numbers below a^3D_3. Its position is actually now found to be at 21925 below a^3D_3. This is based on the results of Mr. R. J. Lang at the University of Alberta who has used an interrupted arc in vacuo and has found the following three lines distinct in character from all others in the region: 1358.84 (12); 1368.00 (2); 1472.48 (1). Using these as the combinations of $^1S_0$ with a^1P_1, a^3D_1' and a^3P_1, the term $^1S_0$ is calculated separately as 21925, 21926, 21925 below $^3D_3$. These are extraordinarily accurate measures at such wave-lengths.

It should be noted here that M. Eugene Bloch wrote to the author in May 1927 suggesting these same lines from his own measurements; but the frequency differences were so far from the necessary values that the author was lothe to accept the assignation. He tenders his acknowledgment of error here.

Unfortunately, the low $^2D(d^9s^2)$ of Ag I, if it exists, is not yet known; but, from the general relations in the spectra of copper, silver, and gold, it is probably much higher than in Cu I. This indeed might account for the failure to observe it since in that case, its strongest combinations with 2^2P would be in the infra-red. If this is correct then the $^1S_0$ of Ag II will lie very far below $5s^3D_3$ and its combinations will be in the far ultra-violet. A rough estimate would place its strongest combination at about $^1S_0-5p^1P_1 = 81000$. Of the other two possible combinations, that with $5p^3D_1'$ would then be 440 wave-numbers towards the short wave-lengths and that with $5p^3P_1$ at 6270 wave-numbers towards longer wave-lengths.

{*Note added in proof.* The author's estimate of the position of $^1S_0(d^{10})$ proves to be too high by almost 9000 wave-numbers. The measures of Mr. H. E. White of Cornell for the three combinations are:

$^1S_0-5p^1P_1$	1112.46 (80)
$^1S_0-5p^3D_1'$	1107.05 (25)
$^1S_0-5p^3P_1$	1195.87 (50)

These give the value of $^1S_0$ as -39163.9 on the basis used in Table I. This means that the ^2D of *Ag.* I must be nearly coincident with 2^2P.}

Since two members of the $^3D^1D(d^9s)$ series are known, an approximate series limit can be evaluated by using a Rydberg formula. The four separate limits so calculated are given in the Term Table. They indicate, as in Cu II, Pd I, Ni I that the $^3D_3$ and $^3D_2$ series converge to one limit which would be the $^2D_3(d^9)$ of Cu III; and the $_3D_1$ and $^1D_2$ series converge to another limit, the $^2D_2$ of Cu III. As pointed out in connection with Cu II, this differs from the theoretical prediction. This question will be discussed more fully in a later paper.

The pentad $4d^95d$ is unusual in that the triplet terms all have very small intervals between the components of higher j, and very large intervals between the components of smaller j. The latter intervals are comparable with the calculated limit separations $^2D_3-^2D_2$ of Cu III, which would indi-

cate that the theoretical predictions may here also be in error. This is, however, in direct apposition to the evidence of the structurally similar set (d^9sd) in Cu I where the whole pentad indicates agreement with theory.

TABLE III

Classified lines of Ag II.

λ	Auth.	Int.	ν	Designation
3372.51	E	1	29643.0	$5p^1D_2'-6s^3D_3$
3269.81	E	1	30574.0	$5p^3D_1'-6s^3D_2$
3223.50	E	3	31013.3	$5p^1P_1-6s^3D_2$
3184.2	E	1u	31396.0	$5p^1F_3-6s^3D_3$
2938.55	E	15u a	34020.5	$5p^3F_2-6s^3D_2$
2934.24	E	30u a	34070.4	$5p^3D_3'-6s^3D_3$
29.37	E	30 A	34127.1	$5s^3D_3-5p^3P_2$
20.07	E	15u a	34235.7	$5p^1D_2'-6s^3D_1$
02.09	E	20u a	34447.9	$5p^3D_3'-6s^3D_2$
2896.50	E	20u a	34514.3	$5p^1D_2'-6s^1D_2$
82.2	E	1u	34685.6	$5p^1D_2'-5d^3S_1$
73.62	E	20u a	34789.1	$5p^3D_1'-6s^3D_1$
37.76	E	1u	35228.7	$5p^1P_1-6s^3D_1$
				$5p^3D_1'-5d^3S_1$
29.2	E	1u	35335.3	$5p^3D_3'-6s^3D_3$
15.57	E	20u a	35506.3	$5p^1P_1-6s^1D_2$
2799.70	E	30u a	35707.6	$5p^3D_2'-6s^3D_2$
86.50	E	2u	35876.8	$5p^1D_2'-5d^3P_1$
67.54	E	75 A	36122.5	$5s^1D_2-5p^3F_2$
56.48	E	35u a	36267.5	$5p^1F_3-6s^1D_2$
43.92	E	15 A	36433.5	$5s^3D_1-5p^3P_2$
12.07	E	40u a	36861.3	$5p^3F_4-6s^3D_3$
11.21	E	15u	36873.0	$5p^1P_1-5d^3P_1'$
2688.39	E	3u	37186.0	$5p^3D_1'-5d^3D_2$
81.38	E	20u a	37283.2	$5p^3P_1-6s^3D_2$
60.49	E	60 A	37575.9	$5s^1D_2-5p^3P_1$
56.92	F	6u	37626.4	$5p^1P_1-5d^3D_2$
56.65	F	4u	37630.2	$5p^1P_1-5d^1S_0$
25.70	E	8u	38073.7	$5p^1F_3-5d^3D_3$
14.56	E	15u	38235.9	$5p^3F_2-6s^3D_1$
06.14	E	15u	38359.5	$5p^3F_3-6s^3D_3$
2598.55	S	3u	38471.5	$5p^1F_3-5d^3F_4'$
95.67	E	8u	38514.2	$5p^3F_3-6s^1D_2$
84.21	E	2u	38685.0	$5p^3F_2-5d^3S_1$
80.77	E	35u a	38736.5	$5p^3F_3-6s^3D_2$
67.21	S	5u	38941.2	$5p^3D_3'-6s^1D_2$
64.41	E	8u	38983.6	$5p^3P_0-6s^3D_1$
53.43	E	5	39151.3	$5s^1D_2-5p^3D_2'$
35.30	E	30 A	39431.2	$5s^3D_3-5p^3P_2$
07.30	E	8u	39871.5	$5p^1D_2'-5d^1P_1'$
06.63	E	60 A	39882.2	$5s^3D_1-5p^3P_1$
04.11	E	8u	39922.3	$5p^3D_2'-6s^3D_1$
2486.72	F	4u	40201.5	$5p^3D_3'-6s^1D_2$
85.78	E	8u	40216.7	$5p^3D_3'-5d^3G_4$
80.41	E	20u a	40303.7	$5p^3D_3'-5d^3P_2'$
79.31	E	1u	40321.6	$5p^3F_3-5d^3D_3$
77.25	E	25u a	40355.2	$5p^3P_2-6s^3D_2$
76.74	E	4u	40363.5	$5p^1D_2'-5d^3G_3$
76.21	E	2u	40372.1	$5p^3D_3'-5d^3S_1$
73.84	E	80 A	40410.8	$5s^3D_3-5p^3D_3'$
72.92	E	5u	40425.8	$5p^3D_1'-5d^1P_1'$
62.26	E	20u a	40600.8	$5p^3F_3-5d^3F_4'$
61.28	E	2u	40617.0	$5p^1D_2'-5d^3D_1$
60.32	E	20u a	40632.8	$5p^3F_3-5d^3D_3$
53.31	E	30u a	40748.9	$5p^3D_3'-5d^3D_3$
47.93	E	80 A	40838.5	$5s^3D_3-5p^3F_3$
46.34	E	10u a	40865.0	$5p^1P_1-5p^1P_1'$
44.22	E	25u a	40900.5	$5p^1D_2'-5d^1D_2$
37.81	E	100R A	41008.0	$5s^3D_2-5p^3P_2$
36.62	E	8u	41028.0	$5p^3D_1'-5d^3F_2'$
29.65	E	35u a	41145.7	$5p^3D_2'-5d^3F_4'$
28.21	E	5u a	41170.1	$5p^3D_1'-5d^3D_1$
22.62	E	2u a	41265.1	$5p^1D_2'-5d^3F_3'$
20.11	E	30u a	41307.9	$5p^1D_2'-5d^1F_3'$
13.23	E	90 R A	41425.6	$5s^3D_3-5p^3F_3$
11.41	E	75A	41450.9	$5s^3D_1-5p^3D_2'$
2409.01	E	2u	41498.2	$5p^3P_1-6s^3D_1$
05.00	E	8u a	41567.4	$5p^3D_3'-5d^3P_1'$
02.60	E	8u a	41608.9	$5p^1P_1-5d^3D_1$
2392.98	E	5u a	41776.2	$5p^3P_1-6s^1D_2$
90.58	E	25u a	41818.1	$5p^3D_3'-5d^3F_3'$
86.32	E	5u a	41892.7	$5p^1P_1-5d^1D_2$
83.17	E	8u a	41948.1	$5p^3P_1-5d^3S_1$
79.7	E	1u	42009.3	$5p^3D_2'-5d^3D_3$
73.71	E	8u a	42115.3	$5p^1F_3-5d^3G_3$
65.69	E	10u a	42258.0	$5p^1P_1-5d^3F_3'$
64.01	E	30u a	42288.1	$5p^3D_2'-5d^3F_3'$
62.20	E	20u a	42320.5	$5p^3D_3'-5d^3D_3$
58.87	E	35u a	42380.2	$5p^1F_3-5d^1G_4$
57.92	E	70 A	42397.3	$5s^3D_1-5p^3P_0$
43.77	E	3u	42653.2	$5p^1F_3-5d^1D_2$
39.17	E	3	42737.1	$5p^3D_1'-5d^3P_2$?
31.40	E	80R A	42879.5	$5s^3D_3-5p^3P_1$
25.12	E	40u a	42995.3	$5p^3F_4-5d^3G_4$
24.68	E	70R A	43003.4	$5s^3D_3-5p^3F_3$
24.48	S	0u	43007.2	$5p^3F_4-5d^3G_4$
21.56	E	5u a	43061.2	$5p^1F_3-5d^1F_3'$
20.29	E	80R A	43084.8	$5s^1D_2-5p^1F_3$
17.05	E	70R A	43145.0	$5s^3D_1-5p^3F_2$
15.32	E	1	43177.3	$5p^1P_1-5d^3P_0'$
12.4	E	1u	43231.8	$5p^3F_3-6s^1D_2$
2295.08	E	8u a	43539.1	$5p^3F_4-5d^3D_3$
80.03	E	75 A	43845.5	$5s^1D_2-5p^1P_1$
77.43	E	10u a	43895.6	$5p^3P_1-5d^3D_2$
75.32	E	25u a	43936.3	$5p^3F_4-5d^3F_4'$
57.41	E	1	44284.8	$5s^1D_2-5p^3D_1'$
53.45	E	30u a	44362.6	$5p^3F_4-5d^3G_4$
48.74	E	75R A	44455.5	$5s^3D_3-5p^3D_3'$
46.43	E	100R A	44501.2	$5s^3D_3-5p^3F_4$
46.14	S	20(u?)a	44507.0	$5p^3F_4-5d^3G_4$
41.80	S	3u	44593.1	$5p^3F_3-5d^3P_2'$
40.39	S	10u	44621.0	$5p^3P_0-5d^1P_1'$
29.53	S	60 A	44838.4	$5s^1D_2-5p^1D_2'$
19.69	S	10u	45037.4	$5p^3F_4-5d^3D_3$
17.87	S	2u	45054.0	$5p^1D_2'-5d^1G_4$
08.49	S	15u	45265.7	$5p^3F_3-5d^3F_3'$
05.95	S	35u a	45317.7	$5p^3F_3-5d^3F_3'$
04.38	S	10u	45350.0	$5p^3F_3-5d^3D_3$
03.64	S	15u	45365.3	$5p^3P_2-5d^3D_1$
02.09	S	40u a	45397.2	$5p^3P_2-5d^3S_1$
2186.76	S	50 A	45715.3	$5s^3D_3-5p^3D_3'$
71.66	S	10	46032.6	$5s^3D_3-5p^3D_3'$
70.87	S	25u	46050.0	$5p^3D_3'-5d^3G_3$
66.51	S	45 A	46142.6	$5s^3D_3-5p^3F_3$
66.05	S	10	46152.4	$5s^3D_1-5p^1P_1$
58.95	S	1u	46304.3	$5p^3D_3'-5d^3D_3$
45.76	S	20u	46588.2	$5p^3P_2-5d^3P_2'$
				$5p^3D_3'-5d^1D_2$
45.60	S	60 A	46592.1	$5s^3D_1-5p^3D_1'$
29.12	S	10u	46952.8	$5p^3D_3'-5d^3F_3'$
25.50	S	18u	47032.8	$5p^3P_2-5d^3D_2$
20.45	S	40 A	47144.9	$5s^3D_1-5p^1D_2'$
13.82	S	80R A	47292.6	$5s^3D_3-5p^3D_3'$
11.43	S	1u	47346.1	$5p^3P_2-5d^3D_2'$
2075.61	S	10u	48163.1	$5p^3P_1-5d^1D_2$
65.90	S	40 A	48389.4	$5s^3D_3-5p^1F_3$
33.92	S	15 L	49150.2	$5s^3D_2-5p^1P_1$
21.65	S	5 L?	49448.4	$5s^3P_1-5d^3P_0'$?
15.89	S	15 L	49589.7	$5s^3D_3-5p^3D_3$
00.68	S	20 L	49966.7	$5s^3D_3-5p^3F_3$
1993.67	S	20 L	50142.5	$5s^3D_3-5p^1D_2'$
32.88	S	8 L	51719.1	$5s^3D_3-5p^1D_2'$

E. Exner and Hascheck Spark.
Kayser. "Handbuch der Spectroscopie. Vol. 7."
F. Frings. (as "E".)
S. Author.
A. a. Appears in arc. A—strong. a—weak.
L. Long line in focussed spark.

The list of identified lines includes practically all the spark lines which appear in the arc. One enhanced line only (λ2395.68 (15)) has not been identified and its presence seems inexplicable unless another structure altogether is assumed to be present. The list gives the authority for the wave-length measurements, the author's intensity estimates, and a note as to the line's appearance or non-appearance in the arc. The arc exposure in the region λ2500—λ2250 was most intense and it will be noticed that in that region very few of the identified lines do not appear in the arc. As a matter of technique, it may be noted that an arc run on small current between pointed electrodes and with large self-induction in the circuit is most favourable to the production of spark lines. For instance, in the present case terms which are approximately 23 volts above the lowest state of the atom are very strongly excited in the arc of this character.

It has frequently been noticed that spark lines measured in the arc yield wave-lengths shorter than in the spark. In silver, the sharp lines are apparently unshifted but all the diffuse lines show a very considerable displacement. A few cases were measured on the assumption that no shift occurs in the sharp lines and gave displacements of the diffuse lines of about 2.2 wave-numbers in the region around λ2350.

PALMER PHYSICAL LABORATORY,
PRINCETON UNIVERSITY,
December 17, 1927.

VIBRATIONAL LEVELS AND HEAT OF DISSOCIATION OF Na_2

By F. W. Loomis

Abstract

According to Kemble's theory of the Zeeman effect in band spectra, there should be a magnetic rotation line at the head of each Na_2 absorption band. It is found that most of Wood's magnetic rotation lines in the blue-green region can be arranged into a band system, and integral vibrational quantum numbers, n' and n'', assigned, in terms of which their frequencies are given by the following polynomial:

$$\nu = 20301.7 + (124.13n' - 0.84n'^2) - (158.5n'' - 0.73n''^2 - 0.0027n''^3)$$

The heat of dissociation is then calculated to be 1.0 ± 0.1 volt. The energies needed to dissociate the molecules which correspond to the upper levels of the blue-green and red systems are shown to be 0.6 volt and 1.25 volt, respectively, within about 0.1 volt. The lower level molecule, in both systems, dissociates by vibration into two normal (3^2S) atoms, while the upper level molecule, in both systems, dissociates into one atom in the normal state and one in a 3^2P state.

When the intensities of the magnetic rotation lines corresponding to the heads are tabulated, in the usual square array, according to n' and n'', a wide open parabola-like figure appears, of a type which Condon has accounted for in terms of an hypothesis of Franck. This affords an explanation of a puzzling phenomenon, reported by Wood, in the spectral distribution of the fluorescent light when excited by light of various frequencies.

THIS paper is based on R. W. Wood's investigations,[1] by means of fluorescence and "magnetic rotation," of the blue-green band system of sodium vapor. This spectrum is now generally attributed[2] to the diatomic molecule, Na_2. Much of the material presented here was included in a paper[3] read before the February 1927 meeting of the American Physical Society.

The absorption spectrum of sodium vapor consists of two distinctly separated band systems, one in the blue-green, the other in the red. These same systems appear, however, in a more extended manner, i.e., developed to higher values of the vibrational quantum numbers n' and n'', in the magnetic rotation and fluorescence spectra, and hence these, especially the magnetic rotation spectrum, afford a better basis for a vibrational energy formula and for the determination of the heat of dissociation.

Wood's magnetic rotation spectrum was obtained by sending the light from the crater of a carbon arc through two Nicols, between which was a tube of sodium vapor within the core of a powerful electromagnet. If the Nicols were set for extinction and the magnetic field then turned on, a spectrum flashed out which was very much simpler than the absorption spectrum. It consisted, in fact, of about 130 sharp lines in the blue-green and 340 in the red. Each of these lines was caused by light whose plane of

[1] R. W. Wood, Proc. Am. Acad. **42**, 235 (1906), Astrophys. J. **30**, 339 (1909).
[2] Pringsheim, Handbuch der Physik, XXIII, pages 504–505.
[3] Loomis, Phys. Rev. **29**, 607A (1927).

polarization had been rotated by the magnetized sodium vapor; and the direction of rotation could be found, in the case of the stronger lines, by determining in which direction the second Nicol had to be rotated to re-extinguish the line.

The classical explanation[4] of magnetic rotation of the plane of polarization is that it occurs in the neighborhood of absorption lines, which are split into Zeeman patterns by a magnetic field. A line which exhibits the normal Zeeman effect, will, when viewed along the lines of force, be split into a right-handed circularly polarized component whose frequency is slightly increased by the field and a left-handed circularly polarized component whose frequency is slightly decreased. Each of these components will exhibit an anomalous dispersion curve of the usual sort, symmetrical about the displaced position of the component. The result will be that the velocity of the right-hand component will exceed that of the left-hand component everywhere except between them; and the region between them, if the magnetic separation is small, will be one of high absorption. Consequently, if plane polarized light enters the vapor, one of the two circularly polarized beams into which it is resolvable will be retarded with respect to the other; that is, the plane of polarization will be rotated. Moreover, the sign of the rotation will be the same for all frequencies near the absorbing line, except between the two magnetically separated components, where the light is largely absorbed. Hence the light which actually gets through will be almost wholly rotated like a right handed screw. A line having a complex Zeeman pattern may rotate in the opposite direction, depending on the relative intensities and separations of the Zeeman components.

The most complete theory, to date, of the Zeeman effect in bands has been published by Kemble.[5] He finds the magnitude of the Zeeman pattern should ordinarily be approximately inversely proportional to j; that is, it should decrease rapidly as one goes away from the origin, and should be very much smaller than in line spectra, except for the band lines nearest the origin. The magnetic rotation should therefore be largest near the origin and not observable at any considerable distance from it. Magnetic rotation should be particularly prominent just on the *violet* side[6] of the heads, since the region is influenced by the strong magnetic rotation due to several neighboring lines of low quantum number, and yet does not coincide with any absorption line.

Many of the strong magnetic rotation lines do actually correspond to heads in this way; and Wood has arranged some of the green ones into five series, whose spacing is approximately that of the fluorescence series and which undoubtedly are n'' progressions. The writer has extended this

[4] Lorentz, Theory of Electrons, page 163.

[5] Kemble, National Research Council Report on "Molecular Spectra in Gases" pp. 337 ff.; Phys. Rev. **27**, 799A (1926); Kemble, Mulliken and Crawford, Phys. Rev. **30**, 438 (1927).

[6] The Na_2 bands are degraded to the red, and the heads are within a few lines of the origins. Cf. Smith, Proc. Roy. Soc. **A106**, 400 (1924).

arrangement by converting wave-lengths to frequencies and applying the usual combination principle methods, and finds that about 90 of the lines, including all the strong lines which rotate normally and none which rotate abnormally, can be assigned to such series. By comparison with the fluorescence series it is possible to assign vibration quantum numbers with certainty. The frequencies of these lines are represented by the following polynomial expression of the usual type:

$$\nu = 20301.7 + (124.13n' - 0.84n'^2) - (158.5n'' - 0.73n''^2 - 0.0027n''^3)$$
$$= \nu_0 + T'(n') - T''(n'') \qquad n' \text{ and } n'' \text{ integral} \qquad (1)$$

Table I exhibits the assignment of vibrational quantum numbers to these lines and the agreement between Eq. (1) and the observed frequencies.

TABLE I

Assignment of vibrational quantum numbers to magnetic rotation lines.

n'	n''	Intensity	Direction of rotation[7]	λ[8]	ν obs.	ν calc. by (1)	observed − calc. by (1)
0	0	10		4924.32	20301.7	20301.7	0.0
0	1	10	−	4962.85	20144.1	20144.0	+0.1
0	2	10	−	5001.57	19988.2	19987.8	+0.4
0	3	9	−	5040.65	19833.2	19833.1	+0.1
*0	4	8	−	5079.78	19680.4	19679.9	+0.5
0	5	8	−	5119.34	19528.3	19528.2	+0.1
0	6	6		5159.1	19377.8	19378.0	−0.2
*0	8	4		5238.9	19082.7	19082.1	+0.6
1	0	6	−	4894.58	20425.1	20425.0	+0.1
1	1	10	−	4932.64	20267.5	20267.3	+0.2
1	2	8		4970.85	20111.7	20111.1	+0.6
1	3	4		5009.4	19956.9	19956.4	+0.5
1	4	8		5048.49	19802.4	19803.2	−0.8
*1	5	8	−	5087.31	19651.3	19651.5	−0.2
1	6	8	−	5126.54	19500.9	19501.3	−0.4
1	7	8	−	5165.85	19352.5	19352.6	−0.1
*2	0	4		4865.59	20546.8	20546.6	+0.2
2	1	3		4903.38	20388.4	20388.9	−0.5
2	2	2		4941.6	20230.7	20232.7	−2.0
2	3	10	−	4979.34	20077.4	20078.0	−0.6
2	4	4		5017.5	19924.7	19924.8	−0.1
2	6	8		5094.78	19622.5	19622.9	−0.4
2	7	8	−	5133.73	19473.6	19474.2	−0.6
2	8	8	−	5172.82	19326.4	19327.0	−0.6
2	9	8		5211.71	19182.2	19181.3	+0.9
3	0	10		4837.49	20666.1	20666.5	−0.4
*3	1	2		4875.1	20506.7	20508.8	−2.1
3	2	6	−	4912.10	20352.2	20352.6	−0.4
3	5	5		5025.66	19892.4	19893.0	−0.6
3	7	4		5102.3	19593.6	19594.1	−0.5
3	8	8		5140.71	19447.2	19446.9	+0.3
3	9	8		5179.71	19300.7	19301.2	−0.5
3	10	8		5219.00	19155.4	19157.0	−1.6
4	0	10		4810.16	20783.5	20784.8	−1.3
4	1	4	−	4846.8	20626.4	20627.1	−0.7

[7] Minus sign indicates "normal" direction of rotation; absence of any sign indicates direction of rotation not reported. No lines in this table show abnormal rotation (i.e.+).

[8] Wave-lengths given to 0.01A are taken from Wood, Proc. Am. Acad., 42, 259 (1906). The others are from Wood, Astrophys. J., 30, 360 (1909).

* Indicates a line which can be assigned quantum numbers in two ways.

TABLE I (continued)

n'	n''	Intensity	Direction of rotation[7]	λ[8]	ν obs.	ν calc. by (1)	observed − calc. by (1)
4	2	4		4883.81	20470.1	20470.9	−0.8
4	4	4		4958.62	20161.3	20163.0	−1.7
4	6	5		5033.54	19861.2	19861.1	+0.1
4	7	8		5071.50	19712.6	19712.4	+0.2
4	9	8		5147.50	19421.5	19419.5	+2.0
4	10	8		5186.70	19274.7	19275.3	−0.6
4	11	8		5225.34	19132.2	19132.6	−0.4
4	12	6		5263.8	18992.4	18991.4	+1.0
5	0	10	−	4782.89	20902.0	20901.4	+0.6
5	1	10		4819.43	20743.6	20743.6	0.0
5	3	6		4892.9	20432.1	20432.8	−0.7
5	5	4		4967.10	20126.9	20127.8	−0.9
*5	8	8	−	5079.78	19680.4	19681.8	−1.4
5	11	8		5192.3	19253.9	19249.2	+4.7
5	12	1		5232.2	19107.1	19108.0	−0.9
5	13	6		5270.3	18969.0	18968.2	+0.8
6	0	10		4756.6	21017.6	21016.2	+1.4
6	1	10	−	4792.4	20860.6	20858.5	+2.1
*6	3	4		4865.59	20546.8	20547.6	−0.8
6	7	4		5012.7	19943.8	19943.8	0.0
6	8	4		5049.56	19798.2	19796.6	+1.6
*6	9	8	−	5087.31	19651.3	19650.9	+0.4
*6	13	4		5238.9	19082.7	19083.1	−0.4
6	14	6		5276.6	18946.3	18944.9	−1.4
7	0	10		4731.4	21129.5	21129.5	0.0
7	1	10		4766.7	20973.0	20971.8	+1.2
7	2	10	−	4802.2	20818.0	20815.6	+2.4
7	3	4	−	4839.	20659.7	20660.8	−1.1
*7	4	2		4875.1	20506.7	20507.6	−0.9
7	9	4		5058.4	19763.6	19764.2	−0.6
7	15	6		5282.6	18924.8	18921.4	+3.4
8	0	10		4706.5	21241.3	21241.0	+0.3
8	1	10	−	4741.8	21083.2	21083.3	−0.1
8	2	4		4777.1	20927.4	20927.1	+0.3
8	3	4	−	4812.2	20774.7	20772.4	+2.3
8	4	4		4848.4	20619.6	20619.2	+0.4
8	16	6		5288.6	18903.4	18897.8	+5.6
*9	0	2		4682.6	21349.7	21350.8	−1.1
9	1	10		4716.9	21194.5	21193.1	+1.4
9	2	10		4752.04	21037.7	21036.9	+0.8
9	3	2		4787.5	20881.9	20882.2	−0.3
9	5	4		4858.3	20577.6	20577.3	+0.3
10	0	2		4658.6	21459.7	21459.0	+0.7
10	2	10	−	4727.52	21146.8	21145.1	+1.7
10	3	10		4762.7	20990.6	20990.4	+0.2
10	16	1		5228.3	19121.4	19115.8	+5.6
10	18	6		5298.9	18866.6	18849.9	+16.7
*11	2	10	−	4703.9	21253.0	21251.6	+1.4
11	3	10	−	4738.5	21097.8	21096.9	+0.9
12	2	2		4681.2	21356.1	21356.4	−0.3
*12	3	10		4715.63	21200.2	21201.7	−1.5
12	4	10	−	4749.3	21049.9	21048.5	+1.4
13	3			4692.54	21304.5	21304.8	−0.3
14	2	2		4636.7	21561.0	21561.0	0.0
14	3	2		4670.4	21405.5	21406.3	−0.8
*14	4	10	−	4703.9	21253.0	21253.1	−0.1
15	2	2		4615.8	21658.7	21660.8	−2.1
15	3	8		4648.9	21504.5	21506.0	−1.5
*15	4	2		4682.6	21349.7	21352.8	−3.1
*15	5	10		4715.63	21200.2	21201.2	−1.0
16	3	2		4628	21601.6	21604.1	−2.5
16	4	2		4661.2	21447.7	21450.9	−3.2

It will be noted that none of the lines to which it has been possible to assign quantum numbers n' and n'', i.e., none of the magnetic rotation lines coinciding with band heads, were found by Wood to show positive magnetic rotation. That is, all the assigned lines either definitely show negative (i.e., normal) rotation, or rotation too slight to permit determination of its sign. The fact that some of the fluorescence series are doublets indicates the presence of R and P branches; while the fact that the bands degrade to the red shows that the heads are on R branches. One is therefore justified in concluding, empirically, that, for the kind of magnetic rotation which occurs near the origins of the Na_2 bands, the lines on the R branch rotate normally $(-)$; and, undoubtedly, those on the P branch rotate abnormally $(+)$. This is the opposite of the rule found by the writer[9] in the iodine bands. Kemble's theory[10] indicates that the rule for Na_2 is what one should ordinarily expect, while that for I_2 is unusual, both in direction and in that the rotation is strong for lines far from the origin.

The cause of the magnetic rotation lines which do not correspond to heads is puzzling. It is natural to suspect that they correspond to perturbations, since perturbed lines are known to show abnormally large Zeeman patterns; but if so they should form n', or possibly n'', progressions, which they do not appear to do. Nor do they, according to Fredrickson and Watson's[11] analysis of fine structure, occur, when on P and R branches, as pairs of lines with the same m'; nor recur in the same locations in bands of a progression.

Before using Eq. (1) to calculate the heat of dissociation of Na_2, it is necessary to decide whether or not it is more suitable for the purpose than the more recent and somewhat different equations which Fredrickson and Watson[12] have published for both the blue-green and the red systems. Their equations are as follows:

$$\text{Green } \nu = 20301.62 + (123.84n' - 0.79n'^2) - (157.57n'' - 0.57n''^2) \quad (2)$$

$$\text{Red } \nu = 15006.68 + (115.69n' - 0.427n'^2) - (157.81n'' - 0.538n''^2) \quad (3)$$

Frequencies calculated by (2) differ systematically from those of the magnetic rotation lines in Table I. The difference amounts to as much as 50 cm^{-1} for lines with large n''. Hence it is evident that (2) is quite inadequate to represent the magnetic rotation lines, particularly those with high quantum numbers; whereas column 8 shows that (1) is about as accurate as the data warrant.

Fig. 1 shows to what extent the three formulas for the term in n'' represent the absorption data of Fredrickson and Watson. The abscissa is n''. The circles represent the terms in n'', obtained, by subtraction, from their data on the green system, according to the equation

$$T''(n'') = \nu(n', 0) - \nu(n', n'') \quad (4)$$

[9] Loomis, Phys. Rev. **29**, 112 (1927).
[10] L.c. page 344.
[11] Fredrickson and Watson, Phys. Rev. **30**, 429 (1927).
[12] L.c., page 430.

The crosses represent $T''(n'')$ obtained, in the same way, from their data on the red system. The magnetic rotation data are omitted to avoid confusing the figure. The continuous curve represents $T''(n'')$ according to (2); the broken curve according to (3). In each case $T''(n'')$ according to (1), i.e.,

$$T''(n'') = 158.5n'' - 0.73n''^2 - 0.0027n''^3 \quad (5)$$

has been subtracted, for convenience in plotting. Hence the axis of abscissas represents $T''(n'')$ according to (1).

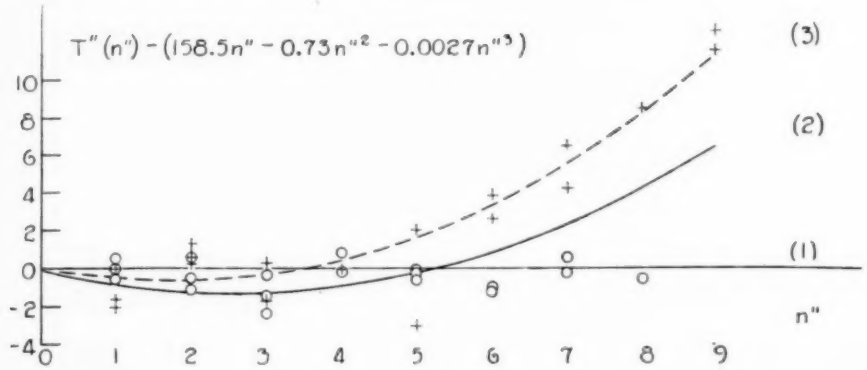

Fig. 1. Comparison of lower level terms, $T''(n'')$ from Fredrickson and Watson's absorption data for green and red systems with those from Eqs. (1), (2) and (3). Circles represent the green system, crosses the red system.

It will be seen that the Eq. (1) represents even Fredrickson and Watson's data on the green system rather better than their own Eq. (2); while it has been shown that Eq. (2) fails badly when extrapolated to cover the magnetic rotation lines of high quantum numbers. It is therefore certain that Eq. (1) is to be preferred as a basis for calculating the heat of dissociation.

It is a little surprising, however, to find that (1) does not represent their data for the red system; and, in fact, that it is impossible to represent $T''(n'')$ for both the green and red systems by the same formula within what appears to be the probable error of their measurements. One is forced to conclude, either that the two systems do not have a common lower level, or that ther is some systematic error in the frequencies of the bands, amounting to as much as 12 cm^{-1} in the extreme red.

The difference is in the wrong direction, and much too large, to be accounted for as due to the use of heads in place of origins. The writer inclines, however, to the belief that the lower levels in the two systems are really identical. Certainly, as is shown below, they both dissociate by vibration into unexcited atoms; and they have sensibly identical values of ω_0''. It is also shown below that Eq. (3) leads to seriously inconsistent estimates of the energies of dissociation. Moreover, the questionable red bands seem to lie anomalously on the intensity diagram.[13] Unfortunately

[13] Fredrickson and Watson, l.c., Table III.

no evidence is available from the red magnetic rotation spectrum, since it is so rich, and contains so many of the anomalous lines discussed above, that the writer has not yet been able to assign quantum numbers to it.

The heat of dissociation can now be calculated from Eq. (1) by the method of Birge and Sponer.[14] By differentiation one finds that the maximum of T'' occurs when $n''=76.3$. The corresponding value of T'' is: $T_{max}''=6644$ cm$^{-1}=0.82$ volt. The writer originally reported this as the heat of dissociation of the normal Na_2 molecule, but Professor Birge has kindly pointed out to him that a more accurate value is usually obtained by disregarding the cubic term in $T''(n'')$, since its effect is to some extent compensated by higher power terms of opposite sign. Moreover, it is likely that the true value lies somewhere between those obtained with and without the use of the cubic term. If the cubic term were disregarded, the calculated heat of dissociation would be $T_{max}''=8604$ cm$^{-1}=1.06$ volt. It is probably safe to conclude that the true heat of dissociation of the unexcited molecule is 1.0 ± 0.1 volt.

Proceeding in the same way with the upper level, for which only a quadratic formula is available, one finds that $T_{max}'=4586$ cm$^{-1}=0.57$ volt.

Since $\nu_0=20302$ cm$^{-1}=2.50$ volt is accurately known, it follows that the excess of energy of the pair of atoms into which the upper level molecule dissociates, over those into which the lower level molecule dissociates, is given by $\nu_0+T_{max}'-T_{max}''=2.50+0.57-1.0=2.07$ volt. Now the lowest excited levels of the sodium atom are the 3^2P, which are the initial states for the emission of the D lines and lie 16973 cm^{-1} and 16956 cm^{-1} or 2.10 volts above the normal level, 3^2S. The next level above 3^2P is 4^2S at 25743 cm$^{-1}=3.18$ volts. Since it has just been shown that the heat of dissociation of the lower level molecule is 1.0 ± 0.1 volt, it is clear, from considerations of stability, that it dissociates into two normal (3^2S) atoms. Inasmuch as an error of over one volt in the above estimate of $\nu_0+T_{max}'-T_{max}''$ is out of the question, there is no other possibility than that the upper level molecule dissociates into one normal (3^2S) atom and one atom in a 3^2P state. Having settled this point, it is possible to set $\nu_0+T_{max}'-T_{max}''=2.10$ volt, the accurately known energy of excitation of the D lines, and to combine it with the above values, $\nu_0=2.50$ volt, $T_{max}'=0.57$ volt, to obtain an independent estimate of the heat of dissociation, $T_{max}''=0.97$ volt. The closeness with which this agrees with the above estimate is probably partly accidental.

It remains to consider the red system. According to Fredrickson and Watson's Eq. (3), $\nu_0=15007$ cm$^{-1}=1.85$ volt; $T_{max}'=7838$ cm$^{-1}=0.97$ volt,[15] $T_{max}''=11570$ cm$^{-1}=1.43$ volt; $\nu_0+T_{max}'-T_{max}''=1.4$ volt. If, however, it is assumed that the lower levels of both red and green systems are identical,

[14] Birge and Sponer, Phys. Rev. **28**, 259 (1926).

[15] The writer finds that $T'(n')=114.94n'-0.353n'^2$ corresponds to most of Fredrickson and Watson's absorption data rather more closely than does Eq. (3). The resulting value of T'_{max} is 9360cm$^{-1}=1.16$ volt, which agrees well with the indirectly and independently calculated value, 1.25 volt.

the much more accurate value of $T_{max}'' = 1.0 \pm 0.1$ volt is available. Combining this with $\nu_0 + T_{max}'$ from Eq. (3) one obtains $\nu_0 + T_{max}' - T_{max}'' = 1.8$ volt. In either case the arguments applied to the green system hold here with even greater force, and show that, in the red system also, the lower level molecule dissociates into normal 3^2S atoms and the upper level molecule into one normal 3^2S and one in a 3^2P state. Hence $\nu_0 + T_{max}' - T_{max}'' = 2.10$ volt, accurately as in the green system. Assuming the lower levels of the two systems to be identical and hence that $T_{max}'' = 1.0$ volt, one obtains $T_{max}' = 1.25 \pm 0.1$ volt. That is, the molecules in the upper state of the red system, although they have a smaller ω_0', and are therefore to be thought of as less tightly bound, than those in the upper state of the green system,

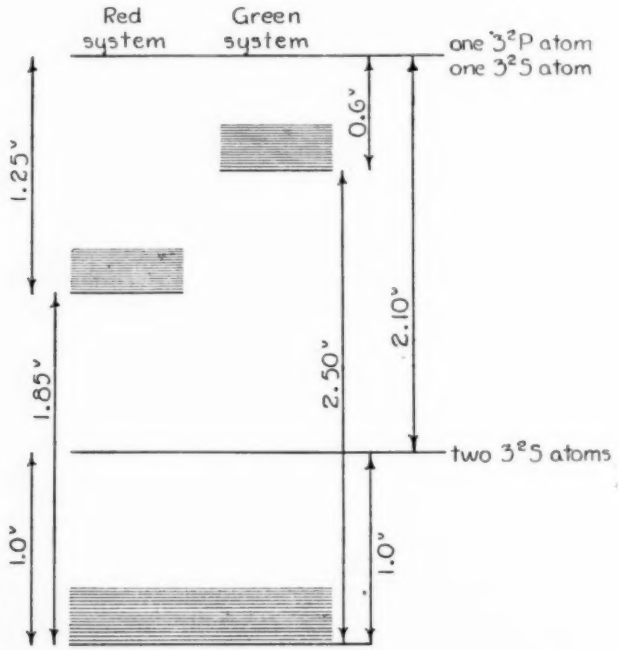

Fig. 2. Vibrational energy levels in the red and green systems.

nevertheless require much more energy to effect dissociation. No conceivable revision of the above figures could affect this conclusion. The assumption that the two lower levels are different and that T_{max}'' is to be taken from (3) as 1.43 volt, would make the T_{max}' for the red system even greater. The above results are summarized in Fig. 2.

In Fig. 3 the intensities of all the magnetic rotation lines in Table I are indicated in the circles opposite the appropriate values of n' and n''. It will be seen that the lines arrange themselves into a well developed parabola-like figure, of a type which Condon[16] has recently explained in terms of an hypothesis of Franck. Indeed, the likeness of Fig. 3 to that given by Condon

[16] Condon, Phys. Rev. **28**, 1182 (1926).

for CO is very striking. Both are of the wide open type which, on Condon's theory, corresponds to an electronic transition which results in a rather large change of moment of inertia. This signifies that the band heads are near the origins and helps to justify the assumptions on which the present analysis is based.

Fig. 3 also affords as explanation of an interesting phenomenon which Wood has reported. When light from a monochromator is used to excite fluorescence, the effect of varying the frequency of the exciting light is shown

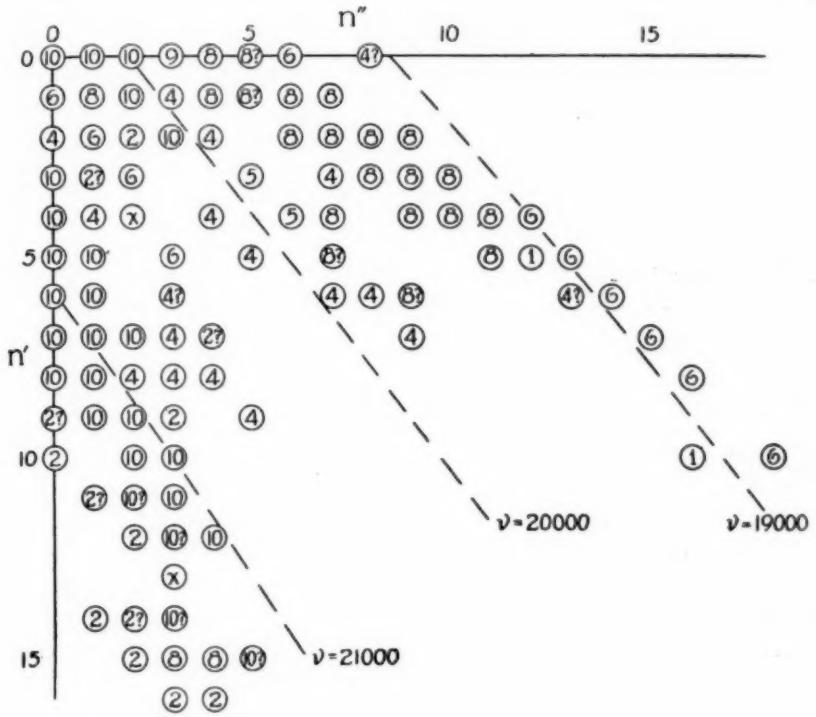

Fig. 3. Intensities in the blue-green magnetic rotation spectrum.

in Fig. 4.[17] It will be seen that when the exciting light, indicated by the double arrow, is in the blue, there are two patches of fluorescent light; one in the blue, the other in the yellow-green. As the wave-length of the exciting light is increased, the two patches move together, and finally fuse. The bluer region always includes the exciting light. By reference to Fig. 3, on which the spectral regions are indicated by the sloping lines, it will be seen that the blue light excites molecules having low n'' and lifts them to high values of n'. When these molecules emit the fluorescent light they may either return to their original n'', or one near it, corresponding to the left arm of the parabola, in which case the fluorescent light will be in the blue, near the exciting light; or they may fall back to a much higher value of n'',

[17] R. W. Wood, Proc. Am. Acad. **42**, Fig. 6c, 235 (1906).

corresponding to the same n' but on the right arm of the parabola, and then the fluorescent light will be in the yellow-green. As the patch of exciting light moves toward lower frequencies, successively lower values of n' will occur and the patches of fluorescent light corresponding to the arms of the parabola will move together and finally fuse at the vertex.

The knowledge of the vibrational energy levels in the lower electronic state makes it possible to plot the fluorescence series excited by various bright line sources, in a way very much like that used for iodine. In many cases the

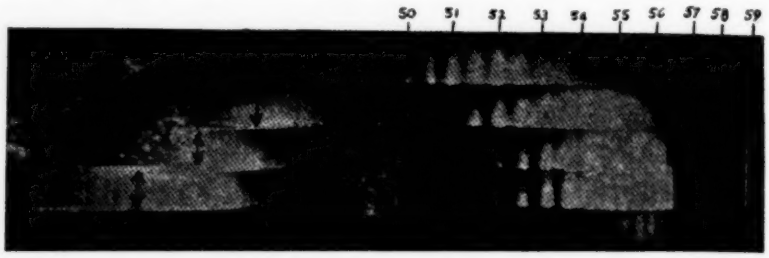

Fig. 4. Effect of varying frequency of exciting light, on intensity distribution of fluorescence. From Wood, Proc. Am. Acad. **40**, 235 (1906) Fig. 6c.

wave-lengths are not accurately enough known, and the possible exciting lines are too numerous, to make unambiguous arrangement into fluorescence series possible. There are, however, enough clear cases to make it evident that there are both singlet and doublet series, with the singlet series predominating. There seem to be no triplet series. Consequently the emission or absorption spectrum must consist of P, Q and R branches, but the initial state for emission of the O branch must be different from that for the P and R branches.

NEW YORK UNIVERSITY,
December, 1927.

CENTRAL FIELDS AND RYDBERG FORMULAS IN WAVE MECHANICS

By J. C. Slater

Abstract

The analogy in wave mechanics is set up for the non-penetrating part of the electron orbits on the older theory, in which the motion of the outer electron is like that in the field of a point charge. The Rydberg formula follows from this as in the older theory. The separate Rydberg series for the various multiplets also are explained. The method previously applied by the writer to the helium problem appears as a next approximation, in which the outer electron moves, not in a hydrogen-like field, but in a somewhat more accurate central field. It is shown that this method should give a good approximation to the energy levels, and also to the wave function, except at very small distances. The attempt to use this function as a starting point for perturbation calculations is shown, however, not to be justified, for the matrix of the Hamiltonian function H, which is used in the perturbation method, greatly magnifies the errors in the wave function. Suggestions are made as to the next step in improving the method, by increasing the accuracy of the wave function for small r's.

IN A recent note[1] the writer described a method for calculating the spectra of atoms, by setting up a central field, and finding the wave function for an electron moving in that field. This was applied to helium with gratifying results. Independently Sugiura[2] has used essentially the same method, and has obtained very similar values. As was stated in the earlier paper, the method yields a set of unperturbed wave functions which, it was supposed, formed fairly good approximations to the truth; and it was hoped to use these to find a further approximation to the energy levels, by letting the Hamiltonian funtion H operate on them, and integrating. This has been done, with a good deal of labor on account of the fact that most of the work must be done numerically or in series development; and the results are disappointing. The average of H over the orbit comes out much farther from the observed energy than the original values found by the central field method directly. In searching for an explanation of this fact, and for a method of overcoming the difficulties that presented themselves, a number of results of general interest have emerged, which apply to other atoms than helium. While these results are not particularly remarkable, they help in visualizing and understanding the problem of finding wave functions of atoms, and seem worth presenting. They relate principally to the fact that the wave functions of atoms must be interpreted in configuration space rather than three dimensional space.

1. In the older quantum theory, a valence electron, when at a distance from its core, described an orbit essentially like that in an inverse square

[1] J. C. Slater, Proc. Nat. Acad. Sci., **13**, 423 (1927).
[2] Y. Sugiura, Zeits. f. Phys., **44**, 190 (1927).

field. Bohr made this the foundation of his theory of spectra, in which the spectrum of hydrogen points the way at every step. We ask, what is the analogue to this in wave mechanics?

In answering, we first note that in wave mechanics there is no clear distinction between the valence electron and any other. In wave functions which are symmetric or anti-symmetric in the electrons, each electron acts as a valence electron for an equal fraction of the time; in other cases (as, for example, in the ordinary spectrum of lithium[3]) the situation is similar, though more complicated. Any electron acts as a valence electron, in the simple cases, when it is far from the nucleus and all other electrons are close up. This limits us to a restricted region of configuration space, and we may expect to find an analogue to the hydrogen-like part of the orbits in the older theory, in any such region. For the simple case of helium, we may visualize this in a schematic way by plotting two coordinates, representing the distances of the two electrons from the nucleus, r_1 and r_2, as in Fig. 1.

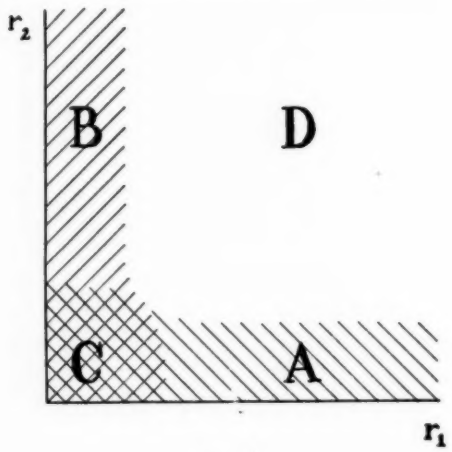

Fig. 1.

The part of this schematic configuration space where we may expect hydrogen-like orbits is divided into two parts, A and B, in the figure, one with r_1 large and r_2 small, the other with r_2 large and r_1 small. In the region C, on the other hand, both electrons are near the nucleus; this is the region described in the older theory as that where the valence electron penetrates the core; but now the electrons both have the same standing in this region, so that we cannot say that one is the valence electron, the other the ionic one. Finally, the region D where both electrons are far from the core is one that has had but little attention; it is unimportant for most practical purposes because of the small value of the wave function there. In more complicated atoms, the situation is less easy to visualize; but we shall always have a hydrogen-like situation when we go out in configuration space along any one of the r axes.

[3] A. Unsold, Ann. der Phys. **82**, 355 (1927). E. Wigner, Zeits. f. Phys. **40**, 492 and 885 (1927).

It is easy to show on wave mechanics that the wave function in a region where one r is large, the others small, really does show a hydrogen-like form as far as the electron with large r is concerned. The wave equation of an atom with nuclear charge Ze, and n electrons, may be written

$$-H\psi=\left[\sum_{i=1}^{n}\nabla_i^2+\frac{2Z}{r_i}-\sum_{j=i+1}^{n}\frac{2}{r_{ij}}\right]\psi=-E\psi, \tag{1}$$

if the r's are measured in terms of a_0, the radius of the first Bohr orbit of hydrogen (this introduces the factor 2 in the potential energy) and if the energy is measured in terms of Rh. We are interested in the region where one r, say r_1, is large, but the others small. Rewriting (1) as

$$\left[\nabla_1^2+\frac{2Z}{r_1}-\sum_{j=2}^{n}\frac{2}{r_{1j}}+\sum_{i=2}^{n}\left(\nabla_i^2+\frac{2Z}{r_i}-\sum_{j=i+1}^{n}\frac{2}{r_{ij}}\right)\right]\psi=-E\psi, \tag{2}$$

we note that in the region in which we are interested, the r_{1j}'s will all be approximately equal to r_1, so that the equation may be approximately replaced by

$$\left[\nabla_1^2+\frac{2(Z-n+1)}{r_1}+\sum_{i=2}^{n}\left(\nabla_i^2+\frac{2Z}{r_i}-\sum_{j=i+1}^{n}\frac{2}{r_{ij}}\right)\right]\psi=-E\psi.$$

In this modified equation, the variables may be separated; we write $\psi=v(x_1y_1z_1)u(x_2y_2z_2,\ \ldots\ ,x_ny_nz_n)$. Then we have the separate equations

$$\left[\nabla_1^2+\frac{2(Z-n+1)}{r_1}+\alpha\right]v=0, \tag{3}$$

$$\left[\sum_{i=2}^{n}\left(\nabla_i^2+\frac{2Z}{r_i}-\sum_{j=i+1}^{n}\frac{2}{r_{ij}}\right)+\beta\right]u=0\ ;\quad \alpha+\beta=E.$$

The first is the equation for the motion of an electron in a hydrogen-like field of charge $Z-n+1$; the second is the equation for the ion. The wave function is the product of the two, indicating in this limit a hydrogen-like electron, and an ion, not influencing each other except for the shielding by the ion; and the energy is the sum of the ionic energy, and the energy of the valence electron.

2. Bohr explained the Rydberg formula by making but two assumptions about the motion of the valence electron: first, that it moves in essentially a Coulomb field when at a distance from the ion, so that its orbit outside the core is essentially a Kepler ellipse; second, that all orbits of the same azimuthal quantum number were almost identical in the penetrating part. Applying this quantum condition, he had $nh=\int_i pdq+\int_o pdq$, where $\int_i$ represents the integration over the inner part of the orbit, which is the same for all terms of a series and $\int_o$ is the integral over the Keplerian part of the orbits, and hence is to a good approximation equal to $h/(-E)^{1/2}$, where E is the energy of the Kepler ellipse, measured in terms of Rh. Thus we have $E=-1/[n-\int_i pdq/h]^2$, a Rydberg formula.

Essentially the same proof can be carried through in wave mechanics. We have already seen the analogue to the first postulate: when one r is

large compared with the others, the wave function is the product of the wave function of a hydrogen problem, and that of the ion. The second postulate also has its analogue: when all the r's are small (C, in Figure 1), the wave function is essentially dependent only on the azimuthal quantum number except for the normalization constant, which is unimportant for the moment. Comparison with the hydrogen wave function for small r's will convince us of this: there the function for azimuthal quantum number k starts off from the origin as r^k, quite independent of the total quantum number.

In following Bohr's argument, we next must apply the analogue to the quantum condition; that is, we must impose the boundary condition that the wave function be finite everywhere. This condition must be applied to a composite wave function of this nature: for all r's small, we take the correct wave function, of which we know only that it is dependent mostly on the azumuthal, not on the total, quantum number; and for any r large, the others small, we take the product of a function of the coordinates of the distant electron which is a solution of the hydrogen equation, and a function of the other coordinates which represents an ion composed of the remaining electrons. For the region where several r's are large, we need make no assumption. The boundary conditions are now (1) that the correct wave function for small r's be finite at the origin, which is automatically satisfied; (2) that each of the hydrogen-like wave functions be zero at infinity, so that the wave function will go to zero as we pass out along any r axis (if we do this, it will undoubtedly go to zero when several r's become infinite together); and (3) that the two sets of wave functions join onto each other as smoothly as possible at the edge of the ion. The conditions on the solution of the hydrogen-like wave problem are thus not those that lead to the hydrogen energy levels; they are rather that the function be finite at infinity, but that it join smoothly onto a known function at a given point, say $r=r_0$. This condition is of the nature of the well-known cases met, for example, in heat flow and vibration problems, [4] $f'(r_0)=\text{constant}\times f(r_0)$. We shall show in the next section that the characteristic numbers of such a problem are not given by $-1/n^2$, $n=1, 2, \ldots$, but approximately by $-1/(n-c)^2$, $n=1, 2, \ldots$. Thus we have again a Rydberg formula.

(3) For our boundary value problem, we are required to find a solution of the hydrogen equation from (3), subject to the condition that the function be zero at infinity, and that it reduce to given values on the surfaces of a sphere of radius r_0 (we may imagine the function in ordinary three dimensional space). Now the general solution of the hydrogen-like problem (3), for a given α, subject only to the condition of single-valuedness, is

$$v_\alpha = \sum_{k,m} C_{k,m} R_{\alpha,k}(r) P_m{}^k(\cos\theta) e^{im\phi},$$

where $R_{\alpha,k}(r)$ is a solution of the equation

$$\left(\frac{1}{r^2}\frac{d}{dr}\left(r^2\frac{d}{dr}\right)+\frac{2(Z-n+1)}{r}-\frac{k(k+1)}{r^2}+\alpha\right)R_{\alpha,k}(r)=0.$$

[4] See, for example, Courant-Hilbert, p. 234.

To fit arbitrary boundary conditions on a sphere, with such a solution and a single value of α, would in general be impossible, since the range of k is limited when α is determined, so that we have only a finite number of functions of the angles at our disposal. We infer, however, from the physics of the problem, that the actual situation is more restricted than this. Empirically, in a simple spectrum (one with but one valence electron outside a closed shell or an S state), the system of quantum numbers is just as in hydrogen (neglecting the electron spin). Thus we infer that the wave function in such a case, at large r, is not merely hydrogen-like, but corresponds to a single term, with a single value of k and m. In a complex spectrum, on the other hand (two or more electrons excited to states other than s states), we know empirically that the electrons still show the properties that indicate that their k's are as in a simple spectrum. Their m's however, no longer have independent meaning; their place is taken, say in atoms with two electrons, by two new quantum numbers; viz., the m of the whole atom, and the quantized vector sum of the k's of the two electrons. We are to infer from this that the perturbations in a complex atom, when the two electrons act on each other, demand for their description not single spherical harmonics of the coordinates of the outer electron, but different zero order unperturbed functions, consisting of linear combinations of the terms, of nature $\sum_m C_m P^k{}_m(\cos\theta)e^{im\phi}$, the coefficients being determined by the standard procedure for finding the correct unperturbed wave functions in a problem of degeneracy. In either of these cases, the simple nature of the wave function at a distance must be reflected in simple boundary conditions on the sphere of radius r_0. We infer then that the boundary conditions are, for a simple spectrum,

$$v(r_0\theta\phi) = f(r_0)P_m{}^k(\cos\theta)e^{im\phi}$$

$$\frac{dv}{dr}(r_0\theta\phi) = f'(r_0)P_m{}^k(\cos\theta)e^{im\phi},$$

and for a complex spectrum

$$v(r_0\theta\phi) = f(r_0)\sum_m C_m P_m{}^k(\cos\theta)e^{im\phi}$$

$$\frac{dv}{dr}(r_0\theta\phi) = f'(r_0)\sum_m C_m P_m{}^k(\cos\theta)e^{im\phi},$$

where k is a fixed integer in either, and m is in the first case. These simple forms of boundary conditions would, of course, be expected to follow from the correct wave functions for small r's, if we could determine them.

The boundary condition at $r = r_0$ now becomes simply $f(r_0) = R_{\alpha,k}(r_0)$, $f'(r_0) = R'_{\alpha,k}(r_0)$, either for simple or complex spectra. Thus we must determine a function $R_{\alpha,k}(r)$ which has a definite value and slope at r_0, and which, in addition, is zero when r is infinite. Returning to the equation for $R_{\alpha,k}(r)$, we see that it has a doubly infinite set of solutions from its two arbitrary constants coming from the fact that it is a second order equation; regarding α as arbitrary also, we have the three adjustable constants needed to satisfy the boundary conditions.

To investigate the values of α determined by these conditions, we first impose the condition at infinity, without that at r_0. Then all values of α are still allowed; but for each α a definite value of $R'_{\alpha,k}(r_0)/R_{\alpha,k}(r_0)$, which we shall call $F(\alpha)$, is determined. We may plot $y=F(\alpha)$ as a function of α or, more conveniently, as a function of $1/(-\alpha)^{1/2}$. On the same graph, we also plot the line $y=f'(r_0)/f(r_0)$, which will be a straight line parallel to the axis of abscissae; each intersection of the two curves will then give a possible value of α. Having determined these α's, we still have one constant at our disposal, a constant factor, by which we give $R_{\alpha,k}(r_0)$ its proper value.

As a first step in the investigation of the function $F(\alpha)$, we consider $R_{\alpha,k}(r)$ itself. If $1/(-\alpha)^{1/2}=n$, an integer, R will be the familiar Laguerre orthogonal function, which, neglecting the normalization factor, and taking for the sake of simplicity the special case of the unit charge on the nucleus, has the following expansion about the origin:

$$R_{\alpha,k}(r)=r^k\{1-r(k+1)^{-1}+r^2[1+(k+1)/2n^2](k+1)^{-1}(2k+3)^{-1}+\cdots\}.$$

It is obvious that, for small r_0's, the function will depend only slightly on n; as $1/(-\alpha)^{1/2}$ comes to each successive integer, the function $R(r_0)$ will come back almost exactly to the same value. Between the integral values, however, the expansion in power series in r is impossible; for the function becomes infinite at the origin as soon as $1/(-\alpha)^{1/2}$ departs from an integer (since we are imposing the condition that it be zero at infinity, for any α). Considering R as a function of r, and letting $1/(-\alpha)^{1/2}$ increase uniformly, the general effect will be that the curve will shift toward greater values of r. New nodes appear infinitely close to $r=0$, and move outward; and this process is repeated almost periodically, when $1/(-\alpha)^{1/2}$ increases by unity. This continuous flow of the function will result in an almost periodic fluctuation of its value at r_0; for each increase of $1/(-\alpha)^{1/2}$ by unity, one node will cross r_0, and the function will pass through a half period of its fluctuation. Thus, very roughly, $R_{\alpha,k}(r_0)$ resembles $A\cos(\pi/(-\alpha)^{1/2}+c)$. To a similar approximation, $R'_{\alpha,k}(r_0)$ resembles $B\sin(\pi/(-\alpha)^{1/2}+c)$: for R' also fluctuates periodically as $1/(-\alpha)^{1/2}$ increases, but is maximum when $R=0$, zero when R is maximum. Thus roughly the function resembles $C\tan(\pi/(-\alpha)^{1/2}+c)$. It becomes infinite once in each unit interval of $1/(-\alpha)^{1/2}$ (at the point where a node is at r_0); in between these points, the function passes through all values between $-\infty$ and $+\infty$. Thus the solution of the equation $F(\alpha)=f'(r_0)/f(r_0)$ determines an infinite number of values of $1/(-\alpha)^{1/2}$, one lying between each integral value; and, since the function is almost periodic in $1/(-\alpha)^{1/2}$, the roots $1/(-\alpha_n)^{1/2}$ will differ almost by integers: $1/(-\alpha_n)^{1/2}=$almost $(n-d)$, $n=$integer, $d=$constant. Thus, approximately, $\alpha_n=-1/(n-d)^{1/2}$ which is a Rydberg formula.

4. The existence of multiplets is not so naturally described by Bohr's method as the simple spectra. The general interpretation of multiplets in wave mechanics has of course been given, but it is of interest to see how they fit into the scheme we have described. The essential point is that terms of different multiplicities have essentially different wave functions in the regions

of small r's; these result in different boundary conditions at the edge of the ion; and hence the different multiplets fall into different Rydberg series. In considering the question more in detail, we first note, of course, that different multiplets are connected with wave functions which have different symmetry relations. We take helium as an example. The singlets of helium are symmetrical in the two electrons, the triplets antisymmetric. This gains a very simple interpretation from Figure 1. The wave function as plotted in the schematic diagram is symmetrical about the 45° line for singlets, and antisymmetric for triplets. Thus the 45° line becomes a node of the triplets. This suggests a further inquiry into the positions of the nodes in configuration space. They are easy to locate in the regions corresponding to A and B, but it seems impossible to find by general considerations anything about their behavior in the region D.

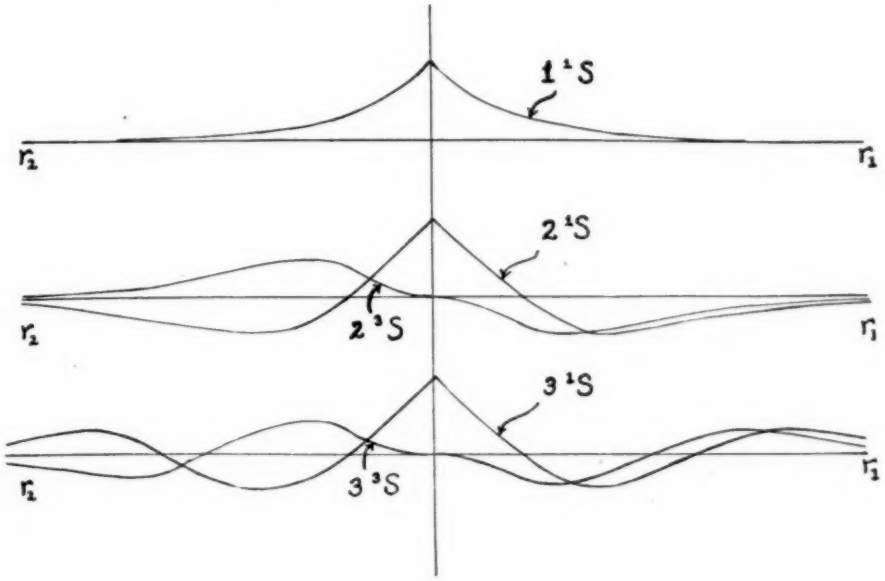

Fig. 2.

There is another instructive way of plotting the wave function, to see the symmetry relations. We may consider the value of the function along the r_1 and r_2 axes. If we plot the r_1 axis to the right from the origin, the r_2 axis to the left, then the wave function can be plotted as an ordinary function of one variable. In Fig. 2, we show this function schematically for several energy levels. In this sort of plot, the symmetry or antisymmetry of the function is made very graphic. Also, the number of nodes exhibited in this way increases by unity going from one energy level to the next higher, as in the one dimensional case. Finally, we see more plainly from it than in any other way just the relation of the singlet and triplet states to the central field method. The triplet state of a given total quantum number has a wave function which, at the edge of the ion, is like the singlet function, only shifted toward the nucleus. To find a hydrogen-like function to join onto this, for

large r's, we must take one corresponding to a tighter binding than for the singlet, since increased tightness of binding shifts the nodes toward the nucleus, and consequently the rest of the function with them. Thus we see that the triplets lie below the singlets. The contrast between the two functions for small r's, leading to the different boundary conditions, is most striking; while the wave function of the singlet S terms is large inside the ion, that of the triplet S is very small all through the ion. This curious fact might easily have interesting applications, for example in collisions problems.

5. We have seen how the qualitative properties of spectra can be described in terms of the simple hydrogen-like sort of wave function when one r becomes large. For quantitative purposes, however, this method is very crude; the function ceases to be hydrogen-like when still a very considerable distance from the core. We shall examine the inaccuracies in this approximate solution uv (see (3)) of the wave equation, as r_1 becomes small. It is readily found that

$$-H(uv)=\left[-(\alpha+\beta)+\frac{2(n-1)}{r_1}-\sum_{j=2}^{n}\frac{2}{r_{1j}}\right]uv.$$

When r_1 is so large, and the other r's so small, that the last two terms cancel, we have a correct solution; for small r's, however, the operator does not transform uv into a constant times itself, but into a function of the r's times itself. We can roughly estimate the error of the wave function by seeing how much this function departs from constancy, in the region we are interested in (r_1 moderately large, the other r's of the order of magnitude of the ionic radius). Then the r_{1j}'s can depart from r_1 by terms of the order of the ionic radius R, so that we have $r_{1j}=r_1\pm\lambda R$, where λ is of the order of unity. Hence $2/r_{1j}=2(1\mp\lambda_j R/r_1)/r_1$ approximately, and

$$\sum_{i=2}^{n}-\frac{2}{r_{1j}}+\frac{2(n-1)}{r_1}=\sum_{i=2}^{n}2\lambda_j\frac{R}{r_1^2} \qquad \text{(approximately).}$$

The errors thus increase, with decreasing r_1, with the inverse square of the distance, and increase with the first power of the ionic radius R.

In seeking a more accurate wave function, we are led to the method of setting up fields used in the previous paper. Fixing our attention on equation (2), we ask first for a solution of the problem

$$\left[\frac{2Z}{r_1}-\sum_{j=2}^{n}\frac{2}{r_{1j}}+\sum_{i=2}^{n}\left(\nabla_i^2+\frac{2Z}{r_i}-\sum_{j=i+1}^{n}\frac{2}{r_{ij}}\right)\right]u=-\epsilon(r_1)u,$$

where $\epsilon(r_1)$, which takes the place of an energy level, is a function of the parameter r_1, and where the boundary condition on u is that it be finite everywhere. If this can be solved, we then solve the equation $[\nabla_1^2-\epsilon(r_1)]v=-\eta v$. We assume for the moment (as we did in the previous paper, and as Sugiura does), that we impose on v the boundary conditions of being finite at infinity and at zero. We take the quantity uv as an approximate wave function. We readily find that

$$-H(uv)=-\eta uv+\text{grad}_1 u\cdot\text{grad}_1 v+v\Delta_1^2 u.$$

In the limit of large r_1, u approaches the wave function of the free ion, and hence becomes independent of the coordinates of subscript 1. Thus in this limit, the last two terms drop out, so that the wave equation is satisfied by uv, with η as a characteristic number. For smaller r_1's, we can show in particular cases at least that $H(uv)$ is more nearly a constant times uv than in the previous approximation. For the problem of helium, the ion problem for determining u becomes the problem of an electron in the field of two coulomb centers. This can be solved in inverse powers of r_1, though unfortunately the series have not a large range of convergence, and the expansion of u, regarding r_1 as large and r_2 as small, commences with the terms $e^{-2r_2-r_2(r_1-r_{12})/4r_1^2}-\cdots$. The first term of the exponent, which alone is present when r_1 becomes sufficiently great, is just the term for the helium ion alone. The next is of order R^2/r_1^2 (where as before R represents a distance of the order of the radius of the ion). When we carry out the differentiation, we find $\text{grad}_1 u \cdot \text{grad}_1 v = \text{constant} \times r_2(r_1-r_{12})uv/r_1^3$ or of the order of $R^2/r_1^3 uv$. The Laplacian is of higher order. Thus we see that the wave function gives an $H(uv)$ which departs from a constant multiplied by uv, by a term R^2/r_1^3, against R/r_1^2 in the previous case. This is a better representation both on account of the small function R, and the large one r_1 in the denominator. Thus we make a real gain in satisfying the differential equation at large distances by this procedure.

6. When this method is actually applied to helium, two principal results are apparent. The values of η are good approximations to the actual energy levels; but the wave functions depart in some region from their true values, for the integrals of H over them are nowhere near the correct energy levels (in the S states, at least). In the light of what we have seen, these facts are to be interpreted in the following way: The wave functions uv are at a distance good approximations to the true functions; for small r's, however, they depart from the truth. As we shall see in a moment, H operating on them, and integrated over the region of small r's, is so far from what it should be that it leads to the error observed in these integrals, and accounts for the failure of the attempt to find the energy to a higher approximation. This incorrectness appears conspicuously, however, only in the differentiation to produce H; it is not large enough in the functions themselves so that the boundary conditions on v which were used (finiteness at zero) and the correct boundary condition (that the function join smoothly to the correct wave function at the edge of the ion) are appreciably different. Thus the values of η do not have any large errors. In the P and D states, where v is small all through the ion, this is particularly true.

We can investigate the errors of the wave function for small r's by expanding u and v in powers of the r's; we find, for all r's small, that $u = e^{-2r_2+r_{12}\cdots}$, and, for S states, $v = e^{-2r_1\cdots}$. These give $uv = e^{-2(r_1+r_2)+r_{12}\cdots}$. On the other hand,

$$-He^{-2(r_1+r_2)+r_{12}} = (2/r_{12}+\cdots)e^{-2(r_1+r_2)+r_{12}}.$$

Thus when r_{12} becomes equal to zero, the differential equation ceases completely to be satisfied by our function uv. It is found that the term $2/r_{12}$ is just the one which, when integrated, gives the incorrect value to our averages of H. It can be easily shown, however, that the correct wave function for the S states should approach $e^{-2(r_1+r_2)+r_{12}/2}$ at small r's; when H operates on this, the result is in terms of zero order in the r's, which never depart very greatly from the proper energy value.[5] As we mentioned in the previous paragraph, this function and uv are not very different, although H operating on them gives very different results. The differentiation enhances the errors.

7. From the experience gained in the calculations on helium described in the preceding section, and from the general results of the present paper, we may draw several conclusions regarding practical methods of calculating the structure of atoms on wave mechanics. Almost any method of setting up approximate wave functions will give fairly good results in the non-penetrating part of the orbit; and it is this part that is of almost complete importance in many practical applications that demand knowledge of the wave function, such as transition probabilities, polarizibility, etc. The operator H, almost alone among the operators of physical interest, puts a severe strain on the most inaccurate part of the wave function, that connected with the penetrating part of the orbit, on account of the differentiations and the factors $1/r$ that it contains. For this reason, a wave function which is decidedly satisfactory for most physical applications may give a very inaccurate matrix of H. Yet it is just this matrix that is used in the perturbation method for solving the atomic structure problem. It seems necessary to conclude from this that the perturbation method is not a satisfactory one for actual calculations.

The only other method of calculation with fair hope of success (except perhaps the Ritz method,[6] which suffers severely from its lack of physical simplicity), seems to be that suggested by the present writer and by Sugiura. This system certainly gives wave functions which, in the physically important range, are close to the true ones. Further, in determining energy values, it has by its nature an essential advantage over the method of perturbations. For it sets up a wave function which obeys the wave equation more and more closely as we go further and further from the nucleus; and it really determines the energy values as the asymptotic values approached by the ratio $H\psi/\psi$ with increasing r's. Thus the energy levels are determined by the most accurate part of the wave function, rather than, as in the method of perturbations, primarily by the most inaccurate part. The only

[5] This simple function is apparently a rather good approximation to the true wave function for the normal state, all over the region where its values are large. Thus, H averaged over it equals $(4+1.71)$, in terms of the Rydberg constant; while the correct value is 4 (for the ionic energy) $+1.807$ (for the ionization potential of normal helium). This is nearly as close an approximation as those obtained by other methods. For Li^+ and other ions, the corresponding functions seem even closer. It is quite likely that this function would be useful in practical applications.

[6] Kellner, Zeits. f. Phys., **44**, 91 and 110 (1927).

way in which the wave function for small r's is concerned is in determining the boundary conditions at the edge of the ion. This can be determined with fair accuracy by a wave function which is really rather incorrect within the ion; and in addition, the wave function at a distance is not very sensitive to small inaccuracies in the boundary conditions. From these arguments, the success of the method in finding energy levels seems quite natural.

To improve the accuracy of our method, then, we must not seek to use it as a starting point for a perturbation calculation; we must simply improve the various assumptions which go into it. The present paper suggests that the next essential step is to find a somewhat more accurate solution for the wave function inside the ion, so as to get better boundary values for the central-field wave function, and use these instead of the plainly incorrect, but not very inaccurate, boundary conditions of the previous paper. This, among other things, will certainly bring the various multiplets (singlets and triplets for helium) correctly into the scheme. As a suggestion for finding this more accurate solution for small r's, the approximate wave function of note 5 seems to point the way. When these more accurate energy levels have been obtained, we can be quite sure that the wave functions found from the central field with the resulting boundary conditions will be close enough approximations to the truth to be of great value in dealing with atomic and molecular problems.

The writer wishes to express his thanks to Dr. J. R. Oppenheimer for valuable discussions on the subject of this paper.

JEFFERSON PHYSICAL LABORATORY,
CAMBRIDGE, MASS.
December, 1927.

NOTE ON HEISENBERG'S INDETERMINATION PRINCIPLE

By E. H. Kennard

Abstract

The *indetermination principle* of Heisenberg is discussed and applied to cases where position and velocity of an electron are observed by allowing it to pass through shutters opened momentarily at known times. The principle requires that such a shutter shall change the speed of the electron in a manner that can only be predicted statistically, in the same way as the frequency of a light quantum passing through such a shutter must usually undergo alteration to correspond with the Fourier resolution of the finite train of waves that gets through while the shutter is open. This effect is small and hard to detect experimentally.

A PAPER[1] read before the American Physical Society by E. A. Ruark suggests that it may be interesting to discuss in somewhat greater detail one or two simple applications of what that author aptly calls Heisenberg's Indetermination Principle.[2] In order to make the matter entirely clear it seems best to begin with a careful statement and explanation of the principle itself. As slightly modified[3] by the present writer, it can be stated as follows:

Two canonically conjugate quantities, such as a coordinate and the correlated momentum, cannot simultaneously be assigned approximately exact physically observable values; if α, β *are the measures of indetermination of the two quantities, then* $\alpha\beta \geqq h/2\pi$. (By measure of indetermination is meant the square root of twice the mean square of departure from the arithmetic mean).

In the case of a coordinate and its momentum the emphasis rests here especially upon the words "simultaneously" and "physically observable." The observation of position is theoretically simple: to locate an electron, for instance, at a time t, we can allow two quanta of light to rebound from it approximately simultaneously and then to pass through two microscopes pointed along different lines at the electron; Heisenberg suggests that unlimited precision in this measurement is, in principle, obtainable by using super-γ-rays of indefinitely short wave-length. By "the value" of a coordinate at a given time as a physically observable quantity is meant the result of such a measurement; such a definition was really implicit even in the classical theory. According to the new theory only a probability curve can usually be assigned for the result that would be, or would have been, yielded by such a measurement at a time t and so for "the value" of the coordinate at that time.

If we turn now to the measurement of velocity we encounter an essential difficulty in fixing the time to which the measurement refers. Suppose, for instance, we wish to measure the velocity of an electron moving in a space

[1] E. A. Ruark, Phys. Rev. **31**, 311 (1928).
[2] W. Heisenberg, Zeits. f. Physik **43**, 172 (1927).
[3] E. H. Kennard, Zeitz. f. Physik **44**, 326 (1927).

free from electric or magnetic field. Heisenberg suggests that we might allow several light-quanta to rebound from it and calculate the velocity from the Doppler effect on their frequency. But to do this with high precision we should have to pass them through a grating or equivalent instrument of high resolving power; we should then have no way of knowing through which slit of the grating the quanta actually passed and, since the optical paths are necessarily unequal for different slits, we should not know very closely at what instant the quanta rebounded from the electron. This indefiniteness in the time is proportional to the resolving power of the grating and so to the precision obtained in the value of the velocity; in the ideal case of infinite precision the indefiniteness of the time becomes infinite.

Similar considerations apply to the simple mechanical method discussed by Ruark, in which the electron is made to pass through two holes placed a known distance apart and opened momentarily at known instants of time. Here indefinitely small holes cannot be employed because of a peculiar "rapid-shutter effect" described below, which would introduce an instrumental variation into the result; we must therefore use large holes placed far apart and the time to which the resulting value for the velocity refers is then again to a large degree indeterminate.

The writer is inclined toward the view that the "interval" of time required for such a measurement really represents physically, with respect to the quantity being measured, only a single "instant." Several other data, at instants which are separate relative to other quantities, may also be obtained during this same "interval;" the first measurement, for which the instant is a single one, is then "physically simultaneous" with all of the others. Perhaps we have here at last, although in a rather unexpected form, the atomism of time predicted long ago by Poincaré.

Whether this view be adopted or not, we can define the "velocity of a particle at an instant t" as the result that would be, or would have been, obtained from an exact measurement occurring or at least beginning at the time t. For this purpose it is necessary that the particle be free from forces. According to Heisenberg we can always imagine the forces to be abolished at any moment to permit of such a measurement; but the physical significance of this assumption has never seemed quite clear to the writer—an alternative view would be that we ought rather to regard the velocity or momentum of a particle in a force-field as incapable of exact physical definition, but this latter view will not be adopted here.

The Indetermination Principle now asserts that we cannot predict with unlimited accuracy the results of precise measurements, to be made at (or to begin at) a given instant, of a coordinate or of the corresponding momentum; nor can we make a similar statement as to what would have been observed at a past instant. We can only assign probability curves for these two alternative results. Nor can it ever be possible to execute both measurements with unlimited precision simultaneously, for then such a statement as to the past would become possible. As here stated the principle refers primarily to the "statistical situation" determined by the experimental conditions and by

our knowledge of them; in Heisenberg's original paper great emphasis was laid upon the errors of a simultaneous observation of both quantities, but the "error" of an observation has no physical meaning unless we can give a meaning to the "true" value from which the observed value differs, and the definition of the true value must already involve the characteristic indetermination.

With this preliminary discussion in mind, let us now consider the application of the Principle to the statistical situation created when an electron leaving one plate of a charged condenser passes through a very small hole in the other plate into a space free from electric and magnetic force; let the hole be closed by a shutter which is opened momentarily for an interval τ at time t_1. Then at time t_1 we know the position of the electron with a certain accuracy, that is, we can predict within certain limits the result of a precise determination of its position at time t_1; and by decreasing τ we can diminish the uncertainty in this prediction *ad libitum*.

Suppose now we try to predict the result of an exact measurement of its velocity after passing through the hole. The classical answer is: $mv^2/2 = eV$ (V = potential difference between the plates), and this relation can be made to yield v with any desired precision. Ruark points out in explanation that the hole and shutter are themselves only statistical aggregates of atoms and concludes that our knowledge of the position of the electron at time t_1 is thereby limited. But this answer does not seem obviously adequate, for we could experiment at absolute zero to get rid of thermal agitation, and it would seem that points in space could then be distinguished with any degree of precision by employing sufficiently elaborate indirect methods, perhaps of statistical character. In any case, if I have understood Professors Bohr and Heisenberg correctly in conversation, they find the solution of such cases in the *wave properties* of electronic motion.

In the parallel case of a monochromatic light-quantum passing through a slit opened momentarily by a shutter the train of waves that gets through is of limited length and represents therefore a spectral region of finite width as found by Fourier analysis. A light-quantum must therefore usually suffer a change of frequency upon passing through such a slit, presumably because of some hitherto unknown interaction with the shutter, the change being sometimes an increase and sometimes a decrease in frequency according to a probability curve that can be calculated from the result of the Fourier resolution.

In a similar way, it is postulated by Bohr that a *particle* passing through a small hole opened momentarily by a shutter suffers in general a change of momentum, which is determined only statistically in accordance with the requirements of the wave theory. This assumption has definite physical meaning, for the velocity might be measured with any accuracy first before and then after the passage through the hole. In the case just considered, the velocity of approach (assumed small relative to the speed of light) is v_0, where $eV = mv_0^2/2$, and may be assumed to be very accurately known; the frequency of the deBroglie waves is then $\nu = mv_0^2/2h$, the number of waves that get

through is $\nu\tau$, and the mean relative variation of their spectral frequency is $1/2\nu\tau$. The mean variation in the momentum of the electron after issuing from the hole (as would be found experimentally from many repetitions of the experiment) is thus $mv_0/2\nu\tau$ or $h/v_0\tau$. The indefiniteness in its position, on the other hand, is of order $v_0\tau$. Thus the product of the two degrees of indetermination is of order h. This change in momentum can be avoided only by enlarging the hole or decreasing the shutter speed so as to make τ large.

This "rapid-shutter" effect upon electronic speed will not be particularly easy to detect by experiment. The wave-length accompanying an electron whose speed v is small relative to that of light is (in cm):

$$\lambda = h/mv = h(2emV)^{-1/2} = 7.2/v = 1.22\times10^{-7}\times V_0^{-1/2}$$

where V_0 = "equivalent volts." Thus even 0.01 volt electrons would have a wave-length of only 1.22×10^{-6} cm. The number of waves getting through in time τ is $N=\nu\tau$ where $\nu = mv^2/2h$, so that

$$\tau = 2N(m/h)\lambda^2 = 0.276N\lambda^2.$$

Thus even if $N=10^6$ and $\lambda=10^{-6}$ (0.01 volt electrons), $\tau=0.3\times10^{-6}$ sec., so that the dispersion of velocity by a shutter will be hard to detect.

Up to this point we have been discussing the statistical situation, as defined in terms of precise observations that might be made. The condenser and hole can, however, also be regarded as an instrument for "observing" simultaneously, with limited precision, both the position and velocity of the electron. In conclusion let us consider such a double observation that might be made upon the electron after leaving the hole.

To measure its velocity we can pass it through an instrument consisting of two more holes equipped with shutters which are opened momentarily in succession. From the known statistical situation and the law of the shutter-effect we can calculate a probability curve for the result of the observation just mentioned, and the relation between this curve and the curve representing the statistical situation will then be an indication of the degree of precision of our instrument; if the statistical situation is so simplified (for instance, by enlarging the hole in the condenser plate) as to reduce its curve sensibly to a single ordinate, then the curve for our instrument reduces to the ordinary curve showing the error-spread of observations.

Our instrument also measures position with a certain accuracy. To improve it in this respect one might be tempted to add a separate determination of the position of the electron at a time t_2, either with γ-ray microscopes or by means of a third hole and shutter placed between the other two; the other holes being then placed far apart for high precision in the velocity. But either type of position measurement disturbs the velocity, the γ-ray observation because of the Compton recoil-effect, the third hole because of the rapid-shutter effect. From no point of view can the observed velocity obtained under these conditions be regarded as the single true physically

observable velocity at the instant t_2 at which the position is known; from the writer's point of view, involving a partial atomism of time, the reason is that the measurements of velocity and position are physically simultaneous no matter what the ratio of the distances from the third hole to the outer two holes, whereas the value obtained for the velocity will depend upon this ratio. This variation in the observed velocity and the variation in the observed position, when the experiment is repeated many times, are easily shown to obey the fundamental inequality $\alpha\beta \geqq h/2\pi$ whatever the statistical situation may be. We have thus a simple application of the Indetermination Principle to the physical precision of simultaneous measurements of two canonically conjugate quantities.

CORNELL UNIVERSITY,
December 29, 1927.

ON THE QUANTUM THEORY OF THE CAPTURE OF ELECTRONS

By J. R. Oppenheimer*

Abstract

In Section 1 the method of a previous paper[1] is applied to find the rate at which α particles capture electrons from atoms. The mean free path for capture varies roughly with the sixth power of the velocity of the α particle, and in good agreement with Rutherford's experiments.[3] The value of the mean free path is computed for capture in air, and agrees with the experimental value.

In Section 2 the probability of radiative recombination of electrons and protons is computed. The cross section for recombination becomes infinite for small relative velocities with the inverse square of the velocity; for high velocities it is given by $10^{-18}W^{-5/2}$, where W is the energy in volts of the incident electrons.

IN THE collision of an α-particle with an atom, one of the atomic electrons will occasionally be captured by the passing particle. In this capture the electron jumps from one bound orbit to another; and the energy difference in the binding is taken up in the relative translational energy of the two heavy particles. The initial and final states have the same energy; but the wave functions representing them are not strictly orthogonal, since it is possible, though not very likely, that the electron, although "bound" to the atom, be found in the immediate neighborhood of the α-particle. If one writes out the scalar product of the initial and final wave functions, e.g., for hydrogen,

$$\epsilon = \int d\tau \psi_{H} \psi_{He^{++}} \psi_{H^{+}}^{*} \psi_{He^{+}}^{*} \qquad (1)$$

where the integral is to be taken over the configuration space, one sees that, for large relative velocities, this becomes very small.[2] The capture thus corresponds to a transition between almost orthogonal states of the same energy, and may be treated by the methods of ref. 1. For this one needs the form of the wave function in the initial state; we shall carry through the calculation for a hydrogen-like atom with arbitrary nuclear charge, and shall consider, subsequently, how, and with what error, this may be applied.

This capture of electrons has been studied both experimentally[3] and theoretically.[4] Our theory will give directly the mean free path for capture as a function of the velocity of the α-particle and the constants of the atom. This has been observed for a considerable range of velocities in air, and will give the most direct check on the theory.

Fowler's theory[4] of the capture is based on considerations radically different from those of this paper. Fowler observes that the loss of the captured

* National Research Fellow.

[1] J. R. Oppenheimer, Phys. Rev., Jan. 1928, Section 3. Referred to as ref. 1.

[2] For this the wave functions must be normalized to dE/h. Cf. ref. 1, Eq. 3.

[3] E. Rutherford, Phil. Mag. **47**, 277, 1924. Hdb. d. Physik, xxiv, 177 (1927).

[4] R. H. Fowler, Phil Mag. **47**, 269, and 416 (1924).

electron of the α-particle may be regarded as a process of ionization by collision with one of the atomic electrons. (We shall adduce evidence that the process of loss is not precisely of this kind, but that is here irrelevant). The reverse process to this is a three body collision: two electrons strike the α-particle; one of them is captured, and the other carries off the excess energy. If now one imagines the electrons to form a gas at the temperature appropriate to the velocity of the α-particles, and assumes that the system is in thermodynamic equilibrium at this temperature, one may use the principle of detailed balancing to compute the probability of capture from the probability of loss by ionization; and this latter probability is approximately known from the classical formulae of Bohr. Fowler has carried through the calculations on this basis. They yield, with certain not very unreasonable assumptions, a satisfactory account of the experiments on the ratio of the number of α-particles with a captured electron to the number of bare α-particles in a beam that has been passed through a film of metal.

The theoretical objection to this calculation is that it completely neglects the rôle of the nuclei, and ascribes to the electrons a velocity relative to each other, and relative to the nuclei, which they have not in fact. We shall see later that encounters in which two electrons take part play an unimportant part in the process of capture. Empirically[3] this is confirmed by the fact that the experiments seem to demand a probability of capture proportional to the first power, and not the square, of the electron density. Fowler's formulae may also be applied, with a slight modification, to the evaluation of the mean free path for capture in air. They give results which do not agree nearly as well as those of the present theory with the experiments, and which seem definitely unsatisfactory.

We shall first compute the first order cross section[5] for capture into the normal state by an α-particle of mass M, charge $2e$, and velocity $\boldsymbol{V}$, for an atom with a single electron of mass m, charge $-e$, and with a nucleus of mass qM, and charge Ze. If we eliminate the motion of the center of gravity of the system as a whole, we may describe the relative motion in terms of the vector $\boldsymbol{R}$ from the center of gravity of the electron and α-particle to the nucleus, and the vector $\boldsymbol{r}$ from this same center of gravity to the electron. The wave function for the initial state, representing a unit stream of α-particles per unit area, is then[6]

$$(2\overline{M}/Kha^3)^{1/2}e^{i(\boldsymbol{K}\cdot\boldsymbol{R})+i\kappa(\boldsymbol{r}\cdot\boldsymbol{R})/R-|\boldsymbol{R}-\boldsymbol{r}|/a} \tag{2}$$

with

$$a=h^2/4\pi^2\mu Ze^2\ ; \qquad \mu=mqM/(m+qM)\ ; \qquad \overline{M}=M^2q/[m+(1+q)M]$$
$$\kappa=2\pi\mu V/h \qquad\qquad \boldsymbol{K}=2\pi\overline{M}\boldsymbol{V}/h. \tag{3}$$

[5] The probability of capture has the dimensions of an area because the initial wave function (2) is normalized to make the incident flux per unit *area* per unit time unity. $\sigma\cdot\lambda=[H]$.

[6] The first two exponential factors give the translational motion of the atom and α-particle; the third gives the motion in the normal state of the atom of the electron about the center of gravity of the atom; the factor is chosen to make the flux of incident α-particles one per unit area per unit time.

The wave function for a final state, with a relative velocity of nucleus and Helium ion $\boldsymbol{V}'$, is

$$1/2(\overline{M}K'/ha_0{}^3\pi^3)^{1/2}e^{i(K'R)-2r/a_0} \tag{4}$$

with

$$a_0=h^2/4\pi^2\mu e^2\ ;\ \boldsymbol{K}'=2\pi\overline{M}\boldsymbol{V}'/h.$$

This is normalized[7] to $dvd\omega$, where $E=h\nu$ is the total energy of the final state, and $d\omega$ is the element of solid angle of the unit vector $\boldsymbol{s}=\boldsymbol{V}'/V'$. The perturbing energy for the capture is the interaction energy of the α-particle and electron:

$$H_1=(-2e^2/r)(\mu/m). \tag{6}$$

The matrix component of this which conserves the energy has a velocity $\boldsymbol{V}_1$:

$$\boldsymbol{V}'=\boldsymbol{V}_1\ ;\quad V^2-V_1{}^2=(h^2/4\pi^2\mu\overline{M})(1/a^2-4/a_0{}^2), \tag{7}$$

and is a function of the direction of $\boldsymbol{V}_1$, or of the vector $\boldsymbol{s}$:

$$H_1(\mathbf{s})=(\overline{M}e^2K_1/ka_0{}^3\pi K')(2z^3/\pi)^{1/2}\int d\boldsymbol{R}$$

$$\int d\boldsymbol{r}/r\cdot e^{i[(K\cdot R)-(K_1R_1)-s(rR)/R]-[2r+|R-r|)]/a}. \tag{8}$$

If we expand the $|R-r|$ in the exponent for small r/R we get

$$H_1(S)=2^{11/2}\pi^{1/2}Z^{-3/2}a_0{}^2\overline{M}e^2(K_1/hK)$$
$$\{4-(Z-ia_0\kappa)^2\}^{-1}\{1+a^2(|\boldsymbol{K}_1-\boldsymbol{K}|)^2\}^{-2}. \tag{9}$$

This gives for the first order cross section[8]

$$\sigma_0=4\pi^2/h^2\int|H_1(\mathbf{s})|^2d\omega=\frac{2^{13}\pi^4\overline{M}^2a_0{}^2e^4}{3h^4ZK^2[a_0{}^4\kappa^4+2(4+Z^2)a_0{}^2\kappa^2\cdots]}\cdot \tag{10}$$

We have now to consider the validity of certain of the approximations involved in this calculation. It was shown in ref. 1. that, if the matrix element of H_1 to some other final state—involving a transition which violates the conservation of energy—is much larger than that responsible for the first order effect, second order terms must be considered. The matrix elements of H_1 have maximum values for $\boldsymbol{V}'$ parallel to $\boldsymbol{V}$, and these values are sensibly independent of V'. In this case, therefore, the second order terms are negligible; and they may be shown, in fact, to vanish more rapidly than σ_0 with increasing V. This applies also to transitions to excited states in He^+.

In evaluating H_1 we have neglected the term $-2Ze^2/R$, which gives the interaction energy of the nucleus and the α-particle, and which gives rise to the Rutherford scattering. The contribution of this term to the probability

[7] Ref. 1, Section 1.
[8] Ref. 1, Section 3, Eq. 7.

of capture is only apparent, and arises from the fact that the wave function for the deflected α-particle and undisturbed atom is not quite orthogonal to that of the deflected α-particle with a captured electron. The contribution of this term to the cross section vanishes more rapidly than σ_0 with increasing V.

The electron may be caught into one of the excited states of He^+. The wave functions for these states corresponding to (4) are

$$(1/2\pi)\left\{\frac{\overline{M}K'(2k+1)(k-m)!(n-k-1)!}{2ha_0^3n^2(k+m)![(n+k)!]^3}\right\}^{1/2} e^{i(K\cdot R)-2r/na_0}$$
$$L_{n+k}^{(2k+1)}(4r/na_0)P_k^{(m)}(\cos\delta)e^{im\phi} \tag{11}$$

where n, k, m are the three quantum numbers of the He^+ orbit. If one uses (11) to estimate the probability of capture into the excited states, one finds that the contribution of states for which $k\neq 0$ vanishes more rapidly than σ_0 by a factor V^{-2}. The only important terms, for large V, for the states n, 0, 0, are those arising from the first term of the Laguerre polynomials. Each such state has a transition probability

$$\sigma_n=\frac{1}{n^3}\frac{2^{13}\pi^4\overline{M}^2a_0^2e^4}{3h^4ZK^2[a_0\kappa^4+2(4/n^2+Z^2)a_0^2\kappa^2\cdots]}. \tag{12}$$

For large V the total probability of capture thus becomes

$$\sigma=\sum_{n=2}^{\infty}\sigma_n+\sigma_0=\sum_{n=1}^{\infty}(1/n^3)\sigma_0=1.2\sigma_0. \tag{13}$$

In the evaluation of $H_1(\mathbf{s})$ the exponent $|\boldsymbol{r}-\boldsymbol{R}|$ was expanded:

$$|\boldsymbol{R}-\boldsymbol{r}|\sim R-(\boldsymbol{R}\cdot\boldsymbol{r})/R \tag{14}$$

The integral as it stands is difficult to evaluate, but we may control this approximation by setting

$$|\boldsymbol{R}-\boldsymbol{r}|=\begin{matrix}R-(\boldsymbol{R}\cdot\boldsymbol{r})/R \text{ For } R>r.\\ r-(\boldsymbol{R}\cdot\boldsymbol{r})/r \text{ For } R<r.\end{matrix} \tag{14a}$$

This introduces into the integral over $\boldsymbol{R}$ new terms of the form

$$\kappa^{-3}e^{-1/a_0[2\pm 1\pm ia_0\kappa]R}. \tag{15}$$

These vanish more rapidly for large V than the terms retained.

Part of the excess of energy of the electron in its initial state over that in its final state may be given off as spontaneous radiation; this may increase the probability of capture, in particular of capture into the normal state of He^+. The cross section for radiative capture is[8]

$$\sigma_r=\int d\omega\int_0^{\nu_0+\nu_1}d\nu(64\pi^4\nu^3/hc^3)|P(\bar{\nu},\mathbf{s})|^2;\quad h(\bar{\nu}-\nu)=h\nu_0=E_0 \tag{16}$$

where $\nu_1=(h^2/8\pi^2\mu a_0^2)(Z^2-4)$, and where $\boldsymbol{P}(\bar{\nu},\mathbf{s})$ is that component of the effective electric moment $-e\underline{r}$ of the system which corresponds to a transition to a state of energy $h\bar{\nu}$, and a direction of relative velocity given by the vector $\mathbf{s}$. The resulting matrix integrals differ from H_1 chiefly in having a factor r in place of $2e/r$; and this introduces a factor $\kappa^{-4}e^{-2}$ into the cross section. The ratio of σ_r to σ turns out[9] of the order of magnitude of

$$\sigma_r/\sigma=\nu_1{}^3h^2K/e^2a\overline{M}c^3\kappa^4. \tag{17}$$

For the range to which we shall apply our formulae this is about 10^{-7}. Stimulated radiative transfers do not occur.

These considerations give, for the mean cross section for capture in atomic hydrogen

$$\sigma=1.2\sigma_0=[2\times10^{-11}/W^2(W+135)] \tag{18}$$

where W is the equivalent electron voltage of the α-particle. This is valid only for velocities for which $50/W$ may be neglected.

For atomic hydrogen captures in which two electrons play a part can not occur. They may occur for other atoms, provided that the sum of the ionization potentials of the two electrons is less than the energy of binding in He^+. But the coupling between the electrons is not very great—compared with the coupling of each to the nucleus—and one may expect such captures to be of the same relative importance as double ionizations in the theory of ionization by collision. One cannot estimate this very accurately without a more detailed knowledge of the periodic and aperiodic wave functions for the atom in question. But Fowler's calculations offer a convenient upper limit, since they make encounters between electrons much more probable than they are in fact, and assume that any electron can absorb any quantum of energy. It will be seen that Fowler's formula gives a cross section for capture by double encounter only about 1/100th of that computed by (10). As has been observed, the probability of the simple capture depends very little on the energy to be taken up by the nucleus.

The most direct way, then, of adapting (18) to experiments on air is to neglect the interaction of the atomic electrons, and use, for the wave function of each electron, that of the normal state of a hydrogen-like atom with such a nuclear charge Z_n as gives the proper ionizing potential for the electron. This yields for λ_c, the mean free path for capture, in air at N.P.T.,

$$\lambda_c{}^{-1}=\Sigma_n(5.4\times10^8/Z_nW^2)\{W+2764+Z_n{}^2)\}^{-1}. \tag{19}$$

where the summation is to be taken over all the electrons of the "air molecule." The value of λ_c depends only slightly on the ionizing potentials.[10]

[9] To evaluate (16) one may use the property of the normalized wave functions for the motion of the ion: $\int d\omega\int d\nu\psi_{H^+}(\nu,\ \mathbf{s},\ \mathbf{R}')\psi_{H^+}{}^*(\nu,\ \mathbf{s},\ \mathbf{R}'')=\delta(\mathbf{R}'-\mathbf{R}'')$

[10] The oxygen molecule has twelve electrons with Z ranging from 1 to 1.7; and four with Z=7.5. The nitrogen molecule has ten electrons with Z ranging from 1.1 to 1.7; and four with Z=6.5. Cf. Hdb. d. Physik, xxiii, 756–760, 1926.

For comparison we may quote Fowler's result[11]:

$$\lambda_c^{-1}=2.7\times10^7\nu_\epsilon^2(e^2h/4\pi^2VW^2)\{W+104\}^{-1}. \tag{20}$$

Here ν_ϵ is the effective density for double encounters of "loosely bound" electrons. If N be the number of such electrons per molecule, and G be the volume of the molecule, we may set, for air at N.P.T.,

$$\nu\epsilon^2=2.7\times10^{19}N(N-1)/G\,;\quad N=10.4\,;\quad G=6\times10^{-23}.$$

The numerical values are given in Table I.

TABLE I

V (cm/sec)	λ_c(mm) computed (20)	λ_c(mm) observed (4)	λ_c(mm) computed (19)
(1.) 1.8×10^9	500	2.2	2.3
(2.) 0.9×10^9	4.4	0.037	0.039
(3.) 0.44×10^9	0.042	0.0008	0.0009
Ratio (1./2.)	115	59	57
Ratio (2./3.)	105	46	44

To apply (19) to find the relative concentrations of He^+ and He^{++} in a beam that has passed through air or metal, we must know the probability for the process of loss. There is some evidence that this is not a simple ionization by electron impact. In the first place, since the probability depends upon the square of the matrix component of the perturbing energy, the probability of ionization due to the nucleus should be Z^2 times that for the ionization due to an electron, whereas that due to all the electrons should be Z times that due to a single electron; for heavy atom the nucleus would thus be the more important. The second point is empirical. For the classical theory gives a probability of ionization which falls off with V^{-2}; and one may readily see by writing down the matrix elements that, for large velocities, the quantum mechanics gives this too; this has been established in detail by Elsasser.[12] But experimentally Rutherford finds that the mean free path for loss varies, in a range for which Bohr's formula should hold, as V^1. It may be shown that the ionization due to a colliding dipole falls off less rapidly with increasing V than that due to a simple charge; so that both discrepancies may be resolved by taking for the ionizing particle the core of the atom.

If one uses Bohr's formula for the rate of loss, the method of this section leads to reasonable values for the ratio of the concentrations of He^{++} and He^+. This ratio then varies as V^4, whereas Rutherford finds $V^{4.6}$.

2. The recombination spectrum for electrons and protons may be studied by canonical methods; and one may compute the cross section for re-

[11] Fowler, ref. 4, Eq. 11.

[12] I am indebted to Dr. Elsasser for informing me of his results.

combination from the known wave functions of the hydrogen atom.[13] For, in spite of the fact that the aperiodic wave functions approach those of free particles only when the distance between the particles r is held constant and their relative velocity V is increased indefinitely, and not when V is held constant and r is increased, one can write down an initial wave in terms of these wave functions which, for large r, represents a unit incident beam per unit area, moving with a velocity V in a given direction ($\cos\delta=0$). This turns out to be

$$\Psi_i=2\kappa^{-1}\pi^{1/2}\sum_{k'=0}^{\infty}(k'+1/2)\,i^{k'}\psi(\nu',k',0) \tag{1}$$

where $\psi(\nu',k',0)$ is the aperiodic wave function for the state $E=h\nu'=\frac{1}{2}mV^2$, orbital angular momentum k', and component of angular momentum parallel to the beam zero, taken real, and normalized to $d\nu'$. For the normal state the wave function is

$$\Psi(0,0,0)=(\pi a_0^3)^{-1/2}e^{-r/a_0}. \tag{2}$$

The interaction energy giving the spontaneous emission may be written

$$H_1=4\pi r(h\nu^3/3c^3)^{1/2} \tag{3}$$

where ν is the frequency of the emitted light. The cross section for radiative recombination to the normal state,

$$\sigma_0=4\pi^2/h^2\left|\int d\tau\;\Psi_i H_1\psi(0,0,0)\right| \tag{4}$$

thus becomes

$$\sigma_0=(2^7\pi e^2h/3m^2c^3g^2)e^{-(4/g)\tan^{-1}g}(1+g^2)^{-2}(1-e^{-2\pi/g})^{-1} \tag{5}$$

where g is the ratio of the initial translational energy of the electron to the energy of ionization of the hydrogen atom. For low velocities the cross section becomes infinite:

$$\sigma_0\sim(2^7\pi e^2h/3e_1^4m^2c^3)g^{-2}. \qquad e_1=2.718\cdots$$

For high velocities it is given by

$$\sigma_0\sim(64e^2h/3m^2c^3)g^{-5}. \tag{7}$$

The extension of (5) to recombination for excited states offers considerable arithmetic difficulties. For high velocities it is easy to modify (7) to take account of the excited states. For, for high velocities, the wave functions of the two body problem approach those for the free particles, and these latter become almost orthogonal to the periodic wave functions, and may be used to evaluate σ. For the initial wave function we may thus take

$$V^{-1/2}e^{i\kappa r\cos\delta}=\kappa^{-1}V^{-1/2}\sum_{k'=0}^{\infty}P_{k'}(\cos\delta)I_{k'}(\kappa r)=\Psi_0 \tag{8}$$

[13] Cf. J. R. Oppenheimer, Z. f. Physik, **41**, 268 (1927), Eqs. 46, 47, 29. Further Y. Sugiura, Journ. d. Physique, VI, **7**, 113 (1927) Eq. 15.

with

$$I_{k'}(\kappa r)=\pi i^{k'}\cdot(2k'+1)(2\kappa/r)^{1/2}J_{k'+1/2}(\kappa r)\,. \tag{9}$$

For that of the final state, with the electron bound in an n,k,m orbit, we have

$$\left\{\frac{(2k+1)(k-m)!(n-k-1)!}{\pi n^2 a_0{}^3(k+m)![(n+k)!]^3}\right\}^{1/2} e^{-r/na_0}L_{n+k}^{(2k+1)}(2r/na_0)$$
$$P_k^{(m)}(\cos\delta)e^{im\phi}=\psi(n,k,m). \tag{10}$$

The *total* cross section for recombination, σ, is then

$$\sigma=4\pi^2/h^2\sum_{n,k,m}\left|\int d\tau\psi_0 H_1\psi(n,k,m)\right|^2. \tag{11}$$

Now the selection rule gives $k-k'=\pm1$. With this limitation one may readily verify that the dominant terms for high V have $k=0$, $k'=1$, and that only the first *two* terms of the Laguerre polynomials corresponding to $k=0$ need be retained; all other terms vanish more rapidly with the velocity. Eq. (11) thus reduces to

$$\sigma=(64\pi^4\nu^3e^2/3ch)\sum_{n=1}^{\infty}(16\pi/a_0{}^3n^3V\kappa^2)\left|\int_0^{\infty}r^3drI_1(\kappa r)e^{-r/na_0}(1-(n-1)r/na_0)\right|^2 \tag{12}$$

This yields

$$\sigma=(2^6e^2h/3m^2c^3)g^{-5}\sum_{n=1}^{\infty}n^{-3}=\sigma_0\sum_{n=1}^{\infty}n^{-3} \tag{13}$$

or numerically

$$\sigma=10^{-18}W^{-5/2} \tag{14}$$

with W the electron voltage of the incident beam. For recombination with a bare nucleus of charge Z, σ must be multiplied by Z^5. For recombination from high velocities, and for recombination to the normal state for all velocities, the light emitted is polarized with its electric vector parallel to the electron beam.

JEFFERSON PHYSICAL LABORATORY,
CAMBRIDGE, MASSACHUSETTS,
December 1927.

COLLISIONS BETWEEN ELECTRONS AND GAS MOLECULES

By Irving Langmuir and Howard A. Jones

ABSTRACT

Using a simple method in which positive ion sheaths serve as perfect grids we have obtained data on the *probability of various types of collisions* occurring between Hg, H_2, N_2, He, Ne and A molecules and electrons of moderate velocity, i.e., 30–250 volts. A theory has been developed and the *mean angular deflection for elastic and inelastic collisions between electrons and gas molecules has been calculated.* Evidence on the mechanism of ionization is presented. The current densities of the various Maxwellian groups of electrons and the average temperatures of these groups are calculated from the data and are shown to be in good agreement with data obtained by us using Langmuir and Mott Smith's probe wire method. The *current density of positive ions* has been measured by both plane and probe wire collectors and the *space potential* both measured and calculated. The evidence in support of negative anode drops has been pointed out and the ions flowing to the anode measured separately by means of a perforated collector. The *maximum number of positive ions produced by an electron* with a given velocity before losing its ionizing power has been measured and shown to be independent of current density and pressure being dependent only on the velocity of the electron and the nature of the gas.

The *mean free path of high velocity electrons* (i.e., above the ionizing potential) for various types of collision can be evaluated from the probability data. The mean free path for inelastic impact has been calculated separately and independently of the reflection of electrons from the collectors. The *small angular scattering of electrons* is discussed in detail. Phenomena, similar to Langmuir's high speed electrons in mercury vapor, have been observed and the curves showing the energy transfer between primary electrons in H_2 and A are given. The *resonance and ionization potentials* observed in the work are also tabulated.

MOST quantitative experiments on the ionization of gases involve the use of a stream of electrons moving with homogeneous and definitely known velocity. For this purpose the electrons from a hot cathode are usually accelerated by a positively charged grid or perforated plate into a region which is made as nearly field-free as practicable. To avoid space charge effects and the resultant uncertainties in potential distribution it is necessary to work with very low currents, which usually involve electrometer measurements. Furthermore, the grids must be of very fine mesh or the perforations in the plate of small diameter to avoid transverse velocity components in the electron stream and to make the effective potential of the grid the same as its actual potential. The customary methods are thus not adapted to the study of certain phenomena which appear only when rather large current densities are employed. With the high intensity of ionization accompanying larger currents it becomes possible, however, to use quite different methods for studying ionization phenomena.

In apparatus of ordinary size and with potentials above 40 volts, electron currents of a few milliamperes cause such intense ionization and high electrical conductivity that the interior of a gas at low pressure necessarily

becomes nearly field free. The potential drop between cathode and anode is then largely confined to a thin layer or sheath covering the surface of the cathode in which there is a positive ion space charge. This sheath has a well defined outer edge beyond which the field of the cathode does not extend. The sheath thus acts as an ideal grid for accelerating the primary electrons from a cathode into a field-free region.

The presence of such a homogeneous beam of electrons may be detected by a small disk-shaped collector placed in the electron stream so that the electrons move normal to its surfaces. When the collector is at a negative potential with respect to the ionized gas it is covered by a positive ion sheath. It collects all the positive ions that reach the edge of the sheath and all the electrons (except those reflected at the collector surface) which have velocity components normal to the surface sufficient to carry them against the retarding field in the sheath.

Thus if the collector is at a potential below that of the cathode it will receive only positive ions, but as soon as its potential is higher than that of the cathode, the primary electrons, which have not lost momentum by collision or otherwise, will be able to pass through the sheath, and reach the collector. The current-voltage characteristic of the collector thus shows a break at the cathode potential. If, however, the collector is turned so that its plane is no longer perpendicular to the direction of propagation of the electrons, the collector potential will have to be raised above that of the cathode by an amount ΔE before primary electrons can be collected. This voltage displacement of the break ΔE is thus a measure of the transverse energy of the electrons, viz., the energy component parallel to the surface of the collector.

Apparatus and Method

Unless the dimensions of the collector are large compared to the thickness of the sheath, the sheath area will vary with the voltage, so that the interpretation of the current-voltage characteristic becomes more complicated. If the cathode is a straight filament the collector should be part of a cylindrical surface having the filament as axis in order that the primary electrons may impinge normally at all points of the collector surface. This suggests that the collector may advantageously be made a complete cylinder surrounding the filament and having a length equal to that of the filament. Such a tube is illustrated in Fig. 1 where F is the cathode filament, C is the coaxial cylinder which may be used to collect the primary electrons that reach it, A and B are end-plates which fit closely within the cylinder C and are provided at their centers with small holes through which the cathode filament passes.

In most cases one of the plates (A) is used as anode, its potential being sufficiently high to give strong ionization of the gas within the cylinder C. The electrons from the cathode are then accelerated in strictly radial directions within the cathode sheath, and at low gas pressures a fraction of these electrons reach the cylinder C with normal incidence after having traveled a definite distance through the gas.

The potential of the ionized gas is approximately that of the anode, and is, in fact, usually a couple of volts above it (negative anode drop). We shall see that at low pressures the mobility of the electrons is so high that the ionized gas constitutes a very satisfactory field-free region.

Any electrode which is at a potential below that of the ionized gas will be covered by a positive ion sheath. If C is a few volts negative (we shall take the negative end of the cathode as of zero potential) the primary electrons which move radially across the tube are retarded within the sheath on C, are brought to rest, and are driven out of the sheath again without having lost energy, and still moving in a radial direction. All the positive ions which diffuse to the edge of the sheath on C will be collected, and the positive ion

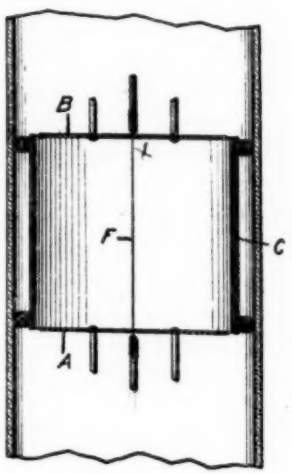

Fig. 1.

current is therefore independent[1,2] of the negative voltage on C. Illustrations of these constant currents may be seen in Figs. 2, 3, 4, etc., for negative voltages. In a similar way the plate B can be made negative and the positive ion current to this electrode measured. Thus by making corrections for the few ions collected by the filament (and by the anode), the total number of ions formed from a given number of primary electrons can be determined. One of the main objects of the investigations to be described in this paper has been to obtain quantitative data on the degree and nature of the ionization produced in a gas by a specified stream of primary electrons of known velocity. A tube of the type of Fig. 1 lends itself admirably to this purpose, not only because of its simple geometry, but also because of the fact that the ionized gas is completely enclosed[3] within metallic electrodes, any one of which may be used as a collector.

[1] Langmuir, Science **58**, 290 (1923).

[2] Langmuir, Gen. Electric Rev. **26**, 731 (1923).

[3] A short preliminary account of the methods of using a tube like that of Fig. 1 to study free paths and ionization phenomena in gases has been published by the present authors in Science **59**, 380 (1924).

If C is made slightly positive the retarding field in its sheath will no longer be able to stop the primary electrons, so that some of these will be collected, and a break in the current voltage curve occurs at the cathode potential (zero) (see Fig. 2). This current discontinuity affords a simple and accurate means of determining electron free paths. The current-voltage curve of the collector C at higher voltages gives data on the velocity distribution (and the distribution of directions of motion) of the various other groups of electrons. Comparisons between the curves obtained with C (Fig. 2) and with B (Fig. 3) as collectors are particularly useful in giving information regarding the directions of motion of the electrons. We can thus estimate the fraction of the primary electrons which make elastic collisions and we also find that practically none of these are scattered through angles as large as 90 degrees.

In a similar way, by analysis of such curves as those of Fig. 2, we find that a certain fraction of the electrons lose an energy corresponding to a resonance potential of the gas (6.7 volts in Fig. 2), but even these electrons are not deflected through large angles. The ionized gas also contains a large number of electrons which move in random directions with velocities distributed according to Maxwell's law.[4,5]

Particularly interesting results are obtainable with tubes like that of Fig. 1 by the use of longitudinal magnetic fields. With weak fields the electron paths are curved so that the electrons reach the cylinder with oblique incidence. The current-voltage curves obtained in this way give good data for measuring the number of electrons that make elastic collisions with gas molecules.

With strong magnetic fields the distribution of electrons and positive ions between two collectors C and B is entirely changed. This furnishes a valuable quantitative method of studying mobilities of electrons and ions. The intensity of ionization near the filament F, even at low pressures of gas, is then many times greater than at C so that relatively large positive ion currents flow to the cathode. This effect, however, is readily studied quantitatively by noting the increase in filament resistance caused by the heating effect of the positive ion bombardment.

Description of Typical Current-Voltage Characteristic Curves

The curves shown in Figs. 2, 3, and 4 were obtained with a tube like that of Fig. 1, in which the cylinder C was 3.1 cm in diameter and had an effective length of 3.8 cm (area 37.0 cm^2). The plates A and B were 3.0 cm in diameter (area 7.0 cm^2 each), and had holes 0.35 cm in diameter through which the filament (of 0.178 mm diameter) passed. To light the filament to a temperature at which 5 milliamperes of electrons were emitted required about 2.5 amperes and 3.3 volts. The electron emission was fairly uniform along the filament up to within about 5 mm of the ends of the filament and then

[4] Langmuir, Jour. Franklin Inst. **196,** 751 (1923).

[5] Langmuir and Mott-Smith, Jr. Gen. Electric Rev. **27,** 449, 538, 616, 762, 810 (1924). See also; Phys. Rev. **28,** 727, (1926) and Zeit. f. Physik, **46,** 271 (1927).

dropped off rapidly because of the cooling effect of the leads, which extended very close to the holes in the plates.

Curve A (Fig. 2) was obtained with mercury at a pressure of 25 baryes (51.5°C), while B corresponds to 102 baryes (75°C) of mercury vapor. The

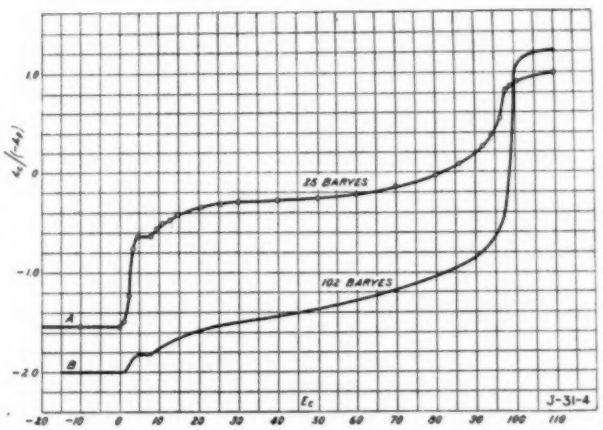

Fig. 2.

two plates A and B were connected together and were used as anode at 100 volts, while the potential of the cylinder C was varied and the current i_C was measured.[6] The filament F was heated by a storage battery and the current i_F of electrons emitted (and positive ions received) was measured

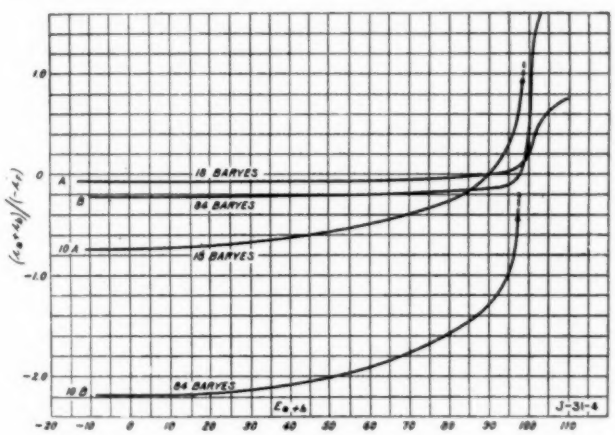

Fig. 3.

directly. This current was maintained at approximately -5 milliamperes. The ordinates in Fig. 2 represent the ratio $i_C/(-i_F)$ and the abscissas are

[6] We adopt the convention that the sign of the current to any electrode is that of the charged particles that it would have to emit in order to carry that current. Thus if F emits electrons or receives positive ions i_F is negative, while i_C is positive if C receives electrons and negative if it receives positive ions.

the collector potentials E_C. It was found in nearly all cases that for moderate variations in i_P the ratio $i_C/(-i_P)$ remained nearly constant.

The curves of Fig. 3 were obtained under similar conditions to those of Fig. 2, except that the functions of the two electrodes $(A+B)$ and C were interchanged. Thus the cylinder C was used as anode and was maintained at $+100$ volts, while the two plates A and B (connected together) were used as collector. The lower curves marked $10A$ and $10B$ are the same as the curves A and B except that the ordinates are multiplied by 10.

The data in Fig. 4 were obtained with argon at a pressure of 30 baryes. The plate A was used as anode at a potential of $+50$ volts, while B and C

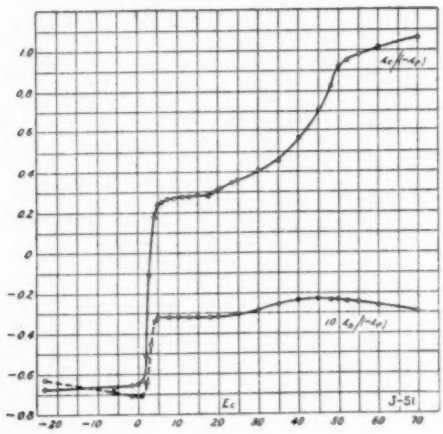

Fig. 4.

were used as collectors. The potential E_C of the cylinder was varied, but the plate B was maintained at a constant potential of -23 volts. The ordinates of the dotted curve representing the current i_B have been multiplied by 10.

Positive Ion Current Density I_P

The practically constant currents that are observed in Figs. 2, 3 and 4 when the collector is at negative potentials measure the rate at which ions diffuse to the edge of the sheath on the collector. These currents divided by the effective areas of the collectors give us a measure of the positive ion current densities I_P in the ionized gas. If the velocities of the positive ions are distributed according to Maxwell's laws corresponding to a temperature T_P, the number of ions per cm^3 can be calculated from the equation (reference 5, p. 455, Eq. (44))

$$n_p = 4.03 \times 10^{13} I_p (m_p/m T_p)^{1/2} \tag{1}$$

where m_P/m is the ratio of the mass of the ion and the electron, and I_P is to be measured in amps. per cm^2. From data which we shall discuss later we may assume T_P is roughly constant and equal to 3000°K, so we are able to estimate the intensity of ionization, i.e., the number of ions per cc, from measurements of the positive ion current densities.

In case the thickness of the positive ion sheath on a collector is appreciable, the effective area of the collector may be different from its actual area. Let us, therefore, determine the thickness of the sheaths in the examples we have cited. In general, the sheath thickness may be calculated from the space charge equations, and these values agree excellently with those obtained by direct visual observation of the dark space surrounding the collector (reference 5, pp. 545, 622). For electrodes having the small curvature of those we are now considering, the space charge equation for parallel planes is applicable:

$$I_p = 2.34 \times 10^{-6} (m/m_p)^{1/2} V^{3/2}/x^2 \qquad (2)$$

Here V represents the voltage drop through a sheath of thickness x (cm).

Table I contains a summary of the data on positive ion currents and sheath thickness from the curves of Figs. 2, 3, and 4. The first column refers to the number of the figure and the designation of the curve, and the second column gives the gas and its pressure in baryes.

TABLE I

Positive ion currents and sheath thicknesses. The currents i_F, I_B and I_C are in milliamperes. Data of Figs 2, 3 and 4.

1	2	3	4	5	6	7	8	9	10
Fig.	Gas	β_B	β_C	i_F	V	Sheath thickness x_B	x_C cm.	Positive current density I_B	I_C
2*A*	Hg 25	—	1.54	−5.4	105	—	0.19	—	0.256
2*B*	Hg 102	—	1.99	−6.3	105	—	0.16	—	0.375
3*A*	Hg 18	0.073*	—	−4.5	105	0.63	—	0.023	—
3*B*	Hg 84	0.218*	—	−5.5	105	0.33	—	0.086	—
4	A 30	0.071	0.65	−4.9	73	0.31	.022	0.054	0.112

* These values of β_B include the currents flowing to the electrode A which in this case was connected to B.

The sheath thicknesses in cm as calculated from Eq. (2) are given in columns 7 and 8. In the case of the data from Figs. 2 and 3 these thicknesses were calculated for an assumed collector potential of −5 volts, but for the data of Fig. 4, E_C was taken to be the same as E_B, which was kept at −23 volts. In columns 3 and 4 β_B and β_C are taken to represent the nearly constant values of $i_B/(-i_F)$ and $i_C/(-i_F)$ corresponding to the negative collector potentials.

The values of the positive ion current densities I_B and I_C in columns 9 and 10 were obtained by multiplying β_B or β_C by i_F (Column 5) and dividing by the areas of the sheaths on the collectors calculated from the values of x_B and x_C.

The intensity of ionization n_P as given by Eq. (1) may now be calculated from these values of I_P. For example, the value $I_C = 0.256$ ma. per cm^2 from the data of Fig. 2 corresponds to 1.1×10^{11} ions per cm^3 if we assume $T_P = 3000°$.

We see from the data of Fig. 4 in Table I that I_C is about twice I_B. This effect is caused by radial electric fields which accelerate the ions outwards. Since the rate of production of ions per unit volume near the filament is greater than near the cylinder, the concentration of ions must decrease as the distance from the filament increases. The electron concentrations must everywhere in the body of the gas be nearly equal to those of the positive ions, and as the electrons have high mobilities they will set up potential differences which are related to their concentrations according to the Boltzmann equation

$$n_1/n_2 = \epsilon^{Ve/kT} \tag{3}$$

where n_1 and n_2 are the electron concentrations in two regions, T is the temperature of the electrons, and V is the potential of the first region with respect to the second. The ratio e/k is equal to 11,600 degrees per volt. Thus if the positive ion space charge is neutralized principally by electrons having a temperature of 10,000° there will be a potential difference of 0.60 volt between two regions in which the positive ion concentrations differ in the ratio of 2 to 1. Since concentration differences of this order of magnitude are to be expected even at the lowest pressure[7] there must be radial potential differences of the order of one volt. The velocity of the ions in a radial direction will therefore be greater than in the direction of the cylinder axis, and this explains the fact that I_C is greater than I_B in Fig. 4.

Comparing the values of I_C from Fig. 2 (Table I) with those of I_B from Fig. 3, we find that the ratios in these cases range from 4 to 11. It must be noted, however, that the values of I_C were measured when $A+B$ was anode, while I_B was measured when C was anode. With C as anode a certain fraction (about 50 percent at 18 baryes) of the primary electrons were removed by this electrode, so that the total number of ions produced was less than if B or $A+B$ had been anode. However, allowing for this effect and for the differences in the pressures for the data of Figures 2 and 3, we find that the ion current densities at the cylinder are still 5 times (at 18 baryes) or 3 times at (at 84 baryes) greater than those at the plates. Experiments with mercury vapor with connections like those of Fig. 4 have given ratios I_C/I_B not exceeding 2, so we must conclude that the high values for this ratio in Figures 2 and 3 are an indication that the radial electric field is greater when C is anode than when an end plate is anode. This conclusion is in accord with our theory of the cause of the radial field, for when C is negative the primary electrons that are reflected back into the gas from the sheath on C produce ions near the surface of C. The removal of these primary electrons by making C anode lowers the concentration of ions near the cylinder relatively more than near the filament and thus increases the radial field.

[7] Direct measurements of the ion concentrations in a tube carrying an arc in mercury vapor at low pressures gave concentrations at the axis about 2 to 4 times greater than those at the wall. See loc. cit. (5) p. 769.

The currents flowing to negatively charged collectors are practically independent of the collector voltage according to the curves of Figures 2, 3, and 4. The dotted curve in Fig. 4, where the lower end of the curve shows a marked negative slope, corresponds to a case in which the current to the plate B is altered by changing the negative potential on the cylinder C. It was found, however, that if B and C were connected together so as to be at the same potential, the current to each electrode remained constant as the negative potential changed. The negative slope of $i_B/-i_F$ is very largely explained by considering the thicknesses of the sheaths on the electrodes. When the potential of C is changed from -23 to 0 volt (in Fig. 4), the sheath on C changes from 0.22 to 0.17 cm. This sheath on C partly covers the plate B and prevents positive ions from being collected near the edge of the plate. The effective diameter of the plate (actual diameter 3.1 cm) thus increases from 2.66 to 2.76 cm, as E_C changes from -23 to 0 volts.

The increase in area is 8 percent, while the positive ion current $(-i_B)$ increases about 14 percent. Thus the change in collecting area accounts for only part of the change.

At higher pressures, where the free paths of the electrons become small compared to the radius of the tube, the radial concentration gradient of ions is determined by diffusion.[8] With a given concentration of ions near the axis the rate of flow to the sheath on C should increase as the sheath increases in thickness because of the decreased distance through which diffusion occurs. With a given rate of production of ions near the axis, the concentration should therefore decrease as the sheath becomes thicker. This effect, together with the decreased collector area, probably explains the negative slope of the left hand part of the curve for i_B in Figure 4. It should be noted that the actual decrease in $i_B/(-i_F)$ from -23 to 0 volts is only 0.009, while the increase in $i_C/(-i_F)$ is 0.02.

Number of Ions Produced by Each Electron (β)

Since the ionized gas (Fig. 1) is completely surrounded by metallic electrodes at each of which the positive ion current density can be measured, we can determine the total number β of ions produced by each electron emitted from the cathode, assuming no recombination.

Let us express by β_A, β_B, etc., the ratio of the positive ion current at any electrode to the current i_F that flows from the filament. Then β_F gives the fraction of the current from F which is carried by the positive ions that strike the filament and $1-\beta_F$ is the fraction carried by electrons. If no recombination of ions and electrons occurs within the ionized gas the total ionization β per electron emitted is evidently

$$\beta=(\beta_A+\beta_B+\beta_C+\beta_F)/(1-\beta_F) \tag{4}$$

[8] Schottky and Issendorff, Zeits. f. Physik **31**, 163 (1925) have developed the mathematical theory of the diffusion of electrons and ions subject to the condition that the concentrations of the ions and the electrons shall everywhere be equal.

In experiments like that which gave Fig. 4 we measure β_B and β_C. The value of β_A corresponds to the positive ion current flowing to the anode. If, as is usually taken for granted, the anode were positively charged with respect to the space near it, we should place $\beta_A = 0$ since the ions would be repelled from the anode. But in general, where the anode is of large area and especially where the gas is strongly ionized by high velocity primary electrons from a hot cathode, the anode will be at a negative potential with respect to the ionized gas. Direct measurements of the space potential by small collectors near the anode have shown these negative anode drops (reference 5, page 767). Compton and Eckart,[9] following a suggestion of one of us, have demonstrated their existence in low voltage arcs at higher pressures.

A. F. Dittmer has suggested the use of plane collectors provided with one or more small round holes (of diameter small compared to the sheath on the collector) back of which is a Faraday cage or a second plate. By this arrangement the positive ions and electrons that pass through the holes can be separated. Measurements recently made by us with such a perforated collector have shown that it receives just as many positive ions when it is anode as when it is at a large negative potential.

We may therefore conclude that we should place $\beta_A = \beta_B$. The only remaining unknown quantity in Eq. 4 is β_F. This may be calculated from space charge equations with the degree of accuracy with which I_P in the neighborhood of the cathode may be estimated. Since β_F is usually very small, this method is often permissible. In further experiments now in progress β_F is being measured by the changes in resistance and in the electron emission of the filament due to the temperature rise that results from the positive ion bombardment.

If the positive ion current to F is limited by the rate at which positive ions reach the sheath surrounding the filament we may calculate β_F by the space charge equation

$$i_F\beta_F = 14.68\times10^{-6}L(m/m_p)^{1/2}V^{3/2}/r\beta_0^2 \tag{5}$$

where L is the length and r the radius of the filament, V is the voltage drop through the sheath of radius a, and β_0 is a function of a/r for which tables are available.[10] As we do not know a we cannot use this equation directly to obtain β_F, but since the outside surface of the sheath is the effective collecting area we may use the relation

$$i_F\beta_F = 2\pi aLI_p \tag{6}$$

and can then change Eq. (5) to the form

$$(a/r)\beta_0^2 = 2.34\times10^{-6}(m/m_p)^{1/2}V^{3/2}/(r^2I_p). \tag{7}$$

[9] K. T. Compton and Carl Eckart, Nature **114,** 51 (1924); Phys. Rev. **25,** 139 (1925). See also; Compton, Turner and McCurdy, Phys. Rev. **24,** 577 (1924).

[10] Langmuir and Blodgett, Phys. Rev. **22,** 347 (1923).

All the quantities of the right hand member are known. Thus by preparing a curve giving $(a/r)\beta_0^2$ as a function of a/r from Table III of paper in ref. 10 we may determine a and then by (6) can find β_F.

For the case of the experiment that gave Fig. 4 let us place (see Table I) $I_P = 1.12\times10^{-4}$ amps. per cm.[2] Putting $V=73$, $(m/m_P)^{1/2}=1/272$ and $r=0.0089$ cm we find by (7) that $(a/r)\beta_0^2$ is 605, which corresponds to $a/r=12$. Thus a, the radius of the sheath on the cathode, is 0.107 cm. If we take I_P near the axis of the tube to be twice as great, viz., 2.24×10^{-4}, we find $a/r=9.4$ and $a=0.084$ cm. By (6) we now calculated β_F, taking ($i_F=4.9$ ma.) $L=3.8$ and find for $I_P=1.12\times10^{-4}$, $\beta_F=0.058$, while for

$$I_p=2.24\times10^{-4},\ \beta_F=0.092.$$

When the radius of the sheath around a cylindrical collector is as great as 10 times that of the collector itself, the tangential components of the velocities of the ions when they enter the sheath may cause a considerable fraction of the ions to describe orbits about the collector and thus pass out of the opposite side of the sheath.

Under these conditions the current flowing to a collector of area A is

$$i=AI_pf \tag{8}$$

where f is a function of a/r, V and T_P, whose value approaches a/r when Ve/kT_P is less than $2(a/r)-2$ and approaches the value $2[(1+Ve/kT_P)/\pi]^{1/2}$ when a/r and T_P are sufficiently large.[11] For the case in hand we find the following values for f

I_p	$f(T_p=5000)$	$f(T_p=10000)$
1.12×10^{-4}	10.52	8.72
2.24×10^{-4}	8.95	7.88

We see that the radius of the sheath, which is proportional to f is comparatively little affected by doubling either I_P or T_P. Taking the higher value of I_P as the more probable, and choosing $f=8.4$, we find from Eq. (8) by placing $i_F=4.9$ m. amp., $A=0.212$ cm^2 and $i_F\beta_F=i$, the most probable value of β_F to be

$$\beta_F=0.081. \tag{9}$$

Inserting $\beta_C=0.67$, $\beta_A=\beta_B=0.062$ and $\beta_F=0.08$ in Eq. (4) gives us for the total ionization the value $\beta=0.95$. That is, in an experiment with argon at 30 baryes, each 50 volt electron produces 0.95 ion before losing its ionizing power.

If the conditions of the experiment are such that no recombination occurs, and all the primary electrons give up their energies to gas molecules before reaching the anode, we should expect β to be independent of pressure, the primary electron current and such geometrical factors as the diameter or length of the cylinder C.

[11] The complete expression for f is given in the G. E. Review article reference,[5] p. 454. A discussion and derivation of these equations has been given by Mott-Smith and Langmuir.[5]

Thus we can understand why it is, in experiments such as that of Fig. 2, that the positive ion current to the negatively charged cylinder is so nearly independent of the potential of the cylinder even when the sheath thickness varies considerably. If the number of ions per cc in the gas remained constant, the current to C should be proportional to the diameter of the sheath, so that the voltage-current curve would have a negative slope for negative cylinder voltages. But if β remains constant and if the current i_A is small compared to i_C, i_C must also be constant, and therefore the intensity of ionization of the gas must increase as the sheath on the cylinder becomes thicker. This effect is due to the reflection of the electrons from the sheath edge, which increases the primary electron current density and makes the rate of ionization per unit volume inversely proportional to the volume.

When A and C are connected together the fact that the curves for i_A and i_C are flat (for negative voltages) is explained by the constancy of β. In the data of Fig. 4, where E_B was kept constant while E_C was varied, we have seen that the negative slope of i_B was about equal to the positive slope of i_C. This is a result of the constancy of β.

Primary Electrons Which Reach the Cylinder C.

If the cylinder C is brought to a positive potential the retarding field is no longer able to prevent primary electrons from reaching it. At pressures low enough for an appreciable fraction γ of the primary electrons to reach the collector C without having collided with atoms, there is thus an abrupt change Δ_C in the value of $i_C/-i_F$ when the potential E_C is raised from negative to positive values. In Fig. 2 we see for mercury vapor at 25 baryes that Δ_C is 0.90, while with a pressure of 102 baryes Δ_C is only 0.18, indicating that as the pressure increases a larger fraction of the electrons from the cathode lose energy by collision.

The change Δ_C is due to two factors: (1) the electrons taken up by C and (2) the decrease in the positive ion current to C resulting from the removal of the primary electrons by C.

The primary electron current from the cathode is $i_F(1-\beta_F)$. Of these electrons the fraction γ reach the cylinder when it is positive, but only the fraction $1-\rho$ of these are collected, where ρ is the reflection coefficient for electrons. Thus the current due to primary electrons which reach the cylinder directly is

$$i_F\gamma(1-\beta_F)(1-\rho) \tag{10}$$

and the current of electrons reflected is $i_F\gamma\rho(1-\beta_F)$. When the potential of the cylinder is only a few volts positive, the primary electrons lose nearly all their energy in traversing the sheath on the cylinder, and for these low velocities the reflection coefficient ρ is small (about 0.2). Although the reflected electrons probably leave the surface of the collector with a distribution of directions approximating to Lambert's cosine law, they are so strongly accelerated by the field in the sheath that they emerge from the sheath moving in a radial direction, so that we may consider the reflection to be specular.

Thus at low pressure some of the reflected electrons pass back across the tube, a fraction γ^2 of them reaching the opposite side of the cylinder, so that the fraction $\gamma^2\rho$ of them are reflected a second time. The total electron current is thus obtained by multiplying that given by (10) by $1+\rho\gamma^2+\rho^2\gamma^4+\cdots=1/(1-\rho\gamma^2)$.

Each primary electron emitted from the cathode produces an ionization which contributes $\beta_C/(1-\beta_F)$ to the positive ion current to C. Similarly, each primary electron removed by the collector C will cause a decrease $\beta_C'/(1-\beta_F)$ in the positive ion current to C. Here β_C' differs from β_C only because the ions produced near the cylinder are more likely to reach the cylinder than if they were produced near the filament, and because the radial potential gradient which draws ions away from the filament is decreased by ions produced near the cylinder. At low pressures it is probable that β_C' and β_C are practically equal.

Since the total change in current to the cylinder, when this becomes positive, is $i_F\Delta_C$ we find

$$\Delta_C=\gamma(1-\rho)(1+\beta_C'-\beta_F)/(1-\rho\gamma^2). \tag{11}$$

Fig. 3 shows that there is no corresponding break in the current to the end-plate if the potential of the plate is varied while C is kept negative. This means that there are no electrons in the ionized gas which move in an axial direction with the velocity of the primaries. However, the current i_B does suffer a break (as in Fig. 4) if E_C, the potential of the cylinder is changed from negative to positive values. Let us represent the change in $i_B/-i_F$ by Δ_B. Each electron from the cathode contributes a fraction of the positive ion current to B equal to $\beta_B/(1-\beta_F)$ and we may assume that each electron taken up by the cylinder C causes a decrease of $\beta_B'/(1-\beta_F)$ in the current to B. Here β_B' and β_B are probably even more closely equal than are the corresponding quantities β_C' and β_C.

By reasoning similar to that used in deriving (11) we find

$$\Delta_B=\gamma(1-\rho)\beta_B'/(1-\rho\gamma^2). \tag{12}$$

By division we obtain from (11) and (12)

$$\Delta_B/\Delta_C=\beta_B'/(1+\beta_C'-\beta_F). \tag{13}$$

The break Δ_B is observed with value unchanged when E_c is raised from a negative to a positive value, whether B is kept at constant negative voltage or is connected to C. While Δ_C is due to changes in both the electron and the ion currents to C, Δ_B is caused solely by the change in ion current.

The experiments show that the ratio of the observed values of Δ_B and Δ_C agrees well with that calculated by Eq. (13). For example, the data from Fig. 4 give $\beta_B=0.071$, $\Delta_B=0.039$, $\beta_C=0.65$ and $\Delta_C=0.92$ and we have already estimated the value of β_F to be 0.08. The value of Δ_B/Δ_C calculated from Eq. (13) by ignoring the distinction between β and β' is thus 0.0451, while the ratio of the observed values of Δ_B and Δ_C is 0.0424. This difference, amounting to 6 percent, is in the direction to be expected, since β_C' should actually be slightly greater than β_C.

Theory of Current-Voltage Characteristic for Primary Electrons Which Make Elastic Collisions.

A detailed analysis of the shape of the current-voltage characteristic of $i_C/(-i_F)$, such as the curve shown in Fig. 4, will enable us to calculate the numbers of electrons which make elastic and inelastic collisions and also to determine the distribution of the angles through which the electrons are deflected or scattered by their collisions with gas molecules.

We have seen that each primary electron moves along a radius until it either reaches the sheath on the cylinder or collides with a gas molecule. Although the kinetic energy of an electron is not appreciably changed by an elastic collision, the velocity no longer remains radial so that when the electron reaches the sheath on the cylinder (used as collector) it is not able to move against so large a retarding potential as if it had not collided. In general, the greater the angle through which the electron has been deflected by the collision, the higher will be the collector potential required to collect the electron. Let us now attempt to calculate what fraction of the electrons which make collisions can reach the collector when this is at any given potential.

In Fig. 5, which shows the tube in cross-section, O is the cathode filament and the circle of radius R is the collecting cylinder. Consider an electron which is projected from the cathode sheath in the radial direction OU and

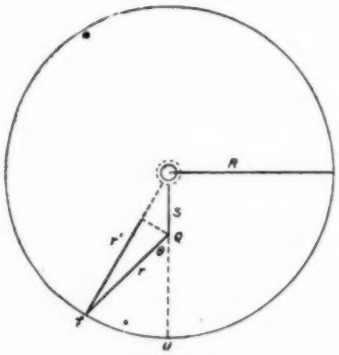

Fig. 5.

let this electron make an elastic collision with a molecule at Q after having moved a distance S from the cathode. After the collision the electron in general will have a velocity component along the axis of the cylinder, but this component will have little effect in determining whether or not the electron will be collected by the cylinder, provided (as we are assuming) that the cylinder is long enough. We therefore need consider only the velocity component perpendicular to the axis. We shall call r the magnitude of this component and θ the angle which its direction makes with the original direction of motion OU. When the electron arrives at the cylinder its radial velocity component is the projection of r on OT, and is thus equal to $r[1-(S^2/R^2)\sin^2\theta]^{1/2}$.

The electron will be collected only if this radial velocity equals or exceeds a certain value u_0 given by

$$u_0 = [2(e/m)(V_0 - E)]^{1/2} \tag{14}$$

where V_0 is the potential of the ionized gas (approximately anode potential) and E is that of the collector, both measured from the cathode. Thus the condition that the electron shall be collected is

$$r^2 - (r^2 s^2/R^2)\sin^2\theta \geqq u_0^2. \tag{15}$$

Scattering through cone of semi-angle θ_M. Let us now consider a large number N_S of electrons which make their collisions with gas molecules in a small element of volume surrounding Q after having traveled a distance S. We will assume provisionally that the velocity vectors after collision are distributed at random through a cone of semi-angle θ_M whose axis is the original direction of motion of all the electrons (OU). In other words the end points of the vectors are distributed with uniform density on a zone of a spherical surface of radius v_0 where v_0 is the magnitude of the original velocity and is given by

$$v_0 = [2(e/m)V_0]^{1/2}. \tag{16}$$

The *projected* velocities r may therefore be represented in a diagram with polar coordinates, r and θ as in Fig. 6, by points lying in a circular segment

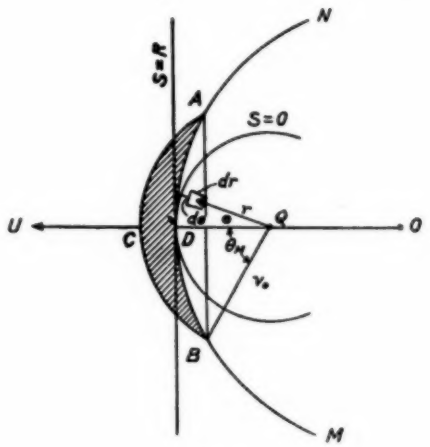

Fig. 6.

ABC of radius v_0 and semi-angle θ_M and it is readily found that the number of points in a specified element of area $rdrd\theta$ is

$$\frac{N_s}{2\pi v_0^2(\sin\frac{1}{2}\theta_M)^2} \cdot \frac{rdrd\theta}{[1-(r^2/v_0^2)]^{1/2}}. \tag{17}$$

Not all of these representative points correspond to electrons which can be collected, but only those which satisfy the condition (15). Thus for any given

value of S the points corresponding to the electrons that can be collected lie, in Fig. 6, to the right of a certain curve, (such as MDN) whose equation is found by taking the equality sign in (15). This curve is in general an ellipse, whose center is at Q and which as indicated in Fig. 6, degenerates into a circle for $S=O$ and into a straight line for $S=R$. For any given distance S the number of electrons collected (N_C) is therefore found by integrating the expression (17) over the shaded region indicated in Fig. 6. This integration is best carried out by expanding the expression (17) into a series in terms of E/V_0. Taking only the first order terms and restricting ourselves to values of θ_M less than about 30° we thus find (approximately)

$$N_C=\frac{N_S R}{S}\cdot\frac{E/V_0}{\sin^2\theta_M} \tag{18}$$

provided that S is greater than a critical value S_1 defined by

$$S_1=R(E/V_0)^{1/2}/\sin\theta_M \tag{19}$$

For this value of S the ellipse MDN of Fig. 6 passes through the points A and B. When S is greater than S_1 the expression for N_C/N_S is the same (except for the proportionality factor $1/\sin^2\theta_M$) as it would be if the electrons were scattered uniformly through *all* angles instead of through a cone of semi-angle θ_M. Thus Eq. (18) is relatively simple.

When, however, S is less than S_1 the limits of integration depend upon θ_M and the expression for N_C/N_S becomes very complicated, but it is found that the function can fairly well be represented by

$$N_C=N_S(E/V_0)^{1/2}k(S)/\sin\theta_M \tag{20}$$

where $k(S)$ is a quantity which is nearly independent of E and of θ_M but varies from $4/\pi$ to 1 as S increases from 0 to S_1.

For collisions taking place near the filament, that is, for $S=0$, Eq. (20) gives for small values of θ_M and E/V_0

$$N_C=(4/\pi)N_S(E/V_0)^{1/2}/\sin\theta_M. \tag{21}$$

If the scattering occurs uniformly through all angles so that $\theta_M=180°$ as in the case of electrons colliding with heavy elastic spheres, a rigorous expression for N_C can readily be worked out by integrating over the whole annular ring between the circles indicated in Fig. 6. We find in this case

$$N_C=N_S(E/V_0)^{1/2}. \tag{22}$$

For collisions occurring near the cylinder, that is, for $S=R$, a rigorous expression for N_C is obtainable:

$$N_C=\frac{N_S[1-(1-E/V_0)^{1/2}]}{2\sin^2(\theta_M/2)} \tag{23}$$

provided that E/V_0 is not greater than $\sin^2 \theta_M$. If E/V_0 is greater than $\sin^2 \theta_M$ then we have

$$N_C = N_S \quad \text{for} \quad \theta_M < 90°$$

or

$$N_C = N_S\left[1 - \frac{(1-E/V_0)^{1/2}}{\sin^2(\theta_M/2)}\right] \text{ for } \theta_M > 90°. \tag{24}$$

Distribution of collisions along the radius. We must now take into account the fact that the collisions of the electrons with molecules can occur at all points along the radius. If λ is the mean distance that an electron travels through the gas before making a collision then $1/\lambda$, which we shall denote by P is the probability of collision per unit length of path. For each particular type of collision that may occur in a gas we shall have a different value of P. We shall use the following notation for the probabilities per unit length of path; P for collisions of all kinds, P_e for elastic collisions, P_k for inelastic collisions, P_i for collisions that cause ionization, P_r for resonance collisions, i.e., those that cause the impinging electrons to lose a definite energy corresponding to a resonance potential of the gas.
The first three of these quantities are related:

$$P = P_e + P_k. \tag{25}$$

We have used γ, according to Eq. (11), to denote the fraction of the primary electrons which reach the sheath on the cylinder C after having undergone some specified change as a result of collisions. In accordance with this use we may let: γ_0 be the fraction of the primaries which reach the sheath[12] on C without colliding with gas molecules; γ_n be the fraction of the primaries which reach the sheath on C after having made n *elastic* collisions but no inelastic collisions (we have γ_1, γ_2, etc., corresponding to $n=1$, $n=2$, etc.); γ_e be the fraction of the primaries which reach the sheath on C after having made one or more elastic collisions, but no inelastic collisions; and γ_r be the fraction of the primaries which reach the sheath on C after making one resonance collision. This includes the electrons which may also have made one or more elastic collisions (either before or after the resonance collision). From these definitions we see that

$$\gamma_e = \gamma_1 + \gamma_2 + \gamma_3 + \cdots \tag{26}$$

$$\gamma_0 = \epsilon^{-RP} \tag{27}$$

We calculate γ_1 as follows. If N_F primary electrons leave the cathode sheath then $N_F P_e \epsilon^{-SP} ds$, of these make elastic collisions with molecules in the distance ds after they have traveled a distance S without having pre-

[12] In these definitions it is specified that the electrons shall reach merely the edge of the sheath, i.e., the boundary between the sheath and the field-free ionized gas, for at present we do not wish to distinguish between the electron that can reach the *cylinder* against the retarding field in the sheath and those that are not able to do so.

viously made inelastic collisions. In accordance with experiments which will be described, we assume that the electrons are deflected by the elastic collisions only through rather small angles so that after the collision the distance the electron must travel before reaching the cylinder is $R-S$. Thus the fraction $d\gamma_1$ of the primary electrons which reach the cylinder after a single elastic collision (but no inelastic collision) is

$$d\gamma_1 = P_e\epsilon^{-SP}\epsilon^{-(R-S)P}ds = P_e\epsilon^{-RP}ds \tag{28}$$

and therefore by integration from $S=0$ to $S=R$

$$\gamma_1 = RP_e\epsilon^{-RP}. \tag{29}$$

In general we find in a similar manner

$$\gamma_n = (1/n!)(RP_e)^n\epsilon^{-RP}. \tag{30}$$

Thus by Eqs. (26) and (27) we obtain

$$\gamma_e = \epsilon^{-R(P-P_e)} - \gamma_0 \tag{31}$$

and by (25)

$$\gamma_0+\gamma_e = \epsilon^{-RP_k}. \tag{32}$$

By elimination of P between Eqs. (29) and (31) we obtain

$$\gamma_0/(\gamma_0+\gamma_e) = \epsilon^{-RP_e}. \tag{33}$$

For the resonance collisions we have, by the method used for Eq. (29),

$$\gamma_r = RP_r\epsilon^{-RP_k} \tag{34}$$

and thus by Eq. (32)

$$\gamma_r = RP_r(\gamma_0+\gamma_e). \tag{35}$$

Let N_e be the average number of elastic collisions that are made by the electrons which reach C after having made *at least one elastic but no inelastic collisions*.

Let N_r be the average number of *elastic* collisions that are made by the electrons which reach C after having made *one resonance* collision.
We see that

$$N_e = \frac{\gamma_1+2\gamma_2+3\gamma_3+\cdots}{\gamma_1+\gamma_2+\gamma_3+\cdots} = \frac{RP_e}{1-\epsilon^{-RP_e}} \tag{36}$$

and

$$N_r = \frac{\gamma_1+2\gamma_2+3\gamma_3+\cdots}{\gamma_0+\gamma_1+\gamma_2+\gamma_3+\cdots} = RP_e. \tag{37}$$

By combining (36) and (33) we obtain the more convenient equation

$$N_e = RP_e(\gamma_0+\gamma_e)/\gamma_e \tag{38}$$

Analysis shows that the electrons which reach the cylinder after having made n elastic collisions have traveled an average distance $R/(n+1)$ since the last collision. In fact it is readily seen if we consider only electrons that reach C after having made one or more elastic collisions, that these collisions are distributed with equal probability along the radius.

Scattering by collisions uniformly distributed along a radius. We wish to consider the current-voltage curve due to electrons, collected by C, which have made single elastic collisions distributed at random along a radius. We have defined γ_1, as the fraction of the primary electrons that reach the sheath on C after having made single elastic collisions. In general, because of the retarding field in the sheath, only the fraction γ of the primary electrons will reach the surface of C. Evidently γ will become equal to γ_1 if the retarding field should disappear, that is if E, the potential of the collector is made equal to V_0, the potential of the gas. The value of γ is found by integrating the expression for N_C/N_S from Eqs. (18) and (20) along the radius. Thus

$$\gamma=(\gamma_1/N_S R)\int_0^R N_C ds. \tag{39}$$

This integration must be carried out in two steps, from $S=0$ to $S=S_1$, by Eq. (20) and from S_1 to R by Eq. (18). Placing for convenience

$$E/V_0=\nu \tag{40}$$

we thus find[13]

$$\gamma=\gamma_1(\nu/\sin^2\theta_M)\left[1+\log(\sin\theta_M/\nu^{1/2})\right]. \tag{41}$$

This equation, like (18) and (20) is based on the assumption that ν and θ_M are small quantities. However, from an examination of the second and third order terms in the expansions it appears that Eq. (41) should give a good approximation (as accurate as the experiments) up to values of ν as high as 0.6 and values of θ_M as high as 30°.

From Fig. 6 we see that all electrons which are scattered through angles of less than θ_M will be collected by the cylinder, no matter where the collisions occur along the radius, if the voltage of the cylinder is raised sufficiently to make the point D meet the line AB or pass to the left of it. This will occur if

$$u_0 \leqq v_0 \cos\theta_M. \tag{42}$$

By Eqs. (14), (16) and (40) we find that this condition is equivalent to

$$\nu \geqq \sin^2\theta_M. \tag{43}$$

When ν becomes equal to $\sin^2\theta_M$, γ should be equal to γ_1, and in fact we see that Eq. (41) gives this value under these conditions. For values of ν

[13] The logarithmic term in the brackets comes from the integration of Eq. (18) between S_1 and R, while the term unity was obtained from the integral of Eq. (20) after having calculated the value of $k(S)$ with some care.

greater than $\sin^2\theta_M$ of course Eq. (41) does not hold but γ remains constant and equal to γ_1.

Although Eq. (41) is not applicable when θ_M is a large angle, it is possible to derive by similar methods the following approximate equation for the case that $\theta_M = 180°$, that is when electrons are scattered equally in all directions by collisions uniformly distributed along a radius

$$\gamma = \gamma_1 \nu [0.88 + \tfrac{1}{4} \log (1/\nu)]. \tag{44}$$

Scattering according to probability laws. We have thus far taken the directions of the scattered electrons to be uniformly distributed within a cone of semi-angle θ_M. If we have n electrons scattered in this way, the angular density η (expressed as electrons per steradian) can be calculated from the relation

$$n = 2\pi\eta(1 - \cos\theta_M) = 4\pi\eta \sin^2(\theta_M/2). \tag{45}$$

When θ_M is small this becomes

$$n = \pi\theta_M{}^2\eta. \tag{46}$$

The error in using (46) in place of (45) is only 2.3 percent for $\theta_M = 30°$ and 1 percent for 20°.

Let us now assume that the scattered electrons instead of having uniform angular density are distributed according to a type of probability law such that

$$\eta = \eta_0 \epsilon^{-\theta^2/\theta_0{}^2} \tag{47}$$

where η_0 is the maximum angular density and θ_0 is the angle at which the angular density of the scattered electrons is $1/\epsilon$ of η_0. It can be readily proved that θ_0 is the root-mean-square deflection of the electrons. The average angle θ_{av} and the most probable angle θ_P of scattering are related to θ_0 as follows

$$\theta_{av} = \tfrac{1}{2}\pi^{1/2}\theta_0 \text{ and } \theta_p = \tfrac{1}{2}2^{1/2}\theta_0. \tag{48}$$

The total number n of electrons that are scattered according to Eq. (47) is approximately (for not too large values of θ_0) given by

$$n = \int_0^\infty 2\pi\theta\eta d\theta = \pi\theta_0{}^2\eta_0. \tag{49}$$

Comparing this result with Eq. (46) we see that the total number of electrons is the same as in a cone of semi-angle θ_0 having electrons distributed with the uniform angular density η_0.

From the results already obtained we may now by an integration process derive an equation for the current collected by C when this is at a voltage E for the case that the electrons are scattered according to probability laws by collisions uniformly distributed along the radius.

If N_F primary electrons leave the cathode $N_F\gamma_1$ of them reach the sheath on C after making single elastic collisions, and we will assume that these are

scattered according to Eq. (47). We may divide these $N_F\gamma_1$ electrons into an infinite number of groups, each group consisting of $N_F d\gamma_1$ electrons scattered through a cone of semi-angle θ (variable for different groups) with a uniform angular density $d\eta$. The number of electrons in a group is thus

$$N_F d\gamma_1 = \pi\theta^2 d\eta .$$

Let the collector C be maintained at a given voltage E, then from Eqs. (43) and (40) we see that if $\theta < \nu^{1/2}$ all the electrons in the group will be collected, but if $\theta > \nu^{1/2}$ only a part will be collected, the fraction collected being, by Eq. (41) equal to

$$(\nu/\theta^2)\left[1+\log(\theta/\nu^{1/2})\right].$$

Thus we find that the total number $N_F\gamma$ of electrons reaching C is

$$N_F\gamma = \int_{\eta_c}^{\eta_0} \pi\theta^2 d\eta + \int_0^{\eta_c} \pi\nu\left[1+\log(\theta/\nu^{1/2})\right] d\eta \tag{50}$$

where η_c is the value of η which, by Eq. (47) corresponds to the critical angle $\theta = \nu^{1/2}$. Thus

$$\eta_c = \eta_0 \epsilon^{-\nu/\theta_0^2}. \tag{51}$$

We may express $d\eta$ in terms of θ by differentiating Eq. (47), and by Eq. (49) we find that

$$\eta_0 = N_F\gamma_1/(\pi\theta_0^2). \tag{52}$$

If we then substitute $y = \theta^2/\theta_0^2$, Eq. (50) becomes

$$\gamma/\gamma_1 = \int_0^x y\epsilon^{-y} dy + x\int_x^\infty \left[1+\tfrac{1}{2}\log(y/x)\right]\epsilon^{-y} dy$$

where

$$x = \nu/\theta_0^2 = E/(V_0\theta_0^2). \tag{53}$$

Carrying out the integration we get

$$\gamma/\gamma_1 = 1-\epsilon^{-x}+\tfrac{1}{2}x\int_x^\infty \epsilon^{-x} dx/x. \tag{54}$$

The integral in Eq. (54) is equal to $-Ei(-x)$ where Ei stands for the "exponential integral" given for example in Glaisher's Tables (Phil. Trans. *140*, 367 (1870)). By means of the series expansion for $Ei(-x)$ we find for small values of x that

$$\gamma/\gamma_1 = x(0.7114-\tfrac{1}{2}\log x)$$

which gives only 3 percent error when $x=1$. For larger values of x a good approximation is

$$\gamma/\gamma_1 = 1-\tfrac{1}{2}\epsilon^{-x}.$$

Table II gives values of γ/γ_1 as a function of x, calculated from Eq. (54).

TABLE II

The fraction of collectable electrons as a function of $x=E/(V_0\theta_0^2)$ as given by Eq (54)

x	γ/γ_1	x	γ/γ_1	x	γ/γ
0.001	0.0042	0.2	0.3035	1.5	0.8519
0.01	0.0301	0.3	0.3950	2.0	0.9136
0.02	0.0534	0.5	0.5334	3.0	0.9698
0.005	0.1105	0.75	0.6553	4.0	0.9892
0.10	0.1863	1.00	0.7418	5.0	0.9961

It is of interest to compare Eq. (54) which is for electrons scattered by probability laws, with Eq. (41) which is for electrons scattered uniformly through a cone. Replacing $\sin\theta_M$ by θ_M in Eq. (41) and by analogy with Eq. (53) placing

$$x'=\nu/\theta^2_M \tag{55}$$

we have

$$\gamma/\gamma_1=x'[1+\tfrac{1}{2}\log(1/x')]. \tag{56}$$

A double logarithmic plot of the function of the right member of Eq. (54) is given in Fig. 8 by the full line ST (also marked $\delta=0$). The corresponding function of Eq. (56) is represented in this figure by the dotted curve. By means of the function given in Table II we shall be able to analyze current-voltage curves such as those of Fig. 2 and thus determine from the

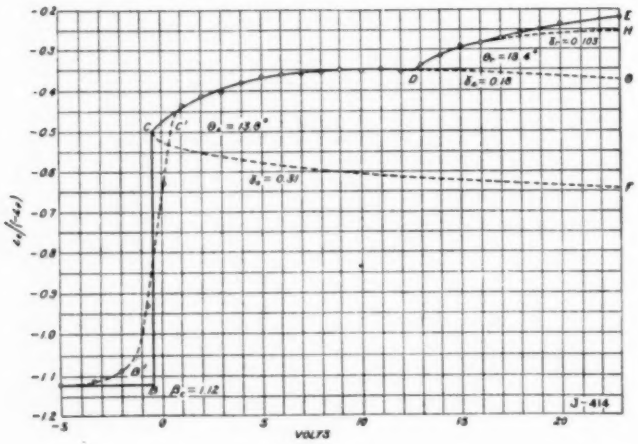

Fig. 7.

experiments the number of electrons that make elastic collisions and the mean angle θ_0 through which they are scattered by the collisions.

Application of the theory for electrons which have suffered collisions. To illustrate the method of using the equations let us consider in some detail a typical example which gave the data recorded in Table III and Fig. 7.

In this experiment nitrogen was used at 50 baryes and 650°K (in the cylinder C). This pressure was corrected for the effect of thermal effusion as will be described later. The cylinder C_r was of molybdenum, 5.0 cm long, 5.2 cm in diameter, and the end-plates were 4.85 cm in diameter and 5 cm apart. One of them, A, was used as anode at 100 volts while the other, B, was maintained at -6.0 volts. The filament F was of tungsten, 5 cm long, 0.0254 cm in diameter, heated to about 2300°K by an intermittent current, which read 5.95 amps. on an A.C. ammeter and about 3.92 on a D.C. meter. A rotating commutator operated by a 60 cycle synchronous motor was used to produce the intermittent filament current and to connect the circuit for measuring the current i_C only in the intervals during which no current flowed through the filament. Thus the effects of voltage drop along the filament were avoided. The circuit for C was closed 43.6 per of the time so that the observed currents as read by a D.C. microammeter were multiplied by 1/0.436 to get the instantaneous current i_C.

Table III, in columns 1 and 2, gives the instantaneous currents to the cylinder C at various cylinder voltages. The currents are expressed as a fraction of the current i_F from the cathode. As these data are given only to illustrate the method used for calculation, alternate readings have been

TABLE III

Typical current voltage data. Nitrogen at 50 baryes and 650°K; $R=2.60$ cm; anode at 100 volts; $\beta_c=1.12$; $\beta_F=0.11$; $\gamma=0.498\Delta/(1-\rho)$; $\Delta=i_c/(-i_F)-1.12$

E_c	$i_c/-i_F$	$1/(1-\rho)$	γ	obs. $\gamma-\gamma_0$	cal. $\gamma-\gamma_0$	Diff.	γ'	E'
2	−0.413	1.100	0.387	0.077	0.076	+ .001	—	—
4	− .384	1.135	.416	.106	.107	− .001	—	—
6	− .362	1.163	.439	.129	.128	+ .001	—	—
8	− .354	1.187	.453	.143	.142	+ .001	—	—
10	− .352	1.208	.462	.152	.152	.000	—	—
12	− .354	1.228	.468	.158	.160	− .002	—	—
14	− .318	1.245	.497	.187	.166	+ .021	.0176	1.2
16	− .286	1.262	.524	.214	.171	+ .043	.0380	3.2
18	− .259	1.278	.548	.238	.173	+ .065	.0583	5.2
20	− .240	1.292	.566	.256	.175	+ .081	.0735	7.2

omitted from the table; all the observed points between -5 and $+23$ volts are indicated by the small circles in Fig. 7. The same data over a wider range of voltages are also given in curve V of Fig. 12.

The points in Fig. 7 lie along a broken curve $AB'C'DE$. The section AB corresponding to $\beta_C=1.12$ gives the positive ion current. The break $B'C'$, which corresponds to γ_0, is due to electrons which reach C without collisions. Along the curved portion $C'D$ the electrons that have made elastic collisions are being collected, while in the range DE the electrons which have made resonance and ionizing collisions are also collected.

We wish now to distinguish between the electron current and the ion current. To do this we let Δ represent the increase in current[14] (at any given

[14] For convenience we shall frequently refer to the current i_C when we really mean $i_C/(-i_F)$

voltage) over the value -1.12 which corresponds to β_C. Then by Eq. (11) we may calculate γ the fraction of the primary electrons that are able to reach the surface of the cylinder at any given voltage. We may neglect the small quantity $\rho\gamma^2$ and thus write Eq. (11) in the form

$$\gamma=\Delta[1/(1-\rho)]/(1+\beta_C-\beta_F). \tag{57}$$

Reflection coefficient for electrons. To use this equation we must know ρ, the reflection coefficient for electrons. Since ρ is a function of the velocity of the electrons, it might seem at first that for groups of electrons which are not all collectable at a definite voltage, the value of ρ should enter Eq. (57) as a complicated integral. For example, if the collector is at $+5$ volts, the electrons collected include those that are just able to move against a retarding field of one volt as well as those that can move against five volts.

However, the electrons in these different groups, since they cannot have made inelastic collisions, must all have the same total energy as the primary electrons, and thus they differ only in their angles of incidence on the collector. There is considerable evidence, experimental and theoretical, that the reflection coefficient, at least on smooth clean surfaces, depends mainly on the total energy of the electrons rather than upon the normal component of the energy. Therefore, for electrons which have made elastic collisions, we are justified in taking ρ the same for all those that are collected at a given voltage. Eq. (57) may thus be used if we take ρ as the reflection coefficient for electrons which are moving with an energy corresponding to the voltage E (the energy of impact on C). Farnsworth[15] has given data for the reflection coefficient ρ of electrons from tungsten surfaces the values 0.20 for 2 volts, 0.32 for 6 volts and 0. 38 volt electrons. Hull's observations with dynatrons indicate that the reflection from molybdenum is considerably less than from tungsten. Petry[16] has published data on the reflection of electrons from molybdenum, but only relative, not absolute values of ρ were given. Mr. Petry has kindly furnished us with the notes of his original observations and from these we have calculated values of 0.11 at 5 volts, 0.17 at 10 volts, 0.19 at 15 and 0.22 at 20 volts. Based partly on these data and partly on other data in this laboratory[17] we have adopted values for ρ which give

$$1/(1-\rho)=1+0.0645E^{1/2}. \tag{58}$$

The potential E in this equation should correspond to the energy of the electrons which reach the collector. Examination of Fig. 7 shows that electrons begin to be collected when E_C is -2 volts and a large fraction are collected before C becomes positive. The initial velocities of the electrons as they leave the filament and any contact potential difference that may exist between the tungsten filament and the molybdenum cylinder tend to produce small displacements of the curves parallel to the voltage axis.

[15] H. E. Farnsworth, Phys. Rev. **25,** 41, (1925).

[16] R. L. Petry, Phys. Rev. **26,** 346, (1925).

[17] We shall see that the data from the present experiments at a series of pressures all indicate that $1(1-\rho)$ at about 15 volts is close to 1.25 in agreement with Eq. (58).

Therefore we take, as our zero point of potential in calculating E, the mid-point on the steep rise $B'C'$ corresponding to the electrons that come through without collisions. Thus $E=E_C+0.4$ volt, not only in Eq. (58) but when we calculate x or ν by Eq. (53).

The data in the 3rd column of Table III are obtained from Eq. (58) in this way. The effect of possible errors in the value of ρ will be discussed later. Taking $\beta_C=1.12$ and assuming $\beta_F=0.1$, $\beta_A=0.11$ we thus find from Eq. (57) the values of γ given in the 4th column. From our theoretical study of the current-voltage curves we concluded that the relation between γ and the voltage E can be expressed by Eqs. (54) or (56) according as the electrons are scattered according to probability laws, or are scattered uniformly through a cone.

Let us now compare our experimental data for γ with those calculated from these equations.

In the range from C' to D in the curve of Fig. 7, the electrons collected, corresponding to γ consist of two parts: those that have made no collisions (γ_0) and those that have made elastic collisions. It is only this second part that corresponds to γ in Eq. (54). From Eq. (53) we see that x is proportional to E. By plotting the logarithms of γ/γ_1 and of x, as in Fig. 8, we thus see

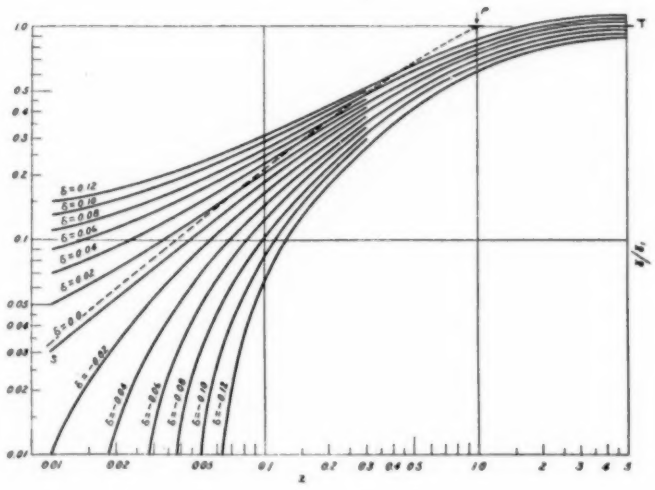

Fig. 8.

that changes in the values of the "unknowns" γ_1 and θ_0 do not alter the shape or size of the curve but result merely in vertical or horizontal displacements of the curve as a whole. On the other hand a change in the value of γ_0 corresponds to the addition or subtraction of a quantity and this does change the shape of the curve.

These latter changes may be studied by plotting a family of curves (as in Fig. 8) from the data of Table II, corresponding to $(\gamma/\gamma_1)\pm\delta$, where δ is given successively the values 0.02, 0.04, 0.06, etc.

We may now use this plot in a very simple way, to determine from the experimental data for γ (Column 4 of Table III) the values of γ_0, γ_e and θ_0. We proceed as follows:

By examination of a plot of γ (from Table III) against E, or directly from a plot such as Fig. 7, we make a rough preliminary estimate of the value of γ_0 which must correspond to the steep initial rise $B'C'$ in current near $E=0$. Suppose we assume $\gamma_0'=0.33$ for this value. We then plot on double-logarithmic paper (using the same scale as in Fig. 8) the values of $\gamma-\gamma_0'$ as ordinates and the voltages E as abscissas, so that we obtain the points which lie near the curve $A'C'$ in Fig. 9. By superposing[18] Fig. 9 on Fig. 8,

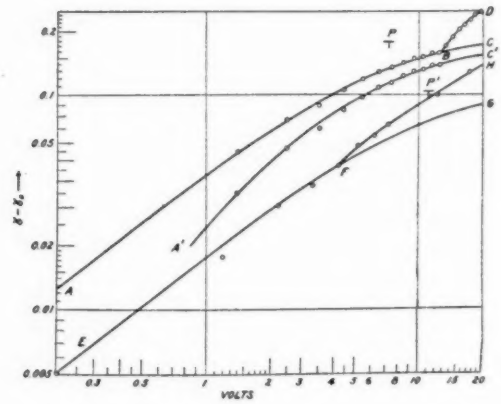

Fig. 9.

keeping the edges of the curve sheets parallel, one figure can be displaced with respect to the other until these points are made to fit as well as possible with one of the family of curves in Fig. 8. We find that the curve $\delta=-0.10$ gives the best agreement. Tracing this curve through on to Fig. 9 we obtain the curve marked $A'C'$.

The curve ST in Fig. 8, for which $\delta=0$, when transferred through to Fig. 9 gives ordinates in Fig. 9 about 0.02 greater than those of the observed points. Therefore we see that if we had chosen 0.31 instead of 0.33 for the value of γ_0, the observed points for $\gamma-\gamma_0$ would lie on the theoretical curve ($\delta=0$). Using this revised value of γ_0 and plotting $\gamma-0.31$ as given in Col. 5 of Table III, we obtain the points indicated in Fig. 9 by circles along the curve ABD. This curve can now be superposed upon ST in Fig. 8. The curve ABC in Fig. 9 is a theoretical curve obtained in this way by tracing through curve ST from Fig. 8. The point P in Fig. 8 at $\gamma=\gamma_1$, and $x=1$ when transferred to Fig. 9, gives the point P marked by the intersection of the short horizontal and vertical lines. The coordinates of this point give $\gamma_e=0.180$ and $E_E=7.2$ volts where E_E is the value of E corresponding to $x=1$. From Eq. (53) for $x=1$,

[18] This is conveniently done by placing one curve sheet on the other, holding both against a glass window by daylight, so that the curves can be seen by transmitted light.

$$E_E = V_0\theta_0^2 \tag{59}$$

and thus, since $V_0 = 100$ volts, we find $\theta_0 = 0.268$ radians or 15.4° as a measure of the angle through which the electrons are scattered by the elastic collisions. Let us denote this value by θ_E.

The good agreement between the observed points and the theoretical curve in Fig. 9 proves that the electrons are scattered at least approximately according to probability laws. By no choice of γ_0, γ_e or θ_M can the experimental data be made to agree with a curve like that shown by the dotted line in Fig. 8 which corresponds to uniform scattering of the electrons through a cone of semi-angle θ_M, according to Eq. (56).

The values of $\gamma - \gamma_0$, as taken from the theoretical curve ABC in Fig. 9, are given in Col. 6 of Table III. Up to $E_C = 12$ volts the agreement is good, the errors (Col. 7) being only about 0.2 percent for the original values of γ. Beyond 12 volts the differences increase rapidly because of electrons which are collected after having made resonance collisions. Let γ' be the fraction of the primary electrons reaching C at any given voltage after they have made one resonance collision. As E_C increases, γ' will approach the limit γ_r which we have already defined. Below the resonance voltage V_r, γ' is zero. In the present case, from inspection of the break at B in Fig. 9, we will take $V_r = 13.2$ volts. Let us place $E' = E - 13.2 = E_C - 12.8$ as in Col. 9. The energy of the electrons which reach C after single resonance collisions is evidently measured by E' and therefore the reflection coefficient for these electrons will be less than for the electrons that have made no collisions or have made only elastic collisions. An analysis shows that γ' may thus be calculated by multiplying the difference given in Col. 7 by the ratio of the values of $1/(1-\rho)$ at E' and at E. For example, at $E_C = 18$ we have $\gamma' = 0.065 \times (1.147/1.278) = 0.0583$, where 1.147 is the value of $1/(1-\rho)$ at $E' = 5.2$ volts and 1.278 is the corresponding value at $E = 18$ volts.

The values of γ' have been plotted in Fig. 9 as the small circles which lie along the curve EFH. By parallel displacement, the curve ST of Fig. 8 has been brought to fit the points in as reasonable a manner as possible, thus giving in Fig. 9 the theoretical curve EFG. The coordinates of the point P' give $\gamma_r = 0.103$ and $E_R = 11.2$ volts, where E_R is the value of E' corresponding to $x = 1$. The corresponding value of θ_0 which we shall denote by θ_R may be calculated from the equation

$$E_R = (V_0 - V_r)\theta_R^2 \tag{60}$$

which is derived from Eq. (53) by considering that the velocity of the "resonance" electrons corresponds to $V_0 - V_r$ instead of V_0. Thus we find $\theta_R = 0.360$ radians $= 20.6°$ as the root-mean-square angle through which the electrons are scattered by resonance collisions.

The angles θ_E and θ_R which we have thus determined are the mean deflections produced by the combined effect of all the collisions that the electrons may have made in traveling from F to C. We are more interested, however, in knowing the deflections of electrons which have made only one collision.

Assuming that the scattering is of the probability type according to Eq. (47), we may let θ_e be the mean deflection corresponding to a single elastic collision and let θ_r be the mean deflection for a single resonance collision. In successive collisions which an electron may make with gas molecules the transverse components of momentum delivered by the separate collisions, are distributed in random directions in the plane normal to the original path of the electron. Therefore θ^2 for the resultant deflection is found by addition of the values of θ^2 for the separate collisions.

Thus for the N_e elastic collisions which are made on the average by each of the electrons in the group corresponding to γ_e we have

$$\theta_E^2 = N_e\theta_e^2 \tag{61}$$

where N_e is given by Eq. (38).

The resonance electrons, corresponding to γ_r, have each made only one resonance collision and, on the average, N_r elastic collisions. Therefore

$$\theta_R^2 = \theta_r^2 + N_r\theta_e^2 \tag{62}$$

where N_r is given by Eq. (37).

Our analysis of the data of Table III (Figs. 7 and 9) has given:

$$\gamma_0 = 0.310 \qquad V_r = 13.2 \text{ volts}$$
$$\gamma_e = 0.180 \qquad \gamma_r = 0.103$$
$$E_E = 7.2 \text{ volts} \qquad E_R = 11.2 \text{ volts}$$
$$\theta_E = 15.4^\circ \qquad \theta_R = 20.6^\circ.$$

From these values by means of Eqs. (27), (33), (25), (35), (37), (38), (61) and (62) we thus derive, placing $R = 2.60$ cm.

$$P = 0.450 \text{ cm}^{-1} \qquad N_r = 0.458$$
$$P_e = 0.176 \text{ cm}^{-1} \qquad N_e = 1.25$$
$$P_k = 0.274 \text{ cm}^{-1} \qquad \theta_e = 13.8^\circ$$
$$P_r = 0.081 \text{ cm}^{-1} \qquad \theta_r = 18.4^\circ.$$

These results have been obtained from an experiment with nitrogen at 650°K and a pressure of 50 baryes. The angles θ_e and θ_r are presumably determined by the nature of single collisions so they should not depend on the pressure of the gas. But the probabilities, P, etc., should be proportional to the number of molecules of gas per unit volume, so that we may recalculate them for the standard temperature and pressure of 20°C and 1000. baryes by multiplying the foregoing values by $(1000/50) \times (650/293) = 44.4$, obtaining

$$P = 20.0 \text{ cm}^{-1} \qquad P_k = 12.2 \text{ cm}^{-1}$$
$$P_e = 7.8 \text{ cm}^{-1} \qquad P_r = 3.6 \text{ cm}^{-1}.$$

The ionization probability P_1 has been determined for a number of gases by Compton and van Voorhis.[19] For nitrogen with 100 volt electrons

[19] K. T. Compton and C. C. Van Voorhis, Phys. Rev. **27**, 724 (1926).

they find for 20°C and 1000 baryes $P_i = 7.7$ cm^{-1}. The inelastic collisions must include those that give ionization and those that produce resonance at 13.2 volts. Thus the remainder P_x given by

$$P_x = P_k - P_r - P_i. \tag{63}$$

measures the probability of all other types of inelastic collisions such as those that excite the molecules to higher energy levels than 13.2 volts. For the case under consideration we find

$$P_x = 0.9 \text{ cm}^{-1}.$$

The curves ABC and EFG in Fig. 9 are the theoretical curves corresponding to the foregoing values of P, γ_0, γ_e, θ_e etc. By taking points from these curves we can calculate values of Δ and compare them with the original observations. Such reconstructed curves are shown in Fig. 7, the whole curve $ABCDH$ being a theoretical curve calculated in this way by our equations. Thus AB is the theoretical line corresponding to a positive ion current of -1.12. The curve $ABCF$ is the theoretical curve corresponding to the positive ion current together with the current of primary electrons ($\gamma_0 = 0.31$) which have made *no* collisions. The negative slope of the line CF shows the effect of the reflection of the electrons from the collector C.

The curve $ABCDG$ includes the current due to the electrons ($\gamma_e = 0.18$) which have made elastic collisions and have thus been scattered through angles which average 12.2° (i.e., $\frac{1}{2}\pi^{1/2} \times 13.8°$). Finally the curve $ABCDH$ includes the electrons that are collected after resonance collisions.

The theoretical curves can thus be made to fit the experimental data within the probable error of the measurements except in the regions where E is close to zero and where E is above the ionizing potential (in this case 17 volts).

When an electron ionizes a gas molecule it must lose an energy corresponding to the ionizing potential, but then in general it must divide its remaining energy with the new electron produced by the ionization. Thus the probability is small that an electron that ionizes a molecule shall lose merely the energy which corresponds to the ionizing potential. Therefore at collector voltages above the ionizing potential the electrons that are collected can no longer be resolved into groups having homogeneous velocities. We see in fact from Fig. 7 that the observed points (along DE) begin to depart from the theoretical line DH at the ionizing potential but this departure begins gradually and not abruptly as in the case of the resonance potential at D.

The experimental data indicated by circles in Fig. 10, were obtained with mercury vapor at 44.5 baryes and 650°K in a tube having a cylinder C of 1.55 cm radius, the anode potential being 50 volts. By an analysis involving a double logarithmic plot it was found that

$\gamma_0 = 0.158$ $\quad V_r = 6.3$ volts

$\gamma_e = 0.159$ $\quad \gamma_r = 0.109$

$E_E = 2.2$ volts $\quad E_R = 2.8$ volts

$\theta_E = 12.0°$ $\quad \theta_R = 14.6°$

and from these were calculated

$P = 1.190$ cm^{-1} $\quad N_r = 0.364$

$P_e = 0.443$ cm^{-1} $\quad N_e = 1.20$

$P_k = 0.743$ cm^{-1} $\quad \theta_e = 11.0°$

$P_r = 0.222$ cm^{-1} $\quad \theta_r = 13.0°$.

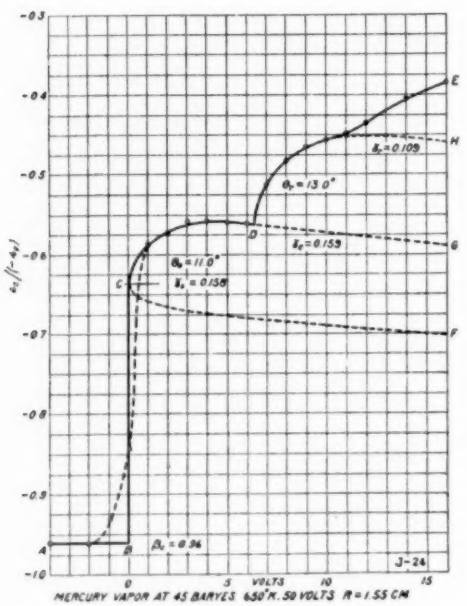

Fig. 10.

Under standard conditions (20°C and 1000 baryes) these probabilities become

$P = 59.0$ cm^{-1} $\quad P_r = 11.0$ cm^{-1}

$P_e = 22.1$ cm^{-1} $\quad P_i = 14.9$ cm^{-1}

$P_k = 36.9$ cm^{-1} $\quad P_x = 11.0$ cm^{-1}.

The curve *ABCDH* in Fig. 10 is the theoretical curve corresponding to the foregoing values of the probabilities and the scattering angles. Although the resonance voltage (6.3) and the ionizing voltage (10.0), corresponding to the resonance potential (6.7) and the ionization potential (10.4) in mercury due to a shift of 0.4 volts at zero, are very different from those of nitrogen, the general agreement with the theory and the character of the results are much the same.

With mercury vapor also the experimental points begin to depart from the theoretical curve DH as soon as the voltage rises above the ionizing potential.

More than two hundred sets of volt-ampere characteristic curves for various gases, pressures and voltages have been analyzed and in all cases it has been found that by suitable choice of P, P_e, P_r, θ_e and θ_r the curve up to the ionizing voltage can be satisfactorily represented by the equations we have developed. The theory is particularly confirmed by the fact that the experimental values of all these constants are practically independent of the gas pressure. A summary of these results is given in Table VIII.

Discussion of the Accuracy of the Results

In fitting the theoretical curves in Fig. 7 to the experimental data we have 6 adjustable constants at our disposal, and it may therefore seem that the accuracy in the determination of all the constants cannot be high. By trial we find that the permissible limits in the choice of the values of γ_0 are rather narrow, so we estimate the probable error of γ_0 to be less than 0.01.

We find, however, that the curves such as AC in Fig. 9 can be displaced a considerable distance in the general direction of their length without greatly altering the agreement between the theoretical curve and the experimental points. Especially is this true with the resonance curve EFG which is more nearly straight and for which agreement with experiment is expected only for a rather limited range of voltage.

Trial shows for the data of Fig. 7 that the agreement becomes poor if E_E is altered by more than about 10 percent which corresponds to a variation of 5 percent in θ_E or θ_e. A 10 percent change in E_E involves about a 4 percent change in γ_e, but for any given value of E_E the probable error in γ_e would be not over 1 or 2 percent.

In the case of the resonance electrons the possible individual errors in γ_r or E_R become relatively large. In Table IV are given a series of pairs of values of γ_r and E_R corresponding to displacements of the curve EFG approximately parallel to the nearly straight line EF.

Table IV

Effect of displacement of curve EFG in Fig. 7

Displacement	γ_r	E_R	P_r	P_z	θ_R	θ_r	E_F
D_1	0.182	25.	6.3	−1.1	30.7°	29.4°	23.
D_2	0.152	19.8	5.3	0.0	26.8	25.7	18.
D_3	0.103	11.2	3.6	+1.7	20.6	18.4	17.
D_4	0.070	7.0	2.4	+3.8	16.3	13.3	14.7
D_5	0.033	2.3	1.2	+4.2	9.3	0.0	13.9

From the values of γ_r and E_R we can calculate P_r, P_z, etc., as given in the table. The displacement D_1 makes P_z negative and therefore must be excluded. The displacement D_2 has been chosen to make $P_z=0$. Thus the maximum possible values of P_r and θ_r are 5.3 and 25.7° respectively.

Displacement D_5 corresponds to the lowest possible value of P_r and the greatest possible value of P_x since any further displacement would make θ_r become imaginary.

For each different displacement, the point corresponding to F in Fig. 9, at which the observed points begin to depart from the theoretical curve, occurs at a different voltage E'. Adding 13.2 volts to these values we obtain the voltages E_F given in the last column of Table IV, and this voltage should presumably be approximately equal to the ionizing potential of the gas (17.0 volts for nitrogen). Thus we are led to choose D_3 as the most probable displacement.

In the analysis of the experimental data on the resonance electrons the displacement of the curve, which determines the value of E_r has usually been chosen so as to make E_F come at the ionizing potential. In other cases, especially when the voltage drop along the filament was not eliminated by using the commutator, the point E_F could not be determined with sufficient accuracy. In order to get approximate values of γ_r and P_r in these cases it was assumed that θ_r could be put equal to θ_e. From this, θ_R, and E_R were then calculated and a displacement was then chosen to give this value of E_R.

The values of P_r and θ_r found by such methods are of course only rough, but it is felt that our main conclusions regarding the rather small angles through which the electrons are scattered by the resonance collisions are not vitally affected thereby.

Estimation of temperature and pressure. To calculate the P's at standard pressure and temperature from the experimental data we must know the pressure and temperature of the gas in the cylinder C. The pressure outside the cylinder was measured by a McLeod gauge but because of the effect of thermal effusion the pressure inside the cylinder was usually considerably higher than that outside.

The radiation from the filament (ranging from 11 to 20 watts in the various experiments) heated the molybdenum cylinder to rather high temperatures. If the cylinder and end-plates had completely surrounded the filament so that the whole energy would be re-radiated from the outside surface, the temperature of the electrodes in the absence of gas, would have been 720° to 790°K. But from the small annular spaces about 2 mm wide between the end plates and cylinder the radiation was nearly that from a black body. Thus the radiative equilibria gave temperatures from 670 to 720°K. The effect of the heat conduction of various gases was calculated, taking into account the Smoluckowski temperature drop at the surfaces.[20] It was found that the cylinder temperature gradually decreased as the pressure rose. For example, argon at 100 baryes would lower the cylinder temperature about 70°. But the heat conduction from the filament tends to raise the gas temperature above that of the cylinder, by amounts that increase as the pressure rises. This effect nearly compensates for the cooling of the cylinder. Thus, the average temperature of the gas along the radius

[20] See I. Langmuir, J. Amer. Chem. Soc. **37**, 421 (1915).

was found to be approximately independent of the pressure and to lie between 650° and 700°K in various typical experiments. At pressures so low that the free-paths of the molecules are large compared to the openings into the cylinder thermal effusion makes the pressure p_c in the cylinder greater than that outside in the ratio of the square roots of the temperatures. The following semi-empirical equation was used in all the experiments to calculate the pressure in the cylinder

$$\frac{p_c}{p_0}=\frac{(T_c/T_0)^{1/2}+bp_0/\lambda_1}{1+bp_0/\lambda_1} \tag{64}$$

where p_0 and T_0 are the pressure and temperature outside the cylinder, while p_C and T_C are those inside; b is the width of the space between the cylinder and end-plates, while λ_1 is the mean free path of the molecules of gas at 1 barye pressure at the temperature of the cylinder.[21]

It will be appreciated that the accuracy in this estimation of the temperature of the gas and the pressure increases by effusion cannot be high. Thus in reducing the observed values P_1, P_e, P_k and P_r to standard conditions errors of perhaps 10 percent have been made. However, it should be noted that the effusion decreases the effect of an error in the estimation of the temperature since the pressure increases as the temperature rises and thus causes a slower variation in the density.

To avoid errors due to uncertainty in the temperature of the cylinder a large number of experiments were made with argon, and helium in tubes in which the "cylinder C" consisted in a vaporized magnesium deposit on the inside of the glass wall of the tube. By a blast of air the tube wall was kept at about 30°C as was measured by the resistance of a fine tungsten wire in close contact with the glass. The average temperature of the gas along the radius was usually about 50° above that of the tube wall, because of heat conducted from the filament.

The values of the probabilities P and P_K found with these tubes were practically the same as those found with the molybdenum cylinders, as will be seen in the summary of results (Table VIII). Thus we are justified in believing that the calculated temperatures of 650° to 700°K in the latter case are not seriously in error.

Small angle deflections. At voltages in the neighborhood of $E_C=0$ the observed currents, as indicated by the dotted line $B'C'$ (Fig. 7) do not rise as abruptly as they should according to the theoretical curve BC, but increase gradually over a range of about 2 or 3 volts, showing that the electrons which have not made collisions with molecules are not moving in strictly radial directions when they strike the cylinder. Possible causes of these small angular deflections from the radial direction are: (1) Initial velocities of electrons due to thermal agitation; (2) Non-axial position of the filament; (3) Transverse magnetic field (earth's field); (4) Scattering by the electric field of ions; (5) Scattering by the fields of molecules; (6) Scattering by

[21] The free-paths λ_1 at 650° were taken to be for Hg 13.1 cm; Ne 51; A 28; He 73; N_2 25 and H_2 47 cm. The slit width b was 2 mm in some cases and 2.5 in others.

energy transferred from other primary electrons. Let us consider briefly the magnitude of these effects.

1. *Initial velocities.* The average kinetic energy of the electrons which leave the filament is $2kT_F$, but the longitudinal component $\frac{1}{2}kT_F$ is not effective in causing them to move against a retarding field at the cylinder. The effective energy $(3/2)\,kT_F$, for a filament temperature of 2300°K corresponds to 0.30 volts, and can thus explain only about one tenth of the observed spread in voltage over which the primary electrons are collected.

2. *Displacement of filament.* If the filament is displaced a distance δ along a radius, the electrons which move along another radius at right angles to the first reach the cylinder with a transverse energy V_T given by

$$V_T = V(\delta/R)^2 \tag{65}$$

where V is the original radial energy. Since in the experiments the filaments were displaced from the center by not more than 1/20th of the radius, V_T for 100 volt primary electrons, cannot have been greater than 0.25 volts.

3. *Effect of earth's field.* The radius of curvature, r, of a V-volt electron in a transverse magnetic field of H gauss is

$$r = 3.36V^{1/2}/H \text{ cm}. \tag{66}$$

If the electron travels a short distance x (small compared to r) perpendicular to the field, the transverse energy, V_T, (in volts) given to the electron by the magnetic field is

$$V_T = 0.089H^2x^2 \tag{67}$$

this energy being independent of the velocity of the electrons. Thus in a tube of 2.6 cm radius (as for the data of Table III and Fig. 7) a transverse field of 0.5 gauss will give a transverse energy of 0.15 volts. Since the electrons which move parallel to the field are not deflected, the primary electrons are thus spread out over a small range. A longitudinal field, however, would give the same transverse energy to all the electrons so would not produce a spread but only a slight displacement of the current-voltage curve.

In our experiments a transverse field of 0.5 gauss may well have been present but this field can have caused only part of the spread in voltage indicated by the lines $B'C'$ in Figs. 7 and 10.

4. *Scattering by ions.* H. A. Wilson[22] in considering the scattering of β-rays by matter has derived equations which are useful in calculating the scattering of electrons by the ions in a gas.

Consider a narrow beam of electrons of energy corresponding to the potential V, passing through a layer of ionized gas of thickness t which contains n univalent charges per unit volume (ions plus electrons). The mean square angular deflection produced by all charges which lie within a distance r of the electron beam is

$$\theta_0^2 = 8\pi nt(r^2/a^2)(1-\pi^2/8+\log a) \tag{68}$$

[22] H. A. Wilson, Proc. Roy. Soc. **A102,** 9 (1923).

where a is a parameter having the value

$$a=2rV/e. \tag{69}$$

In the derivation of Eq. (68) it was assumed that a is large compared to unity and the scattering is thus nearly all due to numerous small deflections, the close encounters which give large deflections being so rare that they contribute little to θ_0. Expressing V in volts, r and t in cm and n in ions per cm^3 we find

$$a=1.39\times10^7 rV$$

and from Eq. (68)

$$\theta_0=1.47\times10^{-6}((nt)^{1/2}/V)(1+0.142\log_{10} rV)^{1/2}. \tag{70}$$

We see that θ_0 becomes infinite if r is infinite so that according to this equation the forces due to the ions at large distances cannot be neglected.

It was assumed in this derivation that the ions were distributed throughout the gas at random. We know, however, from the work of Debye and Huckel[23] that the positive ions tend to accumulate around the negative and vice versa so that the field of a given ion falls to $1/\epsilon$ of the value it should have by Coulomb's law, in a distance λ, which for the case of univalent ions having a temperature T is

$$\lambda=6.92(T/n)^{1/2}\text{ cm}. \tag{71}$$

Thus the value of r in Eq. (70) should be placed equal to λ, since the field due to ions at greater distances cannot be important.

For the example we have considered in Table III and Fig. 7 the positive ion current density I_P corresponding to β_C is 5.3×10^{-5} amps per cm^2. From this by Eq. (1) placing $T_P=3000°$ we find $n_P=0.88\times10^{10}$ ions per cm^3. Since there must be an equal number of negative charges we may take $n=1.76\times10^{10}$. Assuming the temperature T in Eq. (71) (average for electrons and ions) to be 5000°, we find $\lambda=3.7\times10^{-3}$ cm. Taking this for the value of r in Eq. (70) and letting $t=2.6$ cm, the radius of the cylinder we find $\theta_0=0.003$ radians or 0.17° as the mean angular deflection of the electrons due to the electric field of the ions.

The mean transverse energy corresponding to this deflection is $V(\theta_0)^2$ or only 0.0009 volts which is entirely negligible as a cause of the spread of the voltage at which the primary electrons are collected.

5. *Scattering by the field of molecules.* In an electric field of intensity X a molecule becomes a dipole of moment αx where α can be calculated from the dielectric constant D of the gas by the equation

$$\alpha=(D-1)/4\pi n \tag{72}$$

where n is the number of gas molecules per unit volume.

[23] P. Debye and E. Huckel, Phys. Zeits. **24**, 185, 305 (1923).

Because of this polarization, an electron and a gas molecule at a distance r attract one another with the force

$$F = 2\alpha e^2/r^5. \tag{73}$$

An electron which passes a gas molecule with a velocity corresponding to the potential V is thus deflected through an angle θ given by[24]

$$\theta = (3\pi/8)\alpha e/Vr_0^4 \tag{74}$$

where r_0 is the distance of nearest approach. This equation is derived on the assumption that θ is a small angle. The transverse energy $V\theta_0^2$ acquired by the electron is thus

$$V_T = (3\pi/8)^2\alpha^2 e^2/Vr_0^8 \tag{75}$$

expressing V in volts and α and r_0 in terms of cm we find

$$V_T = 2.84\times 10^{-14}\alpha^2/Vr_0^8. \tag{76}$$

The dielectric constant of nitrogen at atmospheric pressure and 0°C is 1.000581, so by Eq. (72) we find for this gas $\alpha = 1.71 \times 10^{-24}$. We have found the probability of collision of electrons with nitrogen molecules at 1000 baryes and 20°C to be 20.0 cm^{-1}. The number of molecules per cm^3 is then 2.48×10^{16} so the target area per molecule is 8.05×10^{-16} cm^2 corresponding to a target radius of 1.60×10^{-8} cm. All 100 volt electrons which pass within this distance of the center of the molecule presumably make elastic or inelastic collisions and are thus acted on by forces which are not of the type we are now considering. We may assume, however, that beyond this distance the force F given by Eq. (73) is effective. Thus placing $r_0 = 1.60 \times 10^{-8}$ cm in Eq. (76) and inserting the value of α we find that the maximum transverse energy that a 100 volt electron can acquire from this force is 0.192 volt.

The transverse energy falls off with a very high power of the distance r_0 so that the effect of multiple scattering is negligible compared with single scattering.

We thus conclude that the scattering due to the forces acting between electrons and molecules resulting from the polarization of the latter, is very small.

6. *Scattering by energy transferred between primary electrons.* It has been shown[25] that with high primary electron current density and low gas pressures the longitudinal energy of some of the primary electrons actually increases as the electrons traverse the space between the cathode sheath and the collector sheath. These electrons may thus reach the collector even when it is many volts negative with respect to the cathode.

In some of the present experiments with hydrogen and argon this effect was studied by varying the electron emission of the cathode from 1 to 90 milliamperes.

[24] F. Zwicky, Physik. Zeitsch. **24**, 171–183 (1923).
[25] I. Langmuir, Phys. Rev. **26**, 585 (1925).

Fig. 11 gives some typical data obtained with a tube having a molybdenum cylinder 5.0 cm in diameter with end plates 5.1 cm apart. The filament diameter was 0.18 mm. The full line curves were obtained with argon at a pressure of 13.4 baryes as indicated on the McLeod gauge, corresponding to 19.1 baryes in the cylinder at 650°K. The anode voltage was 60. Cathode currents, $-i_F$, of 3, 9, 29 and 90 milliamperes were used. To prevent overlapping the ordinates of 3 of the curves were increased by the amounts Δ indicated on the curves.

With a current of only 3 milliamperes the electrons begin to be collected in appreciable numbers when the collector is about 3 volts below the cathode, but as the current is increased to 9, 29 and 90, the voltages at which electrons are first collected become respectively -7, -19 and -32 volts. A more

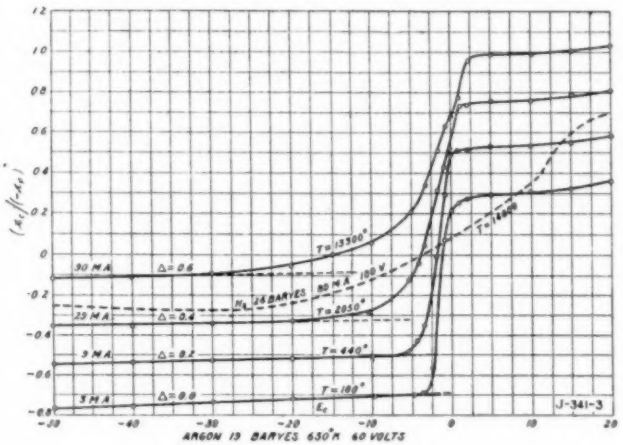

Fig. 11.

rational way of measuring the scattering is to determine[25] the slope of the curve obtained by plotting the electron current against the voltage on probability paper. The square of the reciprocal of this slope divided by 2900 V_0 (V_0 being the energy of the primary electrons in volts) gives the temperature corresponding to the random motion of the electrons which is assumed to be superposed on the translational motion of the beam. The temperatures calculated in this way are indicated on the curves of Fig. 11. The probability plots in these cases were straight only for negative voltages (below about -2 volts) so the slopes were taken from these straight portions.[26] With hydrogen similar effects were obtained as the current density was increased. The dotted curve in Fig. 11 was obtained with the same tube containing hydrogen at 16.4 baryes (24 baryes in the cylinder at 650°K) with a current of 80 milliamperes and an anode voltage of 100.

[26] Experiments have indicated that the deviations from the straight lines at the positive voltages are largely dependent on the fact that a collector is used which nearly completely surrounds the ionized gas. A small disk shaped collector in a discharge in a large spherical bulb gives a much more symmetrical curve which gives a nearly straight probability plot.

This effect was studied at several pressures of argon and hydrogen with various anode voltages. In each case the electron temperatures were calculated from probability plots. A summary of the results are given in Table V. The data given for argon at 19.1 and for hydrogen at 24 baryes are those illustrated in Fig. 11.

The data for argon show that the energy scattering decreases markedly as the pressure is raised, as was previously found for mercury vapor at pressures above 2 baryes[25].

TABLE V

Energy scattering at high currents

Gas	Pressure (baryes at 650°K)	Anode potential	Current $-i_p$	Electron temperatures
Argon	3.9	50 volts	3 ma.	500°K
			9	2000
			30	16000
			90	44000
	19.1	60	3	100
			9	440
			28	2050
			85	13300
	18.6	100.	9	300
			30	2100
			90	12000
	29.	100.	90	6700
Hydrogen	24	100	90	14800
	53	100	9	1200
	53	100	90	70000

On the other hand with hydrogen at a pressure of 53 baryes, a much greater scattering was found than at 24 baryes. With argon, as with mercury vapor, the scattering decreases slightly as the anode voltage is raised.

With 5 ma. emission from the cathode, which was the current usually employed in our studies of electron collisions, the energy scattering effect was always practically negligible.

Effects of current through cathode. In most of the experimental determinations of the current-voltage characteristics of the collector c which have been described, a commutator was used so that there was no current through the filament when the collector current was measured. To avoid the inconvenience of the commutator and the slight irregular variations in current that were sometimes caused by brush trouble, many characteristic curves were made without using the commutator. Two effects are thus introduced, the voltage drop along the filament (about 3-5 volts) caused the breaks in the curves, such as those at B and D in Fig. 7, to be less abrupt, and the magnetic field of the filament current deflects the primary electrons which leave the cathode with energy V_r in a radial direction, so that they acquire axial energy component V_a in the same direction as the motion of the electrons which constitute the heating current in the filament. From the

general equations given by Hull[27] for the motions of electrons near a conductor, we readily find, for the case that V_a is small compared to V_r that

$$V_a = 0.0188 A_F^2 [\log_{10} r/r_F)]^2 \tag{77}$$

where V_a is the axial energy in volts at a distance r from the axis of the filament, r_F is the radius of the filament and A_F is the filament heating current in amperes. The axial energy is thus independent of the anode voltage which determines V_r. The effect of the magnetic field is thus to lower the radial component of the energy by the amount V_a so that the break in the curve (B in Fig. 7) is displaced to the right by the voltage V_a. The experiments show this effect distinctly and in complete agreement with the theory.

The effect of the voltage drop along the filament can be calculated if we know the shape of the volt-ampere characteristic in the absence of this voltage drop. Let i be the current to the cylindrical collector when this is at a voltage E above the cathode and there is no voltage drop along the filament. Let i_M be the measured current when the collector is at a voltage E above the mid-point of the cathode, the voltage drop along the cathode being V_F. Then, if the collector is at a potential above that of the positive end of the filament, we find

$$i_M = (1/V_F) \int_{E-1/2V_F}^{E+1/2V_F} i \, d\, E$$

Expansion by Taylor's theorem and integration gives

$$i_M = i + (1/24) V_F^2 d^2 i/dE^2 + (1/1920) V_F^4 d^4 i/dE^4 + \cdots. \tag{78}$$

If the theoretical relation between i and E is not known, but experiment has given i_M as a function of E, we may use the inverted series,

$$i = i_M - (1/24) V_F^2 \, d^2 i_M/dE^2 + (7/5760) V_F^4 \, d^4 i_M/dE^4 + \cdots$$

and thus obtain the relation between the current and voltage that would exist if there were no voltage drop along the filament.

For the electrons that make elastic collisions, the relation between i and E is given by Eqs. (54) and (53). Eq. (78) can be written

$$\gamma_M = \gamma + (1/24) V_F^2 d^2\gamma/dE^2$$

and by inserting the value of $d^2\gamma/dE^2$ from Eqs. (54) and (53) we find

$$(\gamma = \gamma_M + (1/48) V_F^2 \gamma_\epsilon/(V_0^2 \theta_0^4) \epsilon^{-x} (1 + 1/x) \tag{79}$$

where x is defined by Eq. (53). Since approximate values of θ_0 and γ_ϵ can be obtained from the experimental data by neglecting V_F (or by experiments with a commutator) Eq. (79) can be used to correct the values of γ obtained

[27] A. W. Hull, Phys. Rev. **25**, 652 (1925).

without the use of the commutator. In many cases these corrections have been applied, but usually the corrections are so small as to be unimportant.

Analysis of Current Voltage Curves at Higher Voltages

We have seen from the data of Fig. 3 that in mercury vapor the end plates do not remove any appreciable number of electrons having normal components of energy as large as 80 volts when the primaries have 100 volts energy. We have concluded from this that very few, if any, of the primary electrons are turned through angles as great as 90° by elastic or resonance collisions.

Let us now consider the electrons which begin to be collected when the end plate potential is raised to +20 volts or more. We may make a rough analysis of these groups of electrons by assuming that they consist largely of electrons having a Maxwellian distribution of velocities.

Mutual effect of electron collectors. Let a, b, c and f be the currents from electrodes A, B, C, and F into space, i.e.,

$$a+b+c+f=0. \tag{80}$$

Let a_e and a_p be the electron and positive ion parts of the current from a, so that $a=a_e+a_p$, $b=b_e+b_p$, etc. Let A_a and B_a be the areas of A and B. Then we may write

$$a=A_a I_e \epsilon^{-e(E_s-E_a)/kT}+a_p \tag{81}$$

$$b=B_a I_e \epsilon^{-e(E_s-E_b)/kT}+b_p. \tag{82}$$

Here E_s is the potential of the space which varies with E_a and E_b and is unknown. Eliminating E_s and I_e between Eqs. (81) and (82) we obtain

$$log(b_e/a_e)+log(A_a/B_a)=e(E_B-E_A)/kT \tag{83}$$

We thus plot the electron current to an electrode divided by the electron current to the anode on semi-logarithmic paper against the differences between the collector and the anode voltages. The slope of the straight line through the points gives the temperature or average energy of the electrons, and the ordinate at the space potential divided by the collector area gives the current per unit area of these electrons in space.

We have analyzed the curve marked B in Fig. 3 for the groups of electrons having a Maxwellian distribution of velocities. The curve B represents the current to the end plates A and B when they are in parallel and the potential is varied. The cylinder C was anode in this case.

The electron current to the end plates divided by the electron current to the anode was plotted on semi-logarithmic paper against the differences between the collector and anode voltages. The points lie on a straight line between 30 and 88 volts. The slope of this straight line gives a temperature of 358000 degrees for this group of electrons which we designate the first Maxwellian group.

The experimental points begin to deviate upward from the straight line above 88 volts. By plotting the current differences between these points and the extrapolated straight line, against the differences between the collector and anode voltages on a semi-logarithmic scale we find that the points lie on a straight line between 90 and 96 volts. This straight line has a slope corresponding to a temperature of 30500 degrees for a second Maxwellian group. By again plotting the differences in current between the experimental points and the extrapolated straight line of the second Maxwellian group on a semi-logarithmic scale, we obtain points which lie on a straight line between 96 and 100 volts. The slope of this line corresponds to a temperature of 7150 degrees for this low velocity group of electrons. We designate this group of electrons as the "Ultimate Electrons" since they are always present in any type of electron discharge in gases, carry practically the entire current and neutralize the space charge created by the relatively low velocity positive ions produced as a result of ionization of the gas molecules.

The curve marked B in Fig. 2 has also been analyzed into three Maxwellian groups of electrons. The first Maxwellian group is measurable when the potential of the cylinder C is raised above $+20$ volts. The temperature of this group is 350000 degrees. The second group appears above 88 volts on the collector and has a temperature of 31000°. The third Maxwellian group or the "ultimate electrons" are collected at potentials above 96 volts on the collector and have a temperature of 6900 degrees.

The area of the end plates A and B are 7.0 cm² each and the area of the cylinder C is 37.0 cm² in the experiments shown in curve B, Figs. 2 and 3.

The positive ion current collected on $A+B=4.46\times10^{-4}$ amps or 3.18×10^{-5} amps. cm^{-2} at $+100$ volts potential. By extrapolation we find that in curve B, Fig. 3, 0.4×10^{-5} and 0.44×10^{-5} amps. cm^{-2} of Maxwellian groups 1 and 2 are collected by $A+B$ at $+100$ volts. Similarly the total electron current collected by $A+B$ at 100 volts is 8.18×10^{-5} amps. cm^{-2}. By difference there is 7.34×10^{-5} amps. cm^{-2} of ultimate electrons collected at 100 volts. Hence there are 2.31 electrons for every positive ion collected at 100 volts. At the potential of the space according to Eq. (1), there should be $(T_e m_p/(T_p m))^{1/2}$ or 855 electrons collected to 1 positive ion if $T_p=(1/2)T_e$.

From the Boltzmann Eq. (3), $\log_e n_1/n_0 = Ve/kT$ we have $\log_e(855/2.31) = Ve/kT$, and thus since $T=7150°$, $V=3.65$ volts.

Therefore there is a positive ion sheath with a potential of 3.65 volts when the plates $A+B$ are at the anode potential, i.e., 100 volts positive with respect to the cathode Thus there is a negative anode drop of 3.65 volts. Each collector in the discharge is then receiving all positive ions headed toward it and repelling all electrons which are not able to penetrate through the 3.65 volt sheath.

From Eq. (1) we have $n_p=(4.03\times10^{13}\times3.18\times10^{-5}\times606)/(3570)^{1/2}=1.30\times10^{10}$ positive ions per cc per ma. of emission current.

Similarly the density of electrons in the various groups in space are $n_{e(1)}=2.9\times10^{5}$/cc ma.; $n_{e(2)}=4.1\times10^{6}$/cc ma.; $n_{e(ult)}=1.30\times10^{10}$/cc ma. Thus

we observe that the ultimate electrons neutralize the positive ion space charge and practically the entire current in the discharge is carried by them.

The positive ion current to the collector C is equal to 5.13×10^{-5} amps. cm^{-2} at 100 volts on C in curve B, Fig. 2. The total electron current to C at 100 volts is 2.90×10^{-3} amps. Of this current 5.4×10^{-5} and 4.5×10^{-5} amps. belong to Maxwellian groups 1 and 2 respectively, leaving 2.8×10^{-3} amps. of ultimate electrons, which is equivalent to 7.57×10^{-5} amps. cm^{-2}. Hence there are 1.48 electrons to 1 positive ion collected at 100 volts.

Therefore assuming $T_p=(1/2)T_e$, we have $\epsilon^{Ve/kT}=574$, or $V=3.78$ as the retarding potential for electrons in the sheath when the collector is 100 volts positive with respect to the cathode.

From Eq. (1) we have $n_p=2.10\times10^{10}$/cc ma. emission. Similarly the density of electrons in the various groups in space are $n_{e(1)}=1.8\times10^{5}$/cc ma. emission; $n_{e(2)}=9.1\times10^{6}$/cc ma. emission; $n_{e(ult)}=1.75\times10^{10}$/cc ma. emission.

We have repeatedly checked this method of calculating the negative anode drop in our experiments by means of the probe wire method of Langmuir and Mott Smith.[5]

For example in a typical experiment in mercury vapor at 17.3 baryes, the end plate A and the cylinder C were placed at 100 volts positive with respect to the cathode. A plot of the logarithm of the electron current against the voltage of the probe wire which was at a distance of one cm from the cathode gives us the average temperature of the ultimate electrons. Thus $T_e=3900°K$ in this case and E_s the potential of the space about the probe is 1.25 volts positive with respect to the anode. We find also that $I_e=0.51$ ma. of ultimate electrons per cm^2 per ma. emission, and $n_{e(ult)}/=3.3\times10^{8}$ electrons per cc at the probe wire per ma. emission from the cathode.

The average current density of ultimate electrons reaching the anode is 0.013 ma. cm^{-2} per ma. emission from the cathode. Hence from Eq. (3) the anode is 1.07 volts negative with respect to the space near the collector. This agrees well with the probe wire measurement and also with the results calculated from the volt-ampere curves of the end plates and cylinder.

From the results obtained by analysis of the volt-ampere characteristics of both end plates and cylinder we may draw certain general conclusions. For example, when an electron having 100 volts energy strikes a mercury atom in such a manner that the atom gives up an electron and becomes a positive ion, there is, of course, a 10.4 volt loss by the incident electron in producing an ion. The remaining 90 volts energy is distributed between the incident electron and the electron given up by the mercury atom. The incident electrons and the electrons given up by the atoms give rise to the high velocity Maxwellian group of electrons which become random in direction and in the cases which we have considered have an average energy of about 45 volts.

Additional evidence of the formation of this high velocity Maxwellian group is obtained from the detailed analyses of the curves shown in Figs. 7 and 10. From these curves we see that the experimental curve deviates

gradually from the theoretical curve starting at the ionizing potential in each case.

Fig. 12 shows typical experimental curves in each of the different gases studied. The collector potential, E_c, is plotted against $i_c/-i_f$ in each case.

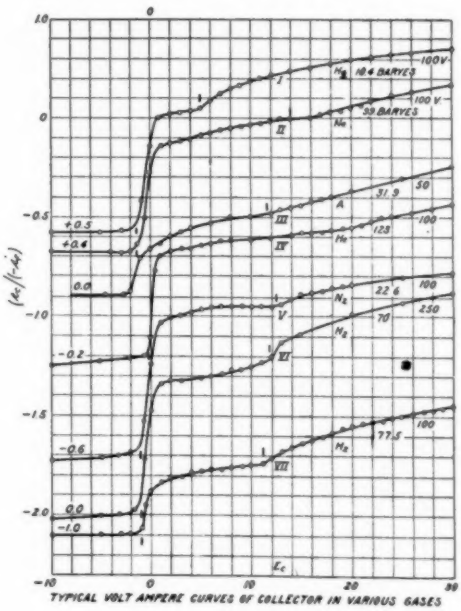

Fig. 12.

The curves have been shifted vertically by the amount indicated at the left end of each curve to prevent over-lapping. For example, curve 1 gives the results obtained in mercury vapor at 10.4 baryes pressure with the anode A at $+100$ volts potential, the curve having been shifted up 0.5 along the ordinate axis.

TABLE VI

Ionization and resonance potentials of various gases used

Gas	Obs. Res. Pot.	Ion. Pot.
Hg	6.7 volts	10.4 volts
Ne	18.5	21.5
A	13.0	15.3
He	21.1	24.5
N_2	13.0	16.8
H_2	12.8	16.1

The resonance potentials at which the kinks appear on the curves for the various gases have been determined from these curves and also from the large scale plots used in the detailed analysis of the groups suffering elastic and inelastic collisions. These potentials are given in Table VI and are probably correct to ± 0.5 volt.

Fig. 13 shows the experimental curves obtained with nitrogen at a series of different pressures. The anode (A) voltage was +75 volts in each case. The curves have been raised along the ordinate by the amounts indicated

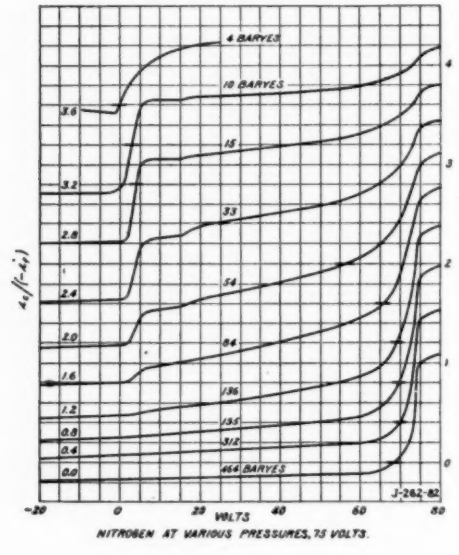

Fig. 13.

on the left side of the curves, the ordinate scale being at the right. The curves at the higher pressures show that no primary electrons reach the cylinder C without having suffered energy losses. As the pressure is decreased, the

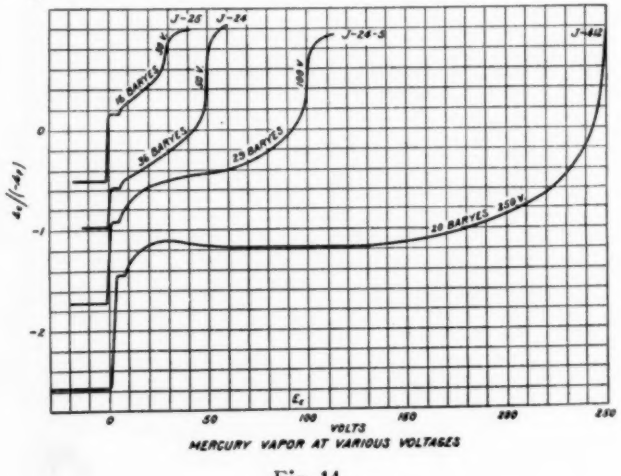

Fig. 14.

primary electrons begin to reach C without loss of energy until finally at 4 baryes pressure the intensity of ionization falls off rapidly at positive voltages on the collector because of the removal of nearly all the primary

electrons before they form ions and thus the positive ion sheaths around the cathode and cylinder over-lap, the current from the cathode drops suddenly to the "space charge" value and our theory no longer applies.

Fig. 14 shows the curves obtained in mercury vapor at a series of different anode voltages. The decrease in current values between +30 and +70 volts on the 250 volt, 20 barye curve is due to the fact that the reflection coefficient of the collector for electrons increases with the electron velocity. The constancy of the positive ion currents collected at negative voltages on the collector, the sharpness of the break at the resonance potential (6.7

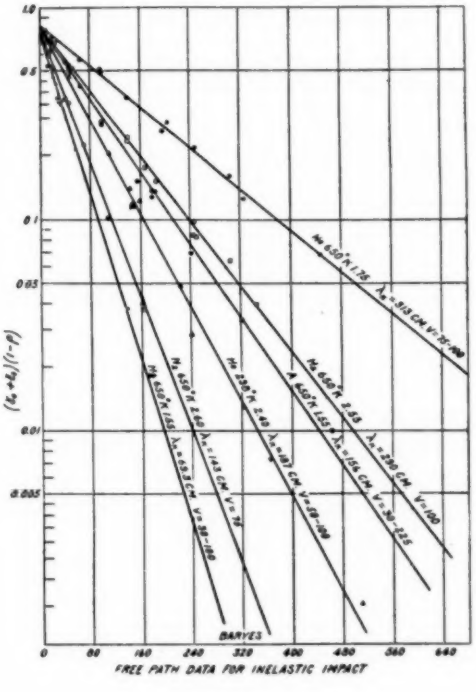

Fig. 15.

volts) and the relatively large number of electrons which suffer a 6.7 volt energy loss show up particularly well in these curves.

Electron Free Paths

The experimental data on the mean free path of high velocity electrons (above the ionizing potential) in the various gases give results in good agreement with the kinetic theory value calculated from viscosity measurements (i. e., $4\cdot(2)^{1/2}$ times the free paths of the gas molecules.)

We have plotted $(\gamma_0+\gamma_e)(1-\rho)$ against the gas pressure in baryes on a semi-logarithmic scale in Fig. 15. This quantity is the fraction of the primary electrons which are collectable by C without having made *inelastic* collisions with molecules and is thus given directly by the experiments when collector voltages just below the resonance potential are used.

Since the free path is inversely proportional to the pressure, we see readily from Eq. (32) that the slope $d \log_e y/dx$ of the lines of the semi-logarithmic plot of Fig. 15 should be R/λ_1, where R is the effective radius of the collector C and λ_1 is the free path of the electrons for inelastic collisions at unit pressure. The intercept of these lines on the vertical axis which corresponds to $1-\rho$ ranges from 0.77 to 0.83. Hence, ρ, the reflection coefficient of the collector for electrons striking with a velocity corresponding to ten to twenty volts varies from 0.17 to 0.23 in good agreement with the values derived from Eq. (58).

The values of λ_1 in cm calculated from the slopes of the lines are given in the 5th column of Table VII. These correspond to a pressure of 1 barye and the temperatures given in the second column. The electron free paths at the same temperature and pressure calculated from the viscosities are given in the 6th column. It is seen that the two sets of values agree rather closely.

In the last column of Table VII are the values of P_k, the probability of inelastic collision per cm at 20°C and 1000 baryes pressure, calculated from λ_1 by assuming that the probability is proportional to the density.

TABLE VII

Free paths for inelastic collisions.

Gas	T°K	R	Anode Voltage	λ_1	Kinetic Theory	P_k
Ne	650	1.75cm	75 and 100	313	288	7.1
H_2	650	2.55	100	290	266	7.6
A	650	1.55	30 50 100	156	160	1.4
He	298	2.40	50 100	187	166	5.4
N_2	650	2.60	75	143	146	1.5
Hg	650	1.55	30 50 100	69.3	72.9	32

We have summarized the results of the detailed analyses of more than two hundred sets of volt ampere characteristic curves for the various gases studied. The final results, expressed in each case at 1000 baryes pressure and 293°K are given in Table VIII. The various quantities in this table have all been defined with the exception of β (max.) The values of θ_r, the mean deflection for a single resonance collison, which appears in brackets, have been assumed to be the same as the mean deflection for a single elastic collision in order to obtain a reasonable value for P_r.

The value β (max.) gives the maximum number of ions which can be produced by an electron having a velocity corresponding to the potential given in the second column. The quantity β is independent of the pressure over a very wide range of pressures. At very low pressures, however, β decreases due to the fact that the sheaths around the cathode and the collector become so thick due to the low intensity of ionization that the electrons travel appreciable distances (compared to the tube radius) in the sheaths, (both in being decelerated and in being accelerated) in which the electrons will not have sufficient energy to produce an ion. If an inelastic collision

occurs under these conditions the electron will suffer a resonance energy loss instead of producing an ion. Then also at low pressures a larger proportion of the electrons will reach the anode while they still retain enough energy to cause ionization.

At pressures above the range in which β remains constant, β again decreases in value. From the theory of the diffusion of ions in ionized gases

TABLE VIII

Summary of data on electron impacts in gases

Gas	Volts	P	P_k	P_e	P_r	P_i	P_x	θ_e	θ_r	E_e	β_{max}
He	50	7.4	5.8	1.6	2.1	0.7	3.0	25	[25]	9.5	1.2
	100	5.6	4.5	1.1	0.5	1.22	2.78	19	16	11	2.9
Ne	75	7.9	7.0	0.9	1.1	1.38	4.52	21	21]	9.8	1.25
	100	7.6	6.9	0.7	1.0	1.80	4.1	19	[19]	11	2.0
A	30	32.4	14.3	18.1	4.4	3.5	6.4	24	[24]	5.3	0.45
	50	29.4	13.8	15.6	1.4	7.1	5.3	18	[18]	5.2	0.9
	100	24.9	14.0	10.9	1.3	8.55	4.15	12	[12]	4.7	1.65
	150	23.4	13.8	9.6	2.0	8.55	3.25	10	[10]	4.5	2.2
Hg	30	61.	36.	25.	13.	10.2	12.8	17	[17]	2.5	1.1
	50	59	36.9	22.1	11.0	14.9	11.0	11	13	3.1	1.4
	100	57.2	37.8	19.4	12.5	16.3	9.0	10	12	3.3	2.7
	250	40	24.	16.	5.0	15.3	3.7	6	[6]	3.2	5.3
H_2	100	10.9	6.9	4.0	2.6	2.9	1.4	5	16	7.3	1.45
	250	10.1	5.4	4.7	1.6	2.7	1.1	9	5	6.7	2.8
N_2	75	26.4	15.2	11.2	4.0	7.0	4.2	16	[16]	5.9	1.32
	100	20.0	12.2	7.8	3.6	7.7	0.9	14	18	5.8	1.65

due to Schottky and Issendorff[2] we find that, where the free paths of the electrons become small compared to the radius of the tube, the cathode may receive as many, or more ions than the collector. The current (i_F) must then be corrected for the large number of ions flowing to the cathode to obtain the true electron emission. When this correction is made and the pressure is not such that the electrons suffer an appreciable number of collisions in the sheaths we find that β agrees approximately with β(max).

In some experiments to test the constancy of β, the electron emission from the cathode ($-i_F$) was varied over a range of five hundred fold without changing the value of β. β being independent of the current density of primary electrons indicates that ionization is a single stage process in our experiments and that no two stage processes are effective in producing any measurable number of ions. It also indicates that recombination of electrons and ions is negligible under the conditions of these experiments up to 1000 baryes pressure.

The authors wish to take this opportunity to correct an erroneous statement made in a preliminary article in Science.[3] In this article it was stated that 60 or even 70 percent of the primary electrons lose nearly all of their energy on their first collisions with atoms producing a highly excited

atom or ion which subsequently caused the ionization of several other atoms. This incorrect statement resulted from our having neglected to consider the change in the reflection coefficient of electrons from the collector with voltage. As a result of our detailed analyses of the experimental curves with the reflection coefficient for each group of electrons treated separately we may safely say, that, if any electrons lose all of their energy in the first collision with an atom, the number suffering such energy loss is small.

The reflection of electrons from the collectors in our experiments is important because the ion sheaths which cover all electrodes (even the anode) act as *accelerating* grids to return the electrons to the field-free space where after reflection and *acceleration* through the positive ion sheath, it may have sufficient energy to cause ionization, resonance, etc. This is not true, however, under negative space charge conditions where the field is positive right up to the collector and any reflected electrons are trapped and collected. Thus, under negative space charge conditions in good vacuum, the three halves power law holds over a wide range of voltages.

The authors take pleasure in extending their thanks to Mr. H. M. Mott-Smith, Jr., for valuable assistance with the mathematical derivations, and to Mr. W. G. Baker for many helpful suggestions rendered during the course of the experimental work.

RESEARCH LABORATORY,
GENERAL ELECTRIC COMPANY,
SCHENECTADY, NEW YORK.

ENERGY DISTRIBUTION OF SECONDARY ELECTRONS FROM COPPER, IRON, NICKEL AND SILVER.

By H. E. Farnsworth

Abstract

This is an extension of previous experiments. An improved form of tube was used from which certain former disturbing factors were eliminated. The energy distribution curves show no evidence of the existence of inelastic collisions, but are found to vary with the metal and to be different for the metal before heating at red heat than after. When the primary voltage is less than about 35 or 40 volts, which varies somewhat with the metal, there are practically no electrons escaping from the metal which have just sufficient energy to do so, but all have an energy of 0.5 equivalent volt or more in excess of that required to escape. A possible interpretation of this result is given.

Introduction

THE experiments here described are a continuation of an attempt to obtain an accurate measure of the energy distribution of secondary electrons from metal surfaces.[1] The especial interest in these experiments developed as a consequence of the results obtained on the magnitude of the secondary electron current from copper and iron as a function of primary or bombarding potential. The curves expressing this relation for these metals were found to have unusual maxima and minima in the low voltage region. As previously pointed out,[1] if these changes in slope have their origin in atomic inelastic collisions similar to those which occur in the vapor state of a metal, one might expect that such inelastic collisions would also result in a characteristic energy distribution of the secondary electrons. Hence, an accurate knowledge of the energy distribution of secondary electrons for low primary voltages should be of value in determining the cause of the unusual secondary electron characteristics mentioned above.

The writer's previous experiments were not decisive for experimental reasons. The results here described were obtained with an improved apparatus from which the disturbing factors of the former apparatus were eliminated. Because of the nature of the results obtained for copper and iron, it seemed advisable to repeat former observations on nickel[2] with the present apparatus. In addition, results on a silver target were obtained.

Apparatus and Procedure

A diagramatic cross-section of the tube is shown in Fig. 1. The advantages of this tube over those previously used are: (1) a new method of obtaining a more intense beam of low velocity electrons with no scattering;

[1] H. E. Farnsworth, Phys. Rev. **25**, 41 (1925); **27**, 413 (1926).
[2] H. E. Farnsworth, Phys. Rev. **20**, 358 (1922).

(2) the use of a larger sphere and a smaller target so that a more nearly radial electric field may be established between them.

A description of the cathode and focusing arrangement, together with measurements on energy distribution of primary electrons, is given elsewhere.[3] C is an insulated diaphragm which forms a part of the sphere D. The Faraday cylinder F and shield E, indicated by the dotted lines, were inserted at first so that measurements could be made on the primary electron beam and were than replaced by the target T. As in former tubes, the target was mounted on quartz rods (not shown in the diagram) and could be removed into the side tube by a magnetic control and there separately heated by high-frequency induction. Evaporated metal was prevented from entering the sphere by a metal diaphragm which was automatically raised in the tube between the sphere and target when the target was pulled back.

The energy distribution of secondary electrons, for a given primary voltage between the cathode and target, was obtained by measuring the

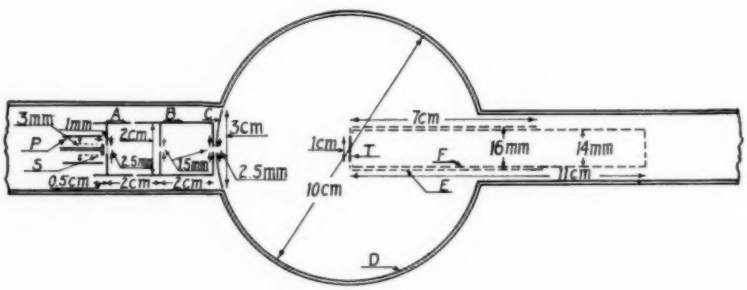

Fig. 1. Apparatus.

ratio of the secondary current (to C and D) to the primary current (to C, D, and T,) as a function of a variable retarding potential on B, C, and D. B and C were kept at the same potential to eliminate scattering in the space between them. Measurements obtained when A was kept at a constant potential with respect to B and C were the same as those obtained when A was kept at a constant potential with respect to the target and ground. The latter method gave the larger primary currents. While obtaining the results given here, A was kept at $+7.5$ volts with respect to the target.

The usual secondary electron curve could be obtained by measuring the above ratio as a function of a variable accelerating potential difference between S and T with B, C, D, and T at zero potential. Multiple reflection between the sphere and target was neglected, but that this must have been small is shown by the sharpness of the breaks in the secondary electron curves. The diaphragm C was covered with sputtered platinum, as was also the inner surface of D, so that their reflection characteristics should have been the same.

Liquid oxygen was used to prevent mercury vapor from entering the tube. A mercury vapor pump, backed by an oil pump, kept the pressure

[3] H. E. Farnsworth, J.O.S.A. & R.S.I. **15**, 290 (1927).

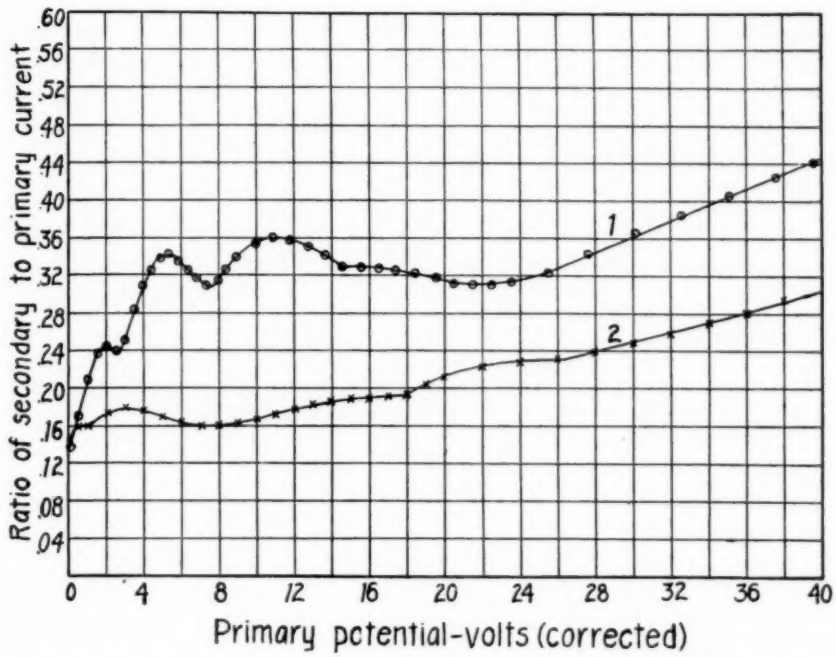

Fig. 2. Secondary electron curves. Curve 1 is for a copper target after red-heat treatment. Curve 2 is for a nickel target after red-heat treatment.

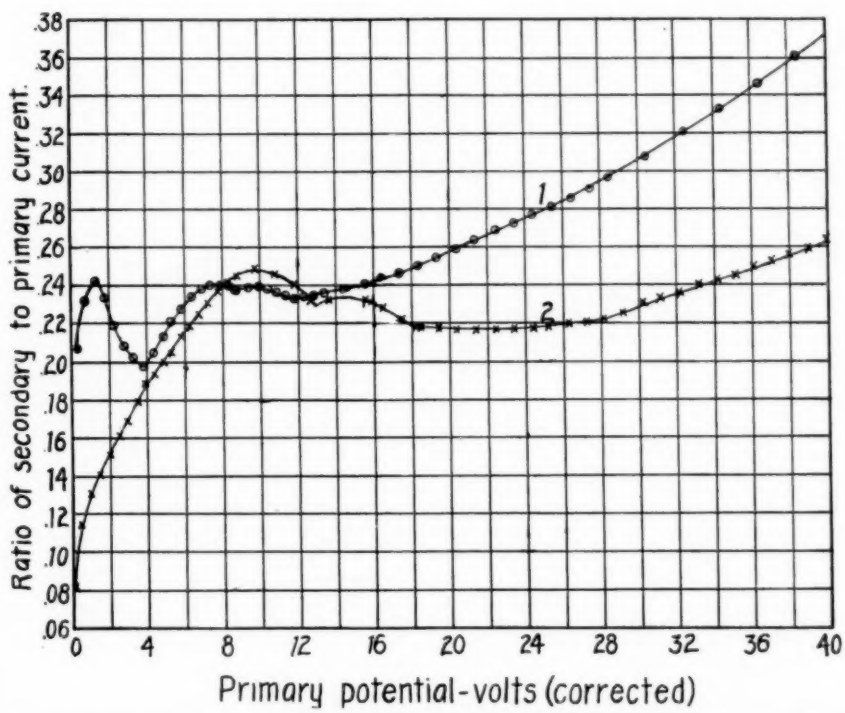

Fig. 3. Secondary electron curves. Curve 1 is for an iron target after red-heat treatment. Curve 2 is for a silver target after red-heat treatment.

less than 10^{-7} mm Hg during observations. During some of the early measurements a ground glass joint was attached at one end of the tube which was sealed on the outside with Khotinsky wax. The joint was later removed and the former measurements checked. While the joint was attached, the tube was exhausted at both ends. Helmholtz coils were used to compensate the earth's magnetic field.

Results and Discussion

Results on the ratio of secondary to primary current, as a function of primary voltage, for Cu, Fe, Ni and Ag are shown in Figs. 2 and 3 for reference. Values of the primary voltage have been corrected. The curves for Cu and

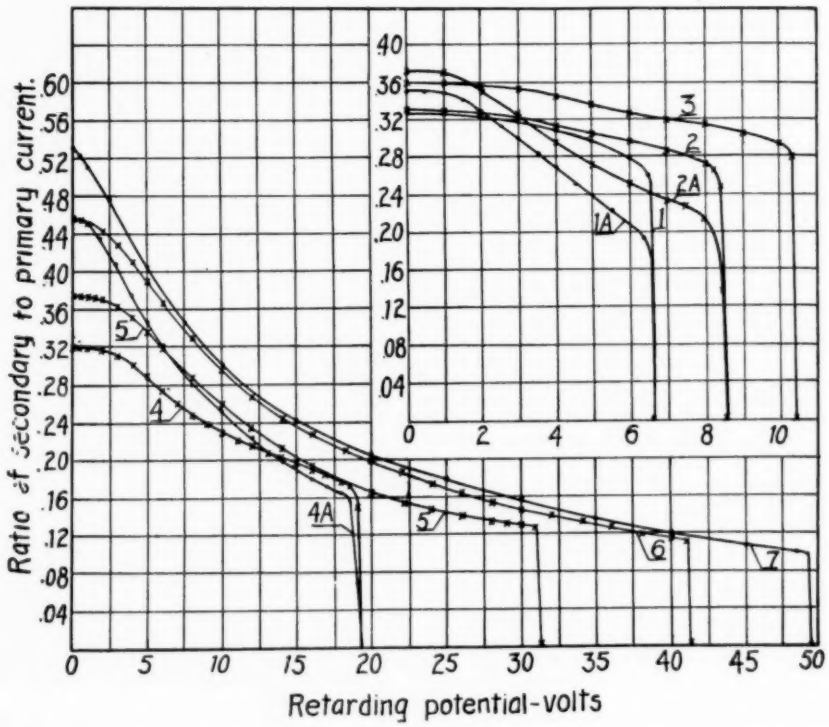

Fig. 4. Energy distribution of secondary electrons from copper. Curve 1, 1A for 6.6 volt (corrected) primary electrons, curve 2, 2A for 8.5 volt electrons, curve 3 for 10.4 volt electrons, curve 4, 4A for 19.0 volt electrons, curve 5 for 31.2 volt electrons, curve 6 for 41.2 volt electrons, curve 7 for 49.2 volt electrons. Curves 1A, 2A, and 4A are for targets subsequent to baking at 350°C, but previous to red-heat treatment. The other curves were obtained subsequent to red-heat treatment of the target.

Fe are similar to those previously obtained,[1] while those for Ni and Ag show more breaks than were obtained with a tube used several years ago.[2]

Energy distribution of secondary electrons from Cu, Fe, Ni, and Ag are shown in Figs. 4, 5, 6 and 7, respectively. Measurements on energy distribution were made for each metal after it had been heated at red heat until the characteristic secondary electron curves shown in Figs. 2 and 3 were obtained.

The above measurements were also made for Cu, Ni and Ag before heating the metals at red heat, but subsequent to baking them at 350°C for several hours. The actual distribution curves, obtained by plotting slopes of the curves shown as ordinates, are not given but their general shapes are apparent. The results on energy distribution of secondary electrons may be summarized as follows:

(1) *No evidence was obtained of critical potentials such as was formerly thought to exist.* The former evidence, because of the inferior tube used,

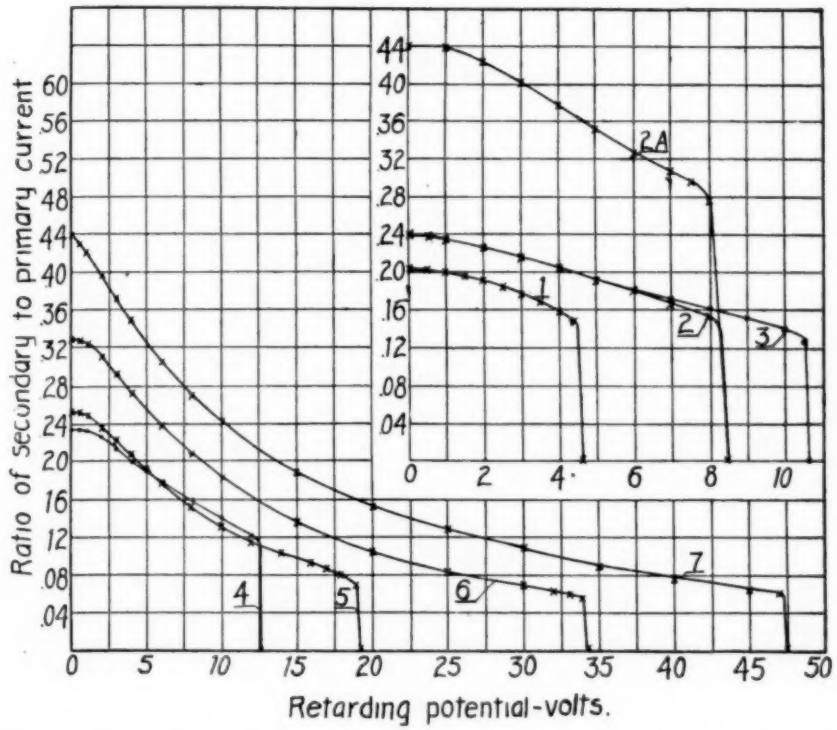

Fig. 5. Energy distribution of secondary electrons from iron. Curve 1 for 4.6 volt (corrected) primary electrons, curve 2, 2A for 8.4 volt electrons, curve 3 for 10.6 volt electrons, curve 4 for 12.5 volt electrons, curve 5 for 19.0 volt electrons, curve 6 for 34.0 volt electrons, curve 7 for 47.4 volt electrons. Curve 2A is for a target subsequent to baking at 350°C, but previous to red-heat treatment. The other curves were obtained subsequent to red-heat treatment of the target.

must then be considered as spurious. One may be led to either of two conclusions: (A) Inelastic collisions occur at the potentials corresponding to the maxima of the secondary electron curve even though no evidence of them is obtained by a measure of energy distribution. This would mean that those electrons which make inelastic collisions lose all of their energy on collision, or are unable to leave the metal even though they retain some energy after collision. (B) The results are not due to atomic inelastic collisions, but to an apparent selective reflection which depends on the structure

of the metal and the energy of the incident electrons. An apparent selective reflection might result from a diffraction phenomenon indicated by results of Davisson and Germer.[4] Brinsmade[5] has also observed a reflection maximum for those electrons leaving an aluminum target in a direction at right angles with the primary beam. Conclusion (B) appears to be much more probable since other results [1,6] indicate that the structure is the determining factor in the appearance of the secondary electron curve.

(2) *For primary voltages below a certain limiting value, which varies with the metal, most of the secondary electrons have energies approximately equal*

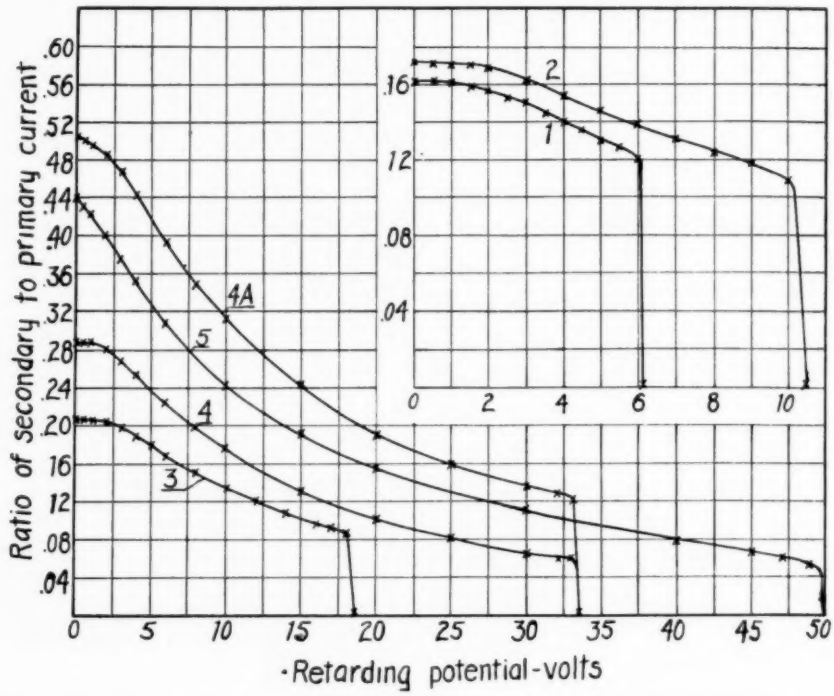

Fig. 6. Energy distribution of secondary electrons from nickel. Curve 1 for 6.2 volt (corrected) primary electrons, curve 2 for 10.4 volt electrons, curve 3 for 18.6 volt electrons, curve 4, 4A for 33.5 volt electrons, curve 5 for 50.0 volt electrons. Curve 4A is for a target subsequent to baking at 350°C, but previous to red-heat treatment. The other curves were obtained subsequent to red-heat treatment of the target.

to the average primary energy. The limiting value is higher for silver than for the other three metals tried.

(3) *As the primary voltage is increased beyond this limiting value, there appear, in addition to the general distribution, two groups of secondary electrons;* the first occurs at a retarding potential of a few volts and the second at a retarding potential nearly, if not quite, equal to the primary potential. The

[4] Davisson and Germer, Nature **119**, 558 (1927); Phys Rev. **30**, 705 (1927).
[5] Brinsmade, Phys. Rev. **30**, 494 (1927).
[6] H. E. Farnsworth, Phys. Rev. **31**, 419 (1928).

relative number of electrons in the first group increases while that in the second group decreases as the primary voltage is increased. The present results for Cu and Ni differ from those previously obtained for these metals in regard to the position of the first group mentioned above. In the results formerly obtained [1,2], the maximum of the first group occurs at very nearly a zero value of the retarding potential. In the present results for these metals, as well as for Fe and Ag, the maximum occurs at a higher value which varies with the metal and primary voltage. As the primary voltage is increased from

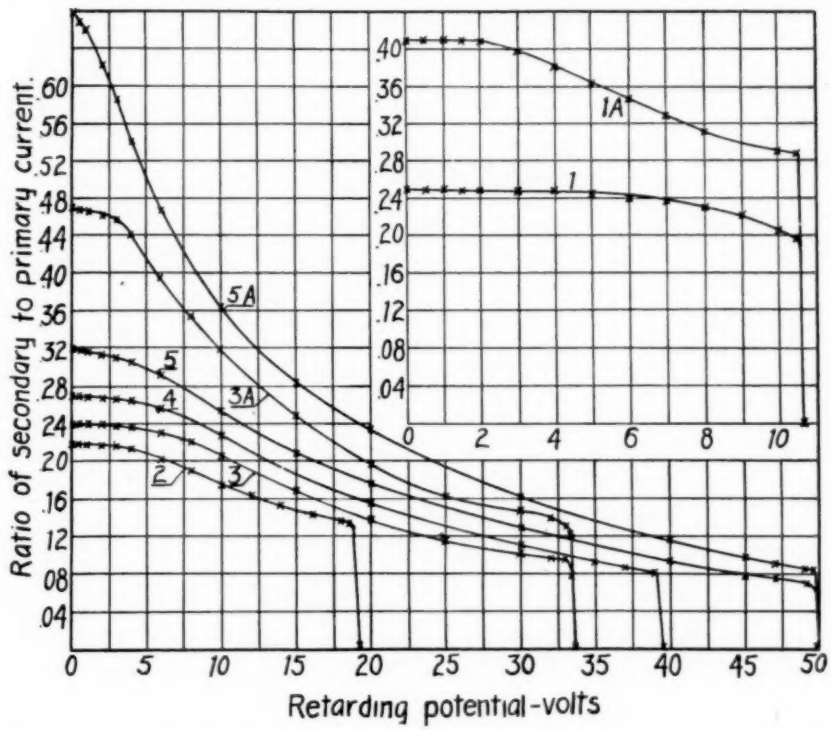

Fig. 7. Energy distribution of secondary electrons from silver. Curve 1, 1A for 10.6 volt (corrected) primary electrons, curve 2 for 18.7 volt electrons, curve 3, 3A for 33.5 volt electrons, curve 4, for 39.0 volt electrons, curve 5, 5A for 50.0 volt electrons. Curves 1A, 3A, and 5A are for targets subsequent to baking at 350°C, but previous to red-heat treatment. The other curves were obtained subsequent to red-heat treatment of the target.

the limiting value to 50 volts, this maximum moves first slightly toward higher and then toward lower retarding potentials, and becomes much broader. In general, it occurs between about 3 and 12 volts for the region investigated. It seems likely that the initial shift toward higher retarding potentials is due to the fact that, for the lower primary voltages, this group consists chiefly of scattered primary electrons which have lost some energy and that the average energy which they retain increases with the primary voltage. The subsequent shift toward lower retarding potentials is then due to an increasing number of emitted electrons whose average energy ap-

parently decreases with increasing primary voltage. For the same primary voltage, the retarding potential corresponding to the maximum of the first group is higher for silver than for any of the other metals tried. The relative number of electrons in the second group is also greatest for silver. The reason for the difference between the present results and those previously obtained is due to the fact that the former tubes did not permit a radial retarding field. This condition causes the indicated value of the average electron energy to be less than the true value.

Brinsmade[5] and Sharman[7], both using the magnetic deflection method, have observed the two groups of secondary electrons. Since the position of the first group varies with the metal, the previous heat treatment of the metal, the primary voltage and probably the angle of emission, a quantitative comparison of their results with the present ones cannot be made, but they appear to be in at least qualitative agreement.

(4) *There are practically no secondary electrons having energies very nearly zero for primary voltages less than about 35 or 40 volts (this varies somewhat with the metal), for any of the four metals.* This seems especially significant, for it denotes that for primary voltages below the above value there are practically no electrons escaping from the metal which have just sufficient energy to do so, but each of those escaping has an energy which exceeds that required to escape by 0.5 or more equivalent volts. This result cannot be a spurious effect caused by the target assuming a negative potential with respect to its surroundings. Although the target was found to be at a negative potential after it had been heated at red heat, this potential was compensated by an applied positive potential while observations were made. As mentioned above, the electrons in the first group probably consist of both scattered primaries, which have lost some energy, and emitted electrons. Taking the final upward rise of the secondary electron curves in Figs. 2 and 3 as being due to an increasing emission, it is apparent that the emission is appreciable for primary voltages considerably below 35 or 40 volts. The results then indicate that all electrons which are emitted from the metal possess energy, immediately after collision, in excess of the equivalent work function of the metal by a certain minimum value, but that, as the primary voltage is increased, electrons are emitted from greater depths and consequently lose more energy before escaping from the metal. This latter condition accounts for the decrease in the average energy of electrons emitted at the surface with increasing primary voltage.

Brinsmade[5] and Sharman[7] both attribute the small number of very low speed secondary electrons in their results to the action of surface forces. It is difficult to see how surface forces might account for the absence of low speed electrons at primary voltages below about 35 or 40 volts and the presence of such electrons about this voltage, as was found in the present experiments.

[7] Sharman, Proc. Camb. Phil. Soc. **23,** 523 (1927).

From measurements on a blackened platinum surface, A. Becker[8] has concluded that the electrons emitted from such a surface have a distribution in energy which is independent of the average energy of the incident electrons, the most probable value being that corresponding to about 2 volts. The present results show that this is not the case for a pure metal which has been thoroughly outgassed.

(5) *The energy distribution of secondary electrons before and after heating the target at red heat is not the same, the percent of low energy electrons being greater before heating than after.* This means that the increased secondary current due to gas on the surface before heating consists chiefly of low energy electrons. Since this is true for all primary voltages tried (0–50 volts), both above and below the ionizing potential of the gas, it follows that the relative number of emitted electrons, as well as the fraction of scattered primary electrons which have lost some energy, is greater for a gas covered surface than for a gas free surface. This is true for the metals Cu, Ni, and Ag. No observations for Fe were obtained previous to heating the target at red heat. It is interesting to note that Jackson[9] has found the electron emission due to positive ion bombardment to be greater from a gas covered surface than from a degassed metal.

It is a pleasure to record here my thanks to Professor A. deF. Palmer and especially to Professor F. G. Keyes, for their interest and assistance in procuring necessary apparatus and material for continuing my investigations in this laboratory.

BROWN UNIVERSITY,
PROVIDENCE, R. I.,
November 1927.

[8] A. Becker, Ann.d. Physik, **78**, 228 (1925).
[9] W. J. Jackson, Phys. Rev. **30**, 473 (1927).

LARGE ANGLE SCATTERING OF LOW VELOCITY ELECTRONS FROM COPPER, IRON, NICKEL AND SILVER.

By H. E. Farnsworth

Abstract

The apparatus permitted a measure of the relative number of electrons leaving the target at angles between 163° and 179° with the primary beam. Measurements were taken at low primary voltages for which the number of emitted electrons is negligible, so that the electrons measured are primary electrons which have been scattered through large angles. For normal incidence the large angle scattering is greater than that necessary to satisfy the cosine law for the metals Cu, Fe, Ni, Ag after they have been heated at red heat in a vacuum, and is different for each metal. Subsequent to baking the tube at 350°C, but previous to heating the target at red heat, the large angle scattering is nearly the same for the four metals and approximately in accordance with the cosine law. The change in large angle scattering appears to be due to a change in the structure of the surface rather than to elimination of gas. For 45° incidence on a copper target, the scattering back in the direction opposite to that of the primary beam is less than for 90° incidence, but the direction of the surface normal is not the only determining factor in the scattering.

McCLELLAND[1] observed many years ago that, when β-rays strike a metal target at normal incidence in a vacuum, the number of electrons leaving the target in any direction is closely proportional to the cosine of the angle between that direction and the normal. This result is to be expected, since the electrons, from an element of volume at a depth in the plate, traverse a thickness inversely proportional to the cosine of the angle between its direction and the normal. Tate[2] observed that, for all angles of incidence and for primary voltages up to 50 volts, the secondary emission from a platinum target is maximum in a direction very nearly straight back on the incident beam, and decreases to zero in directions parallel to the surface of the target. Results of Davisson and Kunsman,[3] and Davisson and Germer,[4] show that reflected electrons, which have been separated from emitted electrons, have a unique angular distribution which depends on the metal and the primary voltage, especially when the latter is more than a few volts. For primary voltages at which the number of emitted electrons greatly exceeds that of the reflected electrons, any unique distribution of reflected electrons would be masked by the effect of the emitted electrons unless the two classes of electrons are separated. Hence, the cosine law would be expected to apply very closely when the relative number of emitted electrons is great. Since measurements on energy distribution,[5] however, show that the relative number of emitted electrons becomes very small for primary

[1] McClelland, Proc. Roy. Soc. **80**, 501 (1908).
[2] John T. Tate, Phys. Rev. **17**, 394 (1921).
[3] Davisson and Kunsman, Phys. Rev. **22**, 242 (1923).
[4] Davisson and Germer, Nature **119**, 558 (1927); Phys. Rev. **30**, 705 (1927).
[5] H. E. Farnsworth, Phys. Rev. **31**, 405 (1928).

voltages of the order of 10 or 15 volts and less, the extension of the cosine law to the case of these low primary voltages becomes questionable.

During the course of measurements on energy distribution of secondary electrons from metals,[5] it was possible, because of the particular construction of apparatus, to obtain a measure of the relative number of electrons which leave the target at angles between 163° and 179° with the primary beam, as a function of the primary voltage. The apparatus is shown in Fig. 1 of the previous article.[5] Referring to this figure it will be noticed that the 3 cm diaphragm C which forms a part of the sphere is electrically insulated from the remainder, so that it is possible to measure the fraction of the current to

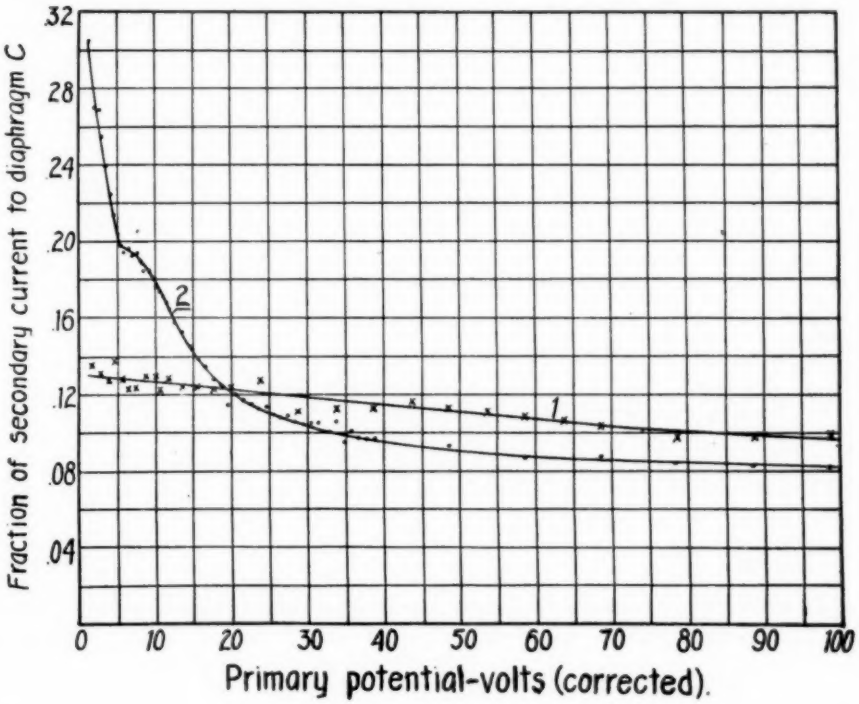

Fig. 1. Large angle scattering from iron. Curve 1 is for a target subsequent to heating at 350°C, but previous to red-heat treatment. Curve 2 is for the target subsequent to red-heat treatment.

the whole sphere which goes to C. This fraction is plotted as a function of the primary voltage for Fe, Cu, Ni and Ag, in Figs. 1, 2, 3, and 4, respectively. The values for the voltage have been corrected.

From Fig. 1 it is seen that, previous to heating the iron target at red-heat, the fraction of the current to C was nearly independent of the primary voltage, showing a slight decrease with increasing primary voltage. Assuming a consine distribution law, a computation shows that, for the dimensions of the apparatus, about 10 percent of the total secondary current should strike C. After heating the target at red heat the fraction of secondary current to C increased rapidly as the primary voltage was decreased, so that

for 1 volt primary electrons about 30 percent of the secondary current went to C. Although the diaphragm C is not a perfect absorber, its reflection characteristics should be the same for the curves taken before and after heating

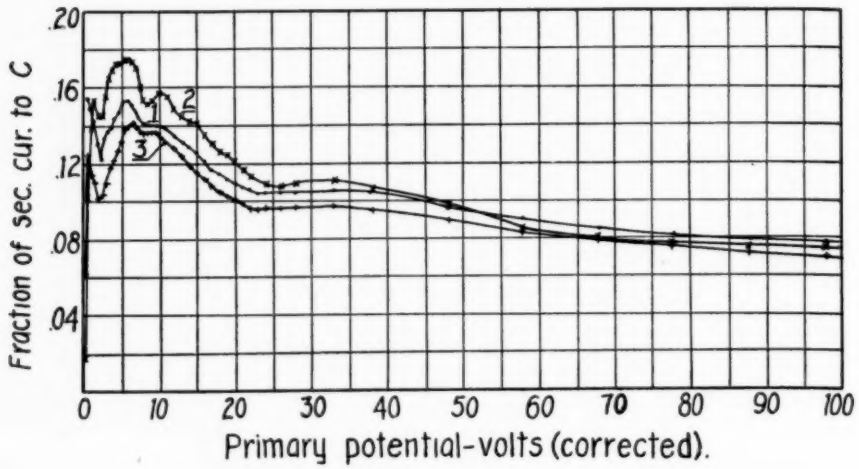

Fig. 2. Large angle scattering from copper. Curve 1 is for a target at normal incidence, subsequent to heating at red-heat for 5 min. Curve 2 is for the target at normal incidence, subsequent to heating at red-heat for more than 30 min. Curve 3 is for the target at 45° incidence, subsequent to heating at red-heat for more than 30 min.

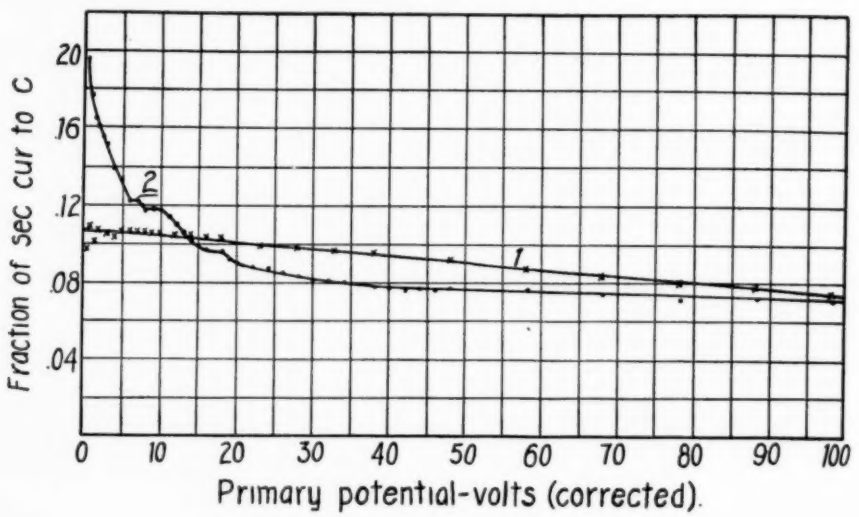

Fig. 3. Large angle scattering from nickel. Curve 1 is for a target subsequent to heating at 350°C, but previous to red-heat treatment. Curve 2 is for the target subsequent to red-heat treatment.

the target at red-heat, so that the difference between the two curves must be due to an effect of heat treatment of the target. The correction to be applied would be such as to increase the value of the current to C which is

shown, and it would be larger for the higher primary voltages. One might expect a result similar to curve 2, Fig. 1, if the target assumed a negative potential due to the heat treatment. A negative potential was found to exist, but curve 2 was obtained with such a positive potential applied to the target as to neutralize this negative potential. In fact, a relatively large current to C was still observed when a considerably greater positive potential was applied to the target than was necessary to compensate the negative potential. Since exposing the iron target to dry air at atmospheric pressure failed to remove the effect, it appears to be due to the surface structure rather than to outgassing. Since energy distribution curves of secondary electrons show that, for low primary voltages, the secondary current consists almost entirely of reflected primary electrons, it follows that the current to C is due to a large angle scattering of primary electrons.

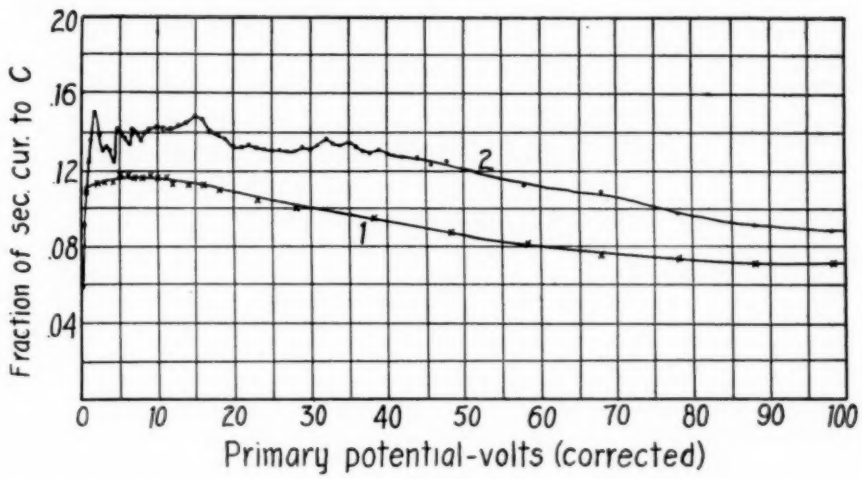

Fig. 4. Large angle scattering from silver. Curve 1 is for a target subsequent to heating at 350°C, but previous to red-heat treatment. Curve 2 is for the target subsequent to red-heat treatment.

Referring to Fig. 2, it is seen that the curve for a copper target, which has been heated at red heat, is entirely different than that for an iron target. To decide whether the plane of the target is a determining factor in the shape of the curve, observations were taken for 45° incidence. Since the tube had to be opened to effect the change of angle, the procedure was as follows: After heating the copper target at red-heat in the vacuum, curve 2 was obtained. The tube was then opened to the air and the position of the target changed for 45° incidence without touching it with the hands. After re-exhausting the tube, baking at 350°C, and separately heating the target at red-heat for 5 min., curve 3 was obtained. To make certain that this change was effected only by the change in the angle of incidence, the tube was again opened to the air and the angle of the target changed back for normal incidence. After re-exhausting and baking the tube at 350°C, and separately heating the target at red heat for 5 min., curve 2 was again

obtained very accurately. Although curves 2 and 3 are widely separated for low primary voltages, there is a considerable similarity in their general form, so that the direction of the surface nornal is not the only determining factor. Curves 1 and 3 appear quite similar. Comparing curves 1 and 2, it appears that the curve continues to change with heat treatment of the metal for some time. Since the sizes of the bombarded crystals increase enormously with heat treatment, the crystal growth is probably a determining factor.

The curves in Figs. 3 and 4 for Ni and Ag, respectively, furnish further evidence that the effect in question varies with the metal. The curve for a Ni target resembles that for Fe. The fact that curve 2, Fig. 4, continues to remain above curve 1 even for the higher primary voltages is in accordance with the result that silver reflects a comparatively large fraction of the incident electrons even for these higher primary voltages[5].

Although observations on a single copper target have been checked after removing the target and again replacing it in the tube without disturbing the surface, it is not certain that the curves for two different targets of the same metal would be the same. If these results depend upon the orientation of the particular crystals and relative number of different crystal faces being bombarded, it seems probable that the results for different targets would be different. Unfortunately no observations on this point were obtained for copper. Observations on two different nickel targets show the general form of the curves to be the same, but one rises much higher for low primary voltages than the other. More observations are needed to settle this point.

Although the present results give only a part of the complete scattering picture which results when very low velocity electrons impinge on a metal surface, they do establish the fact that this scattering varies with the metal bombarded, and is far from that given by the cosine law. A further knowledge of this scattering of very low velocity electrons should be of importance in determining the exact nature of surface forces.

BROWN UNIVERSITY,
PROVIDENCE, R. I.
November 1927.

SECONDARY ELECTRON CURRENT AS A FUNCTION OF CRYSTAL STRUCTURE

By H. E. Farnsworth

Abstract

A summary is given of results formerly obtained which indicate that the breaks in the low voltage region of the secondary electron curve of a metal are characteristic of the arrangement of the atoms at the metal surface, and not of the structure of the atoms themselves. Further evidence in support of this view is as follows: The secondary electron curve for phosphor bronze containing 95.4 percent copper does not show the characteristics of the curve formerly obtained for copper. The curve for targets cut from a single crystal of copper is distinctly different from that previously obtained for a large number of targets taken from copper sheet. Changing the angle of incidence of a copper target from 0° to 45° causes the changes in slope to be much less prominent, and changes the relative positions of some of the breaks.

THE fact that, after a metal target has been properly heat treated in a vacuum, its secondary electron curve (secondary current as a function of primary voltage) shows breaks which appear to be characteristic of the particular metal has led several experimenters[1–3] to attempt a correlation with soft x-ray and optical levels of the atom. The attempts have been far from successful and many of the results indicate no correlation. Krefft[3] has recently reported a correlation for a primary voltage of 70.5 volts in the case of tungsten while at about 1200°K. The writer has previously taken the view that the maxima and minima in the low voltage region of the secondary electron curves for copper and iron are due to inelastic collisions between the incident electrons and the atoms of the metal, although certain results have indicated that these changes in slope are in some way dependent upon the arrangement of the atoms at the surface of the metal. The purpose of this paper is to give further results which it is believed, together with previous observations, furnish convincing evidence that sudden changes in slope of the secondary electron curves in the region investigated (0–40 volts) and for the metal studied are due to the arrangement of the atoms at the surface of the metal and not to the structure of the atoms themselves.

The results previously given elsewhere[4] are briefly summarized here:

1. The temperature at which a copper target has previously been heated, rather than time of heating, appears to be the determining factor which causes the appearance of the various sudden changes in slope in the secondary electron curve for copper.

2. After this curve has been obtained for a copper target, the subsequent exposure of the target to dry air over a considerable range of pressure does not alter the general shape of the curve.

[1] Stuhlman, Science **56**, 344 (1922); Phys. Rev. **25**, 234 (1925).
[2] Petry, Phys. Rev. **26**, 346 (1925).
[3] H. E. Krefft, Phys. Rev. **29**, 908 (1927).
[4] H. E. Farnsworth, Phys. Rev. **25**, 41 (1925); **31**, 405 (1928).

3. The above curve for a copper film deposited by evaporation is considerably different from that for mass metal previously heated. After heating the deposited film, the curve obtained is similar to that for mass metal.

4. After heating a copper target at a temperature near the melting point, the breaks in the curve are less sharp than after heating at a somewhat lower temperature.

5. Measurements of energy distribution of secondary electrons from copper and iron show no such distribution as might be expected to result from atomic inelastic collisions.

Further observations[5] which furnish additional evidence of the influence of surface structure are given in Figs. 1 and 2. If the secondary electron characteristics are an atomic property, they should be observable even

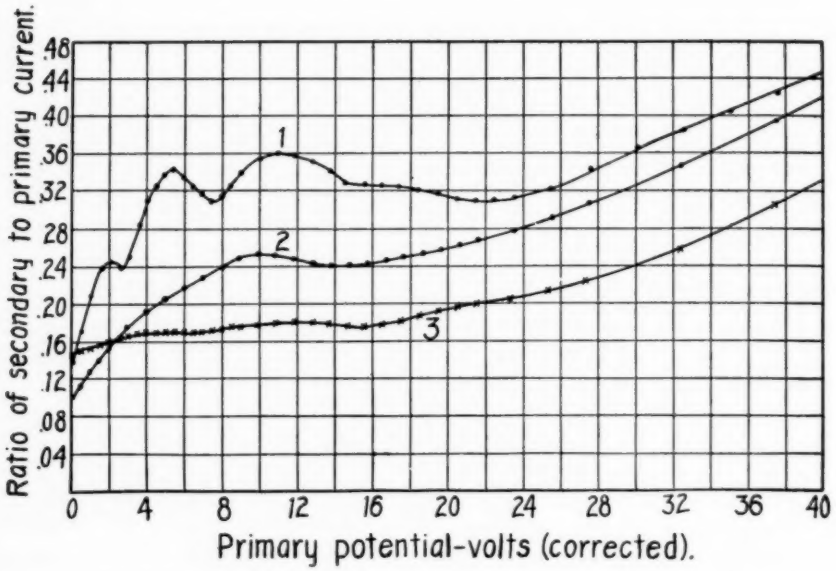

Fig. 1. Secondary electron curves. Curve 1 is for sheet copper. Curve 2 is for sheet phosphor bronze. Curve 3 is for copper cut from a single crystal. All curves were taken subsequent to red-heat treatment of the targets in a vacuum.

though the target contains atoms of other metallic elements, but, if they are a function of the atomic arrangement, the presence of other atoms should produce considerable changes in these characteristics.

Experimental results for a phosphor bronze target containing 95.4 percent copper, 4.5 percent tin and 0.1 percent phosphorus, indicate that structure is the determining factor as is shown by a comparison of curves 1 and 2 in Fig. 1. The positions of the breaks in the curve for copper do not check with any of those in the curve for phosphor bronze. Curve 2 was obtained for 2 different targets taken from the same sheet of metal. Curve 3 is for a Cu target cut from a single crystal in the form of a bar of rectangular cross-

[5] These results were obtained with the tube shown in Fig. 1, Phys. Rev. **31**, 406 (1928).

section. Curves similar to curve 1, Fig. 1, have been obtained for a large number of targets taken from commercial sheet copper as well as from chemically pure sheet copper. Curve 3 was obtained for two different targets cut from the same piece. Precautions were taken not to contaminate the surfaces of the targets before inserting them in the tube, and the surface layers were removed by prolonged heating at red heat while in a vacuum. Since the targets cut from the single crystal were of very pure copper, the only possible reason for the difference between the curves for this and other specimens appears to be a different orientation of the surface crystals. No special attempt was made to keep from breaking the crystals in the targets which were cut from the single crystal, so that they contained a large number of small crystals when placed in the tube. However, these crystals probably retained a certain preferred orientation.

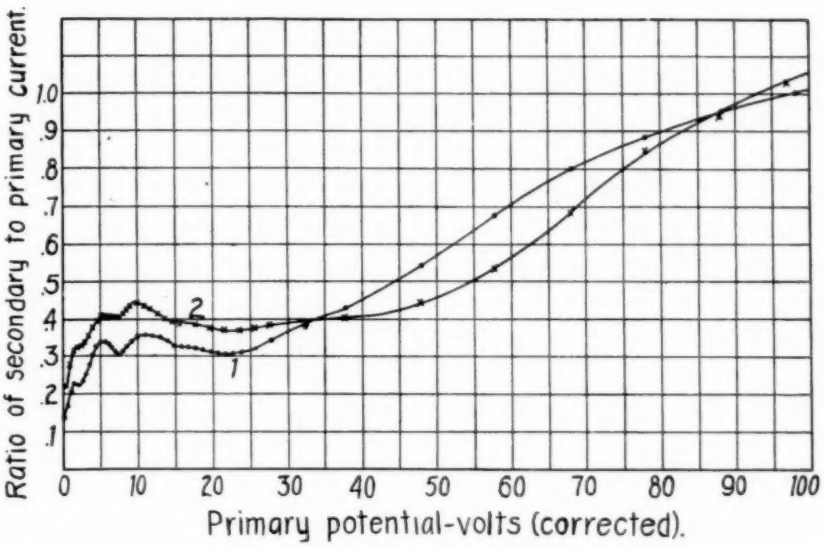

Fig. 2. Secondary electron curves. Curve 1 is for a sheet copper target at normal incidence. Curve 2 is for the same target at 45° incidence.

In looking over the results obtained for copper several years ago, it was found that among a large number of targets tried, there were two for which a curve similar to curve 1, Fig. 1, could not be obtained. The curves for these two targets showed a broad maximum and minimum at about 8 and 14 volts, respectively. At the time these curves were obtained it was thought that they were due to contamination of the metal surface so were not reported. It now seems more probable that they were due to a particular preferred orientation of the surface crystals.

Fig. 2 shows the effect of changing the angle of incidence on the secondary electron curve of a copper target. For the lower primary voltages, where reflected electrons are predominant, the secondary current is increased when the angle of incidence is changed from 0° to 45° with the normal. At some-

what higher primary voltages, where emitted electrons are predominant, the secondary current is decreased by this change. At still higher primary voltages the secondary currents become equal for the two angles of incidence. Thus one effect of increasing the angle of incidence from 0° to 45° is to increase the reflection and decrease the emission for the lower primary voltages. This increase of angle of incidence also causes the changes in slope of the curve to be much less prominent and also changes the relative positions of some of the breaks. However, since the two curves are still similar it appears that a rotation of all of the surface crystals does not produce entirely different characteristics. The distribution in the number of different crystal faces which are exposed may be the determining factor.

In conclusion, a large number of different observations have shown that the secondary electron characteristics of copper, in the low voltage region, are a function of the arrangement of the atoms at the surface of the metal, and are not directly dependent upon the structure of the atoms themselves. This undoubtedly is true for other metals as well as for copper.*

I am indebted to Professor F. G. Keyes for obtaining the copper crystal from which some of the targets were cut.

BROWN UNIVERSITY,
PROVIDENCE, R. I.
November 1927.

* *Note added to page proof:* Since this paper was first written, detailed reports of Krefft's results have appeared (Ann. d. Physik **84,** 639 (1927)); Phys. Rev. **31,** 199 (1928); Jour. Frank. Inst. **204,** 537 (1927). Krefft attributes the differences between his results and those of other observers on tungsten to a more complete elimination of gas from the metal in his experiments. This explanation for all of the differences appears doubtful in view of the present results of the writer which show that structure is a determining factor for copper in the low voltage region. It is impossible to state that this is also true for much higher voltages and for all metals, but in view of the possibility it is obvious that further experiments on critical potentials of metals by the secondary electron method will be of little value unless the metal studied is in the form of a single crystal with known orientation with respect to the incident electron beam. Horton, Davies, and Andrews, (Nature **121,** 192 (1928)) have recently suggested that some of the critical potentials for soft X-ray excitation may also be characteristic of the arrangement of atoms at the surface of the metal.

THE MEAN FREE PATH OF THE ALKALI IONS IN DIFFERENT GASES

By Ralph Brandreth Kennard

Abstract

Retardation and neutralization of caesium and sodium ions in traversing hydrogen, helium and argon.—With caesium ions of 90 volt velocity in hydrogen there is very little neutralization or scattering of the ions even when their path is twenty times the mean free path for a xenon atom in hydrogen. There is a loss of velocity of 1.3 volts per collision. Similar phenomena were observed in helium. Caesium rays of 35 volts velocity in hydrogen are slowly weakened by neutralization or scattering. Sodium ions of 455 volt velocity are also weakened in hydrogen, but the free path for a collision that removes the ion from the bundle is 26 times that of a neon atom in hydrogen. In argon, caesium ions of 90, 35 and 20 volt velocities are rapidly neutralized with a free path only 3.4, 2.6 and 2.3 times that of a xenon atom in argon.

VARIOUS experiments have been made on the scattering and the loss of velocity of positive rays in passing through a gas. J. Koenigsberg and J. Kutschewski[1] experimented with H^+ ions in H_2, O_2 and He, with He^+ in He, and O^+ in O_2, at velocities equivalent to 30,000 to 50,000 volts. They conclude from their observations that the loss of velocity is less than 0.5 percent and that there is little if any scattering. G. P. Thomson,[2] working with H^+ ions at 10,000 volts, in various gases at different pressures found that there was considerable small angle scattering. A. J. Dempster[3] made experiments on the absorption of H^+ ions in helium at from 14 to 1000 volts. Little if any retardation was observed, but considerable scattering of the bundle of protons was found at high pressures. The above experiments were made on relatively light ions, and generally at high velocities. The following experiments have been made with Na^+ and Cs^+ at much lower velocities, and data have been obtained on the neutralization and the slowing up of these rays in different gases.

The method of positive ray analysis developed by Dempster[4] was used in these experiments. The sources of ions were alkali metal catalysts kindly supplied by C. H. Kunsman.[5] This material was placed in a small furnace heated externally by a coil of resistance wire, and insulated with alundum cement. A furnace was chosen in preference to a platinum strip because the material is all at one potential, and also because the larger quantity gives a longer life and greater stability in the emission. For caesium, with the furnace half full, a useful life was obtained of over 100 hours. The furnace,

[1] J. Koenigsberg and J. Kutschewski, Ann. d. Physik **161,** 37 (1912).
[2] G. P. Thomson, Proc. Royal Soc. **102,** 197 (1922).
[3] A. J. Dempster, Phil. Mag. **13,** 115 (1926).
[4] A. J. Dempster, Phys. Rev. **11,** 316 (1918).
[5] C. H. Kunsman, Jour. Ind. & Eng. Chem. **17,** 971 (1925).

A, was made positive with respect to the electrodes B and C which were grounded, B direct, and C through a galvanometer. Electrodes B and C were brass disks with a 5 mm hole in the center across which a few fine wires were stretched in order to get a more uniform electrical field. The beam of

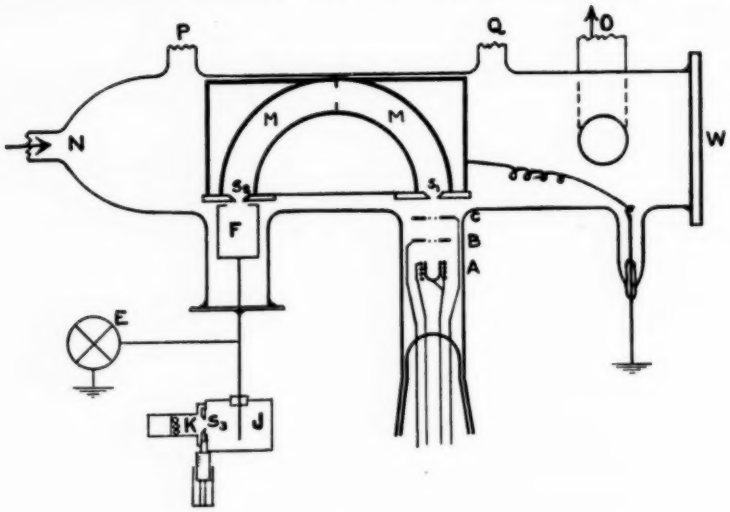

FIG. 1

positive rays was thus approximately parallel before entering the magnetic field, M, through the first slit S_1. In the magnetic field the beam was bent through 180° emerging through the slit S_2 into a Faraday chamber F. The current from the positive rays which entered F was measured by balancing

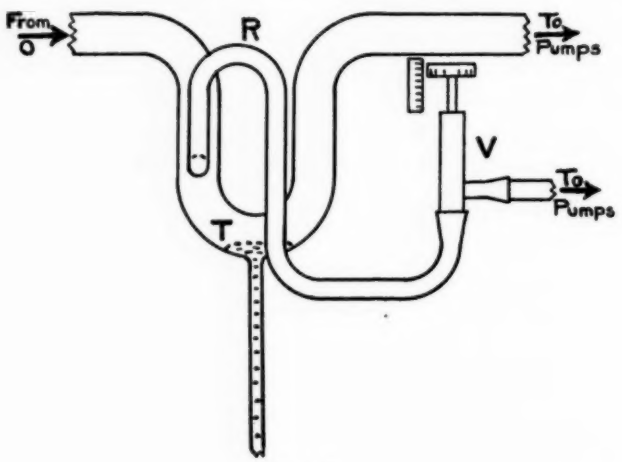

FIG. 2

the positive current by a negative current from an ionization chamber, J.[4] The current in this chamber was proportional to the opening between J and K which contained tubes of radium E, the width of this opening being controlled by micrometer screw reading to 0.01 mm. The current in J could

also be varied by changing the position and the number of radium E tubes in K, three standard arrangements being used.

Gas from a reservoir passed through a very fine capillary, a stop-cock, and a liquid air trap, and entered the system at N. The gas left at O, and passed through a liquid air trap to the pressure control system shown in Fig. 2 and thence to the mercury pumps. When the inflow of gas at N, Fig. 1, was stopped and the trap T, Fig. 2, left open, pressures as low as 10^{-5} mm were obtained. For higher pressures the gas was allowed to flow into the system and the mercury in the trap T was raised so as to force the gas through R and the choke valve V. This valve consisted of a slightly tapered plunger which could be raised or lowered in a cylinder by rotating a divided head. It was found that settings of the head corresponded to definite pressures so that it was possible to duplicate pressures at will. P and Q (Fig. 1) are joined together and lead past an ionization gauge through a liquid air trap to a Macleod gauge. The ionization gauge was used for convenience to indicate when a constant pressure had been reached, and to show any pressure variation that might take place in the course of a set of observations, the Macleod gauge being used as the final measure of all pressures.

In the beginning of a run the freshly filled furnace was heated, at low pressure, and under running conditions, for ten or more hours in order to get a steady emission. The pressure was then adjusted to the desired value and, after the iron in the magnet had been brought into the cyclic condition for a weak field, the current through the second slit was observed for a series of increasing magnetic fields. Although the emission current as measured by the galvanometer connected to C (Fig. 1) was kept constant throughout the readings, the emission of caesium or sodium would not remain constant if the composition of the emission current varied during the course of an experiment. It was found necessary to make an observation of the peaks of the curves when more than one ion was present, in order to reduce the readings to a constant emission of the particular ion under investigation.

Three phenomena may determine the form of the curves observed when gas is present; neutralization of the positive particles, retardation of the rays, and scattering. The positive ions finally observed may also have been subjected to the last two influences simultaneously. If neutralization were the only phenomenon occurring at collisions between the ions and the gas molecules, the curves observed would be weakened as gas is introduced, but would not be broadened or displaced to different values of the magnetic field. A scattering of the rays at collisions would broaden the curves to both higher and lower values of the magnetic field, and in addition would weaken the bundle since the scattering would deflect rays to the sides as well as in the plane in which the magnetic deflection occurs. If retardation occurred alone without neutralization or scattering, the curves would be shifted to smaller values of the magnetic field, and in this case the areas of the curves would remain the same, since the ions are not deflected to the sides. There are thus definite characteristics for identifying the two cases of pure neutralization or pure retardation.

The results of the observations with sodium ions of 445 volts velocity in hydrogen are shown in Fig. 3. The curve observed at the lowest pressure agrees with the curve calculated[4] on the assumption that the beam of ions at S_2 is of the same width as the width of the slit S_1. As gas is introduced the number of ions received is diminished and the curves are spread, mainly to the side of lower magnetic fields. This can be accounted for by the retardation of some of the rays when gas is introduced. There is also possibly some scattering at the higher pressures. Although the three effects cannot be clearly distinguished in this case, it is of interest to note that the combined action of all three is very ineffective in preventing the ions from reaching the second slit, when compared with what we might expect from the kinetic gas theory. The number of ions, N, traversing a distance $x=11.2$ cms at a

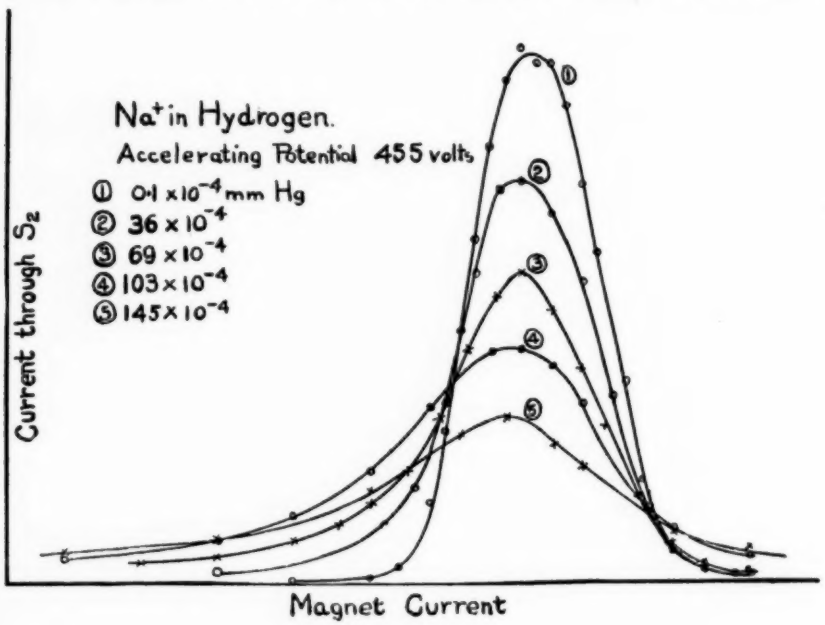

FIG. 3.

pressure of p mms would be expected to decrease with pressure according to the formula $N=N_0e^{-xp/760\lambda}$, where λ is the mean free path, reduced to atmospheric pressure, that the ion traverses before being removed from the group considered. The total number of ions given by the area under the first three curves decreases according to the formula with $\lambda=52\times10^{-5}$ cms. If we consider the maxima of the curves to give the number of ions which have not suffered neutralization or scattering we have for these $\lambda=27\times10^{-5}$ Assuming a radius for the sodium ion equal to that given by the kinetic theory for the neon atom, we find that the mean free path for a collision reduced to atmospheric pressure is only 2×10^{-5} cms. The free paths just deduced from the weakening by neutralization and scattering of the sodium ions in hydrogen are thus from 13 to 26 times as long as the kinetic theory free paths.

It is also of interest to note that the slight shift of the maximum of the curves in Fig. 3 corresponds to a very small loss of velocity even though the

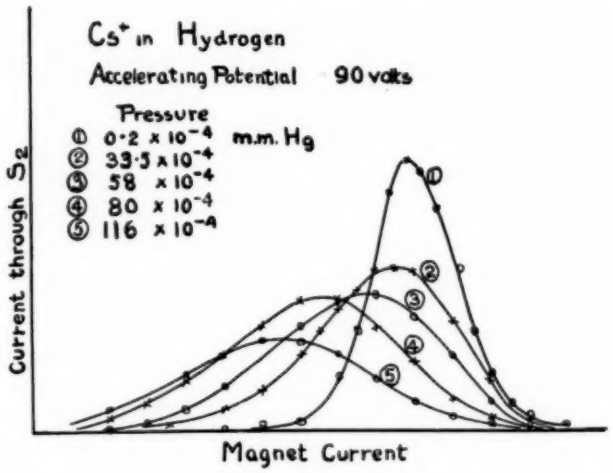

FIG. 4.

ions in curve 5 make 10.7 collisions in traversing this path. The shift at a pressure of 0.01 mm corresponds to a velocity decrease equivalent to 4 volts, or less than one percent.

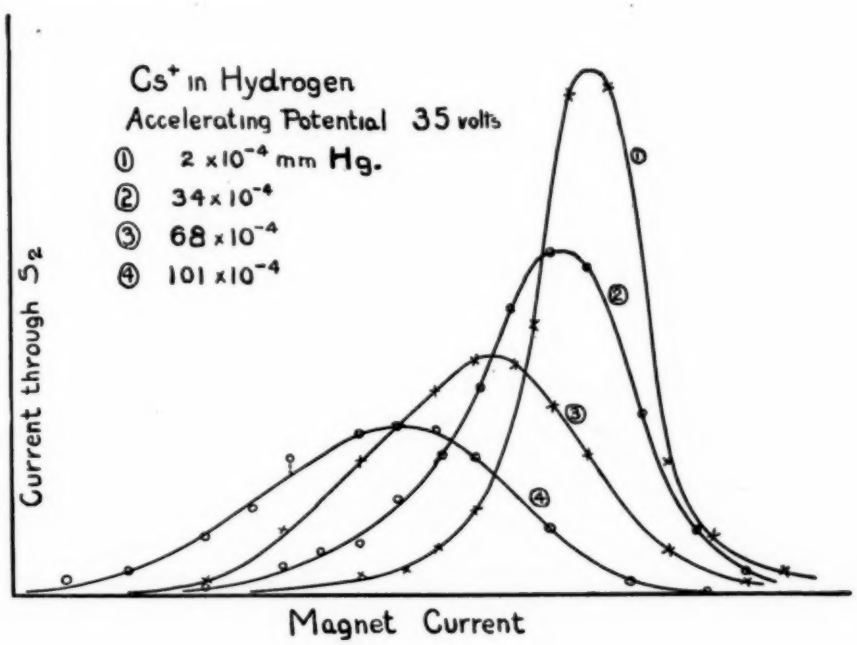

FIG. 5.

With caesium ions quite different phenomena were observed. Whereas with sodium the peaks of the curves (Fig. 3) lie one under the other, with

caesium in hydrogen, the curves (Figs. 4 and 5) spread out in the direction of smaller magnet currents as the pressure is increased. The areas under the first four curves in Fig. 4 are the same, showing no change with increasing pressure. The curve for the highest pressure was not corrected for a change in the relative intensity of the caesium ions. We may then conclude that caesium ions of 90 volt velocity are retarded only, and not neutralized or scattered in passing through hydrogen. With 35 volt rays in hydrogen (Fig. 5) a small decrease in area was observed. The curves for 90 volt rays in helium (Fig. 6) were not corrected for changes in the relative intensity of the caesium rays, but they show the shift of the rays to slower velocities.

In the case of the pure retardation shown by 90 volt caesium rays in hydrogen (Fig. 4) we may estimate the number of collisions made by the

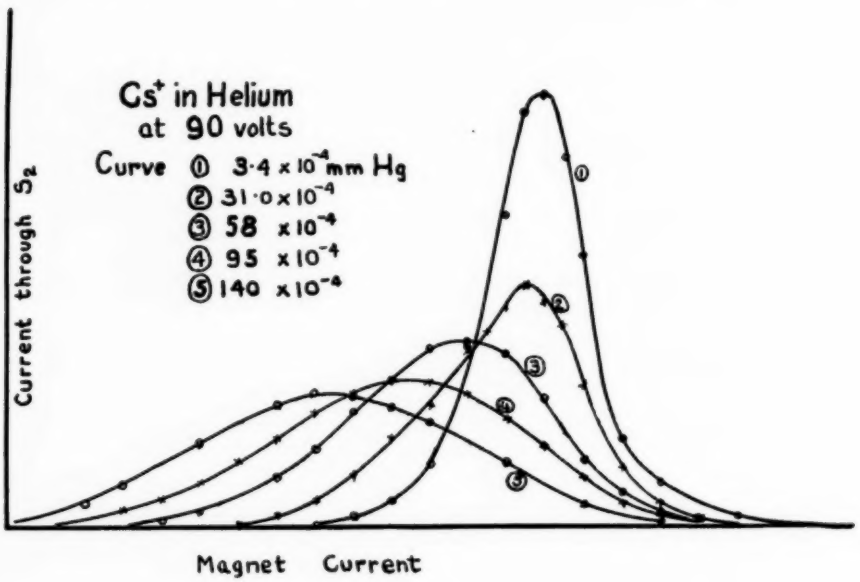

Fig. 6.

ions at the highest pressures. Assuming the diameter of the caesium ions to be the same as that of the xenon atom we find a kinetic theory free path of 5.25 mms at 1.16×10^{-2} mms pressure. Thus the ions giving the fifth curve of Fig. 4 have suffered 21.4 collisions in completing their path of 11.2 cms. The decrease in area of the curves for the 35 volt caesium rays in hydrogen indicates that about 1/5 of the ions are lost by neutralization or scattering after 12 collisions. The results in helium are similar to those in hydrogen although it was not possible in this case to make an exact correction for the emission current. The shift of the maximum of the 90 volt caesium curve in hydrogen would be caused by a loss of velocity corresponding to about 1.3 volts per collision.

When caesium ions pass through argon (98 percent pure) the curves in Fig. 7 are obtained. Here there is a rapid decrease in intensity as the gas

pressure is increased. The ions that remain positive do not suffer a marked loss of velocity. This is, however, to be expected as they have not made

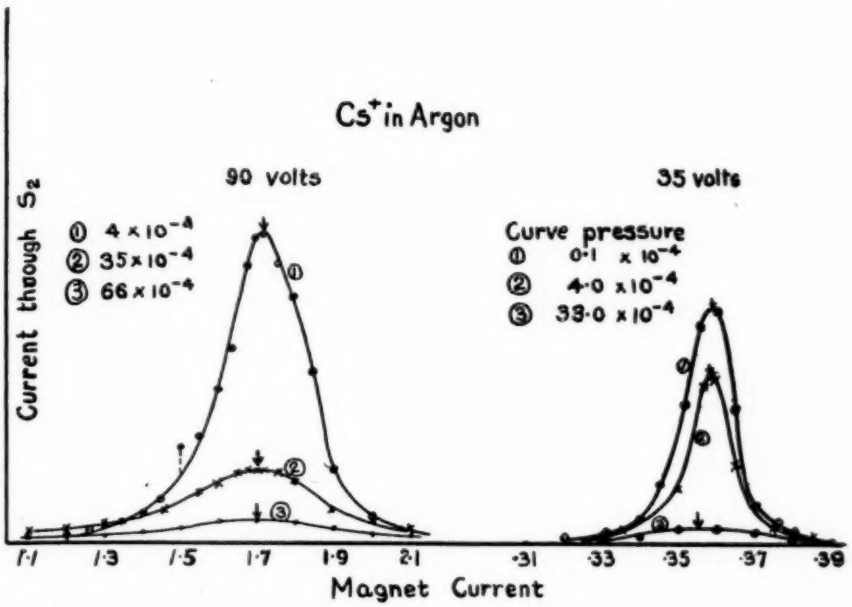

Fig. 7.

many collisions as in the case of the caesium ions in hydrogen. To determine the rate of decrease of the number of ions reaching the second electrode, the

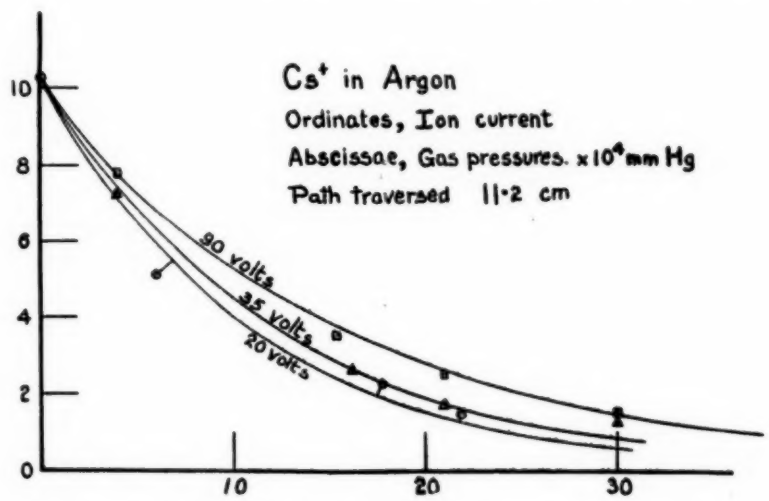

Fig. 8.

decrease of the maximum of the curve was observed. This gives an indication of the areas under the curves in Fig. 7 and may be made rapidly under con-

stant conditions. These observations are given in Fig. 8, and from the curves we may calculate a mean free path for the disappearance of the ion by neutralization or scattering. Reduced to atmospheric pressure we find 22.4×10^{-6} cms at 90 volts; 17×10^{-6} cms at 35 volts, and 15.3×10^{-6} cms at 20 volts. The kinetic theory free path for a rapidly moving xenon atom in argon is 6.5×10^{-6} cms, so that the above values are respectively 3.4, 2.6 and 2.35 times as long.

Experiments were also made on Rb^+ ions in H_2 and it was found that a loss of velocity occurred similar to that for Cs^+, but the work with Rb^+ was discontinued because an exact location of the peak of the curves was im-, possible. This was due to the presence of the two isotopes of Rb, 87 and 85 and of an ion of molecular weight 83, possibly $NaSiO_2^+$ from the alundum cement. All three ions could be separated at a low pressure and their weights determined by a comparison with sodium. The intensities of the two Rb isotopes corresponded exactly to that called for by the atomic weight.

The writer wishes to thank Professor A. J. Dempster for suggesting the above investigation and for his continued advice and encouragement during the progress of the experiments.

RYERSON PHYSICAL LABORATORY,
UNIVERSITY OF CHICAGO,
September 1927.

ON ELECTRICAL FIELDS NEAR METALLIC SURFACES

By Joseph A. Becker and Donald W. Mueller

Abstract

When an electron escapes from a metallic surface it passes through fields which tend to pull it back. Properly directed applied fields partially neturalize the surface fields and hence reduce the work the electron has to do against these fields. That is why i, the thermionic current, increases steadily with F_a, the applied field. Quantitatively $d(\log_{10} i)/dF_a = (11600/2.3\ T) \times s$, where T is the temperature of the surface and s is the distance from the surface at which the surface field F_s is equal to F_a. Hence the slope of an experimental log i vs F_a curve at any F_a yields the value of s corresponding to F_s. For clean or atomically homogeneous surfaces experiment shows that the only force opposing the escaping electron is due to its image field; for composite surfaces other fields, which are ascribed to the adsorbed ions, are superposed on the image field. For 70 percent thoriated tungsten this "adsorption field" is very large close to the surface and in a direction to help electrons escape; it decreases rapidly in strength as s increases until it is zero at about 15 atom diameters; here it reverses its direction and then increases in strength till it attains a maximum value of 8000 volts/cm at 75 atom diameters; beyond this distance it decreases steadily. The intense field close to the surface accounts for the decreased *work function* while the reverse field farther out accounts for the poor saturation at ordinary applied potentials.

The photo-electric long wave-length limit should be shifted toward the red by applied fields. This shift should be particularly noticeable for composite surfaces.

IT IS a matter of common observation that the thermionic current flowing from a heated filament to a nearby anode is never entirely independent of the anode potential. No matter how great a potential difference is applied between filament and anode, a further increase in this potential difference is invariably accompanied by an increase in current. This failure of the thermionic current to saturate with anode potential or this lack of saturation is not very pronounced for homogeneous surfaces such as, for example, clean tungsten. If, however, this surface is partially covered with adsorbed electropositive atoms such as thorium or caesium, the thermionic current from the resulting composite surface saturates very poorly with anode potential. When the tungsten surface is completely covered with a layer of the adsorbed atoms, the lack of saturation is no longer very marked. This effect is illustrated quantitatively in Fig. 1 which shows how the emission current varies with the plate potential for three surfaces. The currents have been multiplied by proper constants such that all three curves pass through the same point for a plate potential of 100 volts. The dashed curve represents the current vs. voltage or i vs. V relation for a clean tungsten filament. The curve marked $\theta = 17$ is an experimentally observed i vs. V curve for a tungsten filament whose surface is partially covered with oxygen and with caesium. θ is the percentage of the surface covered with caesium. The third curve marked $\theta = 120$ is an experimental curve for the same oxidized

tungsten filament when the surface is covered with enough caesium to form 1.2 atomic layers. Note that for a clean tungsten filament the current saturates quite well; when the surface is partially covered with caesium the saturation is very poor indeed; but when the surface is somewhat more than completely covered with caesium the saturation is quite good again. This phenomenon cannot be ascribed to the ionization of gas that may exist between the cathode and anode. Neither can the shape of the $\theta = 17$ curve be explained by the hypothesis that the current is limited by space charge for the largest current is less that 25 microamperes and the structure of the tube is such that a fraction of a volt applied to the plate should produce saturation. The $\theta = 17$ curve illustrates a very striking case of poor saturation. Numerous intermediate stages have been observed in this laboratory in tubes of various shapes and character of filament. *There can be no doubt that this marked failure to saturate is associated with adsorbed electropositive atoms wh ich partially cover electronegative metal surfaces.*

What is the cause of this lack of saturation for composite surfaces? Obviously the applied potential must help electrons escape which otherwise would fail to free themselves from the influence of the surface. It could do this if, in their escape, the electrons had to pass through electrical fields which tended to pull the electron back into the surface. An analysis which follows shows in detail that such a hypothesis does satisfactorily account for the lack of saturation. More than this, it shows just *how to determine the strength of these fields at various distances from the surface.* Before giving this analysis it is desirable to discuss the only published quantitative theory bearing on the lack of saturation and to show that it is inadequate to account for the lack of saturation for composite surfaces.

Schottky's Theory

In 1914 Schottky[1] proposed the hypothesis that when an electron escapes from a metallic surface it induces thereon a charge equal in magnitude but opposite in sign to its own charge, and that the force between these charges prevents the free escape of the electron. This force is given by the well-known image equation $Fe = e^2/4s^2$ where F is the induced field acting on the electron and s is the distance from the surface to the electron. The thermionic "work function" is interpreted quite simply as the work done against this image force in transferring an electron from the surface to an infinite distance from it. When $s = 0$, $F = \infty$ and the integral of Fds is also infinite. To avoid this difficulty, Schottky postulated that the force is constant and equal to $e^2/4s_c^2$ from $s = 0$ to $s = s_c$, a distance characteristic of the metal, but that beyond s_c the force is given by the image equation. It follows from this that half the work function is used in getting to s_c and the other half in going beyond s_c.[2] The values of s_c corresponding to ordinary work functions of 2 to 8 volts are 4 to 1×10^{-8}cm respectively, that is, s_c is of the order of atomic dimensions.

[1] W. Schottky, Phys. Zeits. **15**, 872 (1914).

On the basis of his hypothesis Schottky showed that if a potential gradient is applied at the surface of a filament, an electron need not have as much energy as before in order to escape from the filament, and that consequently the emission current should increase with the applied potential. The relation to be expected between current and potential gradient is given quantitatively by his equation:

$$\log_{10} i = \log_{10} i_0 + 4.39(cV)^{1/2}/2.3T \qquad (1)$$

in which i is the thermionic current in amperes /cm² for the variable plate potential V in volts; $i_0 = i$ when $V = 0$; T, the absolute temperature of the filament; and c the constant, determined by geometry, by which V is multiplied to give the potential gradient at the surface of the filament.

Schottky also showed experimentally that log i for clean tungsten at 1300°K increased linearly with $(cV)^{1/2}$ for values of cV from 10,000 to 50,000 volts/cm and that the rate of increase was within 20 percent of the rate given by Eq. (1). The 20 percent discrepancy could plausibly be accounted for by imperfections in his tube. Since then, no one seems to have made a thorough and careful test of Eq. (1) but many observers must have verified its approximate truth. If it is indeed true, it furnishes strong evidence that

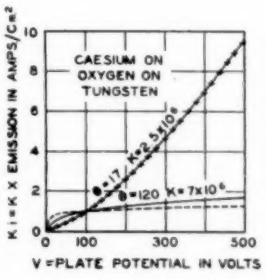

Fig. 1

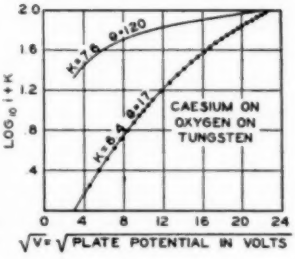

Fig. 2

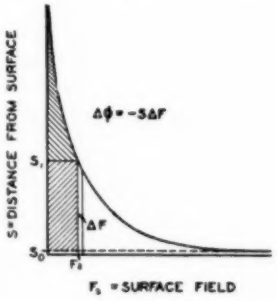

Fig. 3

Fig. 1. The dashed curve is for clean tungsten. The other two are for caesium on oxygen on tungsten. Θ gives the percentage of the surface covered with caesium.

Fig. 2. This shows that the current from composited surfaces does not follow Schottky's equation.

Fig. 3. This is a sketch to illustrate the decrease in the work function ϕ produced by a change in the applied field F_a, when a surface field F_s tends to pull the electron back into the surface.

beyond some small distance from the surface the forces on the electron are image forces and no others. This satisfactorily explains the lack of saturation in *clean surfaces.*

Since the current voltage curves for composite surfaces differ markedly from those for clean surfaces as is illustrated in Fig. 1, it is impossible that Schottky's law given by Eq. (1), can apply in such cases. Numerous tests

[2] This looks like an arbitrary assumption, and actually is unnecessary. We shall show later that it is possible to arrive at Schottky's conclusions by merely assuming that the image law holds for distances beyond about 40 atom diameters. It is unnecessary to make any assumption about the law of force at closer distances.

have shown that log i for such filaments does not vary linearly with $V^{1/2}$ if a sufficiently large range of voltages is investigated. Even when the relation is approximately linear over a small range the slope of the curve differs markedly from that for clean surfaces. Furthermore the ranges of linearity and the slopes change when the amount of surface impurities changes. As an illustration, Fig. 2 shows a plot of log i vs. $V^{1/2}$ for the data shown in Fig. 1. Note that the curve for $\theta=17$ is nowhere linear over an appreciable range while that for $\theta=120$ is quite linear at the higher voltages. Even here the slope is about twice as great as we estimate it should be for the same filament with a clean tungsten surface. For the $\theta=17$ curve the mean slope is about ten times what Schottky's equation requires. It is clear, then, that Schottky's theory does not account for the observed saturation curves for composite surfaces.

A Method of Measuring Surface Fields

To seek the cause of the very poor saturation curves for composite surfaces we can proceed as follows: The emission from a filament obeys Richardson's equation of the type

$$\log_{10} i=\log_{10} A+n \log_{10} T-\phi e/2.3kT \tag{2}$$

where i is the observed current; A is a constant that appears in the thermodynamic argument which leads to Richardson's equation (its value involves numerical constants as well as the well-known constants of nature k, m, e, and h); n is a number which in specific forms of this equation has the value 0, $\frac{1}{2}$, or 2; T is the absolute temperature of the filament; ϕ, the work function; e, charge on electron; k, Boltzmann's constant.

Since the current varies with F_a, the applied field near the surface of the filament, we can differentiate (2). Assuming that A does not vary with F we obtain:

$$\frac{d(\log_{10} i)}{dF_a}=\frac{-e}{2.3kT}\frac{d\phi}{dF_a} \tag{3}$$

This means that the slope of the experimental log i vs F_a curve gives us $d\phi/dF$, the rate at which the work function is being reduced at that field strength. But $d\phi/dF$ is simply related to the s vs F_s curve, where F_s is the surface field which pulls the electron toward the surface when the electron is at a distance s from the surface.

Fig. 3 is a sketch of a general form of such a curve. The surface is defined as the loci of the outermost positive nuclei. The distance s_0 is the greatest distance the electrons can get from this surface and still remain in their orbits. The area to the left of this curve from $s=\infty$ to $s=s_0$ represents that part of ϕ which is due to the surface fields. If we now apply a field F_a there will exist a distance s_1 at which F_a counterbalances F_s and the net field is zero. Beyond s_1 the net field pulls the electron out while inside s_1 the net field pulls it in. Any electron which now reaches s_1 will permanently escape. The work function is reduced for two reasons: (1) while the electron

is going from s_0 to s_1 the applied field is helping it out—this is represented by the shaded area between s_0 and s_1; (2) the electron need not have sufficient energy to overcome the forces represented by the shaded area beyond s_1. In general if the field is increased from any value F_a to $F_a+\Delta F$, the work function is decreased by an amount corresponding to the area $s\Delta F$; or $\Delta\phi = -s\Delta F$; or

$$\Delta\phi/\Delta F = -s \text{ and in the limit } d\phi/dF = -s \tag{4}$$

Substituting this in (3):

$$d(\log_{10} i)/dF = es/2.3kT = 11600s/2.3T \tag{5}$$

Hence *the slope of the log i vs F_a curve at any F_a tells us the distance s from the surface at which the applied field equals the surface field, F_s.* Thus we can readily determine the fields that exist near the surfaces of metals for all regions for which we can neutralize these fields by applied fields.

Critical Discussion

It should be pointed out that the shape of the saturation curves is determined by the value of F beyond s_1 and not at all by its value inside of s_1. Consequently it was unnecessary for Schottky to particularize his theory by assuming that half the work function was used up against image fields and the other half against a constant field very close to the surface. The final deduction is the same no matter what kind of field exists very close to the surface.

In deriving equation (4) it was tacitly assumed that the applied field was uniform from s_0 to s_1. For a smooth surface this would quite likely be true for all values of s that are of appreciable importance. Since filaments are not smooth this assumption might cause serious difficulties. If we could compute the field distribution due to an applied potential, near a rough spot we could still apply the present method. The element of area in Fig. 3 would no longer have vertical sides nor constant width but its area could still be computed. This would modify equations (4) and (5). However, for applied fields less than about 100,000 volts/cm and for ordinary non-uniformities this modification is likely to be negligible. A field of 100,000 volts/cm will neutralize an image field at $s_1 = (300\times 4.8\times 10^{-10}/4\times 10^5)^{1/2}$ or 60×10^{-8}cm. For these conditions, the image field, the applied field and the element of area in Fig. 3 will have about the same value they would have if the roughness were removed. Furthermore Schottky actually found that experiment gave agreement with the image law even for fields of 500,000 volts/cm. Hence ordinary rough spots on the surface do not introduce appreciable errors for ordinary potentials.

Another tacit assumption is that s_0, the largest distance an electron orbit extends from the surface, does not change with the applied field. This too is quite likely for fields less than 10^5 volts cm, since the fields existing near the electron orbits must be of the order of 10^5 volts/cm. The orbits should therefore be inappreciably influenced by these applied fields. For larger

fields we must expect s_0 to be increased and hence ϕ decreased by the applied field. This is probably the cause of the cold discharge due to intense fields.

By experimentally obtaining log i vs F_a curves at various temperatures it is possible to determine s vs F_s curves at these temperatures and consequently determine whether the area underneath them or the corresponding part of the work function is independent of temperature. If F_s is due solely to the image forces, there should be but one s vs F_s curve for all temperatures and the slope of the log i vs $V^{1/2}$ curves multiplied by T should give a constant. Dushman[3] has shown this to be an experimental fact for clean tungsten.

Application of Method: An Illustration

The authors are applying the method to determine a series of s vs F_s curves for thoriated tungsten from a series of experimentally determined log i vs V curves for various values of θ and for various values of T at each θ. From the s vs F_s curves we hope to determine: (1) how much they deviate from the image equation; (2) how this deviation varies with θ; (3) whether the surface fields at a given θ are altered by a change in temperature, that is, whether for thin films $d\phi/dT=0$ as it seems to be for clean surfaces. The

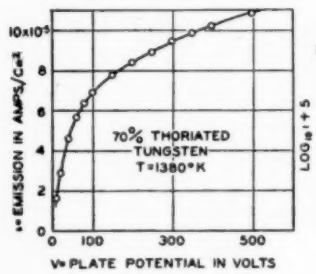

Fig. 4

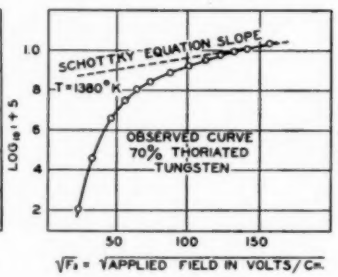

Fig. 5

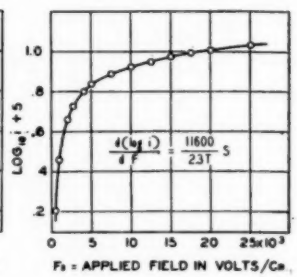

Fig. 6

Fig. 4. This shows that the current from a 70% thoriated tungsten filament saturates poorly.

Fig. 5. This shows that the current does not follow Schottky's equation at low and moderate applied fields.

Fig. 6. The slope of this curve at any value of F_a gives s, the distance from the surface at which the surface field F_s is equal to that particular value of F_a.

s vs F_s curves may also yield quantitative information about: (1) the electrical doublets resulting from the adsorbed thorium; (2) how many of the adsorbed thorium atoms have given up their valence electrons to the surface to become surface ions; (3) whether the number of surface ions at a given θ varies with the temperature as is required by Boltzmann's principle if a surface ionization potential exists. It should also be profitable to study other electropositive materials than thorium, as well as electronegative materials like oxygen, by the same methods and with the same viewpoints.

For all this work the s vs F_s curves are essential. In order to give a concrete illustration of what such a curve is like and the data on which it is

[3] S. Dushman et al. Phys. Rev. **25**, 346 (1925).

based we are including Figs. 4, 5, 6, and 7. Fig. 4 shows an experimental i vs V curve for a 70 percent thoriated tungsten filament 0.0086 cm (3 mils) in diameter stretched along the axis of three nickel cylinders 1.47 cm in diameter. Note the poor saturation. Fig. 5 shows that the observed points do not fall on a straight line on a log i vs $F^{1/2}$ plot and that the slope is considerably greater than that given by Schottky's equation. Note, however, that at the higher potentials the observed curve is more nearly straight and its slope is only slightly greater than Schottky's theory requires. Fig. 6 shows the same data in a log i vs F_a plot. F_a in volts/cm near the surface of the

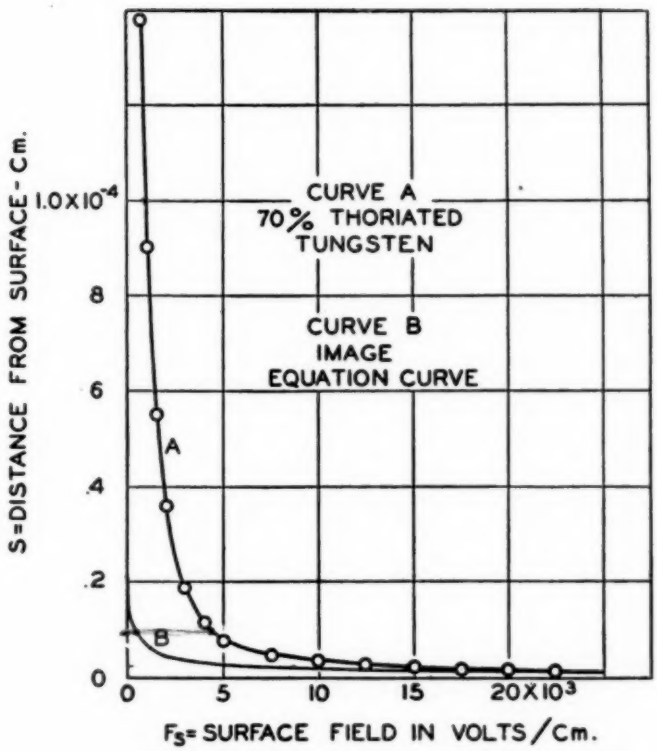

Fig. 7. This shows that the fields near a composite surface differ greatly from those near a homogeneous surface for which they vary according to the image equation. At any s the difference between F_s for curves A and B gives the field due to the adsorbed thorium.

filament is 50 times the plate potential in volts. The slope of this curve at any F_a gives s, the distance from the surface at which the surface field, F_s, equals the applied field, F_a. Finally Fig. 7 shows the s vs F_s curve for 70 percent thoriated tungsten together with the image equation curve, $F=e/4s^2$.

This is the most important figure in this group and hence it warrants some discussion. In a certain sense curve B does not represent a true surface field, since the field does not exist unless the electron under consideration is at a distance s from the surface. Nevertheless the force on the electron

can be spoken of as due to its induced field and it is in this sense that we use the term. Most likely when the electron escapes from the thoriated surface it does work against its image field. Hence at any s it is only the difference between F_s for curve A and curve B which represents the true field which is caused by the presence of the adsorbed thorium. It is very striking that this adsorption surface field has appreciable values at such large distances from the surface. Thus at a distance of 1×10^{-4}cm or 2500 thorium atom diameters away from the surface the field due to the thorium is still 1000 volts/cm; at 1×10^{-5}cm or 250 diameters it is approximately 4000 volts/cm; at 3×10^{-6}cm or 75 diameters it is approximately 8000 volts/cm. Then for still closer distances the field decreases until at something like 6×10^{-7}cm or 15 diameters the field is zero. At all these distances the direction of the field is such as to tend to pull the electron back into the surface. For still closer distances Fig. 7 suggests that the field must rapidly become very large but in a direction to help the electron escape. The net effect of the fields due to the thorium must be to help the electrons escape since the work function of thoriated tungsten is less than that of clean tungsten. Hence curve A must go below B for small values of s. This can be tested by using higher applied potentials or filaments of a smaller diameter. In some preliminary tubes we have actually observed cases in which the A curve crossed the B curve at the higher potential gradients. Since $d(\log i)/dF$ is proportional to s, this means that at high enough potentials, thoriated tungsten saturates as well as or better than clean tungsten. To sum up the picture to which we are led: *the adsorbed thorium or other electropositive material produces fields which close to the surface are very large and in such a direction to help electrons escape; at larger distances the fields are in the opposite direction and may be of appreciable magnitude as far out as 2500 thorium atom diameters.* The huge fields close to the surface are responsible for the decreased work function while the reverse fields farther out are the cause of the marked lack of saturation at ordinary applied potentials.

The fields due to the thorium which are in a direction to hinder the escape of the electrons are astoundingly large at fairly large distances from the surface. They are much larger than one would expect if the thorium ions are rigidly fixed on the surface. It may be that in order to account for these fields, one must assume that an ion is ejected to various distances from the surface by thermal impacts and is pulled back by surface forces. The average distance of all the ions at any one instant may be several times the ion radius and hence the fields produced by these ions may be appreciable at considerable distances from the surface. In the case of caesium on tungsten, some caesium ions are pushed to such large distances from the surface that they are no longer pulled back but permanently escape. Another way to account for these fields is to assume that a composite surface carries a net positive charge. It should also be pointed out that for composite surfaces the A in Richardson's equation may not mean quite the same thing as it does for homogeneous surfaces. Hence it may be that A for composite

surfaces may vary when the applied field is varied which is contrary to the assumption that was made in deriving Eq. (3) above. Whatever the explanation for the fields in question may be, we feel that a fuller discussion had better be left until the present method has been applied to a series of values of θ and T for thorium on tungsten. For the present we wish merely to point out that the surface fields obtained by this method are of such striking magnitude that they require an explanation and that quite likely when we have found this explanation we shall know more about the mechanism of emission from composite surfaces.

In the meanwhile it may not be amiss to point out how the views presented here will modify the conclusions reached in a recent paper on "Electron Emission from Thoriated Tungsten" by Dushman and Ewald[4]. In this paper they computed the current that should be emitted at zero applied potential by assuming that Schottky's equation held for all thoriations and for all applied potentials. As a justification they state "More recent work by Mr. N. B. Reynolds in this laboratory (General Electric Company) has shown that Eq. (4) (which is the same as Eq. (1) above) is also applicable to thoriated tungsten filaments for field strengths which are many times greater than those worked with in the present investigation." Fig. 5 of the present article shows that the emission does approximately follow Schottky's equation at high field-strengths but that it deviates more and more at medium and low field-strengths. It looks as if the field-strength would be about one-tenth that obtained by extrapolating the Schottky line for high field-strengths. Furthermore, the difference between the extrapolated and true currents at zero field-strength will vary with θ and probably also with the temperature. To determine the emission characteristics for zero field-strength it will be necessary to empirically extrapolate the observed values of the current at various low field strengths for each θ and at each temperature and use these in the customary manner; or else to determine A and ϕ_0 for each of a series of low field-strengths and extrapolate the A and ϕ_0 values to zero field-strength. When this is done it may very well be that the A for completely activated thoriated tungsten ($\theta=0$) will be found to have the same value as for clean tungsten i.e., 60.2 amps/cm^2 deg^1.

We should like to point out also that the photo-electric current should be affected by the surface fields in a somewhat similar manner to the thermionic current. It is easy to see that the photo-electric current too should saturate poorly for partially covered surfaces, and that the long wave-length limit should shift toward the red when the applied field is increased from a small value to a larger value. This shift should be more pronounced for partially covered surfaces than for clean or completely covered surfaces. It seems probable that the details of the surface fields can more simply be ascertained from photo-electric than from thermionic effects. An excellent beginning of an experimental study of the photo-electric effects from composite sur-

[4] Dushman and Ewald, Phys. Rev. **29**, 857 (June 1927).

faces has been made in this laboratory by Dr. H. E. Ives and his collaborators.[5]

In conclusion we gratefully acknowledge the criticisms of Dr. W. Wilson and especially Dr. C. J. Davisson which have added to whatever merits this article may have.

BELL TELEPHONE LABORATORIES, INCORPORATED,
NEW YORK, N. Y.
December 1, 1927.

[5] See particularly "Photoelectric Properties of Thin Films of Alkali Metals" by H. E. Ives, Astrophysical Journal **60**, 209–231 (1924).

ELECTRONIC DISCHARGE FROM COLD WIRES IN INTENSE ELECTRIC FIELDS

By Robert J. Piersol

Abstract

Measurements were obtained for cold electronic currents at a pressure of 10^{-8}mm, using thoroughly outgassed electrodes made of a minimum amount of metal. A silver plated glass cylinder served as an anode, with a coaxial tungsten filament cathode. Pure tungsten was used to avoid the changing surface conditions incident to outgassing thoriated tungsten. The gradient necessary for a given current was increased more than three fold by heating the filament for three hours at 2700°K, the approximate period necessary for maximum gradient. The type of current-gradient curve at room temperature verifies the observations of Millikan and Eyring.

Effect of temperature on the discharge of electrons from wires in intense electric fields has been extended by a study of the current-gradient relationship at liquid air temperature. These results show an intrinsic cold electronic phenomenon, possessing a type of current-gradient curve which has characteristics independent of temperature from 90°K to 1000°K.

I. Introduction

WOOD[1] found that electrical conduction starts at one volt across an air gap, 4×10^{-3} cm in width, for ruled speculum metal on quartz. He attributed this to an atmosphere of negative electrons. Broxon[2] tested this theory, using two semi-transparent surfaces of such difference in curvature as to give Newton rings which could be used to measure the distance by interference. He found no disruptive discharge at a 5×10^{-5} cm gap, with an applied voltage producing a gradient of 6.4×10^{5} volts per cm. Hoffman[3] used a vacuum as high as 1×10^{-3} mm. He found that with a gap distance of 4.2×10^{-5} cm, measured by interference, a gradient of 4.8×10^{6} volts per cm was required for conduction. Thus the work of Broxon and Hoffman disproved the negative electron atmosphere theory. In order to account for electronic discharge due to intense electric fields, Schottky[4] set forth a theory based on the thermodynamic agitation of free electrons in a metal. The free electrons are shot out to very small distances from the surface of the metal, the distances depending on the Maxwellian distribution of velocities among the free electrons in the metal. In the absence of intense fields these electrons are attracted back into the metal by their electrical image; but if the field is sufficiently intense (of the order of 10^{8} volts per cm) the applied field is greater than the image field, thereby pulling the electrons

[1] Wood, Phil. Mag. **24,** 316 (1912).

[2] Broxon, Phys. Rev. **20,** 476 (1922).

[3] Hoffman, Zeits. f. Physik **4,** 363 (1921); **5,** 109 (1923); Vehr. d. Deutsch Phys. Ges. **12,** 880 (1910); Phys. Zeits. **11,** 961 (1910); **13,** 480 (1912); **13,** 1029 (1912); Ann. d. Physik **42,** 1196 (1913); **52,** 665 (1917).

[4] Schottky, Jahrb. d. Radioakt. **12,** 200 (1915); Zeits. f. Physik **14,** 80 (1923; **15,** 63 (1923).

away from the metal. Millikan and Shackelford,[5] for two intreated crossed tungsten wires, found the first leak between 1×10^5 and 5×10^5 volts per cm. After heating the tungsten wires at a temperature of 2700°K, the first leak was pushed up to 4.3×10^6 volts per cm. Later Millikan and Eyring[6] used a fine thoriated tungsten filament waxial to a copper cylinder. Outgassing the filament at 2300°K produced a critical potential gradient as high as 7.4×10^5 volts per cm. The current was found to be completely independent of temperature up to 800°C. The writer[7] found a critical gradient of 5.4×10^6 volts per cm between electrodes made from molybdenum plates pressed into hemispherical shells, outgassed at 1400°C by induction heating; this being the highest critical gradient thus far reported. Lilienfeld[8] has used a pointed cathode in a high vacuum x-ray tube. He ascribes the emission as due to the direct action of the applied field on the sharply curved end of the cathode. Unpublished work by Rentschler showed that the normal operation of the Lilienfeld tube is not due to the pulling of the electrons directly out of the metal; but is caused by ionization either from residual gases or impurities pulled from the surface of the electrodes. Nevertheless Rentschler expressed conviction that electrons may be pulled out of pure metals provided the field is sufficiently intense. Hayden[9] found a critical gradient of 1.3×10^6 volts per cm, using outgassed molybdenum spheres 0.306 cm apart. The writer[10] found that the critical gradient between molybdenum electrodes may be increased from 1.2×10^6 to 5.4×10^6 volts per cm by outgassing the electrodes. Preliminary work seemed to indicate that an increase of temperature, up to the thermionic range, influenced both the current and the breakdown voltage. Further investigation showed that this apparent change was due largely to occluded gases diffusing to the surface of the electrodes at higher temperatures. Dushman[11] found a constant ratio between the logarithm of the current and the square root of the plate voltage, for a temperature range between 1470°K and 2239°K, and for plate potentials from 100 to 475 volts. This is in accordance with the theoretical deductions of Schottky. Gossling,[12] in a very extensive research, has shown in a qualitative manner the reality of cold electronic discharge. The results are completely inconsistent with the Schottky variation of current with temperature. Working under Swann, del Rosario[13] obtained results, which he interpreted as casting doubt on the conclusions of previous observers that the currents they obtained were due to the pulling of electrons from the metal surfaces. He interpreted his observations as showing that the effect is due to voltage

[5] Millikan and Shackelford, Phys. Rev. **15,** 239 (1920).

[6] Millikan and Eyring, Phys. Rev. **27,** 51 (1926).

[7] Piersol, Report Brit. A. A. S. p. 359 (1924).

[8] Lilienfeld, Phys. Rev. **2,** 1350 (1921); Akad. d. Wiss. **62,** 31 (1920); Vehr. d. Deutsch Phys. Ges. **2,** 13 (1921); Phys. Zeits. **20,** 280 (1919); **23,** 506 (1922).

[9] Hayden, Jour. A. I. E. E. **41,** 854 (1922).

[10] Piersol, Phys. Rev. **25,** 113 (1925).

[11] Dushman, Phys. Rev. **25,** 338 (1925).

[12] Gossling, Phil. Mag. **1,** 606 (1926).

[13] del Rosario, J. Franklin Inst. **203,** 243 (1927).

rather than field gradient, thereby concluding that the currents observed by Millikan and Eyring might possibly be due to ionization of residual gases in the space between the anode and cathode.

II. Apparatus and Method

The type of tube used, as shown at T in Fig. 1, was made of Corning G702P glass (similar to Pyrex) to permit baking out at 500°C. The filament, 2.92×10^{-3} cm in diameter, was of pure tungsten (non-thoriated), thereby permitting outgassing at 2700°K, without the change of surface conditions due to the diffusion of thorium to the surface. The filament G was suspended by tungsten leads through seals at D and E, being held taut by a helical tungsten spring F. The inside of the tube was silver-plated between the

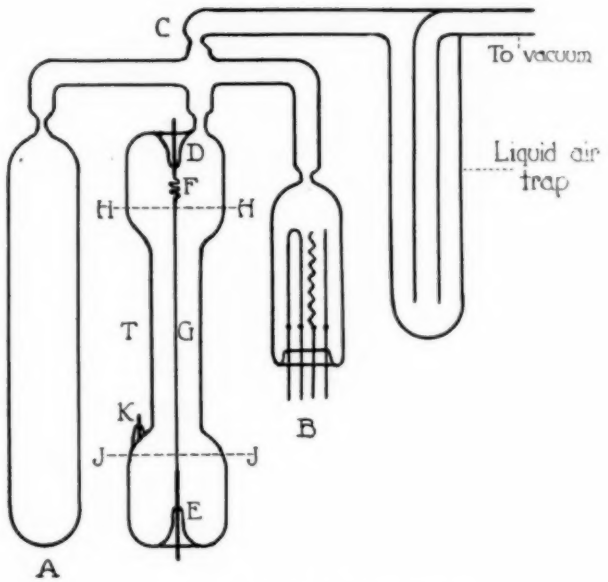

Fig. 1. Tube and exhaust system.

plane HH and the plane JJ. This silver plate on the restricted area of the tube served as an anode, 2.16 cm in diameter, being connected electrically to the tungsten electrode which was sealed in at K. The silver, being of semi-transparent thickness, was far more readily outgassed than a relatively heavy copper cylinder as used by Millikan or nickel cylinder as in the experiment of del Rosario.

As shown in Fig. 1, to the cold electronic tube there was attached a charcoal tube A and a Dushman ionization gauge B, assembled from metal parts of a UX200 radio tube.

Modern high vacuum technique was employed. The tubes were thoroughly outgassed by baking, inductive heating, and bombarding, while the filaments were heated at 2700°K. After evacuation the tubes were sealed off from the system at C, the charcoal tube being submerged in liquid air continuously

until the completion of the experiment. The vacuum remained remarkably constant, being of the order of 10^{-8} mm.

Although this work was completed before the publication of the article by Gossling, identical high tension circuits were used to supply rectified alternating current. Sufficient smoothing capacity was added to reduce the cycle voltage variation to less than one percent when discharging one milliampere. Very exact voltage readings were obtained, by a Shrader electrostatic voltmeter.

III. Experimental Results

For a tungsten filament, 0.00146 cm radius, coaxial to a cylindrical anode, 1.06 cm radius, it may be calculated that the field strength (in volts per cm) at the surface of the filament is 103 times the difference of potential between the electrodes.

As noted by Millikan and Gossling, in the case of wires that have been subjected to extreme heat treatment, sufficiently high gradient may produce a rupture of the surface of the wire, causing the current to jump instantly a thousandfold. In the present experiments this occurred at a gradient necessary to draw a cold electronic current of approximately one milliampere. The resulting conical stream of electrons caused a fluorescent spot to occur, removing the silver from a small area of the glass in a few seconds. This electron stream could be deflected by a magnet. The surface rupture of the wire could be healed by heating the wire for several hours at 2700°K. The rupture of the surface of a filament caused fluctuating current at lower gradients. Therefore all the results reported in this article were obtained for wires where the tube showed no fluorescence in a darkened room. A tube with a ruptured filament was discarded as worthless for reproducible results. Even when reconditioned by heat treatment the tube was not as satisfactory as a new tube.

In all observations the filaments were conditioned, previous to recording data, by drawing a cold electronic current for several minutes at a gradient greater than that to be used. This is because results for decreasing voltages duplicate those for increasing voltages only over a range lower than the conditioning voltage.

In all, 14 tubes were made and used. The results were very uniform from tube to tube. Although 33 sets of observations were obtained, the results may be summarized in three groups showing, first, curves for observations at room temperature for the filament previous to heating; secondly, curves for observations at room temperature for a filament that had been outgassed at 2700°K; and thirdly, curves for observations at liquid air temperature for an outgassed filament. Each curve represents a single set of readings, both for increasing and decreasing voltage, in which the values have not been weighted.

Fig. 2 shows the relation between the logarithm of the current and the potential gradient previous to the heating of the filament at a pressure of 10^{-8} mm as measured by an ionization gauge. Fig. 3 emphasizes the effect

of outgassing the filament at 2700°K for three hours. It should be noted that the gradient necessary to give a cold electronic current of 1×10^{-7} amperes has increased from 4.4×10^{5} volts per cm to 1.5×10^{6} volts per cm.

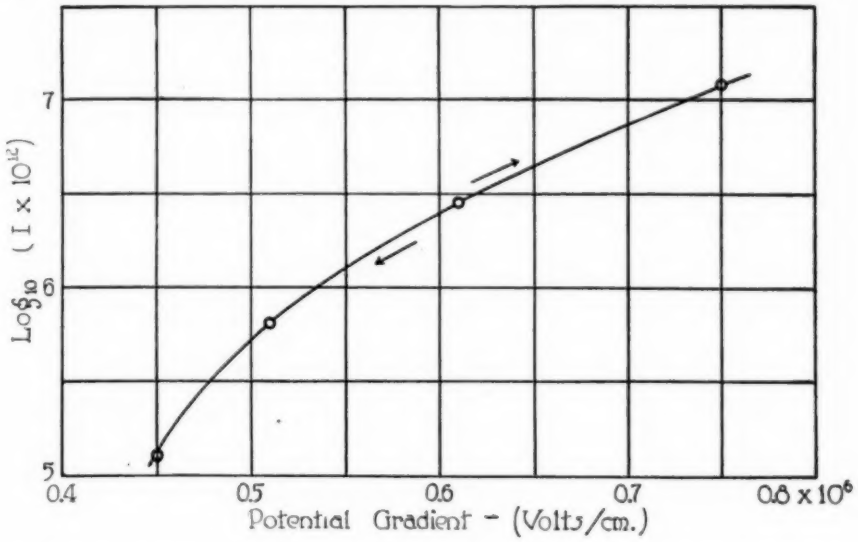

Fig. 2. Relation between the logarithm of the current and the potential gradient before outgassing. Readings taken at 300°K.

At 1×10^{-5} amperes it has increased from 7.3×10^{5} volts per cm to 2.2×10^{6} volts per cm. This shows that it requires over three times the gradient to

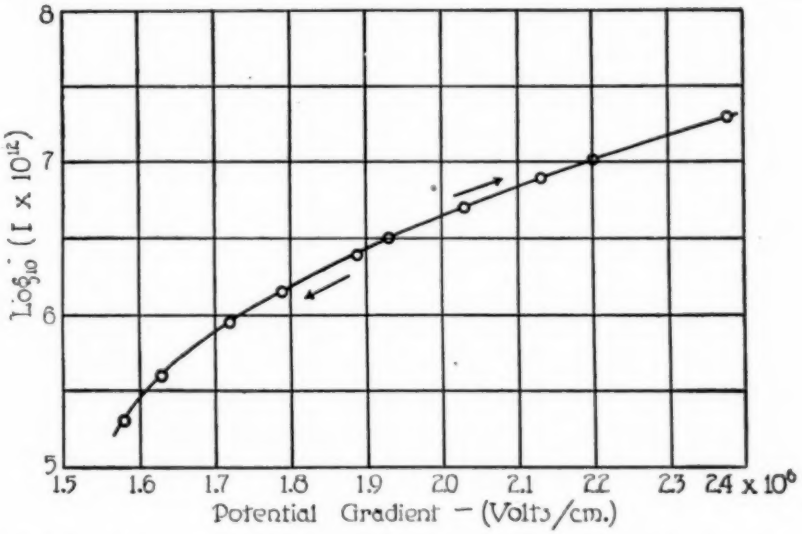

Fig. 3. Relation between the logarithm of the current and the potential gradient after outgassing. Readings taken at 300°K after outgassing at 2700°K for three hours.

give a cold electronic current from an outgassed metal equal to that from the same metal previous to outgassing.

Filaments were outgassed at 2700°K for periods as long as 48 hours. Results showed that there was no appreciable increase in gradient due to outgassing at 2700°K for a length of time longer than three hours.

IV. Influence of Temperature

Fig. 4 gives results when the entire tube was held at a temperature of −180°C. This was done by submerging the cold electronic tube in a large necked thermos bottle filled with liquid air. The liquid air itself is a sufficiently high insulator to prevent measurable leakage except at the frosted area where the leads came out, at which point they were insulated by glass tubing.

The characteristics of this curve are similar to those for an outgassed filament at room temperature. In this particular case the filament had been

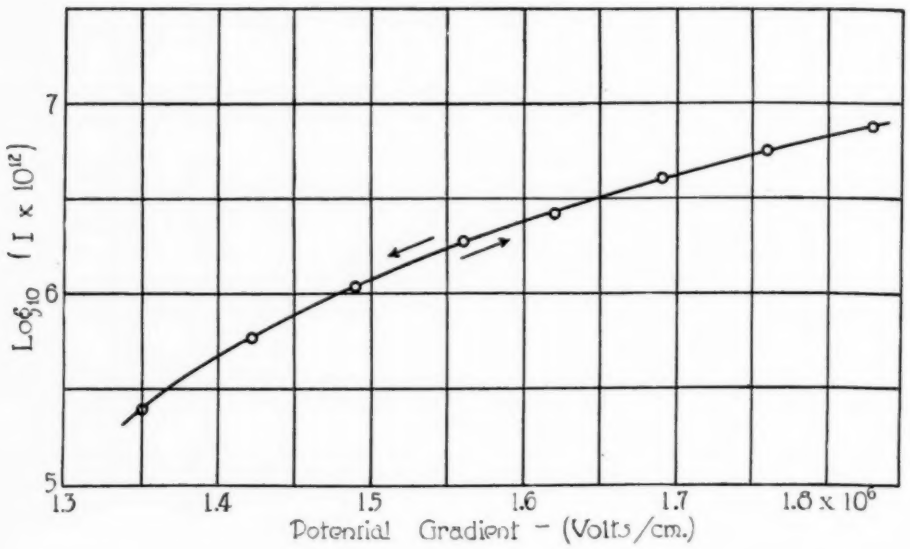

Fig. 4. Relation between the logarithm of the current and the potential gradient at low temperatures. Readings taken at −180°C after outgassing at 2700°K for one hour.

outgassed at 2700°K for a period of one hour as compared to three hours for the filament shown in Fig. 3. Therefore the gradient necessary to produce a certain current was somewhat less. So far as known, these are the first results to be published for liquid air temperature. A series of results on filaments that had been well outgassed showed that observations gave the same characteristic current-voltage curve when the filament was at temperature as high as 1000°K.

V. Discussion

The fact that the Schottky linear relation between the logarithm of the current and the square root of the field gradient does not hold is shown by replotting the previous results. In Fig. 5 curve *A* shows the results at room

temperature for a filament prior to outgassing; curve *B*, the results at room temperature for a filament outgassed three hours at 2700°K; and curve *C*, the results at liquid air temperature for a filament outgassed one hour at 2700°K. Instead of a straight line the curves are continually concave toward the gradient axis. This is precisely the result found by Millikan.

After the experimental results were recorded, it was discovered that these observations, as well as those of Millikan, satisfy a very simple numerical equation, which may be interpreted in terms of the applied field necessary

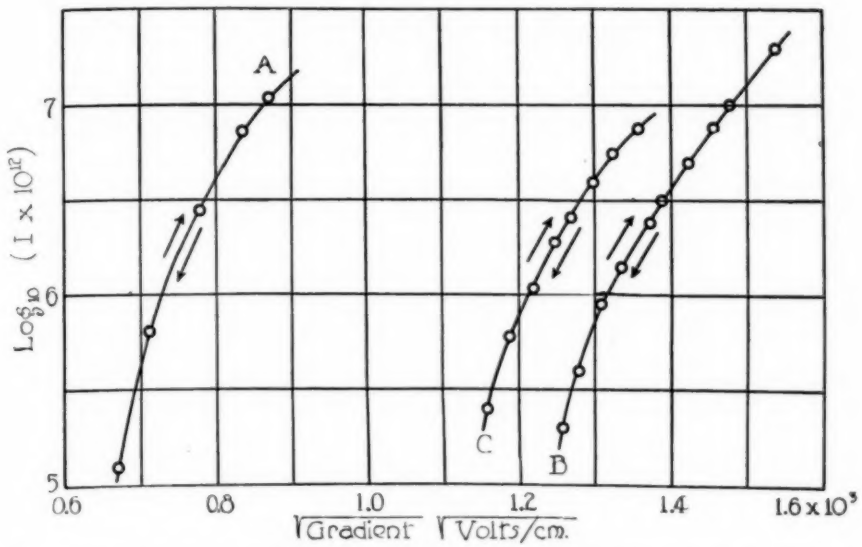

Fig. 5. Relation between the logarithm of the current and the square root of the potential gradient. A refers to Fig. 2, B to Fig. 3 and C to Fig. 4.

to cause the ejection of an electron from its orbit, by overcoming the orbital quantum energy. This theory and its verification by the results of Millikan and the writer will be given in a forthcoming article which is now ready to be presented for publication.

The larger part of the experimental observations were made in the Westinghouse Research Laboratory, prior to the time of the writer left the company. Also acknowledgment of criticism assistance is given to Dr. Slepiam, Dr. Kahler, Mr. Smede, and Mr. Rashevsky.

PITTSBURGH, PENNSYLVANIA,
December, 1927.

CORPUSCULAR THEORY OF LIGHT AND GRAVITATIONAL SHIFT

By G. Y. Rainich

Abstract

Usually the prediction of spectral shift in the light coming from regions of higher gravitational potential is derived by considering the emitting atom as an oscillating mechanism, and the shift is connected with retardation of clocks. In this paper the question is considered from the point of view of the corpuscular theory of light in the form which it takes in the relativity theory. In the special theory the light ray is considered as given by a vector freely movable along the line of its direction. It follows that all rays of light are absolutely equal, the difference in color is due to the difference in position with respect to the reference system (Doppler effect). In the general theory motion of a vector along a curve leads to a geodesic; colors of different rays cannot be compared unless some universal time is introduced; this introduction is easy in the centrosymmetric case; in this case the discussion is completed and leads to the usual result.

IT SEEMS that the wave theory and the corpuscular theory each describe one side of the phenomenon which we call light; the wave theory describes the field of radiation (or some features of the field) and the corpuscular theory describes the symmetry properties of the situation (and here again some features of this symmetry are left out, viz., polarization). We may hope that some time a general theory will be evolved which will embody the essential features of both theories and so give a more adequate picture of the phenomena; in the meantime the number of cases grows in which both theories can be applied with the same results. In this paper one of such cases is discussed. Usually in deriving the gravitational shift of spectral lines the wave theory is used, or if not exactly the wave theory the idea that light is a periodic phenomenon, the emitting mechanism is supposed to possess the same period and the shift is deduced as the effect of the retardation of time on the measuring of these periods. It seems that the more formal treatment based on the corpuscular theory of light which is given in this paper possesses some advantages; it permits us to see more clearly what assumptions we have to make and also how the phenomenon depends on the propagation of light through the intervening space. But even without these advantages it would be interesting, I think, to have an alternative treatment of the question.

1. In the special relativity theory a uniform rectilinear motion of a material particle may be characterized by a straight line in space-time and its four-dimensional momentum vector whose direction is that of the line and which is not attached to any particular point of the line so that we may consider it as freely movable along the line. The corpuscular theory suggests the characterization of the light quantum, or photon, also by a four-dimensional vector freely movable along the line of propagation. The formal

difference between the two cases is that a photon moves with the velocity of light which means that in the second case the momentum vector is a vector of zero square, whereas the momentum vector of a material particle is of negative square (has time direction). The importance of the relativity point of view is emphasized by the fact that this mere difference in direction of the momentum vectors leads to *essential* distinctions, and we know that essential distinctions exist between a material particle and a ray of light; in the classical theory, on the contrary, a difference in velocity is a quantitative difference only.

In the first place, since the square of a vector is its only invariant it follows that all light vectors—all photons—are exactly equivalent, can be transformed one into another by a (pseudo-euclidean) motion in space-time, a Lorentz transformation, whereas material particles may differ in the lengths of their momentum vectors, i.e., in their masses. This seems to be contradicted by our common experience of the existence of different colors but this simply means that the distinction in color (or frequency, to borrow a *term* from the wave theory) is not an absolute distinction, that frequency expresses only the relation of the light ray to the "reference system of the observer" and not an intrinsic property of the ray; though this formulation is not often, if ever, given, probably everybody will agree with its truth. The relation between the light vector (momentum vector of the photon), reference system of the observer, and the frequency is established as follows: frequency is proportional to energy, the energy of a material particle (total energy, consisting of mass and kinetic energy) is the time component of the momentum vector, it is natural to consider the energy of the photon also as the time component of its momentum vector. Frequency is therefore proportional to the time component of the light vector, or *frequency is proportional to the scalar product of the light vector and the unit vector of the time direction* of the observer, or

$$\nu = \kappa q \cdot T \tag{1}$$

where ν is the frequency, q the momentum vector of the photon, T the unit vector along the time axis of the observer and κ a factor of proportionality. Essentially this is nothing but the Doppler principle.

2. When we want to generalize this conception so that it could be applied in *curved* space-time we meet with two difficulties. The one appears when we ask ourselves what we mean here by a vector freely movable along a line; the other is connected with the question of universal time. We shall take up these two difficulties in turn.

How can a vector freely movable along a line be generalized so as to apply to curved space-time? In general, we have here no straight lines so we have to consider a curve as the four-dimensional path of a particle. The momentum vector will be naturally a tangent vector to this curve. We shall speak of a tangent vector freely movable along a curve; what do we mean by freely movable? In the case of flat space it means that the vector is the same in all points of the line. We may say that if we take a

vector equal to the momentum vector at every point of the line these vectors constitute a *field* whose differential along the line, or in the direction of the line, vanishes. Extending this, we shall have to consider a tangent vector at every point of the curve, these vectors constituting a field whose differential in the direction of the curve vanishes. In general, if q^i is the vector of the field $q^i{}_{,\rho}\, dx^\rho$ is the differential which gives the change of the field in the direction of the displacement dx^i; in our case we are interested in the displacement along the curve of which q^i itself is a tangent vector; we have to take dx^i proportional to v^i and write that the result will be zero; omitting the factor of proportionality we have thus $q^i{}_{,\rho}\, q^\rho = 0$, or using the formula for the covariant derivative of a contravariant tensor,

$$(\partial q^i/\partial x^\rho)q^\rho + \Gamma_{\sigma\rho}{}^i q^\sigma q^\rho = 0.$$

Now we consider the curve as given parametrically as $x^i = x^i(p)$. The derivatives dx^i/dp may be considered as the components of a tangent vector and it is always possible to choose the parameter p in such a way that dx^i/dp are equal to the components of given tangent vectors at all points of the curve. Substituting these expressions for q^i in the preceding equation we find after simple transformations

$$\frac{d^2x^i}{dp^2} + \Gamma_{\sigma\rho}{}^i \frac{dx^\sigma}{dp}\cdot\frac{dx^\rho}{dp} = 0. \tag{2}$$

In other words, if there exists a field of tangent vectors whose differential vanishes along the curve it must be possible to choose a parameter p in such a way that Eq. (2) is satisfied, and if such is the case the field of tangent vectors is given by

$$q^i = dx^i/dp. \tag{3}$$

These are things which, in a slightly different form, are very well known, of course; a curve for which such a choice of parameter is possible is called a geodesic, and we have here the case of the parallel displacement of a vector along a geodesic.[1] In curved space-time we have thus to consider a path of a particle a geodesic, i.e., a curve satisfying for some choice of the parameter Eq. (2) and as the momentum vector in every point the vectors given by (3) or vectors proportional to them (because a linear transformation of the parameter is permitted by (2) and such a transformation would result in the multiplication of the right hand sides of (3) by a constant).

All this applies equally to material particles and to light particles. The difference is that in the case of light particles we naturally assume that the vectors v^i are at every point of zero square, i.e.,

$$g_{\rho\sigma}q^\rho q^\sigma = g_{r\sigma}\frac{dx^\rho}{dp}\cdot\frac{dx^\sigma}{dp} = 0 \tag{4}$$

[1] Compare T. Levi-Civita. The Absolute Differential Calculus. Blackie & Son. London 1927, p. 104.

whereas in the case of material particles the left hand side of (4) will be negative. This makes it possible in the case corresponding to a material particle to introduce the arc length as the parameter, and makes it easy to introduce geodesics in this case by means of a minimum property (as the shortest curves). Arc length is zero in the case corresponding to light particles and therefore could not be used as a parameter; we have here to adhere to the definition given by (2).

3. In the special theory of relativity—in flat space-time—the color or frequency is measured, as stated above, by reference to the time axis of the observer. It is true that this time axis is not fixed (as the result of which we have the relativity of color), but if the time axis is fixed for one point it is fixed for the whole space-time; there is no absolute time but *there are universal times*. In the general relativity theory, in general space-time, this does not seem to be so; the choice of a time direction at one point does not seem to impose any restrictions on the choice of time directions at other points; in other words there do not seem to exist in the general space-time any separations into space and time, any stratifications, which are preferred to other stratifications as is the case for flat stratifications in flat space time; it may be true that the consideration of stratifications, of separation of space and time is not necessary for some purposes, e.g., in the discussion of the electromagnetic field; but it seems that in other cases the assumption of definite stratifications, of the existence of universal times is necessary; considerations connected with the possibility of determining the mass constant from the curvature field seem to require such a stratification[2]; and the same applies to the question which interests us here, the question of comparison of colors of different rays of light; if we want to compare two rays of light as to their color we must find the relative orientation of their light vectors with respect to the *same* time direction, we must have, therefore, the notion of the same time direction at different points; the choice of the time direction at one point must determine its choice at other points. It is probable, therefore, that physical space-times are not of the general type, that some restrictions have to be imposed on a mathematical space-time before it can serve as physical space-time, and these restrictions must make it possible to introduce in such spaces natural stratifications, natural separations into space and time. However, this is not the place to discuss further this general question.

4. Fortunately, in the simple case which appears in all applications, in the case of a centrosymmetric field given by

$$ds^2 = (1/\eta)dr^2 + r^2 d\theta^2 + r^2 \sin^2\theta d\phi^2 - \eta dt^2, \tag{5}$$

there exists a natural stratification, the role of the universal time being played by the variable t. We consider the curved space defined by (5) as representing the gravitational field of the sun and we neglect the field of the earth; the function η is given by

$$\eta = 1 - 2m/r \tag{6}$$

[2] Compare G. Y. Rainich. Mass in Curved Space-Time. Proceedings Nat. Acad. Sciences **12**, (February, 1926) pp. 110–113.

We want to study a ray of light which is emitted from the sun radially so that we make θ and ϕ constant; in addition to this we must have along the ray the condition that the tangent vector is of zero square, so that, according to (4) and using the values of the g's given by (5) $(1/\eta)dr^2-\eta dt^2=0$ or

$$dr=\eta dt \tag{7}$$

(we have here $dr=\pm\eta dt$, but the minus sign corresponds to light rays from the earth to the sun). The three conditions which we already have determine a curve and it remains to see whether it is a geodesic. Using the values of the Γ's belonging to the line element (5) (see, e.g., Eddington, Mathematical Theory of Relativity, C.U.P. 1924, p. 84) we find that two of the four equations (2) are satisfied for all choices of the parameter. The remaining two equations

$$d^2r/dp^2+\Gamma_{11}{}^1(dr/dp)^2+\Gamma_{44}{}^1(dt/dp)^2=0$$

and

$$d^2t/dp^2+2\Gamma_{14}{}^4(dr/dp)/(dt/dp)=0$$

are not independent if we take into account (7), and give d^2r/dp^2 the value zero, i.e., the parameter p must be a linear function of r. We may take r itself as our parameter p. The components of the momentum vector are then, according to (3) equal or proportional to

$$q^1=dr/dr=1,\ q^2=0,\ q^3=0,\ q^4=1/\eta. \tag{8}$$

In order to find the color of this ray of light we have to introduce a unit vector of time direction. As we mentioned before, we choose as our time direction the direction $r=$ const., $\theta=$ const., $\phi=$ const.; if T^i is the unit vector of this direction we have by (5)

$$T^1=0,\ T^2=0,\ T^3=0,\ \eta(T^4)^2=1. \tag{9}$$

For the scalar product of the vectors q and T which, according to (1), is proportional to the frequency, we obtain from (8) and (9)

$$1/\eta^{1/2}.$$

This means that if an observer at the distance r_1 from the center of the sun measures the frequency $1/[\eta(r_1)]^{1/2}$ another observer at the distance r_2 measures the frequency $1/[\eta(r_2)]^{1/2}$ for the same ray or an identical ray. If we take the first observer near the surface of the sun and the second on the earth (whose gravitational field, as was mentioned, we neglect) the frequencies will be approximately proportional (by (6)) to $1+m/R$ and 1, respectively, where R is the radius of the sun. This is the customary result. The prediction of the shift follows now from the assumption that identical atoms under all conditions emit light of equal frequencies as judged by a nearby observer for whom the atom is at rest.

ANN ARBOR, MICHIGAN,
December 20, 1927.

EQUIPOTENTIAL SURFACE ELECTRONS AS AN EXPLANATION OF THE PACKING EFFECT

By W. Edwards Deming

Abstract

The mutual mass of ordinary uniformly charged electrons and protons has long been known to account for only a small fraction of the packing effect, ten percent at best. By postulating that the electrons and protons shall be equipotential surface distributions having the usual total charges and radii, the writer shows that any static model for a helium nucleus can give considerably more packing than is possible with ordinary electrons. This idea is applied to two models and found to work out satisfactorily; in fact almost any desired amount of packing could be obtained. Nuclear models in dynamic equilbrium present difficulties which have not been overcome, because the relativity increase in mass of the revolving protons seems to more than annul the negative mutual mass in the two models considered. For the same reason, ordinary electrons in these dynamic models produce negligible packing. So the situation is that with static models of the helium nucleus, packing can be satisfactorily accounted for by equipotential surface electrons but only about ten percent at most by ordinary electrons, and with dynamic models neither kind offers a solution.

ACCORDING to the electromagnetic theory of matter, the packing effect should be accounted for by the negative mutual mass of electrons and protons. The evidence becomes more and more convincing with time that a helium atom must be made up of four protons and four electrons, that is, of four hydrogen atoms. This idea immediately encounters a small difficulty with atomic weights. The atomic weights of hydrogen and helium are known with little doubt to be 1.0078 and 4.000 respectively, whence the amount of packing in helium must be $4\times1.0078-4.000=0.0312$. Harkins and Wilson,[1] by calculating the mutual electromagnetic momentum of two moving charges, found that if the distance between centers of an electron and a proton in the nucleus is about 400 times the radius of a proton, the required amount of negative mutual mass results. But this is obviously an impossible arrangement if the radius of an electron is anything like 1846 times that of a proton, as is suggested by the electromagnetic theory.

It is difficult to imagine any atomic model for helium which could give more packing than one with a half nucleus as shown in Fig. 1, if the two protons are diametrically tangent to the electron.[2] Yet this model yields only about one-tenth the requisite packing, as is easily proved. Thus if a, A, m, M are the radii and masses of electron and proton, e the electronic

[1] W. D. Harkins and E. D. Wilson, J. Amer. Chem. Soc. **37**, 1367–1383, 1383–1396, 1396–1421 (1915). Zeits. f. Anorgan. Chem. **95**, 1–19 (1916).

[2] This arrangement was proposed by W. Lenz, Sitzungsberichte der mathematische-physikalischen Klasse der Bayerischen Akademie der Wissenschaften zu München, p. 355 (1918).

charge in Heaviside-Lorentz units, $m=e^2/6\pi ac^2$, $M=ma/A$; and if in Fig. 1 $AB=2f=2a/Y$, $Y\equiv a:f$, the expression[3]

$$\text{Mutual mass} = (1/6\pi c^2)\sum_{ij} e_i e_j/r_{ij},\ i\neq j \tag{1}$$

for the space average mutual mass gives

$$(2/6\pi c^2)\{-4e^2Y/a+2e^2Y/2a\} = -6Ym\equiv mG(Y) \tag{2}$$

as the space average mutual mass of both halves of the nucleus. The maximum value of Y is practically unity, 1846/1847. The difference 0.0312 between the atomic weights of 4H and He is equivalent to $0.0312\times 1847m/1.0078=57.18m$, since an atomic weight 1.0078 means each atom has the mass $1847m$. 6:57 is roughly 1:10, which accords with the above statement.

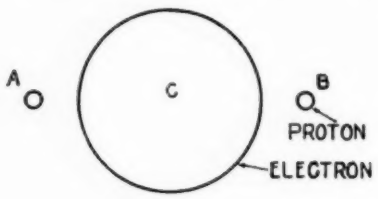

Fig. 1.

This result is independent of any *radial* law of distribution of charge in electron or proton, provided they remain spheres in the inertial system in which they are momentarily at rest, because homogeneous concentric layers of charge behave as if the whole charge were concentrated at the center.

If modern views on the formation of complex atoms, and the electromagnetic theory of mass, are anywhere near correct, there must be some way to account for packing by the same theory. A clue to an explanation arises from the following considerations. The helium nucleus must be an extremely stable structure because there is no evidence that an α-particle has ever been shattered. Consequently one would expect the change from 4H to He to involve a considerable evolution of energy and hence a disappearance of mass. Also the same integral, $\int\int(de_1de_2)/r$ (taken over all charged surfaces, or in fact, volumes), occurs as a factor both for the electromagnetic mass and for the electrostatic energy, of these charged surfaces or volumes. A familiar theorem on electrical energy is[4] "If any number of surfaces are fixed in position, and a given charge is placed on each surface, then the energy is a minimum when the surfaces are placed so that every surface is an equipotential." This suggests that if in Fig. 1 the uniform surface distribution of a Lorentz electron be modified so as to become that on a perfect spherical conductor of radius a, the mutual mass of the nucleus might be sufficiently negative to explain packing. This modification is clearly important only when the electron is extremely close to some other charge (such as in an atomic nucleus) so there is no reason for any anxiety in regard to the many beautiful results obtained in other lines with the Lorentz electron.

Let us proceed to calculate the space average rest mass of two protons separated by an electron as in Fig. 1, treating them as *equipotential* spherical

[3] See, for example, Leigh Page, "An Introduction to Electrodynamics," Ginn & Company, 1922, Eq. 33, p. 56.

[4] J. H. Jeans, Electricity and Magnetism, Cambridge University Press, art. 189.

surface distributions—not by computing directly the electrostatic energy of the combination and multiplying this by $4/3c^2$, as might seem to be the easiest way, but by direct application of the double integral above mentioned, choosing the latter method in order to find incidentally the intrinsic mass of the modified electron itself.

First, we shall need an expression for the electric potential at any point $P(r, \theta)$ produced by an electrified zone of surface density σ and of angle $\alpha, \alpha+d\alpha$. This is known to be

$$\left.\begin{aligned} dV &= 2\pi a\sigma \sin\alpha\, d\alpha \sum_0^\infty (a/r)^{n+1} P_n(\cos\alpha) P_n(\cos\theta), && r>a \\ &= 2\pi a\sigma \sin\alpha\, d\alpha \sum_0^\infty (r/a)^n P_n(\cos\alpha) P_n(\cos\theta), && r<a \\ &= 2\pi a\sigma \sin\alpha\, d\alpha \sum_0^\infty P_n(\cos\alpha) P_n(\cos\theta), && r=a \end{aligned}\right\} \tag{3}$$

P_n stands for Legendre's nth coefficient.

Next we must find the surface density σ on the electron. Consider a conducting sphere with center at C, radius a, total charge $-e$. Point charges e are at A and B. Images of A, B are at D, E of amount $-ea/f$ each. (See Fig. 2.) It is easily found that

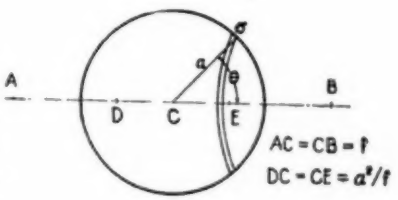

Fig. 2.

$$\sigma = \frac{e}{2\pi af} - \frac{e}{4\pi a^2} - \frac{e(f^2-a^2)}{4\pi a}\left\{\frac{1}{(a^2+f^2+2af\cos\theta)^{3/2}} + \frac{1}{(a^2+f^2-2af\cos\theta)^{3/2}}\right\}$$

If $(A+x)^{-3/2} = \sum_0^\infty a_n P_n(x)$, then by the usual process

$$a_n = \frac{1}{2}(2n+1)\int_{-1}^{+1} (A+x)^{-3/2} P_n(x)\, dx,$$

and

$$\sigma = \frac{e}{2\pi af} - \frac{e}{4\pi a^2} - \frac{e(f^2-a^2)}{2\pi a(2af)^{3/2}} \sum_0^\infty a_{2n} P_{2n}(\cos\theta)$$

$$\sigma = \sum_0^\infty b_{2n} P_{2n}(\cos\theta) \tag{5}$$

$$\left.\begin{aligned} a_0 &= (2af)^{1/2} 2a/(f^2-a^2) \\ a_{2n} &= a_0(4n+1)(a/f)^n \end{aligned}\right\} \tag{6}$$

$$\left.\begin{aligned} b_0 &= e/2\pi af - e/4\pi a^2 - e(f^2-a^2)a_0/2\pi a(2af)^{3/2} = -e/4\pi a^2 \\ b_{2n} &= b_0 2(4n+1)(a/f)^{2n+1} \qquad n=1, 2, 3, \ldots. \end{aligned}\right\} \tag{7}$$

Write $a:f \equiv Y$.

$$\sum_0^\infty b_{2n}^2/(4n+1)^2 = b_0^2 + \sum_1^\infty b_{2n}^2/(4n+1)^2 = b_0^2 + 4b_0^2(Y^6+Y^{10}+Y^{14}+Y^{18}+\cdots)$$
$$= b_0^2[1+4Y^6/(1-Y^4)], \tag{8}$$

an expression which is needed later on.

We are now ready to compute the double surface integral $\int\int (de_1 de_2)/r$ over the surface of the electron. de_1 and de_2 are elements of charge on the electron, r the distance between them. Suppose de_1 lies on a zone of angle interval θ_1, $\theta_1 + d\theta_1$, and de_2 on one of angle interval θ_2, $\theta_2 + d\theta_2$. Let σ_1 and σ_2 be the surface densities at the angles θ_1 and θ_2. Then use $de_1 = \sigma_1 a^2 \sin\theta_1 d\theta_1 d\phi_1$ and $de_2 = \sigma_2 a^2 \sin\theta_2 d\theta_2 d\phi_2$. Now de_2/r integrated with respect to ϕ_2 is merely the expression for the potential at de_1 produced by the zone θ_2, $\theta_2 + d\theta_2$, and this is given by Eq. (3). Put $\mu_1 \equiv \cos\theta_1$ and $\mu_2 \equiv \cos\theta_2$ whenever convenient.

$$\int\int \frac{de_1 de_2}{r} = \int\int\int_{\theta_2=0}^{\theta_2=\pi} de_1 2\pi a\sigma_2 \sin\theta_2 d\theta_2 \sum_0^\infty P_n(\cos\theta_1) P_n(\cos\theta_2)$$
$$= 4\pi^2 a^3 \int_{-1}^{+1}\int_{-1}^{+1} d\mu_1 d\mu_2 \cdot \sum_0^\infty b_{2n} P_{2n}(\mu_1) \cdot \sum_0^\infty b_{2n} P_{2n}(\mu_2) \times \sum_0^\infty P_n(\mu_1) P_n(\mu_2)$$
$$= 4\pi^2 a^3 \int_{-1}^{-1} d\mu_2 \sum_0^\infty b_{2n} P_{2n}(\mu_2) \cdot \sum_0^\infty \frac{2b_{2n}}{4n+1} P_{2n}(\mu_2)$$
$$= 4\pi^2 a^3 \sum_0^\infty b_{2n}^2 [2/(4n+1)]^2 = 16\pi^2 a^3 \sum_0^\infty \frac{b_{2n}^2}{(4n+1)^2}$$
$$= 16\pi^2 a^3 \frac{e^2}{16\pi^2 a^4}[1+4Y^6/(1-Y^4)] = \frac{e^2}{a}[1+4Y^6/(1-Y^4)] \tag{9}$$

With these preliminaries we are now ready to find the space average rest mass of the electron. This is known[5] to be $(1/6\pi c^2)\int\int de_1 de_2/r$ for a charge of arbitrary distribution. For our particular electron, we have calculated this integral. Inserting its value just found, we get

$$(e^2/6\pi a c^2)[1+4Y^6/(1-Y^4)] \tag{10}$$

for the intrinsic space average rest mass of our electron. Of course this reduces to $e^2/6\pi a c^2$ when f becomes large.

Seeing that the mass of this electron has been increased by postulating that it is to be an equipotential surface rather than a uniform distribution, it is natural to enquire into possible changes, caused by the same assumption, in the mass of the two protons A and B. The easiest way to dispose of this

[5] See, for example, Leigh Page, ibid., p. 52.

question is to treat the protons as if they are in a uniform field F. Proton B is acted upon by charges e at A, $-eY$ at D and E, $2eY-e$ at C. $AB=2f$, $DB=f(1+Y^2)$, $EB=f(1-Y^2)$.

$$F=\frac{e}{4\pi f^2}[1/4-Y/(1+Y^2)^2-Y/(1-Y^2)^2+2Y-1] \tag{11}$$

F can never be infinite because the center of a proton can not touch the surface of an electron. With the aid of Fig. 3, consider proton B as a conducting sphere of radius A and charge e in a uniform field F. The potential at $P(r, \theta)$ is $V=-F(r-A^3/r^2)\cos\theta+e/4\pi r$ The radial and tangential components of the resulting field at P are

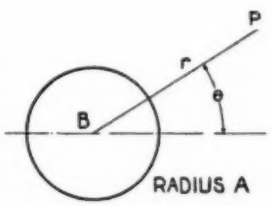

Fig. 3.

$$-dV/rd\theta=-(F/r)(r-A^3/r^2)\sin\theta$$
$$-dV/dr=-F(1+2A^3/r^3)\cos\theta+e/4\pi r^2$$

On the surface where $r=A$ they are 0 and $-3F\cos\theta+e/4\pi A^2$. Consequently the density of electrification at any point (A, θ) on the proton is

$$w=-3F\cos\theta+e/4\pi A^2=H\cos\theta+K=HP_1(\cos\theta)+KP_0(\cos\theta).$$

Just as in dealing with the electron, take two elements of charge $de_1=w_1A^2\sin\theta_1 d\theta_1 d\phi_1$ and $de_2=w_2A^2\sin\theta_2 d\theta_2 d\phi_2$ at points where θ is θ_1 and θ_2. Again use $\mu_1\equiv\cos\theta_1$ and $\mu_2\equiv\cos\theta_2$. Then over the surface of the proton

$$\int\int\frac{de_1de_2}{r}=\int\int\int de_1 2\pi A\, w_2 d\mu_2\sum_0^\infty P_n(\mu_1)P_n(\mu_2)$$

$$=4\pi^2A^3\int_{-1}^1\int_{-1}^1 d\mu_1 d\mu_2\{KP_0(\mu_1)+HP_1(\mu_1)\}\{KP_0(\mu_2)+HP_1(\mu_2)\}$$

$$\times\sum_0^\infty P_n(\mu_1)P_n(\mu_2)$$

$$=4\pi^2A^3\int_{-1}^1 d\mu_2\{KP_0(\mu_2)+HP_1(\mu_2)\}\{2KP_0(\mu_2)+\tfrac{2}{3}HP_1(\mu_2)\}$$

$$=4\pi^2A^3\{4K^2+4H^2/9\}=4\pi^2A^3(4e^2/16\pi^2A^4+36F^2/9)$$

$$=e^2/A+16\pi^2F^2A^3$$

So the space average rest mass of the proton will be

$$\frac{1}{6\pi c^2}\int\int\frac{de_1de_2}{r}=\frac{e^2}{6\pi Ac^2}\left(1+\frac{16\pi^2F^2A^4}{e^2}\right)=M\left\{1+\frac{16\pi^2F^2a^4}{e^2(1846)^4}\right\} \tag{12}$$

which differs from M only by an insensibly small quantity unless the proton is many times closer to the surface of the electron than will shortly be

found necessary to give the desired packing effect. It must be remembered that Eq. (12) is not valid anyway if the proton is extremely close to the electron surface, because the field is then no longer even approximately uniform over the proton. In this case a more exact treatment would be to consider proton B acted on only by its image E. The rather surprising result is that, although the intrinsic mass of the proton is thus increased, the mutual mass of proton and image is sufficiently negative to give a net gain in packing. But values of Y so close to unity will be left entirely out of the discussion and the mass of the protons taken as M exactly.

The mass of each proton remains persistently so close to M because of the small ratio $A:a$. This is also why secondary images can be neglected and the protons regarded accordingly as point charges in dealing with their electrical effects at points external to them.

The space average intrinsic rest mass of the half nucleus is

$$2M+m(1+4Y^6/[1-Y^4])=2\times 1846m+m(1+4Y^6/[1-Y^4]) \quad (13)$$

To this must be added the mutual mass of the half nucleus which is given by Eq. (1). This can be resolved into six partial summations, for convenience.

(i) Let e_i be proton A and e_j be the charge of the zone θ, $\theta+d\theta$ on the electron. $e_i=e$, $e_j=2\pi a\sigma \sin\theta\, d\theta$, and $r_{ij}=(a^2+f^2+2af\cos\theta)^{1/2}$. σ is given by Eq. (4). This partial summation is

$$e\int\int (a^2+f^2+2af\cos\theta)^{-1/2}\sigma\, dS=-e^2/f+2ae^2/f-e^2a/(f^2-a^2)-e^2a/(f^2+a^2) \quad (14)$$

As might have been anticipated, this is the same result as would have been obtained on replacing the electron by charges $-ea/f$ at D and E, and $2ea/f-e$ at C.

(ii) Let e_i be proton A and e_j be proton B. This partial summation is $e^2/2f$.

(iii) Let e_i be the charge on the zone θ, $\theta+d\theta$ and e_j be proton A. This has the same result as (i).

(iv) Let e_i be the charge on the zone θ, $\theta+d\theta$ and e_j be proton B. This has the same result as (i).

(v) Let e_i be proton B and e_j be proton A. This gives the same result as (ii).

(vi) Let e_i be proton B and e_j be the charge on the zone θ, $\theta+d\theta$; same as (i).

The sum of these six partial summations gives for the space average mutual mass of the half nucleus

$$(1/6\pi c^2)\sum_{ij} e_ie_j/r_{ij}=(1/6\pi c^2)\{4(-e^2/f+2ae^2/f-e^2a/(f^2+a^2)-e^2a/(f^2-a^2))+e^2/f\}=-m\{3Y-8Y^2+8Y^2/(1-Y^4)\} \quad (15)$$

The mass of the entire helium atom is

$$\text{Intrinsic Mass}+\text{Mutual Mass}=2\{m+2\times 1846m+m(1+4Y^6/[1-Y^4])$$
$$-m(3Y-8Y^2+8Y^2/[1-Y^4])\}$$

which must amount to

$$[4/(4\times 1.0078)]\times 4m\times 1847=4m\times 1847(1-.00774\cdots)$$

Then

$$F(Y)\equiv 2(4Y^6/[1-Y^4]-3Y+8Y^2-8Y^2/[1-Y^4])=-(8Y^6/[1-Y^4]+6Y)$$
$$=-4\times 1847\times .00774\cdots=-57.18\cdots \qquad (16)$$
$$=-57 \text{ closely enough.}$$

The equation $8Y^6-6Y^5+57Y^4+6Y-57=0$ has one positive root. It is $Y=.966249\cdots$, $Y^{-1}=1.0349\cdots$. So if $f=1.035a$ the requisite amount of packing is obtained. The separation between the center of either proton and the surface of the electron will then be $0.035a$, which is sixty-five times the radius of a proton.

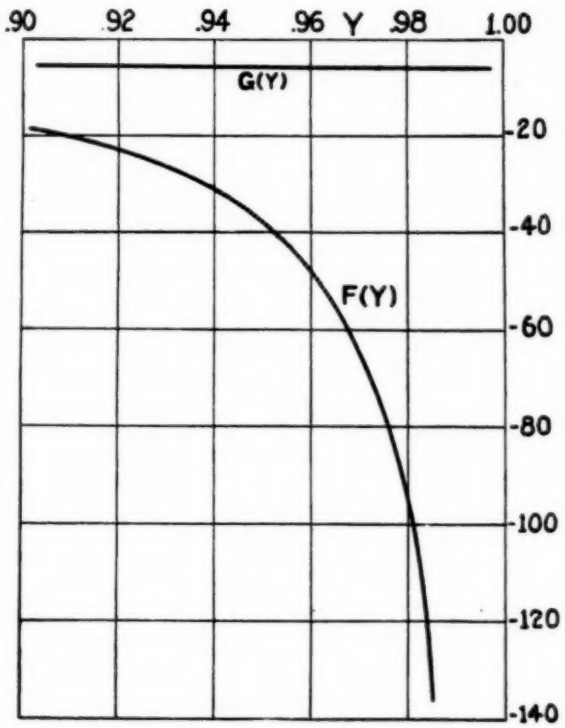

Fig. 4. $F(Y)$ and $G(Y)$ as functions of Y.

$-mF(Y)$ is the resulting packing effect of the helium atom using equipotential electrons. $-mG(Y)=6Ym$ is the corresponding packing with ordinary electrons. $F(Y)$ and $G(Y)$ are plotted in Fig. 4, which shows that as the distance $f=a/Y$ decreases, the packing $-mF(Y)$ increases almost without limit.

It thus appears that the idea of treating electrons and protons as equipotential spheres rather than uniformly charged ones works out very well. This modification can be expected to increase considerably the packing effect over that given by ordinary electrons, regardless of the model adopted for the nucleus, since the statements made in the opening paragraphs may be considered as a general proof. In order to test the idea, *some* model must be tried. That of Fig. 1 is probably unequalled for simplicity and definiteness, because the expression found for σ is exact and not merely an approximation, as there are no multiple images when the protons are treated as points and no other electron is near. Unfortunately this is not regarded as the best model, the main reason being that the helium nucleus or α particle is probably a unit and there seems to be no way in which the above two half nucleii could hold rigidly together.

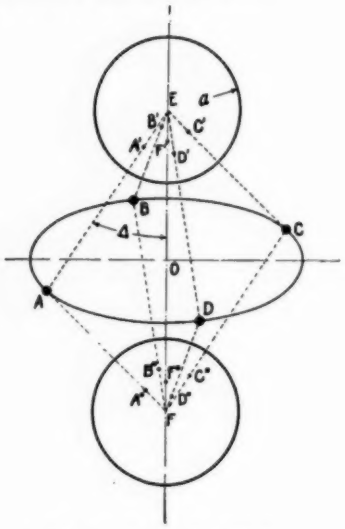

Fig. 5. Lenz Model II

The writer has applied the idea of equipotential surface electrons to the inverted oxygen model[6] (Lenz Model II) of Fig. 5 with similar success. A, B, C, D are the four protons, E, F the centers of the two electrons. A', B', C', D' and A'', B'', C'', D'' are the images of the protons in the electrons. F' is the image in E of the uniform distribution of charge on F, and F'' is the image in F of that on E. No account will be taken here of secondary images. The tedious but straightforward details of the calculation will be omitted and the work merely outlined. Let

$$EA=EB=EC=ED=EA''=\cdots=f=a/Y, \quad Y\equiv a:f.$$
$$Z\equiv a:EF, \quad \Delta=EAF=BEF=\cdots$$

On electron E there will be six distributions $S_1, S_2, \cdots, S_6$ of surface charge, whose densities at any point are $\sigma_1, \sigma_2, \cdots, \sigma_6$, say. Their electrical effects at points on and outside the sphere are the same as if they are point charges

$$\begin{aligned} &q_1=e(4Y-1)/(1-Z) \text{ at } E. && q_4=-eY \text{ at } B'(\alpha_4=0,\ aY)\\ &q_2=-q_1Z \text{ at } F'(\theta=0,\ aZ) && q_5=-eY \text{ at } C'(\alpha_5=0,\ aY) \qquad (17)\\ &q_3=-eY \text{ at } A'(\alpha_3=0,\ aY) && q_6=-eY \text{ at } D'(\alpha_6=0,\ aY) \end{aligned}$$

[6] Also proposed by W. Lenz, loc. cit. Described in Sommerfeld's Atombau und Spektrallinien, 3. Auflage, p. 118.

respectively. $\Sigma q_i = -e$ as they should. The polar axis $\theta = 0$ is the line EF, and the polar axes $\alpha_i = 0$ are the lines EA, EB, EC, ED for $i = 3, 4, 5, 6$.

$$\sigma_i = -e(f^2-a^2)/4\pi a(a^2+f^2-2af\cos\alpha_i)^{3/2} = -\frac{e}{4\pi a^2} Y \sum_0^\infty (2n+1) Y^n P_n(\cos\alpha_i),$$

$$i = 3, 4, 5, 6. \tag{18}$$

To get σ_2, replace α_i by θ, Y by Z, $-e$ by $-q_2$.

$$\sigma_2 = -\frac{q_1}{4\pi a^2} Z \sum_0^\infty (2n+1) Z^n P_n(\cos\theta) \tag{19}$$

To calculate $\int\int de_1 de_2/r$ over electron E.

This integration may be divided into six parts, corresponding to de_1 as an element of $S_1, S_2, \cdots$, or S_3. Let de be an element of S_i and r_j the distance from de to q_j.

$$\int\int \frac{de_1 de_2}{r} = \sum_{i=1}^6 \int\int \left(\frac{de}{r_1} q_1 + \frac{de}{r_2} q_2 + \cdots + \frac{de}{r_6} q_6\right) \tag{20}$$

Use a, θ, ϕ for the coordinates of de, then $de = a^2\sigma_i \sin\theta\, d\theta\, d\phi$. $\int_{S_i}\int de/r_j$ is the mathematical expression for the potential at q_j produced by the surface distribution S_i. If h_j, β_j are the coordinates of q_j (the axes $\beta_j = 0$ and $\theta = 0$ being coincident), Eqs. (3) give

$$q_j \int_{S_i}\int de/r_j = 2\pi a \int_{-1}^1 \sigma_i d\mu \sum_{j=1}^6 \sum_0^\infty q_j (h_j/a)^n P_n(\cos\beta_j) P_n(\mu) \equiv I_i \text{ say.}$$

$$\int\int \frac{de_1 de_2}{r} = \sum_{i=1}^6 I_i$$

$$I_1 = 2\pi a \int_{-1}^{+1} (q_1/4\pi a^2) d\mu \Big\{ q_1 + q_2 \sum_0^\infty Z^n P_n(\mu) \cdot P_n(1) + 4q_3 \times \sum_0^\infty Y^n P_n(\mu) P_n(\cos\Delta) \Big\}$$

$$= \frac{q_1}{a}(q_1 + q_2 + 4q_3)$$

$$I_2 = 2\pi a \int_{-1}^1 d\mu (-q_1/4\pi a^2) Z \sum_0^\infty (2n+1) Z^n P_n(\mu) \Big\{ q_1 + q_2 \sum_0^\infty Z^n P_n(\mu) P_n(1) + 4q_3 \sum_0^\infty Y^n P_n(\mu) P_n(\cos\Delta) \Big\} = -(q_1 Z/a) \Big\{ q_1 + q_2 \sum_0^\infty Z^{2n} P_n(1)$$

$$+4q_3\sum_0^\infty Y^nZ^nP_n(\cos\Delta)=(-q_1Z/a)\{q_1+q_2/(1-Z^2)$$

$$+4q_3/(1+Y^2Z^2-Y^2)^{1/2}\}$$

remembering that $(1+r^2-2rx)^{-1/2}=\sum_0^\infty r^nP_n(x)$

$$I_3=2\pi a\int_{-1}^{1}(d\cos\alpha_3)(-e/4\pi a^2)Y\sum_0^\infty(2n+1)Y^nP_n(\cos\alpha_3)$$

$$\times\Big\{q_1+q_2\sum_0^\infty Z^nP_n(\cos\alpha_3)P_n(\cos\Delta)+q_3\sum_0^\infty Y^nP_n(\cos\alpha_3)P_n(1)$$

$$+q_4\sum_0^\infty Y^nP_n(\cos\alpha_3)P_n(\cos^2\Delta)+q_5\sum_0^\infty Y^nP_n(\cos\alpha_3)P_n(\cos 2\Delta)$$

$$+q_6\sum_0^\infty Y^nP_n(\cos\alpha_3)P_n(\cos^2\Delta)\Big\}$$

$$=(-eY/a)\Big\{q_1+q_2\sum_0^\infty Y^nZ^nP_n(\cos\Delta)P_n(1)+q_3\sum_0^\infty Y^{2n}P_n^2(1)$$

$$+2q_4\sum_0^\infty Y^{2n}P_n(1)P_n(\cos^2\Delta)+q_5\sum_0^\infty Y^{2n}P_n(1)P_n(\cos 2\Delta)\Big\}$$

$$=(-eY/a)\{q_1+q_2/(1+Y^2Z^2-Y^2)^{1/2}+q_3/(1-Y^2)+2q_3/(1+Y^4-2Y^2\cos^2\Delta)^{1/2}$$

$$+q_3/(1+Y^4-2Y^2\cos 2\Delta)^{1/2}\}=I_4=I_5=I_6.$$

The space average intrinsic rest mass of each electron is therefore

$$\frac{1}{6\pi c^2}\int\int\frac{de_1de_2}{r}=\frac{1}{6\pi c^2}\sum_1^6 I_i=m+m\{-1+(4Y-1)^2/(1-Z)$$

$$-Z(4Y-1)^2/(1-Z)^2-8Y(4Y-1)/(1-Z)+Z^2(4Y-1)^2/(1-Z)^2(1-Z^2)$$

$$+8YZ(4Y-1)/(1-Z)(1+Y^2Z^2-Y^2)^{1/2}+4Y^2/(1-Y^2)$$

$$+8Y^2/(1+Y^4-2Y^2\cos^2\Delta)^{1/2}+4Y^2/(1+Y^4-2Y^2\cos 2\Delta)\}$$

$$\equiv m+m\,\tfrac{1}{2}I(Y,Z) \qquad (21)$$

where $I(Y,Z)$ denotes twice the quantity enclosed by the braces. $I(Y,Z)$ vanishes when Y and Z are both zero.

In finding the mutual mass of this nucleus, let (A,B) denote q_Aq_B/AB, that is, the charge effective at A multiplied by the charge effective at B, divided by the distance AB. $(A,B)=(B,A)$. The space average mutual mass of the nucleus will be

$$\frac{1}{6\pi c^2}\sum\sum(A,B),\quad A\neq B,$$

and in which A and B never lie inside the same sphere. This will be a sum of 180 terms, not all different. The result is

$$\begin{aligned}
\textit{Mutual Mass} = (2/6\pi c^2)\,[&8(E,A)+(E,F)+2(E,F'')+8(E,A'')+(F',F'')\\
&+8(F',A)+8(F',A'')+8(A',A)+16(A',B)+8(A',C)+4(A',A'')\\
&+8(A',B'')+4(A',C'')+4(A,B)+2(A,C)\,] = 2m\{8Y(4Y-1)/(1-Z)\\
&+(4Y-1)^2Z/(1-Z)^2-2Z^2(4Y-1)^2/(1-Z^2)(1-Z)^2\\
&-8YZ(4Y-1)/(1-Z)(1+Y^2Z^2-Y^2)^{1/2}+Z^3(4Y-1)^2/(1-Z)^2(1-2Z^2)\\
&-8YZ(4Y-1)/(1-Z)(1+Y^2Z^2-Y^2)^{1/2}+8YZ(4Y-1)/(1-Z)\\
&\qquad\qquad [(1-Z^2)^2+2Y^2Z^2-Y^2]^{1/2}\\
&-8Y^2/(1-Y^2)-16Y^2/(1+Y^4-2Y^2\cos^2\Delta)^{1/2}-8Y^2/(1+Y^4-2Y^2\cos 2\Delta)^{1/2}\\
&+4Y^2Z/(1-Y^2)+8Y^2Z/[(1-Y^2)^2+2Y^2Z^2\sin^2\Delta]^{1/2}\\
&+4Y^2Z/[(1-Y^2)^2+4Y^2Z^2\sin^2\Delta]^{1/2}+4Z(2)^{1/2}\cot\Delta+2Z\cot\Delta\} \equiv m\,M(Y,Z)
\end{aligned}$$

$M(Y,Z)$ vanishes when Y and Z become zero.

The intrinsic mass of the entire atom is $4\times 1846+2m+m\{2+I(Y,Z)\}$. The intrinsic mass plus mutual mass is $4(1846+1)m+m\{I(Y,Z)+M(Y,Z)\}$, which must amount to $4\times 1847m(1-.00774\cdots)=4\times 1847m-57m$, closely enough. So

$$I(Y,Z)+M(Y,Z)=-57$$

to account for the packing in the helium atom.

The greatest packing effect is obtained when the electrons are touching. Then $Z=\frac{1}{2}$.

$$\begin{aligned}
I(Y,\tfrac{1}{2})+M(Y,\tfrac{1}{2}) = 2\{&-1+5(4Y-1)^2/3-2Y^2/(1-Y^2)-8Y^2/(1-Y^4)^{1/2}\\
&-4Y^2/(1-Y^2)^{1/2}(1+3Y^2)^{1/2}-16Y(4Y-1)/(4-3Y^2)^{1/2}\\
&+16Y(4Y-1)/(9-8Y^2)^{1/2}+4(2)^{1/2}Y^2/(2-3Y^2+Y^4)^{1/2}\\
&+(2Y^2+3.83Y)/(1-Y^2)^{1/2}\}
\end{aligned} \tag{22}$$

$I(Y,\frac{1}{2})+M(Y,\frac{1}{2})$ is plotted in Fig. 6 which shows that the requisite packing occurs when Y is about .98. The object of the above work is not to find the numerical value of Y which yields the requisite packing, but to prove that the required amount *can* be obtained. The object has been accomplished, even under the adverse condition of excluding all but primary images. Indeed, even more than the required $-57m$ is obtained by making Y still closer to unity. With closer approximations we should probably find that Y could be adjusted to decrease the atomic weight perhaps a half; this is only a hazardous guess, of course.

As has been remarked, secondary and further images have been left out of the reckoning, in order to leave the problem simple enough to be attractive. If the images A''', B''', C''', D''' in electron E of A'', B'', C'', D'', and A^{IV}, B^{IV}, C^{IV}, D^{IV} in F of A', B', C', D' had been included the value of $I(Y,\frac{1}{2})+M(Y,\frac{1}{2})$ would have been much smaller, i.e., the mutual mass would have turned out to be considerably more negative for any value of Y than the results exhibited in the graph. The inclusion of A''', B''', C''', D''', A^{IV}, B^{IV}, C^{IV}, D^{IV}, they being all positive, would increase the packing in several ways. (i) Their direct effect on the intrinsic mass of each electron would be a decrease, because placing a positive distribution on the negative distributions would give a smaller value of $\int\int de_1 de_2/r$. (ii) q_2 would change from $-(4Y-1)Z/(1-Z)$ to $-[(4Y-1)e-A''']Z/(1-Z)$. This would also decrease the value of $\int\int de_1 de_2/r$. (iii) q_1 would change from $(4Y-1)/(1-Z)$ to $[(4Y-1)e-4A''']/(1-Z)$. This, too, would lower $\int\int de_1 de_2/r$, thus decreasing still more the intrinsic mass. This new value of q_1 would also lower the mutual mass through the terms $(E,A)\cdots$, $(F,A)\cdots$. (iv) The new terms like (A''',A''), $(A''',B'')\cdots$, $(A^{IV},A')\cdots$, being 32 in number would lower the mutual mass by nearly offsetting the positive terms (A',A''), $(A',B'')\cdots$, $(A'',A')\cdots$. A slight disadvantage would arise from terms such as (A,A'''), $(A,B''')\cdots$, $(A,A^{IV})\cdots$, (D,D^{IV}), but the net result would be a much greater packing effect.

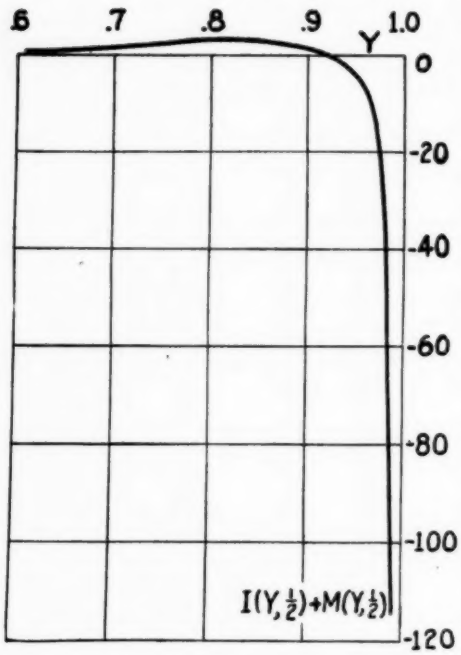

Fig. 6

A rigorous computation of $I(Y,\frac{1}{2})+M(Y,\frac{1}{2})$, using an infinite series of images, would yield a negative quantity for all values of Y, as is evident from considerations of electrostatic energy—yet the curve in Fig. 6, being only an approximation, crosses the Y axis. Surely, then, a better approximation will lower the whole curve, and instead of .98 for Y we might find something like .95 or less.

The force on electron E turns out to be of comparatively large magnitude and in the direction EF. This means that the electrons are being pulled together with great force. So the Lenz Model II would be very stable with equipotential electrons. This accords with our knowledge on the stability of α particles.

So far, the postulate of equipotential surface electrons seems to be highly successful in explaining the packing effect when applied to static models. The protons, in each of the two models above considered, must be revolving

in order to be in dynamic equilibrium. This at once introduces complications because the relativity increase in mass of the protons, brought about by their orbital speed necessary for dynamic equilibrium, offsets the gain in packing for all values of Y, certainly in the Lenz Model I, and in II as far as primary images indicate. The changes in a dynamical model from conditions prevailing in a static model appear to be: (a) The relativity increase in mass of the revolving protons; (b) the relativity increase in mass of the rotating non-uniform surface distributions on the electrons (whether or not the uniform distribution on the electrons be assumed in rotation or not is of no practical importance because the angular velocity is not high enough) (c) the relativity decrease (algebraic) in mutual mass which arises from the same cause as (a), viz., the transformation of acceleration from one coordinate system to another moving relatively to the former.

(a) is undoubtedly larger than (c) because the radius A of the protons is so much smaller than all the other distances entering into the problem. (b) is comparatively unimportant. So difficulties with dynamic equilibrium appear to be an obstacle, but the reason for this may be the particular models chosen to test the postulate, and not with the postulate itself. As stated previously, the writer has no desire to discuss the merits of any nuclear model, but merely chose these two because they are perhaps the best known.

At the beginning of this paper the statement was made that ordinary electrons give only one-tenth the required packing at best, with the static model I. In the static model II they yield at most even less than one-tenth, only the equivalent of three electrons in fact, which is only about one-twentieth the required amount. Now if these models, using ordinary electrons, are put into dynamic equilibrium, the net result is a packing effect of $2.25m$ in the first model and $2.90m$ in the second, and this is scarcely any better than none at all. If dynamic equilibrium is necessary, then ordinary electrons produce no appreciable packing.

The writer takes this opportunity to express his gratitude to Professor Leigh Page, who suggested the fundamental postulate of this paper, for the inspiration and assistance which he has so freely given, and which can best be appreciated by those who have known him as their teacher.

SLOANE LABORATORY,
YALE UNIVERSITY,
June 8, 1927.

THE LUMINOSITY OF FLAMES CONTAINING SODIUM VAPOR

By Gordon L. Locher

Abstract

Variation of the luminosity of sodium flames with thickness. For concentrations of sodium vapor varying from 1 to 10,000 in arbitrary units, the luminosity of a sodium flame is found to be proportional to the square root of its thickness, except for the very low concentrations where it is more nearly proportional to the first power of the thickness. This is in general agreement with the work of Gouy.

Variation of the luminosity of sodium flames with the amount of metal in the flame.—The amount of light from a fixed amount of metallic vapor uniformly distributed in a flame of variable thickness is independent of the concentration of the vapor. The combined luminosity of two flames in tandem is approximately proportional to the square root of the total mass of metal in the flames; this indicates that the luminosity of a flame is independent of the distribution of the emitting vapor in it.

THE first accurate and extensive study of the luminosity of flames containing salt vapors was made by Gouy[1] in 1879–80. He used a photometer suited to the examination of a limited portion of the spectrum and made intensity measurements on spectral lines of flames of various thicknesses and with various concentrations of salts of the alkali and alkaline-earth metals sprayed into them. Gouy placed two identical flames one behind the other in line with the slit of his spectrometer and measured the intensity from first one and then both of these. The ratio of intensities was found to be $2^{1/2}$, approximately.

In 1913, Zahn[2] published an account of experiments in which he compared the intensity of light from a flame with the intensity from the same flame with a mirror behind it. The concentrations of salt vapor employed were very small, in the case of sodium, the solutions sprayed in being between 1/384 and 1/128-normal. The ratios of intensities with and without the mirror were 1.88 to 1.72 for these concentrations, compared with 1.41 if the square root relation held.

Solutions of much larger concentrations were used by H. A. Wilson[3] in examining the relation between conductivity and luminosity of flames. The square root relation was sustained by the results of these experiments for concentrations up to about 0.5 molar, not only for the luminosity, but also for the electrical conductivity. A continuation of similar optical experiments, with greater thickness ratios, is the subject of this paper.

[1] Gouy, Ann. d. Physique et de Chimie **18,** 5 (1879), also Jour. d. Physique **9,** 19 (1880).
[2] Zahn, Deut. Phys. Ges. Ber. **15,** 1203 (1913).
[3] H. A. Wilson, Phil. Trans. Roy. Soc. **A216,** 63 (1915).

Experimental Procedure and Results

(1) Luminosity and thickness of flame. A special burner designed by Professor Wilson was used, providing nine nearly equal, separate flames in a row. The intensity from any number of these, viewed endwise, could be compared with a constant intensity of light of the same wave-length from an incandescent lamp, by means of a Nutting[4] photometer attached to a Hilger wave-length spectrometer; a set of very narrow diaphragms limited the size of the beams of light which entered the spectrophotometer so that there should be no falling off of intensity of light from the more distant of the burners due to their greater distance from the instrument. The salt vapor was introduced into the flames by a sprayer, gasoline gas and compressed air being the fuel. Constancy of gas supply was effected by a rather sensitive balance arrangement which operated a valve in the gas line, the extent of opening of which depended on the pressure in the mains. Air pressure, as indicated by a mercury manometer, was regulated by a mercury blow-off; the small irregularities of pressure of both air and gas were smoothed out by carboys in series with the lines. Precautions were taken against concentration of the solutions in the sprayer, due to evaporation of water, each solution being used for only a short time and then thrown away. Contamination of the burner by deposition of salt was also avoided by frequently washing it out and by making observations with increasing concentration of solution.

In order to minimize observational error arising, particularly, from the necessity of judging just when the portions of the spectral line in the two halves of the field of view were of the same intensity, a large number of observations were made with each concentration of salt. The values recorded in the table are the means of values taken under seemingly optimum experimental conditions, without regard for their mutual agreement.

Table I

Luminosity of sodium flames: I_4/I_1 is the ratio of the intensity of the *D* lines of sodium from four flames to that from one flame. I_9/I_1 is tha ratio for nine and one flames.

Concentration (gr/liter)	Concentration Molar×100	I_4/I_1	I_9/I_1	Percent deviation from square root law	
0.1 NaCl	0.17	2.73	5.25	+36	+75
1.0	1.7	2.08	3.10	+ 4	+ 3
5.0	8.6	1.99	3.05	− .5	+ 1.6
10.0	17.0	2.00	3.05	0	+ 1.6
50.0	86.0	2.02	3.18	+ 1	+ 6
100.0	170.0	2.05	3.30	+ 2.5	+10
240.0 NaOH	830.0	1.99	2.80	− .5	− 6.6
480.0	1660.0	2.05	3.03	+ 2.5	+ .6

Table I shows the results obtained for solutions of concentrations between 0.0017 molar (NaCl) and 16.60 molar (NaOH), a range of ten thousand to one. For the larger concentrations, sodium hydroxide was substituted for

[4] Nutting, Bull. Bureau Stds. **7**, 239 (1911).

sodium chloride because of its greater solubility. It will be noticed that for the 0.17 molar solution, the intensities are much greater than those indicated by the square root law. This is in keeping with the results of Zahn.

(2) Luminosity from a fixed amount of salt. The results of Gouy indicate that the luminosity is a function of the mass of metal per unit area in the flame, independently of its concentration. This was investigated by making observations with a fixed amount of salt distributed through flames of different thicknesses; for example, the luminosity of one flame containing salt vapor of density $4n$ should be the same as that of four flames containing salt vapor of density n. This was found to be the case, within the limits of error. As shown by Table II, the small differences of intensity observed are well within the limits of experimental error.

TABLE II

Results showing that the luminosity depends on the mass of metal per unit area of the flame.

Concentration Molar×100	Number of Flames	(Relative) Intensity	Difference (percent)
1	4	2.02	1.5
4	1	1.99	
4	8	2.06	0.0
16	2	2.06	
16	8	2.12	1.5
64	2	2.15	
25	8	2.15	2.5
100	2	2.20	
100	4	2.28	2.0
200	2	2.24	
10	4	2.06	0.5
20	2	2.07	

(3) The emission from two equal flames containing different amounts of sodium. The experiments described above suggest that the light emitted is proportional to the square root of the total amount of sodium per square centimeter in all the flames used. If, then, the light from two equal flames A and B, one behind the other, is observed and if one gives light of intensity I_A and the other I_B, then the intensity I_C due to the two together should be given by $I_C=(I_A^2+I_B^2)^{1/2}$. For if flame A contains sodium of concentration C_A and flame B sodium of concentration C_B, then $I_A \propto C_A^{1/2}$, $I_B \propto C_B^{1/2}$ and $I_C \propto (C_A+C_B)^{1/2}$. The following results show that this is approximately the case. Table III gives results obtained when the concentration of sodium in

the front flame, A, was kept constant. The calculated values of I_C/I_A were given by the equation $I_C/I_A=[1+(I_B/I_A)^2]^{1/2}$. Table IV contains results obtained when the concentration of the back flame, B, was kept constant. In this case $I_C/I_B=[1+(I_A/I_B)^2]^{1/2}$.

TABLE III

Concentrat on of sodium in flame $A=0.25$

Concentration n B	0.01	0.04	0.09	0.16	0.25	0.50	1.00	2.00
I_B/I_A	.30	.425	.65	.71	1.04	1.08	1.65	2.84
I_C/I_A (found)	.99	1.04	1.12	1.17	1.33	1.36	1.81	2.80
I_C/I_A (calculated	1.04	1.09	1.19	1.23	1.44	1.47	1.93	3.01

TABLE IV

Concentration of sodium in flame $B=0.25$

Concentration in A	0.01	0.04	0.09	0.16	0.25	0.50
I_A/I_B	.234	.364	.62	.83	1.29	1.01
I_C/I_B (found)	.98	.98	1.45	1.39	1.65	1.30
I_C/I_B (calculated)	1.03	1.06	1.18	1.30	1.63	1.42

In most cases the found and calculated values agree fairly well. Very close agreement could not be expected because of variations of the flames. The conclusion is that the luminosity of a flame is proportional to the square root of the mass of salt vapor per square centimeter in it, regardless of what the *distribution* of the vapor may be.

In conclusion, I wish to acknowledge my indebtedness to Dr. H. A. Wilson for the suggestion of this problem and my appreciation of his interest and many valuable suggestions made during the course of this work.

THE RICE INSTITUTE,
HOUSTON, TEXAS,
December 5, 1927

THE ELECTROLYTIC CAPACITANCE OF PLATINUM-SULPHURIC ACID CELLS

By W. M. Pierce

Abstract

Capacitance of an electrolytic cell as determined from the time constant of a circuit on which a constant e.m.f. is impressed.—An electrolytic cell containing platinum electrodes in a solution of sulphuric acid has its electrolytic capacitance determined by a new d.c. method, which consists essentially in observing the current-time record when a small, constant potential is impressed on the circuit containing the cell. The method is described and is used to ascertain whether the capacitance of the cell is a function of the time constant of the circuit in which it is placed. The results show that the capacitance is not a function of the time constant.

Variation of the capacitance of an electrolytic cell with the frequency of the impressed e.m.f.—Alternating and direct current measurements are made on the same cell. The a.c. observations are shown to group with those of others under the general relation $C\omega^n = A$, C being capacitance, ω the angular frequency ($\omega = 2\pi f$), and A a constant. The value of n is shown to vary with the frequency, thus necessitating a modification in the Warburg theory of electrolytic capacitance, which demands that n be 0.5. An empirical relation of the form $(\omega+\omega_0)(C-C_0)=D$ is found, connecting the capacitance of the cell with the frequency of the current flowing through it. The relation fits the combined set of a.c. and d.c. observations very closely.

I. Capacitance of an Electrolytic Cell as Determined From the Time Constant of the Circuit

IT IS well known that an electrolytic cell behaves in many ways as if it contains a capacitance. Such a cell has often been regarded as equivalent to a capacitance in series with a resistance. The capacitance as measured by a. c. methods is found to depend[1] on the frequency of the alternating current. Considering the d. c. capacitance as analagous to the a. c. capacitance, and the time constant of the d. c. circuit as analagous to the period of the a. c. circuit, it seemed reasonable to assume that the d. c. capacitance of the cell might vary as the time constant of the d. c. circuit is varied. No one seems previously to have tested this point.

Suppose we close a circuit containing an electrolytic cell, an adjustable resistance, a galvanometer, and a battery, all in series. Let the resistance of the galvanometer and cell be g (the resistance of the cell being small); let the adjustable resistance be r, and let the capacitance of the cell be C. Then if C, g and r be constant, the current i at any time t will be given by

$$i = i_0 e^{-t/\tau} \tag{1}$$

where τ, $(r+g)C$, is the time constant of the circuit, that is, the time in which the current reaches $1/e$ of its final value. If the deflections of the cur-

[1] For a summary of the results of various investigators, see Lattey, Phil. Mag. **50**, 444 (1925).

rent measuring instrument are proportional to current, and the instrument has no time lag, then

$$y = y_0 e^{-t/\tau} \tag{2}$$

where y is the deflection at time t. Therefore

$$\log_e y = -t/\tau + \log_e y_0. \tag{3}$$

This would be a straight line if $\log_e y$ were plotted against t. The slope is the reciprocal of τ, the time constant of the circuit. In this way we may obtain values of τ corresponding to various values of the external resistance, r.

Now

$$\tau = RC = (r+g)C \tag{4}$$

where R is the total resistance of the circuit. Therefore the relation between the external resistance r and the time constant τ is given by

$$r = \tau/C - g. \tag{5}$$

This should be the equation of a straight line if r is plotted against τ, and if C is constant and independent of τ. But if, as suggested above, C is a function of τ, and therefore also of r, equation (5) will not be a straight line.

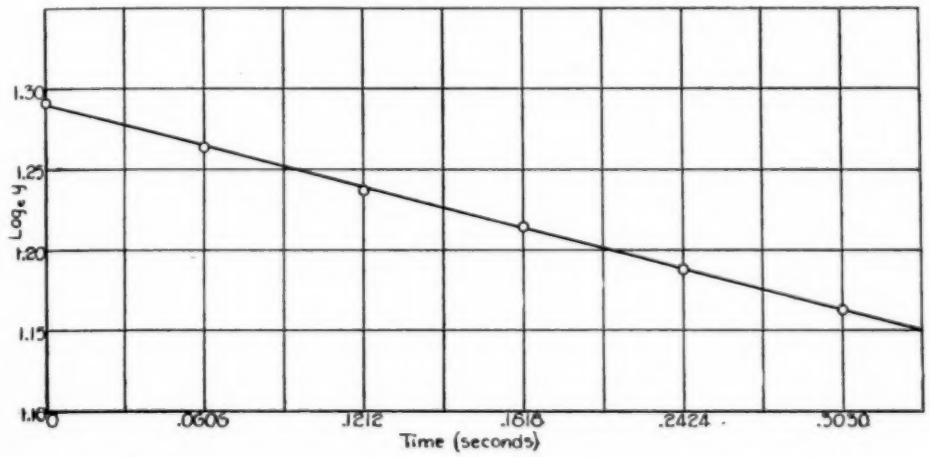

Fig. 1. Observed relation between the logarithm of the galvanometer deflection and the time.

An electrolytic cell, containing platinum electrodes in sulphuric acid, was placed in a circuit containing an adjustable resistance and a string galvanometer. A photographic record of the relation between current and time was obtained for the first few tenths of a second after the circuit was closed, a vibrating reed, of known period, serving as a time marker. The photographic plate was automatically ruled in equi-spaced horizontal lines. One of these was selected as a base line; the position of the trace of the string with reference to this line was read, at the intervals of the time marker. Let this reading be called d. The zero position of the string was also read

with reference to the same base line. Let this reading be called δ. The value of the deflection y is then given by $y=d+\delta$.

Fig. 1 shows the observed relation between $\log_e y$ and t. The plot is seen to be a straight line.

Now by varying r, several curves of tbe above type were obtained, the reciprocals of their slopes giving various values of the time constant, τ. In Fig. 2 a curve is plotted between external resistance r and time constant τ.

Several sets of data were taken on cells having different concentrations of electrolyte. As conditions varied between experiments, and as no effort

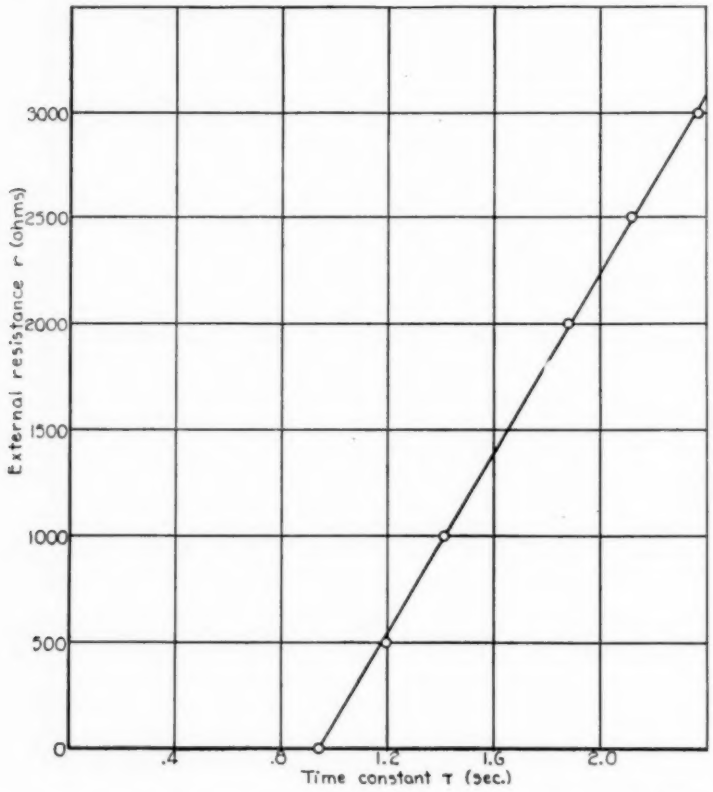

Fig. 2. Variation of the time constant of the circuit with the external resistance.

was made to keep them constant, no conclusion as to variation of capacitance with concentration can be drawn. The curves, plotted as in Fig. 2, were all straight lines, showing that, for these cells, C was constant, independent of τ.

II. Variation of Capacitance with Frequency of the Impressed E. M. F.

Several observers[1] have studied the capacitance of cells using a. c. methods. They find, in general, the relation.

$$C\omega^n=A \tag{6}$$

C being capacitance, ω the angular frequency, and A a constant. $\omega = 2\pi f$, where f is frequency in cycles per second. A tabulation of certain of the experimenters, together with their values of the exponent n and the frequency range they investigated, is presented in Table I.

TABLE I

Observed values of n in the relation $C\omega^n = constant$.

Observer	n	Frequency range (f)	
Jolliffe[2]	0.5	11×10^4	210×10^4
Wolff[3]	0.5	3×10^4	30×10^4
Wolff[3]	0.3	0.02×10^4	3×10^4
Present investigation	0.15	0.0512×10^4	0.1024×10^4
Haworth[4]	0.14	0.0250×10^4	0.1000×10^4

Equation (6) would give an infinite value for C if $\omega = 0$. This is inconsistent with the results described in the first part of this paper, where the capacitance is shown to have a finite value at zero frequency, that is, using direct current. It seemed of interest, therefore, to take both a. c. and d. c. observations on the same cell. A cell was accordingly set up and short circuited for a time, to bring it to a steady condition. It was found that reproducible d. c. observations could be taken almost at once, but that the cell had to be kept short curcuited for a much longer time before reproducible a. c. observations could be taken. This may indicate some fundamental difference in the character of the d. c. and a. c. capacitances.

The a. c. observations were made by balancing the cell on a bridge.[5] A vacuum tube oscillator was used to obtain all the frequencies except the sixty cycle; this was obtained from the laboratory supply. Telephones were used as indicators on the bridge except for the sixty cycle observation, where a vibration galvanometer was used.

The a. c. observations satisfied the relation

$$C\omega^{0.15} = A\,.$$

The frequency range used here was between $f = 512$ and $f = 1024$ cycles per second.

Refering to Table I, it is seen that as the frequency decreases, the value of n decreases. If n be variable, as the results seem to indicate, it is probably a function of frequency. This would call for a modification of the Warburg[6] theory, which theory demands that the value of n be 0.5. So far, no such modification has been proposed.

As has been previously stated, the relation $C\omega^n = A$ would give an infinite value for C if $\omega = 0$. On observing the d. c. capacitance of this cell by the method outlined in part one, it was found to be finite, 1185 microfarads.

[2] Jolliffe, Phys. Rev. **22**, 293 (1923).
[3] Wolff, Phys. Rev. **27**, 755 (1926).
[4] Haworth, Trans. Far. Soc. **16**, 355 (1920).
[5] Hague, A. C. Bridge Methods, p. 232.
[6] Warburg Wied. Ann. 311, p. 125 (1901).

Equation (6) is seen to represent a rectangular hyperbola if C is plotted against ω^n. This relation, approximately verified over a narrow range of frequencies, suggested that there might be some kind of an hyperbolic relation between ω and C. A search for such a relation[7] resulted in the following empirical equation:

$$(\omega+494)(C-526)=325,550. \tag{7}$$

The following table lists values of C observed, and also those computed from

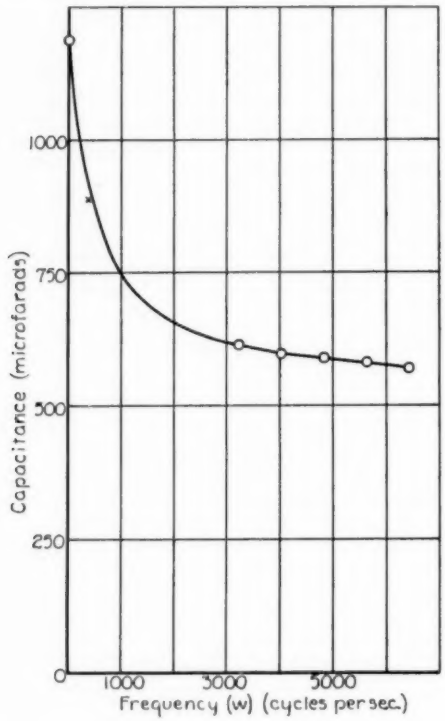

Fig. 3. Variation of the observed values of the capacitance with the frequency of the impressed e.m.f.

Equation (7), for various values of ω. The curve of Fig. 3 shows the observed values of C plotted against the corresponding values of ω.

TABLE II

Comparison of observed capacitances with those computed from Eq. (7).

Frequency (ω)	C(observed)	C(computed)
6430	571	573
5627	582	579
4824	589	587
4020	598	598
3215	614	614
0	1185	1185

[7] For method, see Running, Empirical Formulas, p. 53 (1917).

A value of C at $f=60$ was not observed with these data, but was observed in another run taken a day later. In order to see where the point would fall among the above data, it was computed, the value obtained being 887 microfarads. This is plotted by a cross on the graph, and will be seen to fall fairly close to the curve as drawn. The value demended by the curve equation is 900 microfarads.

The author wishes to take this opportunity to express his thanks to Professor C. C. Murdock, under whose direction the work was done, for helpful criticism and suggestions, to Professor F. K. Richtmyer for suggestions in the interpretation of the results, and to Professor M. W. White for stimulating and helpful discussion of the work.

PHYSICAL LABORATORY,
CORNELL UNIVERSITY.

THE BEHAVIOR OF GLASS AS A DIELECTRIC IN ALTERNATING CURRENT CIRCUITS: I. RELATION OF POWER FACTOR AND DIELECTRIC CONSTANT TO CONDUCTIVITY

By Louise S. McDowell and Hilda Begeman

ABSTRACT

Power factor, dielectric constant at 1000 cycles and apparent resistivity for six glasses of varying composition, both lead glasses and borosilicates with and without lead, all at 20°C. The values of the apparent resistivity at 20°C were found by linear extrapolation, by means of the equation $\rho = e^{k/T}$, from values of the apparent resistivity calculated from measurements of the resistance of small rods at temperatures ranging from 100°C to 500°C. In two cases studied the power factor of strained samples was about 50 percent greater than after annealing. No explanation is offered. For glasses of relatively similar composition both the power factor and the dielectric constant are found to increase with increasing conductivity. The results indicate a close relation between the phenomena of absorption and of ionic conductivity and are shown to be qualitatively in agreement with the theory of Joffé that the phenomena of absorption are due to a counter-electromotive force of electrolytic polarization. Possible alternative molecular explanations are suggested.

OF THE six glasses chosen for investigation numbers 1 and 3 were lead glasses; numbers 2, 4 and 5 were borosilicates without any heavy metals and number 6 was a lead borosilicate. These glasses were chosen because they are known to vary widely in power factor and conductivity. Measurements were made: (1) of the power factor of each glass at 1000 cycles per second, at approximately 20°C; (2) of the dielectric constant at 1000 cycles per second and approximately 20°C; (3) of the apparent resistivity at temperatures ranging from 100°C to 500°C.

Methods of Measurement

The values of the power factor were calculated from measurements of the equivalent series resistance and capacitance made with a capacitance bridge elsewhere described.[1,2] A potential difference in the neighborhood of 100 volts was applied to the bridge terminals. Power was furnished by an electron tube generator of the Hartley circuit type with a 50-watt tube, placed in another room to avoid stray coupling. The test condensers were beakers with mercury electrodes. The beakers were thoroughly washed, rinsed with distilled water and dried in an oven. The mercury was also cleaned and dried. The test beaker was floated in a second beaker containing the mercury which formed the outer electrode and held in place by a wire frame dipping into the mercury and grounded. To maintain constant temperature the entire condenser was placed in an electric furnace with heating coil grounded.

[1] H. J. MacLeod, Phys. Rev. **21,** 53 (1923).
[2] L. S. McDowell, Phys. Rev. **23,** 507 (1924).

The frequency was measured by a frequency meter consisting of a large four-step inductor and a variable oil condenser, calibrated at intervals during the experiments by comparison with tuning forks. This meter was placed about ten feet from the oscillator and the resonance frequency found by telephones connected unilaterally. Usually measurements were made at several frequencies and the value of the power factor at 1000 cycles obtained by interpolation.

For the measurements of dielectric constant, the glass was in the form of plates, 16 cm square, ground plane parallel to a thickness of about 2 mm. The average thickness was determined by means of a Randolph and Stickney dial gauge reading to a thousandth of a millimeter. Readings were taken at thirteen points fixed by a pattern which divided the area of the upper electrode into equal parts. The dried plates were floated on mercury which formed the lower electrode; the upper electrode was an amalgamated copper ring about 13 cm in diameter, 7 millimeters in height, filled with mercury. The capacitance was measured at 1000 cycles, by means of a series inductance bridge with a third arm, since the capacitance bridge used in the power factor measurements was not at the time available. No correction was made for the effect of lack of uniformity of the field at the edge.

The measurements of resistivity at temperatures above 100°C were made upon samples in the form of rods from 2 to 6 cm in length, and about 6 mm in diameter. Contact was made by Dumet wires pushed into the ends of the heated rod. The specimen to be measured was suspended vertically in a cylindrical furnace by the Dumet wires which extended through Pyrex tubes embedded in asbestos stoppers, at opposite ends of the furnace, and were soldered outside to small copper rods. The temperature was measured by a chromel-alumel thermocouple in conjunction with a Wolff potentiometer. The resistance was calculated from the applied electromotive force, usually 50 volts, and the current. For the current measurements a Leeds and Northrup galvanometer of high current sensitivity was used with suitable shunts so calibrated as to permit the calculation of the resistance directly from the applied electromotive force and the galvanometer deflection. To test for errors due to leakage through the furnace a trial run was made with the specimen removed. The error from this cause was found to be less than one percent and at the higher temperatures amounted to only one or two parts in a thousand. To minimize errors in the resistivity, calculated in ohms per cubic centimeter, due to the shape of the specimen and the consequent impossibility of measuring the dimensions with accuracy, at least two samples of different length were measured for each glass, and the effective length found by comparison.

As a check upon the measurements at high temperatures, the resistivity in the case of glasses numbers 1 and 2, at room temperature, was calculated from values of the resistance of the thoroughly annealed glass plates used in the measurement of the dielectric constant. The same mercury electrodes were used with the addition of a guard ring connected to the grounded side of the galvanometer, to prevent the measurement of the current leaking

over the surface. The applied electromotive force was 270 volts. The ratio of the current through the glass to the current through a resistance of one megohm was found by direct substitution, with the aid of an Ayrton shunt to alter the sensitivity of the galvanometer. For the glasses of higher resistivity the galvanometer was not sufficiently sensitive to permit the use of this method.

The power factor was calculated from the relation

$$\text{Power factor} = \cos\theta = \sin\phi$$

where ϕ is the phase difference. For small values of ϕ, $\sin\phi \approx \tan\phi$ and $\tan\phi = R\omega C$, where R and C are respectively the equivalent series resistance and capacitance of the condenser.

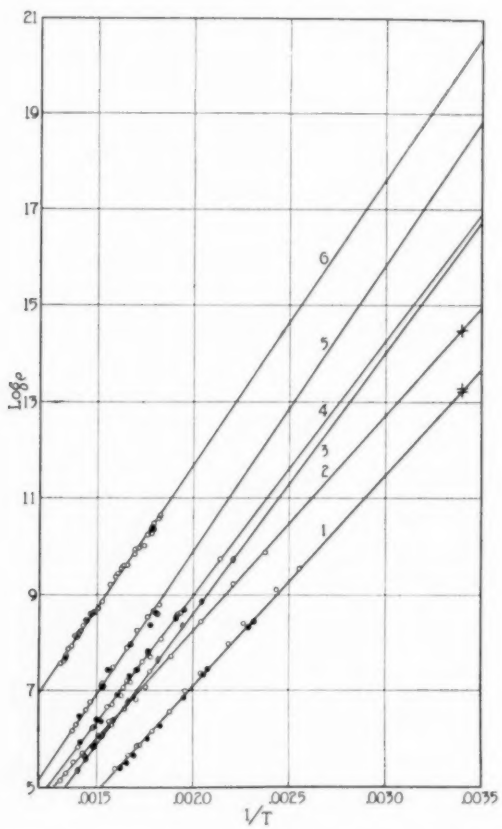

Fig. 1. Logarithm of the resistivity as a function of the reciprocal of the absolute temperature.

RESULTS

Fig. 1 shows the values of the logarithm of the resistivity plotted as a function of the reciprocal of the absolute temperature. Within the errors

of observation the points lie on a straight line in accordance with the relation

$$\rho = e^{k/T}$$

first found by Rasch and Hinrichsen[3] to hold true for various insulators in which the conductivity is now considered to be electrolytic. The values measured at room temperature for glasses 1 and 2 are indicated by the crosses. The agreement between these measured values and the extrapolated values is considered to be sufficiently good to warrant the use of the extrapolated values for the other glasses.

Table I gives the values of apparent resistivity at 20°C, of the tangent of the phase difference at 1000 cycles, and of the dielectric constant at 1000 cycles, for the six glasses divided into two groups according to composition.

TABLE I

Values of the resistivity, of the tangent of the phase angle and of the dielectric constant for six glasses

No.	$\rho(20°C)$	Tanϕ(1000 cycles)	K(1000 cycles)
	a. Lead glasses		
1	2.3×10^{13}	0.0132	7.5
3	2.0×10^{15}	0.0031	6.8
6	8.1×10^{19}	0.0022	5.3
	b. Borosilicates without lead or any heavy metal		
2	3.1×10^{14}	0.0082	5.0
4	2.5×10^{15}	0.0039	4.7
5	3.5×10^{16}	0.00077	4.1

In each group the order of decreasing conductivity is also the order of decreasing power factor and decreasing dielectric constant.

It should be noted that the values of resistivity given are those of apparent initial resistivity, taken a brief, unmeasured interval of time after the application of the potential difference, which is doubtless considerably less than the final conductivity. Race,[4] for example, obtains for "PYREX" laboratory glass (glass No. 2) a value of the resistivity of 8.6×10^{16} ohms per cubic centimeter, 5000 minutes after the application of the potential difference and of 4.9×10^{15} ohms per cubic centimeter, one minute after the application of the potential difference.

To show to what extent the power loss might be supposed to be due to conduction, the power factor was calculated from the relation

$$1/R_p = P/E^2 = \omega C \tan\phi$$

where R_p, the resistance of the condenser, was calculated from the measured resistivity and the dimensions of the condenser. For glass No. 1 the power factor so calculated was 1.05×10^{-5}, for No. 6, 5.41×10^{-10}. These values are negligibly small in comparison with the measured power factors, and if the final resistivity had been used would have been still smaller.

[3] Rasch and Hinrichsen, Zeits. f. Elektrotech. **14**, 41 (1908).

[4] H. H. Race, Thesis, Cornell University, 1927 (to be published).

Since the dielectric constant was measured at a frequency of one thousand cycles it might be supposed that the correlation between the dielectric constant and the conductivity is to be accounted for entirely by the increase in the apparent dielectric constant due to the absorbed charge. However, the rate of change of the dielectric constant with frequency does not seem to be sufficiently great for the glasses of large conductivity and power factor to alter the order as given in Table I. For instance, for glass No. 1 at the frequency of one million cycles per second, the value of the dielectric constant was found to be 7.3.

The Effect of Annealing

To test the effect of annealing, the power factor of two glasses was measured before and after annealing. The results are given below:

Glass	Condition	Power Factor
2	Strained	0.0113
	Annealed	0.0074
4	Strained	0.0055
	Annealed	0.0034

No explanation is offered for the large decrease in the power factor produced by annealing. Despite the rather large increase due to strain, the values of the power factor for different specimens of glass of fairly uniform composition, when well annealed, agree reasonably well. This is illustrated by the following values for "PYREX" laboratory glass measured, at intervals extending over more than a year, and upon specimens from different melts:

Specimen	Form	Power Factor
a	Beaker	0.0085
b	"	0.0089
c	Flat dish, 6mm thick	0.0083
d	" " " "	0.0090
e	" " " "	0.0084
f	" " " "	0.0078
g	" " " "	0.0074
h	Plate 2mm "	0.0084
i	Test tube	0.0073

Specimens *f* and *g* were used in the experiments to determine the effect of annealing and were probably annealed with unusual thoroughness.

Interpretation of Results

The results indicate a close relation between the phenomena of absorption and ionic conductivity. They seem therefore less favorable to the theories of Maxwell and Wagner[5] which explain absorption as due to a variation in the ratio of the dielectric constant to the resistivity for the different layers or constituents which compose the dielectric and more favorable to an explanation on the basis of the behavior of the individual molecules and ions. Qualitatively the results are in agreement with the theory of Joffé, as set forth by Sinjelnikoff and Walther,[6] that the phenomena of absorption are

[5] K. W. Wagner, Archiv. f. Elektrotech. **2**, 371 (1914).

[6] Sinjelnikoff and Walther, Zeits. f. Physik, **40**, 786 (1927).

due to a counter electromotive force of electrolytic polarization, P, such that the final current, $i=(V-P)/R$, where R, the true resistance, is constant and of magnitude sufficient to account for the power loss in an alternating field, if the effect of space charge be taken into account. As alternative explanations, it seems possible to suppose either that the ions, because of assymmetry, possess an electric moment and are slowly rotated as they drift, or that there are present some dipole molecules the orientation of which is retarded because of the influence of the fields of force of the ions, due to the close packing of molecu'es and ions in a solid. If either the theory of Joffé or the first of the suggested alternative molecular explanations is accepted, however, it would seem difficult to account for the complete absence of absorption phenomena in liquids.

A second paper, in preparation, will discuss the effect of frequency and temperature upon the power loss.

The measurements of resistance were made in the Physics Laboratory of Cornell University and the measurements of dielectric constant in the Capacitance Laboratory of the Bureau of Standards during the year 1925–26, while the senior author was a guest in the laboratory. It is a pleasure to acknowledge the many courtesies extended in both laboratories and in particular the friendly interest in the investigation shown by both Dr. H. L. Curtis and Dr. Chester Snow of the Bureau of Standards.

WELLESLEY COLLEGE,
August 1, 1927.

THE EFFECT OF HORNS OF SHORT LENGTHS ON THE INTENSITY OF SOUND FROM A TELEPHONE UNIT

By B. L. Steele

Abstract

By means of a condenser microphone associated with a multi-stage resistance-coupled amplifier, a vacuum thermocouple, and a micro-ammeter the effect of very short horns on the intensity of the sound output of a telephone unit was determined. The response-frequency curves for twelve conical horns of varying flare and length, together with the output-frequency curve for the telephone unit itself showed that by the use of these short horns the intensity of the sound radiated was considerably increased over a wide range of frequencies extending from the upper limit used, 4000, to frequencies much lower than that corresponding to a wave-length equal to four times the length of the horn. The flare of the horn materially affected the sound output. The heights of the peaks in the response-frequency curves, but not their distribution, were affected by the material of the horn. These horns have little value as loud speakers.

Introduction

THE theory of the manner in which horns of various shapes are known to function has been developed by Rayleigh,[1] Barton,[2] Webster,[3] Stewart,[4] Slepian and Hanna,[5] and Minton and Goldsmith.[6] Information concerning the performance of horns as "receivers" of sound has been furnished by Miller[7] and by Stewart,[4] and as "transmitters" of sound by Slepian and Hanna[5] and by Minton and Goldsmith.[6]

Miller found that, as a receiver in conjunction with the diaphragm of the phonodeik, a horn functions as an open pipe, resonating to the complete series of partials. He states that response to frequencies lower than the fundamental of the horn is very feeble. The work of Minton and Goldsmith showed that, in the behavior of a rather long conical horn coupled with a particular telephone unit as a loud speaker, resonance of the horn as an air column closed at one end played an important part. The horn gave considerable amplification for any frequency nearly equal to or greater than that corresponding to a wave-length equal to four times the length of the horn, and peaks appeared in the response-frequency curves for frequencies corresponding closely to the resonance frequencies of a closed pipe. The horns used in the above investigations were rather long, ranging from slightly more than thirty centimeters to more than three hundred centimeters in

[1] Rayleigh, Theory of Sound, Vol. II, Chap. XIV.
[2] Barton, Phil. Mag. **15,** 68–81 (1908).
[3] Webster, Proc. Nat'l Acad. of Sciences **2,** 275 (1919).
[4] Stewart, Phys. Rev. **16,** 313 (1920).
[5] Slepian and Hanna, Trans. A. I. E. E. **43,** (1924).
[6] Minton and Goldsmith, Proc. I. R. E., Aug. 1924.
[7] Miller, The Science of Musical Sounds.

length. This paper gives information concerning the performance of rather short conical horns when used as loud speakers with telephone units.

Apparatus and Experimental Details

Table I gives the dimensions of the horns used, together with the approximate values of their resonance frequencies as closed air columns. The twelve numbered horns were made of galvanized iron 0.053 centimeters thick.

TABLE I

Dimensions of horns

Number of horn	Diam. small end (cm)	Diam. large end (cm)	Flare of horns	Axial length (cm)	Effective length (cm)	Approximate resonant frequencies as closed pipes
1	1.6	1.6	0	8.2	10.4	830, 2490
2	1.6	2.5	6°30′	7.9	10.4	4150, 5810
3	1.6	3.8	16°40′	7.5	10.4	
4	1.6	5.0	26°55′	7.1	10.4	
5	1.6	2.5	3°	16.7	19.2	450, 1350
6	1.6	5.1	12°40′	15.9	19.2	2250, 3150
7	1.6	7.6	22°10′	15.1	19.2	4050,
8	1.6	10.2	34°10′	14.0	19.2	
9	1.6	3.8	5°	25.2	28.0	308, 924
10	1.6	7.6	14°20′	23.8	28.0	1540, 2156
11	1.6	11.4	24°40′	22.4	28.0	2772, 3388
12	1.6	15.2	34°40′	21.8	28.0	4004

The diameter of the small end of the horn was determined by the fact that the opening of the telephone unit used was 1.6 cm in diameter. The effective length of the horn, as given in the table, was obtained by making two additions to the axial length. First, the cylindrical neck of the loud speaker unit was 1.6 cm long. Second, according to Stewart,[4] the end correction for the large end is 0.7 of the radius of that end.

A loud speaker telephone unit was used as the source of sound for all of the horns. The alternating current operating the unit was supplied by a vacuum tube, beat-frequency oscillator manufactured by the General Electric Company. The design of the oscillator was such as to give practically a constant output voltage over the range of frequencies from 60 to 6000 complete cycles per second. Also, the output voltage-curve was practically a pure sine wave. It was found necessary frequently to check the accuracy of the oscillator calibration by comparison with a standard tuning fork.

The sound intensity measuring apparatus consisted of a condenser microphone and a four-stage vacuum tube amplifier, the output of which was measured by means of a vacuum thermocouple and a micro-ammeter. The general theory of the condenser microphone has been given by Wente.[8] The particular condenser microphone used was of the latest type made by the Western Electric Company. Fig. 1 gives the details of the sound measur-

[8] Wente, Phys. Rev. **10**, 39 (1917).

ing circuit. Fig. 2, furnished with the microphone and the sound measuring circuit, gives quite accurately the frequency-response calibration curve of the entire sound measuring apparatus.

The experimental work was carried out in a specially constructed acoustic laboratory, the floor, ceiling and walls of which were covered with acoustic plaster and with both balsam wool and hair felt. Although the absorption

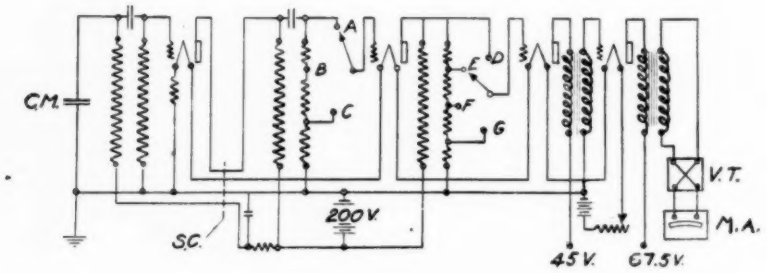

Fig. 1. Sound measuring circuit. C. M. condenser microphone, S. C. shielded cable, V. T. vacuum thermocouple, M. A. micro-ammeter.

coefficient of the walls, floor, and ceiling was very high, yet, with the sustained tones used, the air in the room was thrown into three-dimensional standing waves. These standing waves, although relatively faint, were of sufficient intensity to affect slightly the readings of the apparatus unless it

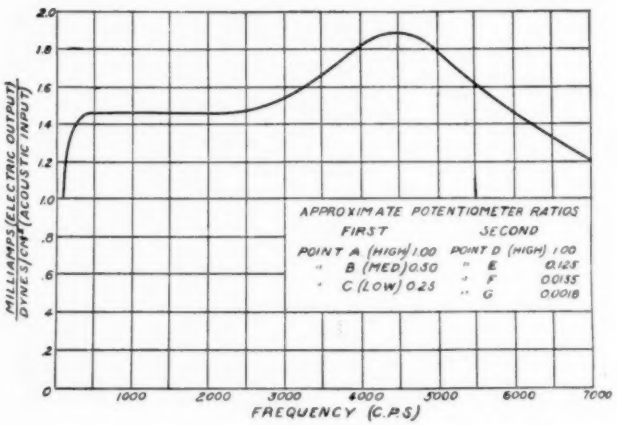

Fig. 2. Characteristic of sound measuring circuit.

was placed near the geometrical center of the room, that is, as far as possible from any of the walls, and, even then, unless the condenser microphone was placed no farther than twenty-five centimeters from the source of the sound. The effect of these standing waves was greatly diminished by using numerous hairfelt baffles eighteen inches wide along the sidewalls, ceiling and floor together with a pair of obliquely placed reflecting surfaces.

In using the telephone unit without a horn, the opening into the unit was considered to be the source of the radiating sound wave. When a horn was used, it was fitted air-tight to the unit by means of a rubber washer, and its large open end was considered to be the source of the radiating sound wave. In making a test with any horn, the center of the condenser microphone diaphragm was placed approximately on the axis of the horn with its plane parallel to, and fifteen centimeters distant from, the plane of the open end of the horn.

To obtain a value which is approximately proportional to the sound pressure change, for any particular horn and at any particular frequency, the procedure was as follows: As the particular pitch was produced by adjustment of the condenser setting of the oscillator, the second and third stage potentiometers of the amplifier were adjusted so that the micro-ammeter reading was 200 or less. If the potentiometer positions were *A* and *D*, the thermo-junction heater coil current in milli-amperes was obtained directly from the calibration curve. If the potentiometer positions were *B* and *D*, the value of the heater current taken from the curve was multiplied

TABLE II

Frequency-response data of telephone unit and numbered horns for low frequency range

Frequency	Telephone unit	10.4 cm horns				19.2 cm horns				28 cm horns			
		1	2	3	4	5	6	7	8	9	10	11	12
		Kx Dynes per sq. cm.				Kx Dynes per sq. cm.				Kx Dynes per sq. cm.			
22	0.0	0.0	0.0	0.0	0.0	0.0	0.0	0.0	0.0	0.0	0.0	0.0	0.1
42	0.0	0.0	0.0	0.0	0.0	0.0	0.0	0.0	0.0	0.0	0.0	0.0	0.1
62	0.0	0.0	0.0	0.0	0.0	0.0	0.0	0.0	0.0	0.0	0.1	0.05	0.1
82	0.0	0.0	0.0	0.0	0.0	0.0	0.0	0.0	0.0	0.1	0.1	0.1	0.1
104	0.0	0.0	0.0	0.0	0.0	0.0	0.0	0.0	0.0	0.1	0.1	0.1	0.2
128	0.05	0.0	0.0	0.0	0.1	0.1	0.04	0.1	0.1	0.3	0.1	0.1	0.3
152	0.05	0.0	0.0	0.0	0.1	0.1	0.1	0.1	0.1	0.1	0.1	0.1	0.1
178	0.05	0.0	0.0	0.1	0.1	0.1	0.1	0.1	0.6	0.2	0.9	0.3	0.3
198	0.1	0.05	0.05	0.1	0.1	0.1	0.1	0.2	0.4	0.3	0.3	0.7	0.4
207	0.1	0.1	0.1	0.1	0.05	0.1	0.1	0.2	0.3	0.4	0.3	0.6	0.6
215	0.1	0.3	0.1	0.1	0.1	0.2	0.15	0.3	0.4	0.4	0.2	0.4	0.5
230	0.2	0.4	0.1	0.1	0.1	0.3	0.2	0.5	0.5	0.5	0.2	0.3	0.4
252	0.2	0.2	0.2	0.1	0.15	0.35	0.35	0.7	0.6	0.6	0.4	0.4	0.4
268	0.2	0.05	0.3	0.2	0.2	0.4	0.5	0.8	0.5	0.7	0.5	0.5	0.5
284	0.2	0.3	0.35	0.3	0.2	0.5	0.3	0.6	0.7	1.0	0.7	0.6	0.6
300	0.2	0.4	0.4	0.4	0.3	0.6	0.4	0.5	0.9	1.8	0.9	0.8	0.7
325	0.35	0.5	0.5	0.4	0.4	0.7	0.4	0.5	0.8	7.2	1.2	1.0	1.3
335	0.4	0.5	0.6	0.4	0.3	0.8	0.5	0.6	0.7	5.4	1.3	1.1	1.2
350	0.45	0.6	0.6	0.5	0.3	1.2	0.6	0.7	0.8	3.5	1.4	1.2	1.1
375	0.5	0.7	0.6	0.8	0.4	1.5	0.7	0.8	0.9	2.5	1.6	1.3	1.2
400	0.6	1.0	0.8	0.8	0.4	4.0	1.1	1.2	0.9	1.4	3.5	1.4	1.5
430	0.7	1.5	1.0	0.9	0.45	7.6	1.4	1.4	1.0	1.4	7.0	2.7	2.5
450	0.8	1.8	1.2	1.0	0.5	3.9	1.6	1.5	1.2	1.4	10.0	3.8	3.2
490	1.1	3.9	1.7	1.3	0.6	2.1	2.1	2.1	1.4	1.5	19.4	11.0	6.8
500	1.1	6.0	2.0	1.5	0.7	1.9	3.0	2.9	1.2	1.5	16.0	14.7	7.2
530	1.2	9.6	2.9	1.8	0.8	1.5	4.8	3.9	1.8	1.5	4.5	10.0	8.5

by the factor 2; if *C* and *D*, by 4; if *A* and *E*, by 8; and so on for other combinations, the multipliers being obtained from the values of the potenti-

ometer ratios given in Fig. 2. To convert the heater current in milli-amperes to dynes per square centimeter, it was necessary to use the divisor indicated by the calibration curve of Fig. 2 for the particular frequency. Attention should be called to the fact that while the values obtained for the sound output are only approximate, relatively they are quite satisfactory.

Discussion of Results

Table II gives the output-frequency data in the low range of frequencies for the telephone unit alone and the response-frequency data in the same range for the telephone unit coupled to the numbered horns. The curves

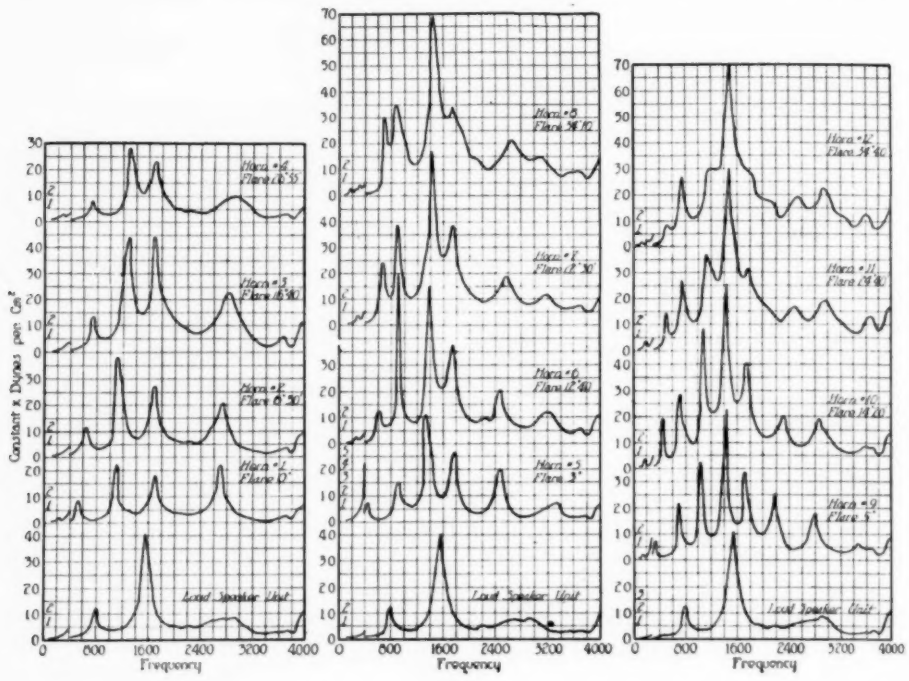

Fig. 3. Fig. 4. Fig. 5.

Fig. 3. Output-frequency curves for 10.4 cm horns.
Fig. 4. Output-frequency curves for 19.2 cm horns.
Fig. 5. Output-frequency curves for 28 cm horns.

of Fig. 3 cover the entire range of frequencies studied. The output-frequency curve of the telephone unit has one very large sharp diaphragm resonance peak and several smaller ones. These peaks are so pronounced as greatly to affect the character of the response-frequency curves of the short horns coupled to this unit. Notwithstanding this very apparent defect, and this is a defect from the point of view of the distortionless transformation of the electric energy input into sound energy output, this unit was selected from a large number as being the most suitable. The corresponding data and response-frequency curves for the other horns are given in Table II and Figs. 4 and 5.

When a conical horn is attached to a telephone unit the intensity of the sound radiated from the horn for any frequency impressed by the harmonically varying current on the diaphragm of the telephone unit is determined by the combined behavior of the diaphragm and the horn, functioning as a coupled system, and is influenced by the resonance frequencies of both the diaphragm and the horn, and the exact character of the response-frequency curve is determined in part by the relative importance of the resonance peaks of the diaphragm and those of the horn. An examination of Tables I and II and Fig. 3 shows that in the case of these 10.4 cm horns coupled with the particular telephone unit the peaks in response-frequency curves correspond neither to the resonance frequencies of the horns nor to the resonance frequencies of the diaphragm. The use of these short horns resulted in an increase in the intensity of the sound output for frequencies much lower than 830, their fundamental resonance frequency at the average laboratory temperature. For frequencies between 300 and 700 the amplification ratio for the first three horns ranged approximately from two to sixty. This increase in intensity for these low frequencies may have been due in part to upper partials in the diaphragm to which the short horns resonated. Facilities were not available with which to determine the character of the sound output of the telephone unit for these low frequencies. It may be, also, that it was due in part to the phenomenon of multiple resonance described by Barus.[9]

An examination of Table II and the curves of Figs. 4 and 5 indicates that, with slight modifications, the observations regarding the behavior of the 10.4 centimeter horns apply to the other lengths as well. The most noticeable exception is to be found in the case of horn No. 9.

In addition to these horns, made of heavy galvanized iron, horns of the same dimensions as number 7, and made of very thin aluminum sheet, of drawing paper, and of three ply gum-wood veneer were used. For every one of them the response-frequency curve was essentially the same as for horn number 7, but the intensity of the sound radiated at a given frequency was less than that at the same frequency for the more rigid walled iron horn.

The resonance peaks are too pronounced on the one hand and the average sound intensity amplification is too slight on the other to render the use of any of these short horns of any value as loud speakers.

The author is pleased to acknowledge his obligation to Professor Arthur L. Foley for his assistance and advice and to offer his thanks to Professor R. R. Ramsey for helpful suggestions.

PHYSICAL LABORATORY,
INDIANA UNIVERSITY,
May, 1926.

[9] Barus, Carnegie Institute of Washington, Publication No. 310, part III.

BOOK REVIEWS

The Mathematical Theory of Relativity by TH. DE DONDER. Pp. 102, figs. 8. Massachusetts Institute of Technology, Cambridge, 1927. Price $2.75.—This book contains ten lectures delivered at the Massachusetts Institute of Technology during the Spring of 1926. It covers the special and general relativity, including in the latter electromagnetic as well as gravitational fields. In the last chapter, entitled "Relativistic Quantization," the author shows that the relativity theory leads to an equation of the form of Schrödinger's equation for the ψ waves.

The author has condensed so much material into one hundred pages that it is difficult to follow his mathematical developments unless one is already very conversant with the subject. The book is not free from typographical errors. For instance, equation 32, lecture 2, which is referred to both on page 19 and on page 29, is entirely missing from the text.

LEIGH PAGE

Physikalisch-Chemische Metamorphose und einige Piezochemische Probleme. ERNST COHEN. Pp. 135, figs. 58, Akademische Verlagsgesellschaft, Leipzig, 1927.—For a review of the original English version, see Phys. Rev. **30**, 225, 1927.

F. H. MACDOUGALL

Leçons de Chimie Physique. By P. MAURICE VÈZES. Pp. 545+X, 293 figs. Librairie Vuibert, Paris, 1927.—In this elementary treatise on physical chemistry we have a clear and interesting account of a number of fields that are of importance to the chemist. At the same time we gain a rather exaggerated notion as to the contributions made to the subject by French scientists. The author devotes about 160 pages to the phase rule and its application to systems with degree of freedom from zero up to four. The treatment of electrochemistry is characterized by simplicity and is not complicated by taking into account the recent advances that have been made in the theory of electrolytic solutions. The only part of this volume which would be likely to be helpful to American readers is the comprehensive treatment of heterogeneous systems.

F. H. MACDOUGALL

Lehrbuch der Thermostatik. Erster Teil. Allgemeine Thermostatik. VAN DER WAALS-KOHNSTAMM. Pp. 390+xvi, 38 figs. Verlag von Johann Ambrosius Barth, Leipzig, 1927. Unbound 22 RM. bound 24 RM.—This treatise on thermodynamics can be confidently recommended to the attention of all serious students of the subject. Of special interest is the fact that the author establishes the general laws of equilibrium not only according to the classical methods but also by means of the axioms of Carathéodory. Of great importance are his chapters on equilibrium in systems under the influence of external forces and the section devoted to the thermodynamic theory of capillarity. The book deserves very high praise.

F. H. MACDOUGALL

Lehrbuch der Thermostatik. Zweiter Teil, Binäre Gemische. DR. J. D. V. D. WAALS, AND DR. PH. KOHNSTAMM. Second edition. Pp. 402, 220 figs. Johann Ambrosius Barth, Leipzig, 1927.—This is the second edition of the second volume of the well known "van der Waals-Kohnstamm," the first edition of which appeared in 1912. Unlike many editions of standard physics texts, this second edition has been greatly altered from the first, more than half the material being new or so radically rewritten as not to be easily recognizable.

The object of the book is to give a qualitative survey of the extraordinarily complicated behavior of binary mixtures from which gaseous, liquid, and solid phases separate. This qualitative survey is given by a discussion of the geometrical character of the various surfaces

which plot the functional relations between such variables as composition, temperature, pressures, and thermodynamic potentials. The geometrical properties of the surfaces are principally characterized by the behavior with respect to the "Faltenspunktskurve," so that the presentation "has rather the character of Analysis Situs than of Function Theory." Special assumptions as to the nature of the characteristic equation have almost entirely disappeared from the treatment. The book is brought up to date by a discussion of the geometrical characteristics of the recent theory of polymorphism of Smits, but it is not in the nature of the book to consider in detail the numerical results of experiment.

The book is unique, and so highly special that many physicists will find it entirely outside their domain of interest, but to those working in this field it is indispensable.

P. W. BRIDGMAN

The Evolution of Scientific Thought from Newton to Einstein. A. D'ABRO. Pp. 544, figs. 21. Boni and Liveright, New York, 1927. Price $5.00.—This book, which is ostensibly of a semi-popular character, is devoted primarily to presenting the subject of relativity, and by way of introduction gives a long preliminary discussion of geometrical and mechanical matters to prepare the mind of the reader for the exposition of the new ideas.

It may be that this book will fill a popular need—the treatment covers many more topics than any other popular book in English of which I know, and there are many admirable features in the presentation—but to the Physicist, for whom this review is written, I believe the book will be unsatisfactory. There is so much repetition that it is long to the point of prolixity. Too often, when confronted by a topic difficult to explain without technicalities, the author adopts the easy authoritarian point of view, and as part of these tactics finds it necessary to exalt the mathematician and physicist at the expense of the philosopher. Whatever the faults of the philosopher, it will make uncomfortable reading for at least the physicist to find himself treated like a little tin god, aware as he is of the many short comings of his own subject.

The physicist must deprecate the decision of the author that when, in discussing technicalities, it became a "question of presenting these subjects loosely or leaving them out of the picture entirely, it appeared preferable to sacrifice accuracy to general comprehensiveness," particularly when this decision can lead to such a statement as "light intensities inferior to a quantum had been observed" on page 396.

Finally, the fundamental point of view of the author which demands the objectification of the absolute space of Newton or the space-time of Einstein, seems to me meaningless, in spite of the strictures of the author against those who are so dull as to be unable to find any meaning here. The treatment given these matters in many places strikes me as pretty close to rationalization. Certainly the temper of such a statement as: "Newton, however, after he had established the existence of absolute space scientifically, proceeded to weld it in with his theological ideas, identifying it with the existence of the Divine Being," on page 541, a statement made apparently merely on the basis of reasonableness without examination of the historical facts, is entirely opposed to the temper of such a discussion, for example, as Burtt has given in his recent book, Metaphysical Foundations of Physics, of the historically actual origin of Newton's metaphysical ideas.

P. W. BRIDGMAN

Materialprüfung mit Röntgenstrahlen. By RICHARD GLOCKER. Pp. 377+vi, 255 figs. Julius Springer, Berlin, 1927. Price, bound 31.50 RM.—This book very neatly closes a gap in the bibliography of x-rays. It gives for the first time in any language a readable account of radiographic methods for non-medical diagnosis, and a reasonably complete review of the most recent researches on preferred orientations of crystals in crystal aggregates. It also contains tables of known crystal structures which are unique in giving the arrangement of atoms in intermetallic compounds and solid solutions. In respect to other compounds the entries are more nearly up-to-date than those in the International Critical Tables and rather more convenient in form, but suffer from some curious omissions (e.g., the structure of ice is not mentioned). The mathmatical appendices comprehend a variety of useful formulae.

The more conventional parts of the book, dealing with the production and properties of x-rays and with the description of crystal structures are adequate but not inspired. Here some inconsistencies may be noted. As the author has already called attention to one of these in a "Druckfehler-Berichtigung" it may be allowed to note on the same point that the order of lines in Fig. 75 on p. 93 should be $\beta_2\beta_1\alpha_1\alpha_2$, not $\beta_1\beta_2\alpha_2\alpha_1$. In several places the wave-lengths quoted in the text do not agree with those found in the tables. There is a slip in the definition of X.E. on p. 83; the arrangement of three-fold screw axes in Fig. 125 on p. 162 does not possess three-fold symmetry which might well be expected; K and L are interchanged at the close of the paragraph below Fig. 79 on p. 98; Fig. 173 on p. 231 identifies μ_2, μ_3 in a manner inconsistent with the text; on p. 278 annealing just below the "solidus" rather than the "liquidus" is undoubtedly meant. Certain formulae only true for the cubic system are first introduced without restriction, e.g. $\cos \alpha' : \cos \beta' : \cos \gamma' = h:k:l$ on p. 148. The term "ideal crystal" is used on p. 143 in a manner quite distinct from that made familiar to us in the papers of Smekal; Fig. 93 shows a $(1\bar{1}0)$, not a (110) plane; CuZn is not, in spite of the remarks on p. 154, based on a body-centered cubic space-lattice.

The section on spectral analysis by emission lines is particularly good. It contains a very complete table, prepared by Hadding, giving the various possible origins of lines for which only the approximate wave-length is known. Use of such a table is necessary before it can be concluded that any suspected element is really present in a mixture. In the section on the evaluation of fibering, complete or limited (i.e., preferred orientation of crystallites) the author follows very closely his own already classical papers on the structure of silver foils. The more complicated sorts of fibering, described in the periodical literature by Weissenberg, are only mentioned.

Students of materials who depend in any great degree upon the information which they can gain by applying x-ray methods will find this book particularly convenient. The frequent numerical examples are especially to be commended. The paper, typography and binding are excellent.

L. W. McKeehan

Essentials of Transformer Practice. By Emerson G. Reed. Pp. 401, figs. 185. D. Van Nostrand Company, New York, 1927. Price $5.00. The transformer is a very important link in our present day transmission and distribution systems. Its proper installation and operation is, therefore, of utmost importance. The designing engineer aims to build his apparatus for the most severe conditions that are apt to arise in service. The operating engineer must be familiar with the effects of abnormal loads and abnormal voltages, he must be able to solve economic problems, balancing first cost against cost of operation for the peculiar conditions of a given installation.

The author, a designing engineer, discusses the problems of transformer operation in a a clear and thorough manner. The chapters on the general design relations are interesting and valuable because they show how the various transformer characteristics depend upon one another. A valuable discussion of the theory and characteristics of instrument transformer is also included. Vector diagrams are used extensively and mathematical analyses are not avoided. The large number of numerical examples used to illustrate mathematical formulas add greatly to the value of the book.

J. H. Kuhlman